

BULLETIN OF RUSSIAN STATE MEDICAL UNIVERSITY

BIOMEDICAL JOURNAL OF PIROGOV RUSSIAN NATIONAL
RESEARCH MEDICAL UNIVERSITY

EDITOR-IN-CHIEF Denis Rebrikov, DSc, professor

DEPUTY EDITOR-IN-CHIEF Alexander Oettinger, DSc, professor

EDITORS Valentina Geidebrekht, Nadezda Tikhomirova

TECHNICAL EDITOR Evgeny Lukyanov

TRANSLATORS Ekaterina Tretiyakova, Vyacheslav Vityuk

DESIGN AND LAYOUT Marina Doronina

EDITORIAL BOARD

Averin VI, DSc, professor (Minsk, Belarus)

Alipov NN, DSc, professor (Moscow, Russia)

Belousov VV, DSc, professor (Moscow, Russia)

Bogomilskiy MR, corr. member of RAS, DSc, professor (Moscow, Russia)

Bozhenko VK, DSc, CSc, professor (Moscow, Russia)

Bylova NA, CSc, docent (Moscow, Russia)

Gainetdinov RR, CSc (Saint-Petersburg, Russia)

Gendlin GYe, DSc, professor (Moscow, Russia)

Ginter EK, member of RAS, DSc (Moscow, Russia)

Gorbacheva LR, DSc, professor (Moscow, Russia)

Gordeev IG, DSc, professor (Moscow, Russia)

Gudkov AV, PhD, DSc (Buffalo, USA)

Gulyaeva NV, DSc, professor (Moscow, Russia)

Gusev EI, member of RAS, DSc, professor (Moscow, Russia)

Danilenko VN, DSc, professor (Moscow, Russia)

Zarubina TV, DSc, professor (Moscow, Russia)

Zatevakhin II, member of RAS, DSc, professor (Moscow, Russia)

Kagan VE, professor (Pittsburgh, USA)

Kzyshkowska YuG, DSc, professor (Heidelberg, Germany)

Kobrinskii BA, DSc, professor (Moscow, Russia)

Kozlov AV, MD PhD (Vienna, Austria)

Kotelevtsev YuV, CSc (Moscow, Russia)

Lebedev MA, PhD (Darem, USA)

Manturova NE, DSc (Moscow, Russia)

Milushkina OYu, DSc, professor (Moscow, Russia)

Mitupov ZB, DSc, professor (Moscow, Russia)

Moshkovskii SA, DSc, professor (Moscow, Russia)

Munblit DB, MSc, PhD (London, Great Britain)

Negrebetsky VV, DSc, professor (Moscow, Russia)

Novikov AA, DSc (Moscow, Russia)

Pivovarov YuP, member of RAS, DSc, professor (Moscow, Russia)

Platonova AG, DSc (Kiev, Ukraine)

Polunina NV, corr. member of RAS, DSc, professor (Moscow, Russia)

Poryadin GV, corr. member of RAS, DSc, professor (Moscow, Russia)

Razumovskii AYu, corr. member of RAS, DSc, professor (Moscow, Russia)

Rebrova OYu, DSc (Moscow, Russia)

Rudoy AS, DSc, professor (Minsk, Belarus)

Rylova AK, DSc, professor (Moscow, Russia)

Savelieva GM, member of RAS, DSc, professor (Moscow, Russia)

Semiglazov VF, corr. member of RAS, DSc, professor (Saint-Petersburg, Russia)

Skobolina NA, DSc, professor (Moscow, Russia)

Slavyanskaya TA, DSc, professor (Moscow, Russia)

Smirnov VM, DSc, professor (Moscow, Russia)

Spallone A, DSc, professor (Rome, Italy)

Starodubov VI, member of RAS, DSc, professor (Moscow, Russia)

Stepanov VA, corr. member of RAS, DSc, professor (Tomsk, Russia)

Suchkov SV, DSc, professor (Moscow, Russia)

Takhchidi KhP, member of RAS, DSc, professor (Moscow, Russia)

Trufanov GE, DSc, professor (Saint-Petersburg, Russia)

Favorova OO, DSc, professor (Moscow, Russia)

Filipenko ML, CSc, leading researcher (Novosibirsk, Russia)

Khazipov RN, DSc (Marsel, France)

Chundukova MA, DSc, professor (Moscow, Russia)

Shimanovskii NL, corr. member of RAS, DSc, professor (Moscow, Russia)

Shishkina LN, DSc, senior researcher (Novosibirsk, Russia)

Yakubovskaya RI, DSc, professor (Moscow, Russia)

SUBMISSION <http://vestnikrgmu.ru/login?lang=en>

CORRESPONDENCE editor@vestnikrgmu.ru

COLLABORATION manager@vestnikrgmu.ru

ADDRESS ul. Ostrovityanova, d. 1, Moscow, Russia, 117997

Indexed in Scopus. CiteScore 2020: 0.4



Indexed in WoS. JCR 2020: 0.4



Five-year h-index is 6



Indexed in RSCI. IF 2018: 0,5



Listed in HAC 31.01.2020 (№ 507)



Open access to archive



Issue DOI: 10.24075/brsmu.2021-04

The mass media registration certificate № 012769 issued on July 29, 1994

Founder and publisher is Pirogov Russian National Research Medical University (Moscow, Russia)

The journal is distributed under the terms of Creative Commons Attribution 4.0 International License www.creativecommons.org



Approved for print 31.08.2021

Circulation: 100 copies. Printed by Print.Formula
www.print-formula.ru

ВЕСТНИК РОССИЙСКОГО ГОСУДАРСТВЕННОГО МЕДИЦИНСКОГО УНИВЕРСИТЕТА

НАУЧНЫЙ МЕДИЦИНСКИЙ ЖУРНАЛ РНИМУ им. Н. И. ПИРОГОВА

ГЛАВНЫЙ РЕДАКТОР Денис Ребриков, д. б. н., профессор

ЗАМЕСТИТЕЛЬ ГЛАВНОГО РЕДАКТОРА Александр Эттингер, д. м. н., профессор

РЕДАКТОРЫ Валентина Гейдебрехт, Надежда Тихомирова

ТЕХНИЧЕСКИЙ РЕДАКТОР Евгений Лукьянин

ПЕРЕВОДЧИКИ Екатерина Третьякова, Вячеслав Витюк

ДИЗАЙН И ВЕРСТКА Марины Дорониной

РЕДАКЦИОННАЯ КОЛЛЕГИЯ

В. И. Аверин, д. м. н., профессор (Минск, Белоруссия)

Н. Н. Алипов, д. м. н., профессор (Москва, Россия)

В. В. Белоусов, д. б. н., профессор (Москва, Россия)

М. Р. Богомильский, член-корр. РАН, д. м. н., профессор (Москва, Россия)

В. К. Боженко, д. м. н., к. б. н., профессор (Москва, Россия)

Н. А. Былова, к. м. н., доцент (Москва, Россия)

Р. Р. Гайнэтдинов, к. м. н. (Санкт-Петербург, Россия)

Г. Е. Гендлин, д. м. н., профессор (Москва, Россия)

Е. К. Гинтер, академик РАН, д. б. н. (Москва, Россия)

Л. Р. Горбачева, д. б. н., профессор (Москва, Россия)

И. Г. Гордеев, д. м. н., профессор (Москва, Россия)

А. В. Гудков, PhD, DSc (Буффало, США)

Н. В. Гуляева, д. б. н., профессор (Москва, Россия)

Е. И. Гусев, академик РАН, д. м. н., профессор (Москва, Россия)

В. Н. Даниленко, д. б. н., профессор (Москва, Россия)

Т. В. Зарубина, д. м. н., профессор (Москва, Россия)

И. И. Затевахин, академик РАН, д. м. н., профессор (Москва, Россия)

В. Е. Каган, профессор (Питтсбург, США)

Ю. Г. Кжышковска, д. б. н., профессор (Гейдельберг, Германия)

Б. А. Кобринский, д. м. н., профессор (Москва, Россия)

А. В. Козлов, MD PhD (Вена, Австрия)

Ю. В. Котелевцев, к. х. н. (Москва, Россия)

М. А. Лебедев, PhD (Дарем, США)

Н. Е. Мантуррова, д. м. н. (Москва, Россия)

О. Ю. Милушкина, д. м. н., доцент (Москва, Россия)

З. Б. Митупов, д. м. н., профессор (Москва, Россия)

С. А. Мошковский, д. б. н., профессор (Москва, Россия)

Д. Б. Мунблит, MSc, PhD (Лондон, Великобритания)

В. В. Негребецкий, д. х. н., профессор (Москва, Россия)

А. А. Новиков, д. б. н. (Москва, Россия)

Ю. П. Пивоваров, д. м. н., академик РАН, профессор (Москва, Россия)

А. Г. Платонова, д. м. н. (Киев, Украина)

Н. В. Полунина, член-корр. РАН, д. м. н., профессор (Москва, Россия)

Г. В. Порядин, член-корр. РАН, д. м. н., профессор (Москва, Россия)

А. Ю. Разумовский, член-корр., профессор (Москва, Россия)

О. Ю. Реброва, д. м. н. (Москва, Россия)

А. С. Рудой, д. м. н., профессор (Минск, Белоруссия)

А. К. Рылова, д. м. н., профессор (Москва, Россия)

Г. М. Савельева, академик РАН, д. м. н., профессор (Москва, Россия)

В. Ф. Семиглазов, член-корр. РАН, д. м. н., профессор (Санкт-Петербург, Россия)

Н. А. Скоблина, д. м. н., профессор (Москва, Россия)

Т. А. Славянская, д. м. н., профессор (Москва, Россия)

В. М. Смирнов, д. б. н., профессор (Москва, Россия)

А. Спаллоне, д. м. н., профессор (Рим, Италия)

В. И. Стародубов, академик РАН, д. м. н., профессор (Москва, Россия)

В. А. Степанов, член-корр. РАН, д. б. н., профессор (Томск, Россия)

С. В. Сучков, д. м. н., профессор (Москва, Россия)

Х. П. Тахиди, академик РАН, д. м. н., профессор (Москва, Россия)

Г. Е. Труфанов, д. м. н., профессор (Санкт-Петербург, Россия)

О. О. Фаворова, д. б. н., профессор (Москва, Россия)

М. Л. Филипенко, к. б. н. (Новосибирск, Россия)

Р. Н. Хазипов, д. м. н. (Марсель, Франция)

М. А. Чундокова, д. м. н., профессор (Москва, Россия)

Н. Л. Шимановский, член-корр. РАН, д. м. н., профессор (Москва, Россия)

Л. Н. Шишкина, д. б. н. (Новосибирск, Россия)

Р. И. Якубовская, д. б. н., профессор (Москва, Россия)

ПОДАЧА РУКОПИСЕЙ <http://vestnikrgmu.ru/login>

ПЕРЕПИСКА С РЕДАКЦИЕЙ editor@vestnikrgmu.ru

СОТРУДНИЧЕСТВО manager@vestnikrgmu.ru

АДРЕС РЕДАКЦИИ ул. Островитянова, д. 1, г. Москва, 117997

Журнал включен в Scopus. CiteScore 2020: 0,4

Журнал включен в WoS. JCR 2020: 0,4

Индекс Хирша (h⁵) журнала по оценке Google Scholar: 6

Scopus®

WEB OF SCIENCE™

Google
scholar

Журнал включен в РИНЦ. IF 2018: 0,5

Журнал включен в Перечень 31.01.2020 (№ 507)

Здесь находится открытый архив журнала

e
**НАУЧНАЯ ЭЛЕКТРОННАЯ
БИБЛИОТЕКА**
LIBRARY.RU



ВЫСШАЯ
АТТЕСТАЦИОННАЯ
КОМИССИЯ (BAK)

CYBERLENINKA

DOI выпуска: 10.24075/vrgmu.2021-04

Свидетельство о регистрации средства массовой информации № 012769 от 29 июля 1994 г.

Учредитель и издатель — Российский национальный исследовательский медицинский университет имени Н. И. Пирогова (Москва, Россия)

Журнал распространяется по лицензии Creative Commons Attribution 4.0 International www.creativecommons.org



Подписано в печать 31.08.2021

Тираж 100 экз. Отпечатано в типографии Print.Formula
www.print-formula.ru

REVIEW**5****Dermatology and telemedicine: goals, advantages and disadvantages**

Dvornikov AS, Minkina OV, Grebenshchikova EG, Vvedenskaya EV, Mylnikova IS

Дерматология и телемедицина: цели, преимущества и недостатки

А. С. Дворников, О. В. Минкина, Е. Г. Гребенщикова, Е. В. Введенская, И. С. Мыльникова

ORIGINAL RESEARCH**10****Retinal abnormalities in transgenic mice overexpressing aberrant human FUS[1-359] gene**

Soldatov VO, Kukharsky MS, Soldatova MO, Puchenkova OA, Nikitina YuA, Lysikova EA, Kartashkina NL, Deykin AV, Pokrovskiy MV

Ретинальные аномалии у трансгенных мышей, суперэкспрессирующих аберрантный человеческий ген FUS[1-359]

В. О. Солдатов, М. С. Кухарский, М. О. Солдатова, О. А. Пученкова, Ю. А. Никитина, Е. А. Лысикова, Н. Л. Карташкина, А. В. Дейкин, М. В. Покровский

ORIGINAL RESEARCH**16****Evaluation of SARS-CoV-2 viability on experimental surfaces over time**

Nikitrova MA, Siniavina AE, Shidlovskaya EV, Kuznetsova NA, Gushchin VA

Оценка жизнеспособности SARS-CoV-2 на экспериментальных поверхностях во времени

М. А. Никиторова А. Э. Синявин, Е. В. Шидловская, Н. А. Кузнецова, В. А. Гущин

ORIGINAL RESEARCH**20****Features of the pathogenetic mechanisms of tuberculous peritonitis in an experiment**

Plotkin DV, Vinogradova TI, Reshetnikov MN, Ariel BM, Zyuza YuR, Zhuravlev VYu, Sinitsyn MV, Bogorodskaya EM, Yablonsky PK

Особенности патогенетических механизмов туберкулезного перитонита в эксперименте

Д. В. Плоткин, Т. И. Виноградова, М. Н. Решетников, Б. М. Ариэль, Ю. Р. Зюза, В. Ю. Журавлев, М. В. Синицын, Е. М. Богородская, П. К. Яблонский

ORIGINAL RESEARCH**28****Labelling of data on fundus color pictures used to train a deep learning model enhances its macular pathology recognition capabilities**

Takhchidi HP, Gilznitsa PV, Svetozarskiy SN, Bursov AI, Shusterzon KA

Разметка цветных фотографий глазного дна улучшает распознавание макулярной патологии с помощью глубокого обучения

Х. П. Тахчиди, П. В. Гильзница, С. Н. Светозарский, А. И. Бурсов, К. А. Шустэрзон

ORIGINAL RESEARCH**34****Role of mast cells in skin regeneration after thermal burn treated with melatonin-enriched dermal film**

Osikov MV, Ageeva AA, Fedosov AA, Ushakova VA

Роль тучных клеток в репарации кожи после термической травмы при применении дермальной пленки с мелатонином

М. В. Осиков, А. А. Агеева, А. А. Федосов, В. А. Ушакова

ORIGINAL RESEARCH**43****Effectiveness of hybrid intraperitoneal mesh repair for paracolostomy hernia**

Malgina NV, Dolgina TYu, Epifanova AD, Rodoman GV

Оценка эффективности применения гибридной интраперитонеальной аллопластики при параколостомических грыжах

Н. В. Мальгина, Т. Ю. Долгина, А. Д. Епифанова, Г. В. Родоман

ORIGINAL RESEARCH**50****Experimental assessment of biological potential of collagen membranes in reconstruction of full-thickness hyaline cartilage defects**

Lazishvili GD, Egiazaryan KA, Nikishin DV, Voroncov AA, Klinov DV

Экспериментальная оценка биологического потенциала коллагеновых мембран при реконструкции полнослойных дефектов гиалинового хряща

Г. Д. Лазишили, К. А. Егизарян, Д. В. Никишин, А. А. Воронцов, Д. В. Клинов

Fluorescence detection of amyloid deposits in human tissues using histochemical dyes

Guseinikova VV, Sufieva DA, Tsypa DL, Korzhevskii DE

Применение гистохимических красителей для флуоресцентного выявления амилоидных скоплений в тканях человека

В. В. Гусельникова, Д. А. Суфиева, Д. Л. Цыба, Д. Э. Коржевский

Hardiness and personal resources of red zone staff: psychological analysis

Yasko BA, Kazarin BV, Gorodin VN, Chugunova NA, Pokul LV, Skripnichenko LS, Skorobogatov VV

Жизнестойкость и персональные ресурсы врачей «красных зон» ковид-госпиталей: психологический анализ

Б. А. Ясько, Б. В. Казарин, В. Н. Городин, Н. А. Чугунова, Л. В. Покуль, Л. С. Скрипниченко, В. В. Скоробогатов

DERMATOLOGY AND TELEMEDICINE: GOALS, ADVANTAGES AND DISADVANTAGES

Dvornikov AS, Minkina OV, Grebenschikova EG ✉, Vvedenskaya EV, Mylnikova IS

Pirogov Russian National Research Medical University, Moscow, Russia

COVID-19 pandemic has made changes to conventional health care. In view of the need for "social distancing", telemedicine services became most in demand, which constituted a reform of the previous doctor-patient relationship format; dermatology was no exception. Increased use of teledermatology (TD) all over the world elevated the relevance of the set of challenges related to teledermatology potential and limits, particularly in the light of the expectations of the technology broader application during the post-pandemic period. The review addresses the issues related to accounting for quality of health care, understanding the social and humanitarian context of TD, as well as the impact on professional education.

Keywords: COVID-19, telemedicine, dermatology, teledermatology, bioethics

Author contribution: Dvornikov AS — study concept and design, manuscript editing; Minkina OV — study concept and design, manuscript writing; Grebenschikova EG — study concept and design, manuscript writing; Vvedenskaya EV — literature analysis, text writing; Mylnikova IS — literature analysis, text writing.

✉ **Correspondence should be addressed:** Elena G. Grebenschikova
Ostrovitianova, 1, Moscow, 117997; aika45@ya.ru

Received: 17.08.2021 **Accepted:** 27.08.2021 **Published online:** 31.08.2021

DOI: 10.24075/brsmu.2021.041

ДЕРМАТОЛОГИЯ И ТЕЛЕМЕДИЦИНА: ЦЕЛИ, ПРЕИМУЩЕСТВА И НЕДОСТАТКИ

А. С. Дворников, О. В. Минкина, Е. Г. Гребенщикова ✉, Е. В. Введенская, И. С. Мыльникова

Российский национальный исследовательский медицинский университет имени Н. И. Пирогова, Москва, Россия

Пандемия COVID-19 внесла изменения в традиционное медицинское обслуживание. В связи с необходимостью «социального дистанцирования» особенно востребованными стали услуги телемедицинской помощи, что изменило прежний формат взаимоотношений врача и пациента; дерматология не стала исключением. Активное использование теледерматологии (ТД) во всем мире актуализировало комплекс проблем, связанных с ее возможностями и недостатками, особенно в свете ожиданий более широкого применения этой технологии в постпандемический период. В обзоре освещены вопросы оказания медицинской помощи, понимания социогуманитарных контекстов развития ТД и последствий для сферы профессионального образования.

Ключевые слова: COVID-19, дерматология, телемедицина, теледерматология, биоэтика

Вклад авторов: А. С. Дворников — концепция и дизайн исследования, редактирование статьи; О. В. Минкина — концепция и дизайн исследования, написание статьи; Е. Г. Гребенщикова — концепция и дизайн исследования, написание статьи; Е. В. Введенская — анализ источников, написание текста; И. С. Мыльникова — анализ источников, написание текста.

✉ **Для корреспонденции:** Елена Георгиевна Гребенщикова
ул. Островитянова, д. 1, г. Москва, 117997; aika45@ya.ru

Статья получена: 17.08.2021 **Статья принята к печати:** 27.08.2021 **Опубликована онлайн:** 31.08.2021

DOI: 10.24075/vrgmu.2021.041

Teledermatology as a section of telemedicine

Telemedicine (TM) is an information and communication technology for provision of health care and medical services, based on remote data communication aimed at diagnosis and treatment of the disorders, clinical and laboratory assessment data analysis, and remote patient monitoring. The technology can also be used as a professional educational resource ("remote healing and specialized learning"). In the Russian Federation, the term TM was established in 2001 in the project of Coordination Council for TM of the Ministry of Health of the Russian Federation, the Concept of TM Technology Development in the Russian Federation. In 2017, the concept of "telemedicine technology" was introduced at the federal legislative level, which included two spheres of use: remote care provision and electronic flow of medical documents [1]. Teledermatology (TD) involves the use of digital technology making it possible to freely advise patients with disorders of skin or its appendages regardless of the distance and time zone; analyze the results of various types of studies, including dermatoscopy images, by data transmission performed at a time appropriate both for the patient and the physician; run remote collegiate conferences in the situations, where the expert opinion is required.

Conventional TD technologies are as follows: asynchronous TD, or SAF (Store-and-Forward), which involves time delay estimation of spatially dispersed images or any other supplementary data; synchronous TD, or RT-TD (real-time teledermatology), involving real-time video consultations; hybrid model (SAF + RT-TD) and mobile TD [2]. Earlier, TD most often involved the store-and-forward models. The number of interactive RT-TD communication significantly increased during the COVID-19 pandemic. Survey about the effects of the pandemic on TD performed in May and June 2020, involving 591 dermatology practitioners being the AAD (American Academy of Dermatology) members, showed that only 14.1% of respondents used TD before the pandemic compared with 96.9% after the COVID-19 emergence; 58.0% of dermatologists assumed they would use TD in the future regardless of the epidemiological situation; 72.0% of physicians rated hybrid model as the most accurate [3].

According to a number of researchers, TD and face-to-face consultations have comparable diagnostic accuracy [4; 5]. The real-time work has certain definite advantages, such as first-hand opportunity to ask clarifying questions, resolve disputes and explain obscure points in a timely manner, control patient's understanding of the recommendations received. However, the quality of video used in RT-TD is usually lower than the

quality of static images used in SAF, particularly with respect to teledermatoscopy and ultrastructural analysis of features in melanocytic, vascular or keratinized cutaneous neoplasms.

In 2021, the results of 2632 TD consultations, conducted from 16.03.2020 to 01.05.2020, were published: SAF accounted for 36.2% consultations, and RT-TD accounted for 63.8%. A total of 54.2% medical service providers preferred synchronous consultations for the reason of benefits provided by face-to-face doctor-patient communication. No preference was expressed for selection of TD modification for initial visit, however, 66.7% of medical service providers selected RT-TD for return visit; 87.5% preferred synchronous consultations for patients with connective tissue diseases and immunobullous disorders, as well as for patients receiving biological therapy [6]. TD modification with greater differential diagnosis variability in relation to particular patient was determined: with the use of RT-TD, the number of diagnoses varied in the range of 1–5; with the use of SAF, it varied in the range of 1–3. RT-TD provides conditions as close as possible to in-person visit, therefore the doctor-patient relationship can deviate from simple analysis of actual data, which expands differential diagnosis and, in turn, affects the diagnosis accuracy.

TD could prove indispensable for remote in-patient assessment given insufficient staffing of hospitals all over the world with dermatologists. The study of diagnostic impressions and therapeutic recommendations in facility-based clinician, external dermatologist (ED) and SAF teledermatologist (SAF-TD) involving 100 patients revealed no substantial differences in the diagnosis accuracy and subsequent prescribing therapy between facility-based dermatologist and SAF-TD: ED advice resulted in diagnosis change in 50.9% of cases, and SAF-TD in 54.7% of cases respectively; ED changed systemic therapy in 41.5% of cases, and SAF consultations resulted in treatment adjustment in 47.2% of cases. When comparing ED and SAF-TD, diagnostic complete and partial agreement were 52.8% and 84.9%, respectively; systemic therapy agreement was reached in 77.4% of cases [7].

Mobile TD and teledermatoscopy (TDS) include the expanded specialized TM services allowing one to send and receive data via smartphones and appropriate applications. Survey of dermatology practitioners in Australia showed that more than 50% of respondents sent and received clinical images on their smartphones at least weekly; this value in young professionals and interns was 89% [8].

The researchers consider the opportunity to significantly improve and quicken access to specialized health care in remote regions understuffed with specialists the main advantage of TD, making it possible to eliminate health inequalities. Moreover, TD can improve access to treatment in patients, who face certain social and economic barriers: childcare periods; decreased mobility; severe social anxiety; complex work schedule [9]. In these cases, there is particular interest in the use of asynchronous TD: the physician performs assessment of images, video and examination results without any in-person visits, and usually spends less time on dealing with each individual case, which can be considered an advantage given the shortage of professionals. It is assumed, however, that the patient would not deal with lack of attention from the doctor during the remote consultation. In a survey of 52 patients with acne, who used TM services during the pandemic, 92.3% rated the attention paid by the dermatologist regarding their disease as favourable; 86.5% of patients were satisfied with the duration of the visit [10].

Moreover, at the level of general practitioner, TD enables screening for various dermatological diseases assigning the

patients an urgency category ("immediate" and "delayed") for further specialized care provision. Simple techniques allowing the patients to improve the quality of skin lesion images to be used during the further general therapeutic SAF consultations themselves have been proposed: "tape dermatoscopy" technique (immersion fluid placed on the lesion, covering the lesion with transparent adhesive tape, recording the image with a smartphone) [11]; "drop TD" technique (applying clear alcohol-based sanitizer with subsequent recording of the image using no adhesive tape) [12].

Limitations of teledermatology

Although the potential benefits of TM are obvious, and dermatology, being a discipline based a lot on the use of images, seems to be the most appropriate area of medicine for the use of TM, the widespread adoption of TM in this area meets serious resistance from healthcare professionals. For example, poor stream video quality or sharing poor-quality image files can complicate the doctor-patient relationship and result in various errors. Images of affected body regions having insufficient resolution, as well as restricted photographing private parts covered with rashes, could be a serious obstacle to morphological elements assessment, analysis of the disease development, diagnosis, and determining the required scope of the examination.

When working in the TD format, there could not only be technical difficulties, such as data networks integration, as well as the issues related to licensing of TM systems, combining TD data with electronic patient records, and financial reporting, but also ethical dilemmas related to confidentiality of the information provided, quality control in healthcare, and regulation of the subsequent physician's liability being the result of "long-distance" examination performed by specialist, even in case the physician and the examined person come from different jurisdictions [13].

The loss of real-life communication between the physician and the patient is one the major ethical issues related to TD. During the in-person consultation, dermatologist performs general and specialized instrumental examination of the patient, e.g. luminescence-based examination, diascopy, etc., helping to distinguish dozens of disorders and establish the presumptive diagnosis, *inter alia* based on the patient's scent, skin peeling pattern, tactile sensation in palpation, and staining of the skin with special dyes. TD consultation deprives the physician of this possibility. The vast majority of patients reported satisfaction with the quality of healthcare services during the study aimed to assess the patients' perception of technical expertise on the use of synchronous TM during the COVID-19 outbreak. However, 68.7% of patients pointed out they would prefer an in-person consultation for their next visit rather than virtual consultation [14].

Despite years of efforts to implement TD and TDS for skin cancer screening [15], as the pandemic continued its progress, it became apparent that extended remote follow-up, delayed face-to-face assessment and surgery can result in exacerbation of chronic disorders, and delayed cancer detection and treatment. One notable limitation of TDS is inability to perform full examination of skin on a regular basis. Since the incidence of melanoma has increased more rapidly compared to any other cancer type during the pre-pandemic period [16], TDS innovations can exacerbate this dangerous trend [17] and result in reduced early diagnosis and increased mortality. The impact of time to definitive stage I–III melanoma surgery on overall survival was assessed by using the National

Cancer Database (153,218 patients) data [18]. Multivariate analysis of cases in all stages showed that the patients who were treated between 90 and 119 days, and more than 119 days after biopsy, had a higher risk for mortality compared with those treated within 30 days of biopsy. It should be reminded that survival rate in patients whose melanoma is detected early reaches 99% [19]. The intra-group stage-based analysis performed during this study revealed higher mortality risk in patients with stage I treated more than 30 days after biopsy; surgical timing did not affect survival in stages II and III.

Inability to perform procedures is one more notable limitation of TD [20]. It was recognized in the beginning of the pandemic [21], which reflected the situation in other areas of medicine, where the need for various manipulations being a difficult if not impossible task for a layman at home had become a problem.

Thus, despite the enthusiasm related to access to dermatological care, clearly understandable during the pandemic, TD still cannot compete with face-to-face medical consultations and can be used in the situations with no alternatives by fully qualified dermatologists. Moreover, confirming the professional competence of the physician, usually contacted by patients from anywhere in the world, also becomes a problem.

It is also important to point out that TD cannot fully address the problem of access to health care services, since not every patient has the required level of literacy, as well as access to broadband Internet and equipment for photography and videoconferencing. This problem is urgent for many countries and regions all over the world. Thus, in India, where the shortage of dermatologists is particularly acute, TD has been treated as a promising opportunity to revolutionize dermatological care during the COVID-19 crisis. However, availability of stable Internet connection and technological illiteracy have become a serious obstacle for widespread adoption of TD in this country [22].

Teledermatology and specialists' education

TM in the "doctor-to-doctor" format is also considered an important educational tool for improving professional competence in medical students, dermatology residents, and professionals with little practical experience [23]. Some professionals believe that integration of TD in residency training programs could have a significant impact on the dermatologists' professional competence formation.

Furthermore, such online education technologies as video lectures, interactive teleconferencing, virtual microscopy, and clinical simulation have become very popular among medical students and resident physicians, and have proved to be effective; these technologies could constitute a significant proportion of self-directed clinical education and enable objectification of the subsequent knowledge assessment. According to the survey of dermatology residency program directors conducted in 2016, 69% of respondents were interested in potentially incorporating TM into their curriculum [24].

However, to practice to the fullest extent, dermatologist should have not only deep theoretical knowledge and large visual memory storage capacity, but also possess various surgical and procedural skills. To date, online broadcasting of surgery performed by highly qualified professionals is quite common. However, despite the attractiveness of TM, productive TM applicability in students, resident physicians and experienced physicians differs [25]. The experience of Netherlands and Australia, where TD is integrated into health system as an important supplement to conventional dermatological care, and the electronic records are accessible

to all users of the system, is a successful model of using new technology [26].

Teledermatology in the context of healthcare digitalization

The use of TM in dermatology is a part of a broader trend of health care digitalization, improvement of health care capacity due to strong deployment of information and communication technologies at different levels of the health system organization, as well as in extra-clinical sphere as a result of rapid development of the mobile health (mHealth) market.

The clinical decision support programmes based on deep learning and artificial intelligence (AI) technologies are being vigorously developed. The results of the diagnostic performance comparative analysis performed in 2020 in human subjects and ResNet34 system, being a convolutional neural network (CNN), involved construction of contemporary computer vision models in multiple settings. In an effort to identify optimal conditions for further beneficial human-computer collaboration, a total of 302 physicians from 41 countries were surveyed: board-certified dermatologists accounted for 56.0%, dermatology residents for 25.5%, and general practitioners for 12.6%. During testing with the use of benchmark test set (1412 dermoscopic images) of various cutaneous neoplasms (melanoma, basal cell carcinoma, actinic keratosis, intraepithelial carcinoma, melanocytic nevi, benign keratinized neoplasms, dermatofibroma, vascular lesions), the ResNet34 sensitivity in all categories of images was 77.7%, and the accuracy was 80.3%. ResNet34 was most beneficial in assessment of such pigmented lesions as actinic keratosis and intraepithelial carcinoma compared to other types of lesions. Medical decision-making support with AI-based multiclass probabilities improved the accuracy of human raters' work from 63.6% to 77.0%, however, it was of little effect when predicting lesion malignancy in laboratory settings. According to the authors, the AI-based computer system performance should be tested not only in real world, but also by the target user. These systems should not be recommended as standalone devices for widespread use [27].

It is quite clear that AI-based diagnostic systems would not replace dermatologists in the near future. However, significance of such systems for diagnosis and increased provision of care cannot be denied. Both physicians and patients aware of the advantages and limitations of health care technological innovation given the specificity of dermatology as the field of medicine should be ready to use the AI-based technologies.

Conclusion

The experience of the TD broader use during the pandemic revealed both TD potential and limitations, many of which had been previously discussed by the specialists. It is obvious that most of the issues would gradually be resolved due to new technology development (for example, image quality improvement), development of ethical standards and legal norms (issues of confidentiality protection), bridging the digital divide between the generations, active incorporation of TD programmes into medical education, and would encourage the further development of this field of medicine. However, the development of TD in a socially responsible and patient-oriented manner requires understanding both dermatological care peculiarities (the need for visual and instrumental examination, as well as for face-to-face contact) and the features of doctor-patient relationship, which largely determine the diagnosis and treatment success.

References

1. Приказ Министерства здравоохранения РФ от 30.11.2017 № 965н «Об утверждении порядка организации и оказания медицинской помощи с применением телемедицинских технологий». Доступно по ссылке: <http://www.pravo.gov.ru>. Russian.
2. Kanthraj GR. Teledermatology: Its role in dermatosurgery. *J Cutan Aesthet Surg.* 2008; 1 (2): 68–74. PubMed PMID: 20300347.
3. Kennedy J, Arey S, Hopkins Z, Tejasvi T, Farah R, Secret AM, et al. Dermatologist perceptions of teledermatology implementation and future use after COVID-19 demographics, barriers, and insights. *JAMA Dermatol.* 2021; 157 (5): 595–7. PubMed PMID: 33787839. DOI: 10.1001/jamadermatol.2021.0195.
4. Moreno-Ramirez D, Argenziano G. Teledermatology and mobile applications in the management of patients with skin lesions. *Acta Derm Venereol.* 2017; Suppl 218: 31–35. PubMed PMID: 28676881.
5. Lee JJ, English JC III. Teledermatology: A review and update. *Am J Clin Dermatol.* 2018; 19 (2): 253–60. PubMed PMID: 28871562.
6. Kazi R, Evankovich MR, Liu R, Liu A, Moorhead A, Ferris L K, et al. Utilization of asynchronous and synchronous teledermatology in a large health care system during the COVID-19 pandemic. *Telemedicine and e-Health.* 2021; 27 (7): 771–7. PubMed PMID: 33074786.
7. Keller JJ, Johnson JP, Latour E. Inpatient teledermatology: diagnostic and therapeutic concordance among a hospitalist, dermatologist, and teledermatologist using store-and-forward teledermatology. *J Am Acad Dermatol.* 2020; 82 (5): 1262–7. PubMed PMID: 31972258.
8. Abbott LM, Magnusson RS, Gibbs E, Smith SD. Smartphone use in dermatology for clinical photography and consultation: Current practice and law. *Australas J Dermatol.* 2018 May; 59 (2): 101–7. PubMed PMID: 28247404.
9. Pulsipher KJ, Presley CL, Rundle CW, Rietcheck HR, Millitelo M, Dellavalle RP. Teledermatology application use in the COVID-19 era. *Dermatology Online Journal.* 2020; 26 (12). PubMed PMID: 33423415.
10. Ruggiero A, Megna M, Annunziata MC, Abategiovanni L, Scalvenzi M, Tajani A, et al. Teledermatology for acne during COVID-19: high patients' satisfaction in spite of the emergency. *J Eur Acad Dermatol Venereol.* 2020; 34 (11): e662–e663. PubMed PMID: 32534472.
11. Blum A, Giacomet J. «Tape dermatoscopy»: constructing a low-cost dermatoscope using a mobile phone, immersion fluid and transparent adhesive tape. *Dermatol Pract Concept.* 2015; 5 (2): 87–93. PubMed PMID: 26114061.
12. Kaliyadan F, Jayasree P, Ashique KT. Drop dermoscopy for teledermatology. *Journal of the American Academy of Dermatology.* 2021; 84 (1): e25–e26. PubMed PMID: 32771542.
13. Adelekun A, Sager MA, Lipoff JB. Bridging the divide, virtually: ethics of teledermatology. *Dermatoethics. Contemporary ethics and professionalism in dermatology.* Springer Nature Switzerland AG. 2021: 59–58.
14. Pearlman RL, Le PB, Brodell RT, Nahar VK. Evaluation of patient attitudes towards the technical experience of synchronous teledermatology in the era of COVID-19. *Arch Dermatol Res.* 2021; 5:1-4. PubMed PMID: 33403572.
15. Kroemer S, Fröhlauf J, Campbell TM, Massone C, Schwantzer G, Soyer HP, et al. Mobile teledermatology for skin tumour screening: diagnostic accuracy of clinical and dermoscopic image tele-evaluation using cellular phones. *Br J Dermatol.* 2011; 164: 973–9. PubMed PMID: 21219286.
16. Okhovat JP, Beaulieu D, Tsao H, Halpern AC, Michaud DS, Shaykevich S, et al. The first 30 years of the American academy of dermatology skin cancer screening program: 1985–2014. *J Am Acad Dermatol.* 2018; 79: 884–91. PubMed PMID: 30057360.
17. Rustad AM, Lio PA.. Pandemic pressure: teledermatology and health care disparities. *J Patient Exp.* 2021; 8: 2374373521996982. PubMed PMID: 34179385.
18. Conic RZ, Cabrera CI, Khorana AA, Gastman BR. Determination of the impact of melanoma surgical timing on survival using the National Cancer Database. *J Am Acad Dermatol.* 2018; 78 (1): 40–46.e7. PMID: 29054718.
19. American Cancer Society. Cancer Facts and Figures. January 8, 2021. Available from: <https://www.cancer.org/content/dam/cancerorg/research/cancer-facts-and-statistics/annual-cancer-facts-and-figures/2020/cancer-facts-and-figures-2020.pdf>.
20. Farr MA, Duvic M, Joshi TP. Teledermatology during COVID-19: an updated review. *American Journal of Clinical Dermatology.* 2021; Apr 9: 1–9. PubMed PMID: 33835345.
21. Perkins S, Cohen JM, Nelson CA, Bunick CG. Teledermatology in the era of COVID-19: experience of an academic department of dermatology. *Journal of the American Academy of Dermatology.* 2020; 83 (1): e43–e44. PubMed PMID: 32305442.
22. Ashique KT, Kaliyadan F. Teledermatology in the wake of COVID-19 scenario: An Indian perspective. *Indian Dermatology Online Journal.* 2020; 11 (3): 301. PubMed PMID: 32695684.
23. Boyers LN, Schultz A, Bacevieciene R, Blaney S, Marvi N, Dellavalle RP, et al. Teledermatology as an educational tool for teaching dermatology to residents and medical students. *Telemedicine and e-Health.* 2015; 21 (4): 312–4. PubMed PMID: 25635528.
24. Wanat KA, Newman S, Finney KM, Kovarik CL, Lee I. Teledermatology education: current use of teledermatology in US residency programs. *J Grad Med Educ.* 2016; 8 (2): 286–7. PubMed PMID: 27168912.
25. Jones VA, Clark KA, Puyana C, Tsoukas MM. Rescuing medical education in times of COVID-19. *Clin Dermatol.* 2021; 39(1): 33–4.
26. Tensen E, Van Der Heijden JP, Jaspers MWM, Witkamp L. Two decades of teledermatology: current status and integration in national healthcare systems. *Curr Dermatol Rep.* 2016; 5 (2): 96–104. PubMed PMID: 27182461.
27. Tschandl P, Rinner C, Apalla Z, Argenziano G, Codella N, Halpern A, et al. Human-computer collaboration for skin cancer recognition. *Nature Medicine.* 2020; 26 (8): 1229–34. PubMed PMID: 32572267.

Литература

1. Приказ Министерства здравоохранения РФ от 30.11.2017 № 965н «Об утверждении порядка организации и оказания медицинской помощи с применением телемедицинских технологий». Доступно по ссылке: <http://www.pravo.gov.ru>. Russian.
2. Kanthraj GR. Teledermatology: Its role in dermatosurgery. *J Cutan Aesthet Surg.* 2008; 1 (2): 68–74. PubMed PMID: 20300347.
3. Kennedy J, Arey S, Hopkins Z, Tejasvi T, Farah R, Secret AM, et al. Dermatologist perceptions of teledermatology implementation and future use after COVID-19 demographics, barriers, and insights. *JAMA Dermatol.* 2021; 157 (5): 595–7. PubMed PMID: 33787839. DOI: 10.1001/jamadermatol.2021.0195.
4. Moreno-Ramirez D, Argenziano G. Teledermatology and mobile applications in the management of patients with skin lesions. *Acta Derm Venereol.* 2017; Suppl 218: 31–35. PubMed PMID: 28676881.
5. Lee JJ, English JC III. Teledermatology: A review and update. *Am J Clin Dermatol.* 2018; 19 (2): 253–60. PubMed PMID: 28871562.
6. Kazi R, Evankovich MR, Liu R, Liu A, Moorhead A, Ferris L K, et al. Utilization of asynchronous and synchronous teledermatology in a large health care system during the COVID-19 pandemic. *Telemedicine and e-Health.* 2021; 27 (7): 771–7. PubMed PMID: 33074786.
7. Keller JJ, Johnson JP, Latour E. Inpatient teledermatology: diagnostic and therapeutic concordance among a hospitalist, dermatologist, and teledermatologist using store-and-forward teledermatology. *J Am Acad Dermatol.* 2020; 82 (5): 1262–7. PubMed PMID: 31972258.
8. Abbott LM, Magnusson RS, Gibbs E, Smith SD. Smartphone use in dermatology for clinical photography and consultation: Current practices and law. *Australas J Dermatol.* 2018 May; 59 (2): 101–7. PubMed PMID: 28247404.

9. Pulsipher KJ, Presley CL, Rundle CW, Rietcheck HR, Millitelo M, Dellavalle RP. Teledermatology application use in the COVID-19 era. *Dermatology Online Journal*. 2020; 26 (12). PubMed PMID: 33423415.
10. Ruggiero A, Megna M, Annunziata MC, Abategiovanni L, Scalvenzi M, Tajani A, et al. Teledermatology for acne during COVID-19: high patients' satisfaction in spite of the emergency. *J Eur Acad Dermatol Venereol*. 2020; 34 (11): e662–e663. PubMed PMID: 32534472.
11. Blum A, Giacomet J. «Tape dermatoscopy»: constructing a low-cost dermatoscope using a mobile phone, immersion fluid and transparent adhesive tape. *Dermatol Pract Concept*. 2015; 5 (2): 87–93. PubMed PMID: 26114061.
12. Kaliyadan F, Jayasree P, Ashique KT. Drop dermoscopy for teledermatology. *Journal of the American Academy of Dermatology*. 2021. 84 (1): e25–e26. PubMed PMID: 32771542.
13. Adelekun A, Sager MA, Lipoff JB. Bridging the divide, virtually: ethics of teledermatology. *Dermatoethics. Contemporary ethics and professionalism in dermatology*. Springer Nature Switzerland AG. 2021: 59–58.
14. Pearlman RL, Le PB, Brodell RT, Nahar VK. Evaluation of patient attitudes towards the technical experience of synchronous teledermatology in the era of COVID-19. *Arch Dermatol Res*. 2021. 5:1-4. PubMed PMID: 33403572.
15. Kroemer S, Frühauf J, Campbell TM, Massone C, Schwantzer G, Soyer HP, et al. Mobile teledermatology for skin tumour screening: diagnostic accuracy of clinical and dermoscopic image tele-evaluation using cellular phones. *Br J Dermatol*. 2011; 164: 973–9. PubMed PMID: 21219286.
16. Okhovat JP, Beaulieu D, Tsao H, Halpern AC, Michaud DS, Shaykevich S, et al. The first 30 years of the American academy of dermatology skin cancer screening program: 1985–2014. *J Am Acad Dermatol*. 2018; 79: 884–91. PubMed PMID: 30057360.
17. Rustad AM, Lio PA.. Pandemic pressure: teledermatology and health care disparities. *J Patient Exp*. 2021; 8: 2374373521996982. PubMed PMID: 34179385.
18. Conic RZ, Cabrera CI, Khorana AA, Gastman BR. Determination of the impact of melanoma surgical timing on survival using the National Cancer Database. *J Am Acad Dermatol*. 2018; 78 (1): 40–46.e7. PMID: 29054718.
19. American Cancer Society. *Cancer Facts and Figures*. January 8, 2021. Available from: <https://www.cancer.org/content/dam/cancerorg/research/cancer-facts-and-statistics/annual-cancer-facts-and-figures/2020/cancer-facts-and-figures-2020.pdf>.
20. Farr MA, Duvic M, Joshi TP. Teledermatology during COVID-19: an updated review. *American Journal of Clinical Dermatology*. 2021; Apr 9: 1–9. PubMed PMID: 33835345.
21. Perkins S, Cohen JM, Nelson CA, Bunick CG. Teledermatology in the era of COVID-19: experience of an academic department of dermatology. *Journal of the American Academy of Dermatology*. 2020; 83 (1): e43–e44. PubMed PMID: 32305442.
22. Ashique KT, Kaliyadan F. Teledermatology in the wake of COVID-19 scenario: An Indian perspective. *Indian Dermatology Online Journal*. 2020; 11 (3): 301. PubMed PMID: 32695684.
23. Boyers LN, Schultz A, Baceviciene R, Blaney S, Marvi N, Dellavalle RP, et al. Teledermatology as an educational tool for teaching dermatology to residents and medical students. *Telemedicine and e-Health*. 2015; 21 (4): 312–4. PubMed PMID: 25635528.
24. Wanat KA, Newman S, Finney KM, Kovarik CL, Lee I. Teledermatology education: current use of teledermatology in US residency programs. *J Grad Med Educ*. 2016; 8 (2): 286–7. PubMed PMID: 27168912.
25. Jones VA, Clark KA, Puyana C, Tsoukas MM. Rescuing medical education in times of COVID-19. *Clin Dermatol*. 2021; 39(1): 33–4.
26. Tensen E, Van Der Heijden JP, Jaspers MWM, Witkamp L. Two decades of teledermatology: current status and integration in national healthcare systems. *Curr Dermatol Rep*. 2016; 5 (2): 96–104. PubMed PMID: 27182461.
27. Tschandl P, Rinner C, Apalla Z, Argenziano G, Codella N, Halpern A, et al. Human-computer collaboration for skin cancer recognition. *Nature Medicine*. 2020; 26 (8): 1229–34. PubMed PMID: 32572267.

RETINAL ABNORMALITIES IN TRANSGENIC MICE OVEREXPRESSING ABERRANT HUMAN FUS[1-359] GENE

Soldatov VO¹✉, Kukharsky MS², Soldatova MO³, Puchenkova OA¹, Nikitina YuA², Lysikova EA², Kartashkina NL⁴, Deykin AV¹, Pokrovskiy MV¹

¹ Belgorod State National Research University, Belgorod, Russia

² Institute of Physiologically Active Substances, Moscow, Russia

³ Kursk State Medical University, Kursk, Russia

⁴ Sechenov First Moscow State Medical University, Moscow, Russia

Retinal damage is an optional sign in a number of neurodegenerative diseases, including amyotrophic lateral sclerosis (ALS). The aim of this work was to assess the structural and functional state of the retina in a murine model of ALS caused by overexpression of the aberrant FUS protein [1-359]. The retinal examination was carried out on 12 transgenic and 13 wild-type mice of 2.5–3 months of age. The study revealed not statistically significant higher level of ophthalmoscopic violations in FUS[1-359] mice. Moreover, gene expression assay confirmed an increased expression of the inflammatory genes *Vegfa*, *Il1b*, *Il6*, *Icam1*, *Tnfa*. However, despite the detected structural and functional abnormalities, western blot analysis and quantitative PCR did not detect the expression of the protein and mRNA products of the FUS transgene in the retina of FUS[1-359] mice.

Keywords: FUS protein, transgenic mice, ALS, retinopathy, inflammation

Funding: the study was carried out with the financial support of the Russian Foundation for Basic Research within the framework of the scientific project № 19-315-90114.

Author contribution: Soldatov VO — the main idea, design of the experiment, ophthalmoscopy, writing an article, design of primers for gene expression assay; Kukharsky MS — the main idea, design of the experiment, writing an article, western blot analysis; Soldatova MO — RNA isolation, qPCR; Puchenkova OA — retina and spinal cord collection, RNA extraction, qPCR; Nikitina YuA — preparation of animal populations, genotyping, western blot analysis; Lysikova EA — preparation of animal populations, genotyping, western-blot analysis, writing an article; Kartashkina NL — interpretation and scoring of ophthalmoscopic picture; Deykin AV — consultation on the main idea and design of the study; Pokrovskiy MV — consultation on the main idea and design of the study.

Compliance with ethical standards: animal procedures were approved by the local ethics committee of the Belgorod State National Research University (protocol № 5 / 19-25 dated september 25. 2019). All manipulations were carried out in compliance with the requirements of the International Recommendations of European Convention for the Protection of Vertebrate Animals used for Experimental and Other Scientific Purposes (1997).

✉ Correspondence should be addressed: Vladislav O. Soldatov
Pobedy, 85, 308015, Belgorod; pharmsoldatov@gmail.com

Received: 19.08.2021 Accepted: 28.08.2021 Published online: 31.08.2021

DOI: 10.24075/brsmu.2021.043

РЕТИНАЛЬНЫЕ АНОМАЛИИ У ТРАНСГЕННЫХ МЫШЕЙ, СУПЕРЭКСПРЕССИРУЮЩИХ АБЕРРАНТНЫЙ ЧЕЛОВЕЧЕСКИЙ ГЕН FUS[1-359]

В. О. Солдатов¹✉, М. С. Кухарский², М. О. Солдатова³, О. А. Пученкова¹, Ю. А. Никитина², Е. А. Лысикова², Н. Л. Карташкина⁴, А. В. Дейкин¹, М. В. Покровский¹

¹ Белгородский государственный национальный исследовательский университет, Белгород, Россия

² Институт физиологически активных веществ, Москва, Россия

³ Курский государственный медицинский университет, Курск, Россия

⁴ Первый Московский государственный медицинский университет имени И. М. Сеченова, Москва, Россия

Повреждение сетчатки является неклассическим симптомом ряда нейродегенеративных заболеваний, включая боковой амиотрофический склероз (БАС). Целью работы было оценить морфофункциональное состояние сетчатки в мышьиной модели БАС, связанной с суперэкспрессией aberrантного белка FUS[1-359]. Исследование проводили на 12 трансгенных и 13 диких мышах 2,5–3-месячного возраста. Выявлено, что трансгенные мыши демонстрируют выраженную, но не достигающую статистической значимости тенденцию к развитию офтальмоскопических аномалий сетчатки. Кроме того, молекулярно-биологический анализ подтвердил увеличение экспрессии провоспалительных генов *Vegfa*, *Il1b*, *Il6*, *Icam1*, *Tnfa*. При этом, несмотря на обнаруженные структурные и функциональные аномалии, вестерн-блот анализ и количественная ПЦР не выявили экспрессию белкового и мРНК продукта трансгена FUS в сетчатке мутантных мышей.

Ключевые слова: белок FUS, трансгенные мыши, БАС, ретинопатия, воспаление

Финансирование: исследование выполнено при финансовой поддержке РФФИ в рамках научного проекта №19-315-90114.

Вклад авторов: В. О. Солдатов — разработка идеи и дизайна эксперимента, проведение офтальмоскопии, написание статьи, подбор праймеров для оценки экспрессии генов; М. С. Кухарский — разработка идеи и дизайна эксперимента, написание статьи, проведение иммуноблотинга; М. О. Солдатова — выделение РНК, проведение ПЦР в реальном времени; О. А. Пученкова — забор материала для молекулярно-биологических исследований, выделение РНК, проведение ПЦР в реальном времени; Ю. А. Никитина — подготовка популяции животных, генотипирование, написание статьи; Карташкина Н. Л. — описание офтальмоскопической картины, написание статьи; А. В. Дейкин — консультация по основной идеи и дизайну исследования; М. В. Покровский — консультация по основной идеи и дизайну исследования.

Соблюдение этических стандартов: исследование одобрено локальным этическим комитетом Белгородского государственного национального исследовательского университета (протокол № 5/19-25 от 25 сентября 2019 г.), проведено с соблюдением требований Международных рекомендаций Европейской конвенции по защите позвоночных животных, используемых при экспериментальных исследованиях (1997).

✉ Для корреспонденции: Владислав Олегович Солдатов
ул. Победы, д. 85, 308015, г. Белгород; zinkfingers@gmail.com

Статья получена: 19.08.2021 Статья принята к печати: 28.08.2021 Опубликована онлайн: 31.08.2021

DOI: 10.24075/vrgmu.2021.043

The retina is the most accessible for examination part of the nervous system and it is one of the most vulnerable sensory tissues. Such properties make the study of neurodegeneration ophthalmic correlates highly relevant, opening up opportunities for improving the diagnostics and study of neurodegenerative processes. Due to embryonic commonality and similarity of proteomic composition, the retina can serve as a platform for the development of pathological cascades the central nervous system is prone to [1]. In particular, retinal damage was found in amyotrophic lateral sclerosis (ALS) [2, 3], a disease caused by accumulation of insoluble protein aggregates leading to progressive death of motor neurons [4].

Protein inclusions in ALS have a complex composition and can consist of various proteins, such as RNA-binding proteins or the antioxidant enzyme superoxide dismutase 1, as well as neurofilaments or ubiquitin [5]. In 5% of familial cases, ALS is associated with the accumulation of aggregates, the main component of which is the FUS protein. One of the cause for the development of FUS proteinopathy is mutations in the nuclear localization signal (NLS) domain and the leak of the protein from the nucleus into the cytoplasm, where it is prone to form insoluble aggregates [6].

With all this background the aim of this study was to assess the relationship between neuronal expression of the pathological form of the FUS protein and the activation of several pathological pathways in the retina.

METHODS

Animals

Transgenic mice carrying the sequence of the aberrant human *FUS* gene encoding a protein with artificially truncated NLS (*FUS*[1-359]) [7] were used as a model recapitulating *FUS* proteinopathy. The *FUS*[1-359] murine model is characterized by progressive paralysis with onset at the age of 3–4 months accompanied by the development of morphological and molecular signs of neurodegeneration, including neuronal death and neuroinflammation [8].

The study was carried out on 25 CD-1 mice (both sexes), 12 of which were *FUS* hemizygotes, and 13 served as wild-type controls. The mice were kept in conditions of constant access to water and food. Light cycle — 12 h/12 h, illumination — 40–50 lx, temperature — 23 ± 1 °C, humidity — $42 \pm 5\%$. At the age of 80–90 days, mice were sedated (Zolazepam + Tiletamine + Xylazine) for ophthalmoscopy. A brief clinical examination performed before sedation allowed to exclude animals with signs of inflammatory changes in the anterior chamber of the eyeball. Ophthalmoscopic examination was performed after application of 1% atropine sulfate. To perform quantitative objective analysis, the ophthalmologist assessed the fundus picture on a point scale from 0 to 5, where 0 points — no violations, and 5 points — severe abnormalities. Ophthalmoscopy scoring results presented as $M \pm SD$; statistical significance for intergroup differences was challenged using the Kruskall-Wallis test. After ophthalmoscopic examination, the animals were euthanized with an overdose of anesthesia for further collection of biomaterial: totally 24 retinal samples were taken from 6 animals from each group for gene expression assay, and 8 retinas and 4 lumbar spinal cord samples were collected from 4 animals for western blot analysis.

Quantitative PCR

Contralateral retinas from each animal were pulled and incubated for 15 min in ExtractRNA solution (Evrogen; Russia).

After lysis of the sample in the reagent, it was subjected to chloroform extraction. The formed RNA precipitate was washed sequentially with isopropyl alcohol and 70% ethanol. The resulting precipitate was diluted in 20 µL of water, and the concentration of the isolated RNA (~ 200 ng/µL) was measured using an IMPLENNanoPhotometer® spectrophotometer (Implen; Germany). Reverse transcription was performed using the MMLVRTSK021 kit in accordance with the manufacturer's protocol (Evrogen; Russia).

Primers for quantitative PCR were designed with use of Primer-BLAST resource (NCBI) in compliance with the following requirements: 1) melting temperature 59–61°C; 2) one of the primers in a pair should span exon-exon junction; 3) forward and reverse primers should not form auto- and cross dimers; 4) the size of the PCR product should be from 95 to 200 bp; the primers must be specific to the maximum number of gene transcripts.

Quantitative PCR was performed in a BioRad CFX96 amplifier using the SYBR® Green Master Mix intercalating dye (Bio-Rad Laboratories, Inc.; USA) and oligonucleotide primers (Evrogen; Russia) (Table 1). The expression level of genes of interest (GOI) was assessed relative to the housekeeping genes (HKG) Gapdh and Actb. Expression at a specific point was calculated using the formula: Gene expression = $2^{(Ct(HKG) - Ct(GOI))}$.

Western blot

Retinal samples were pulled from two animals belonging to the same group. After separation in the gel, the proteins were transferred by semi-dry electroblotting onto a Hybond-P polyvinylidene fluoride membrane (Cytiva; UK) pretreated with 100% methanol, washed with MilliQ water, and soaked in transfer buffer containing 25 mM Tris, 0.15 mM glycine and 20% methanol. Then the membrane with gel placed between tightly pressed two sheets of soaked 3MM Whatman paper and transferred into a semi-dry blotter (GE Healthcare Amersham; USA) allowing proteins to diffuse to the membrane for 30 min at 50 mA (1.2 mA by 1 cm²). After electroblotting, the membrane was washed in Tris-Tween buffer (TTB; 50 mM Tris-HCl pH 7.4, 150 mM NaCl, 0.1% Tween-20) 3 times for 5 min. The membrane was blocked in a 4% solution of nonfat dry milk in TTB for 1 h at room temperature, then incubated with primary antibodies in the same solution at 4 °C overnight. After incubation with primary antibodies, the membrane was washed in TTB 3 times for 5 min and incubated with secondary antibodies for 1.5 h at room temperature, and then re-washed in TTB 3 times for 5 min. Detection of specific binding of antibodies was performed using ECL Plus reagents (Cytiva; UK) according to the manufacturer's instructions. X-ray film was used to detect chemiluminescence. Semi-quantitative assay of the westerns was performed using densitometric analysis using a BioSpectrum AC Chemi HR410 instrument and Vision Works LS software (UVP; Great Britain). When carrying out densitometric analysis, the specific signal from the analyzed protein was normalized in relation to the signal from β-actin (after the membrane reincubation with the corresponding antibodies) for each lane separately.

RESULTS

FUS[1-359] transgenic mice show mild ophthalmoscopic abnormalities.

In both groups, some of the animals were found to have vascular anomalies and edema of the optic disc, which is

Table 1. Primers, used for gene expression assay

Target gene	Forward primer sequence	Reverse primer sequence	Product length, b.p.
<i>Actb</i>	5'-CGC AGC CAC TGT CGA GTC-3'	5'-GCC CAC GAT GGA GGG GAA TA-3'	195
<i>Gapdh</i>	5'-AGG AGA GTG TTT CCT CGT CC-3'	5'-TGA GGT CAA TGA AGG GGT CG-3'	145
<i>Icam1</i>	5'-CAT GCC GCA CAG AAC TGG AT-3'	5'-GGT GTC GAG CTT TGG GAT GG-3'	116
<i>Il6</i>	5'-AAA GCC AGA GTC CTT CAG AGA GA-3'	5'-TGG AAA TTG GGG TAG GAA GGA CT-3'	100
<i>Il1b</i>	5'-GCC ACC TTT TGA CAG TGA TGAG-3'	5'-GAC AGC CCA GGT CAA AGG TT-3'	95
<i>Tnfa</i>	5'-ACT GAA CTT CGG GGT GAT CG-3'	5'-ACT TGG TGG TTT GTG AGT GTG-3'	105
<i>Vegfa</i>	5'-GCA CTG GAC CCT GGC TTT AC-3'	5'-CCA CCA GGG TCT CAA TCG GA-3'	152
<i>Bdnf</i>	5'-CCT GCA TCT GTT GGG GAG AC-3'	5'-GCC TTG TCC GTG GAC GTT T-3'	175
<i>Atg7</i>	5'-GCG GCG ACA GCA TTA GGA TT-3'	5'-ATG GCA GGA AAG CAG TGT GG-3'	118
<i>Atg5</i>	5'-TCA GCT CTT CCT TGG AAC ATC AC-3'	5'-AAG TGA GCC TCA ACC GCA TC-3'	95
<i>Bax</i>	5'-CGA GAG GTC TTC CGG GT-3'	5'-TCT TGG ATC CAG ACA AGC AGC-3'	197
<i>Bcl2</i>	5'-CTG GGA TGC CTT TGT GGA ACT-3'	5'-GGC AGG TTT GTC GAC CTC A-3'	155

routine finding for CD-1 mice [9, 10]. Statistical analysis did not reveal significant differences between transgenic and wild-type animals; however, FUS[1-359] mice showed a tendency towards more pronounced violations in all studied parameters (Fig. 1).

Truncated FUS is not expressed in the retina

Western blot analysis did not reveal the presence of a FUS-immunopositive signal in the retinal tissues of transgenic mice (Fig. 2). Furthermore, quantitative PCR also did not detect *FUS* at the mRNA level. Thus, expression assay did not confirm retinal expression of the transgene at either the transcriptome or protein levels.

Transgenic FUS[1-359] mice are characterized by increased expression of proinflammatory genes in the retina

Gene expression assay found increased levels of proinflammatory factors *Vegfa*, *Icam1*, *Il6*, *Il1b*, and *Tnfa* in the retina of transgenic FUS[1-359] mice. No pronounced changes in the expression of genes related to neuroplasticity (*Bdnf*), autophagy (*Atg7*, *Atg5*), and regulation of apoptosis (*Bax*, *Bcl2*) were found (Fig. 3).

DISCUSSION

Retinal involvement has been found in various neurodegenerative diseases, including Alzheimer's disease [11], Parkinson's disease [12, 13], and frontotemporal dementia [14]. Not surprisingly, mild ophthalmic abnormalities are also a frequent non-motor symptom of ALS [15]. Among typical clinical findings, color vision impairment [16], as well as thinning of the retina [17] and macula [18–20], are described.

In our study, we did not find significant differences in the severity of ophthalmoscopic changes in the studied animals. Nevertheless, for all studied parameters, an obvious tendency towards more pronounced disorders was revealed in transgenic FUS[1-359] mice. Particularly bright differences were found in relation to the retinal vasculature, which is consistent with the results of the previous report [21].

Since transgene is not expressed in the retina, we aimed to elucidate the mechanisms of retinal degeneration by studying the activity of the most common molecular pathways of neurodegenerative damage to motor neurons. In this regard, as the primary targets we focused on genes related to inflammation, apoptosis, and autophagy. Although pathways of autophagy [22–24] and apoptosis [25] are deeply involved in

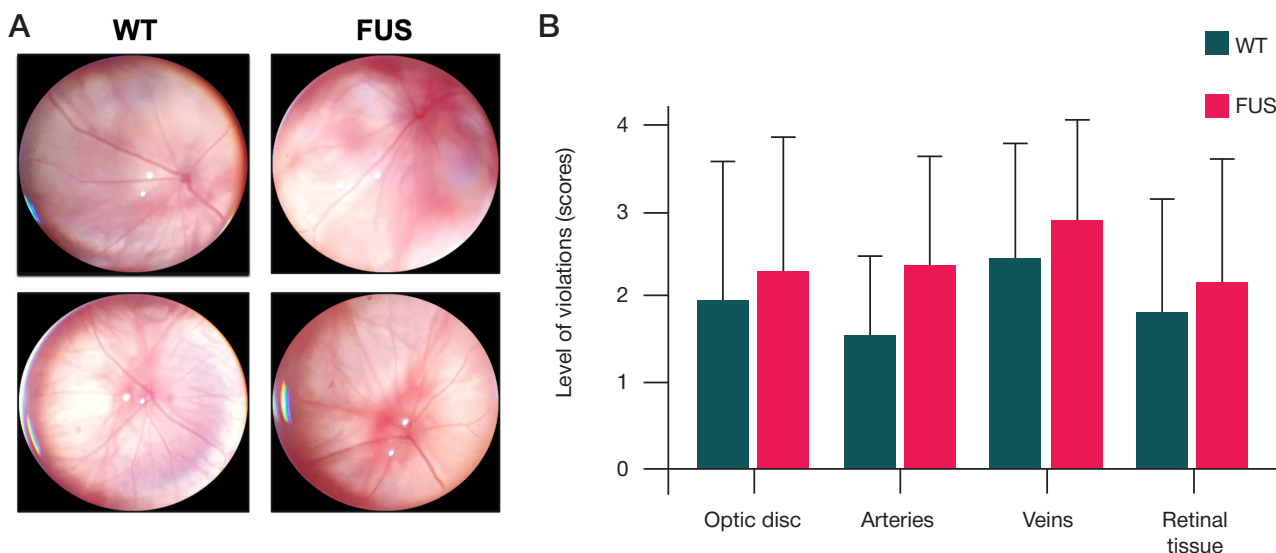


Fig. 1. Results of ophthalmoscopic examination. **A.** Representative ophthalmoscopic pictures of experimental animals. **B.** Results of scale scoring of ophthalmoscopic picture

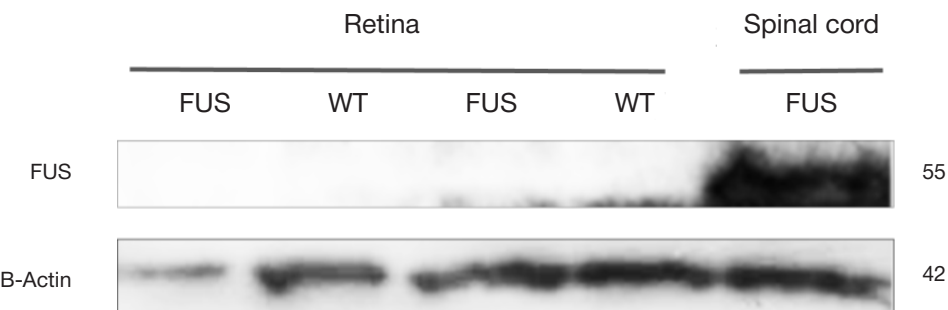


Fig. 2. Absence of truncated FUS protein in retinal tissues of transgenic mice

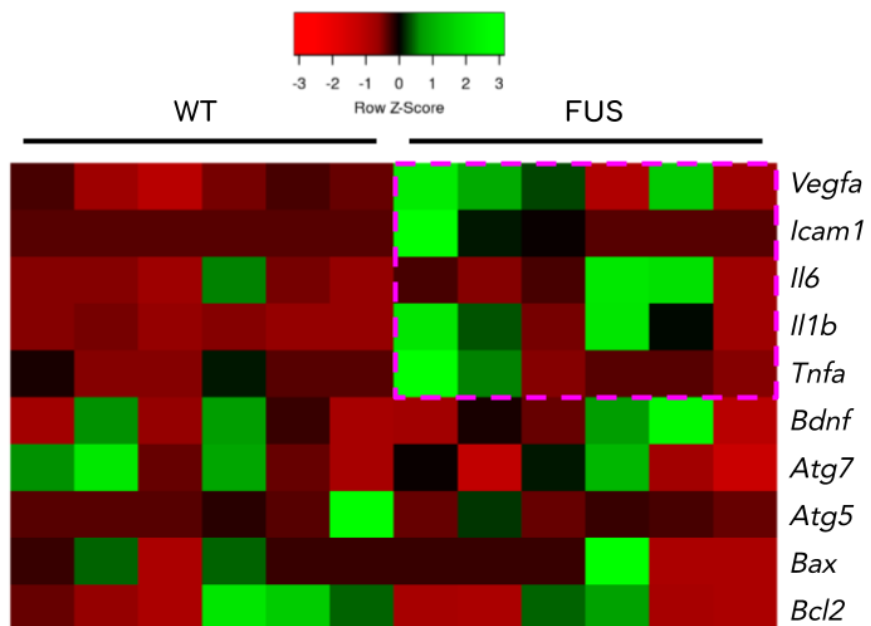


Fig. 3. Normalized heatmap for relative expression of genes related to inflammation (*Vegfa*, *Icam1*, *Il6*, *Il1b*, and *Tnfa*), neuroplasticity (*Bdnf*), autophagy (*Atg7*, *Atg5*), and regulation of apoptosis (*Bax*, *Bcl2*)

ALS as confirmed by various *in vivo* and *in vitro* studies, we did not find changed expression of genes *Atg7*, *Atg5*, *Bax*, *Bcl2*. However, the expression of the *Vegfa*, *Icam1*, *Il6*, *Il1b*, and *Tnfa* genes was altered markedly, indicating the role of inflammation in the mechanisms of retinal degeneration in FUS[1-359] mice. These findings are consistent with previous results regarding the dramatic role of inflammatory activation (and its pharmacological suppression) in the FUS[1-359] mouse model [26, 27].

Thus, despite truncated FUS protein is not expressed in retinal tissue, transgenic animals show signs of retinal abnormalities. Potential mechanisms of damage to the eye

fundus may include activation of microglia [28], vascular regression [20], and neuro-phthalamic interactions through the glymphatic system [29].

CONCLUSIONS

The study has demonstrated that transgenic FUS[1-359] mice are prone to the development of structural and functional abnormalities of the eye fundus, despite the absence of transgene expression in the retina. Further detailing of identified violations can highlight the most significant pathways of FUS-associated retinopathy.

References

- Yap TE, Balendra SI, Almonte MT, Cordeiro MF. Retinal correlates of neurological disorders. *Ther Adv Chronic Dis.* 2019; 10: 2040622319882205. doi:10.1177/2040622319882205
- Cerveró A, Casado A, Riancho J. Retinal changes in amyotrophic lateral sclerosis: looking at the disease through a new window. *J Neurol.* 2021; 268 (6): 2083–9. DOI: 10.1007/s00415-019-09654-w.
- Rojas P, de Hoz R, Ramírez AI, et al. Changes in Retinal OCT and their correlations with neurological disability in early ALS Patients, a Follow-Up Study. *Brain Sci.* 2019; 9 (12): 337. DOI: 10.3390/brainsci9120337.
- Zarei S, Carr K, Reiley L, Diaz K, Guerra O, Altamirano PF, et al. A comprehensive review of amyotrophic lateral sclerosis. *Surg Neurol Int.* 2015; 16 (6): 171. DOI: 10.4103/2152-7806.169561.
- Batra G, Jain M, Singh RS, Sharma AR, Singh A, Prakash A, et al. Novel therapeutic targets for amyotrophic lateral sclerosis. *Indian J Pharmacol.* 2019; 51 (6): 418–25. DOI: 10.4103/ijp.IJP_823_19.
- Zou ZY, Che CH, Feng SY, Fang XY, Huang HP, Liu CY. Novel FUS mutation Y526F causing rapidly progressive familial amyotrophic lateral sclerosis. *Amyotroph Lateral Scler Frontotemporal Degener.* 2021; 22 (1–2): 73–79. DOI: 10.1080/21678421.2020.1797815.
- Shelkovnikova TA, Peters OM, Deykin AV, et al. Fused in sarcoma (FUS) protein lacking nuclear localization signal (NLS) and major RNA binding motifs triggers proteinopathy and severe motor

- phenotype in transgenic mice. *J Biol Chem.* 2013; 288 (35): 25266–274. DOI: 10.1074/jbc.M113.492017.
8. Funikov SY, Rezvykh AP, Mazin PV, Morozov AV, Maltsev AV, Chicheva MM, et al. FUS(1-359) transgenic mice as a model of ALS: pathophysiological and molecular aspects of the proteinopathy. *Neurogenetics.* 2018; 19 (3): 189–204. DOI: 10.1007/s10048-018-0553-9.
 9. Mukaratiwa S, Petterino C, Naylor SW, Bradley A. Incidences and Range of Spontaneous Lesions in the Eye of Crl:CD-1(ICR) BR Mice Used in Toxicity Studies. *Toxicol Pathol.* 2015; 43 (4): 530–5. DOI: 10.1177/0192623314548767.
 10. De Groef L, Dekeyster E, Geeraerts E, Lefevere E, Stalmans I, Salinas-Navarro M, et al. Differential visual system organization and susceptibility to experimental models of optic neuropathies in three commonly used mouse strains. *Exp Eye Res.* 2016; 145: 235–47. DOI: 10.1016/j.exer.2016.01.006.
 11. Hart NJ, Koronyo Y, Black KL, Koronyo-Hamaoui M. Ocular indicators of Alzheimer's: exploring disease in the retina. *Acta Neuropathol.* 2016; 132 (6): 767–87. DOI: 10.1007/s00401-016-1613-6.
 12. Mohana Devi S, Mahalaxmi I, Aswathy NP, Dhivya V, Balachandar V. Does retina play a role in Parkinson's Disease? *Acta Neurol Belg.* 2020; 120 (2): 257–65. DOI: 10.1007/s13760-020-01274-w.
 13. Huang L, Zhang D, Ji J, Wang Y, Zhang R. Central retina changes in Parkinson's disease: a systematic review and meta-analysis. *J Neurol.* 2020; 10. DOI: 10.1007/s00415-020-10304-9.
 14. Harrison IF, Whitaker R, Bertelli PM, O'Callaghan JM, Csincsik L, Bocchetta M, et al. Optic nerve thinning and neurosensory retinal degeneration in the rTg4510 mouse model of frontotemporal dementia. *Acta Neuropathol Commun.* 2019; 7 (1): 4. DOI: 10.1186/s40478-018-0654-6.
 15. Soldatov VO, Kukharsky MS, Belykh AE, Sobolev AM, Deykin AV. Retinal Damage in Amyotrophic Lateral Sclerosis: Underlying Mechanisms. *Eye Brain.* 2021; 13: 131–46. DOI: 10.2147/EB.S299423.
 16. Boven L, Jiang QL, Moss HE. Diffuse colour discrimination as marker of afferent visual system dysfunction in amyotrophic lateral sclerosis. *Neuroophthalmology.* 2017; 41 (6): 310–4. DOI: 10.1080/01658107.2017.1326153.
 17. Rohani M, Meysamie A, Zamani B, Sowlat MM, Akhouni FH. Reduced retinal nerve fiber layer (RNFL) thickness in ALS patients: a window to disease progression. *J Neurol.* 2018; 265 (7): 1557–62. DOI: 10.1007/s00415-018-8863-2.
 18. Fawzi AA, Simonett JM, Purta P, et al. Clinicopathologic report of ocular involvement in ALS patients with C9orf72 mutation. *Amyotroph Lateral Scler Frontotemporal Degener.* 2014; 15 (7–8): 569–80. DOI: 10.3109/21678421.2014.951941.
 19. Ringelstein M, Albrecht P, Sudmeyer M, et al. Subtle retinal pathology in amyotrophic lateral sclerosis. *Ann Clin Transl Neurol.* 2014; 1 (4): 290–7. DOI: 10.1002/acn3.46.
 20. Rojas P, Ramírez AI, Fernández-Albarral JA, López-Cuenca I, Salobrar-García E, Cadena M, et al. Amyotrophic Lateral Sclerosis: A Neurodegenerative Motor Neuron Disease With Ocular Involvement. *Front Neurosci.* 2020; 14: 566858. DOI: 10.3389/fnins.2020.566858.
 21. Crivello M, Hogg MC, Jirström E, Halang L, Woods I, Rayner M, et al. Vascular regression precedes motor neuron loss in the FUS (1-359) ALS mouse model. *Dis Model Mech.* 2019; 12 (8): dmm040238. DOI: 10.1242/dmm.040238.
 22. Rudnick ND, Griffey CJ, Guarneri P, Gerbino V, Wang X, Piersant JA, et al. Distinct roles for motor neuron autophagy early and late in the SOD1(G93A) mouse model of ALS. *Proceedings of the National Academy of Sciences of the United States of America.* 2017; 114: E8294–E8303.
 23. Evans CS, Holzbaur ELF. Autophagy and mitophagy in ALS. *Neurobiol Dis.* 2019; 122: 35–40. DOI: 10.1016/j.nbd.2018.07.005.
 24. Strohm L, Behrends C. Glia-specific autophagy dysfunction in ALS. *Semin Cell Dev Biol.* 2020; 99: 172–82. DOI: 10.1016/j.semcdb.2019.05.024.
 25. Ghavami S, Shojaei S, Yeganeh B, Ande SR, Jangamreddy JR, Mehrpour M, et al. Autophagy and apoptosis dysfunction in neurodegenerative disorders. *Prog Neurobiol.* 2014; 112: 24–49. DOI: 10.1016/j.pneurobio.2013.10.004.
 26. de Munter JPJM, Shafarevich I, Liundup A, Pavlov D, Wolters EC, Gorlova A, et al. Neuro-Cells therapy improves motor outcomes and suppresses inflammation during experimental syndrome of amyotrophic lateral sclerosis in mice. *CNS Neurosci Ther.* 2020; 26 (5): 504–17. DOI: 10.1111/cns.13280.
 27. Ninkina N. Stem cell therapy and FUS[1-359]-transgenic mice: A recent study highlighting a promising ALS model and a promising therapy. *CNS Neurosci Ther.* 2020; 26 (5): 502–3. DOI: 10.1111/cns.13302
 28. Ramirez AI, de Hoz R, Salobrar-Garcia E, Salazar JJ, Rojas B, Ajoy D, et al. The Role of Microglia in Retinal Neurodegeneration: Alzheimer's Disease, Parkinson, and Glaucoma. *Front Aging Neurosci.* 2017; 9: 214. DOI: 10.3389/fnagi.2017.00214.
 29. Dolzhikov AA, Bobyntsev II, Belykh AE, Shevchenko OA, Pobeda AS, Dolzhikova IN, et al. Pathogenesis of neurodegenerative pathology and new concepts of transport and metabolic systems of the brain and eye. *Kursk Scientific and Practical Bulletin "Man and His Health".* 2020; (1): 43–57. DOI: 10.21626/vestnik/2020-1/06.

Литература

1. Yap TE, Balendra SI, Almonte MT, Cordeiro MF. Retinal correlates of neurological disorders. *Ther Adv Chronic Dis.* 2019; 10: 2040622319882205. doi:10.1177/2040622319882205
2. Cerveró A, Casado A, Riancho J. Retinal changes in amyotrophic lateral sclerosis: looking at the disease through a new window. *J Neurol.* 2021; 268 (6): 2083–9. DOI: 10.1007/s00415-019-09654-w.
3. Rojas P, de Hoz R, Ramírez AI, et al. Changes in Retinal OCT and their correlations with neurological disability in early ALS Patients, a Follow-Up Study. *Brain Sci.* 2019; 9 (12): 337. DOI: 10.3390/brainsci9120337.
4. Zarei S, Carr K, Reiley L, Diaz K, Guerra O, Altamirano PF, et al. A comprehensive review of amyotrophic lateral sclerosis. *Surg Neurol Int.* 2015; 16 (6): 171. DOI: 10.4103/2152-7806.169561.
5. Batra G, Jain M, Singh RS, Sharma AR, Singh A, Prakash A, et al. Novel therapeutic targets for amyotrophic lateral sclerosis. *Indian J Pharmacol.* 2019; 51 (6): 418–25. DOI: 10.4103/ijp.IJP_823_19.
6. Zou ZY, Che CH, Feng SY, Fang XY, Huang HP, Liu CY. Novel FUS mutation Y526F causing rapidly progressive familial amyotrophic lateral sclerosis. *Amyotroph Lateral Scler Frontotemporal Degener.* 2021; 22 (1–2): 73–79. DOI: 10.1080/21678421.2020.1797815.
7. Shelkovnikova TA, Peters OM, Deykin AV, et al. Fused in sarcoma (FUS) protein lacking nuclear localization signal (NLS) and major RNA binding motifs triggers proteinopathy and severe motor phenotype in transgenic mice. *J Biol Chem.* 2013; 288 (35): 25266–274. DOI: 10.1074/jbc.M113.492017.
8. Funikov SY, Rezvykh AP, Mazin PV, Morozov AV, Maltsev AV, Chicheva MM, et al. FUS(1-359) transgenic mice as a model of ALS: pathophysiological and molecular aspects of the proteinopathy. *Neurogenetics.* 2018; 19 (3): 189–204. DOI: 10.1007/s10048-018-0553-9.
9. Mukaratiwa S, Petterino C, Naylor SW, Bradley A. Incidences and Range of Spontaneous Lesions in the Eye of Crl:CD-1(ICR) BR Mice Used in Toxicity Studies. *Toxicol Pathol.* 2015; 43 (4): 530–5. DOI: 10.1177/0192623314548767.
10. De Groef L, Dekeyster E, Geeraerts E, Lefevere E, Stalmans I, Salinas-Navarro M, et al. Differential visual system organization and susceptibility to experimental models of optic neuropathies in three commonly used mouse strains. *Exp Eye Res.* 2016; 145: 235–47. DOI: 10.1016/j.exer.2016.01.006.
11. Hart NJ, Koronyo Y, Black KL, Koronyo-Hamaoui M. Ocular indicators of Alzheimer's: exploring disease in the retina. *Acta Neuropathol.* 2016; 132 (6): 767–87. DOI: 10.1007/s00401-016-1613-6.

12. Mohana Devi S, Mahalaxmi I, Aswathy NP, Dhivya V, Balachandar V. Does retina play a role in Parkinson's Disease? *Acta Neurol Belg.* 2020; 120 (2): 257–65. DOI: 10.1007/s13760-020-01274-w.
13. Huang L, Zhang D, Ji J, Wang Y, Zhang R. Central retina changes in Parkinson's disease: a systematic review and meta-analysis. *J Neurol.* 2020; 10. DOI: 10.1007/s00415-020-10304-9.
14. Harrison IF, Whitaker R, Bertelli PM, O'Callaghan JM, Csincsik L, Bocchetta M, et al. Optic nerve thinning and neurosensory retinal degeneration in the rTg4510 mouse model of frontotemporal dementia. *Acta Neuropathol Commun.* 2019; 7 (1): 4. DOI: 10.1186/s40478-018-0654-6.
15. Soldatov VO, Kukharsky MS, Belykh AE, Sobolev AM, Deykin AV. Retinal Damage in Amyotrophic Lateral Sclerosis: Underlying Mechanisms. *Eye Brain.* 2021; 13: 131–46. DOI: 10.2147/EB.S299423.
16. Boven L, Jiang QL, Moss HE. Diffuse colour discrimination as marker of afferent visual system dysfunction in amyotrophic lateral sclerosis. *Neuroophthalmology.* 2017; 41 (6): 310–4. DOI: 10.1080/01658107.2017.1326153.
17. Rohani M, Meysamie A, Zamani B, Sowlat MM, Akhoundi FH. Reduced retinal nerve fiber layer (RNFL) thickness in ALS patients: a window to disease progression. *J Neurol.* 2018; 265 (7): 1557–62. DOI: 10.1007/s00415-018-8863-2.
18. Fawzi AA, Simonett JM, Purta P, et al. Clinicopathologic report of ocular involvement in ALS patients with C9orf72 mutation. *Amyotroph Lateral Scler Frontotemporal Degener.* 2014; 15 (7–8): 569–80. DOI: 10.3109/21678421.2014.951941.
19. Ringelstein M, Albrecht P, Sudmeyer M, et al. Subtle retinal pathology in amyotrophic lateral sclerosis. *Ann Clin Transl Neurol.* 2014; 1 (4): 290–7. DOI: 10.1002/acn3.46.
20. Rojas P, Ramírez AI, Fernández-Albarral JA, López-Cuenca I, Salobrar-García E, Cadena M, et al. Amyotrophic Lateral Sclerosis: A Neurodegenerative Motor Neuron Disease With Ocular Involvement. *Front Neurosci.* 2020; 14: 566858. DOI: 10.3389/fnins.2020.566858.
21. Crivello M, Hogg MC, Jirström E, Halang L, Woods I, Rayner M, et al. Vascular regression precedes motor neuron loss in the FUS (1-359) ALS mouse model. *Dis Model Mech.* 2019; 12 (8): dmm040238. DOI: 10.1242/dmm.040238.
22. Rudnick ND, Griffey CJ, Guarnieri P, Gerbino V, Wang X, Piersant JA, et al. Distinct roles for motor neuron autophagy early and late in the SOD1(G93A) mouse model of ALS. *Proceedings of the National Academy of Sciences of the United States of America.* 2017; 114: E8294–E8303.
23. Evans CS, Holzbaur ELF. Autophagy and mitophagy in ALS. *Neurobiol Dis.* 2019; 122: 35–40. DOI: 10.1016/j.nbd.2018.07.005.
24. Strohm L, Behrends C. Glia-specific autophagy dysfunction in ALS. *Semin Cell Dev Biol.* 2020; 99: 172–82. DOI: 10.1016/j.semcd.2019.05.024.
25. Ghavami S, Shojaei S, Yeganeh B, Ande SR, Jangamreddy JR, Mehrpour M, et al. Autophagy and apoptosis dysfunction in neurodegenerative disorders. *Prog Neurobiol.* 2014; 112: 24–49. DOI: 10.1016/j.pneurobio.2013.10.004.
26. de Munter JPJM, Shafarevich I, Liundup A, Pavlov D, Wolters EC, Gorlova A, et al. Neuro-Cells therapy improves motor outcomes and suppresses inflammation during experimental syndrome of amyotrophic lateral sclerosis in mice. *CNS Neurosci Ther.* 2020; 26 (5): 504–17. DOI: 10.1111/cns.13280.
27. Ninkina N. Stem cell therapy and FUS[1-359]-transgenic mice: A recent study highlighting a promising ALS model and a promising therapy. *CNS Neurosci Ther.* 2020; 26 (5): 502–3. DOI: 10.1111/cns.13302.
28. Ramirez AI, de Hoz R, Salobrar-Garcia E, Salazar JJ, Rojas B, Ajoy D, et al. The Role of Microglia in Retinal Neurodegeneration: Alzheimer's Disease, Parkinson, and Glaucoma. *Front Aging Neurosci.* 2017; 9: 214. DOI: 10.3389/fnagi.2017.00214.
29. Dolzhikov AA, Bobyntsev II, Belykh AE, Shevchenko OA, Pobeda AS, Dolzhikova IN, et al. Pathogenesis of neurodegenerative pathology and new concepts of transport and metabolic systems of the brain and eye. *Kursk Scientific and Practical Bulletin "Man and His Health".* 2020; (1): 43–57. DOI: 10.21626/vestnik/2020-1/06.

EVALUATION OF SARS-COV-2 VIABILITY ON EXPERIMENTAL SURFACES OVER TIMENikiforova MA¹✉, Siniavin AE^{1,2}, Shidlovskaya EV¹, Kuznetsova NA¹, Gushchin VA^{1,3}¹ Gamaleya National Research Center for Epidemiology and Microbiology, Moscow, Russia² Shemyakin-Ovchinnikov Institute of Bioorganic Chemistry, Moscow, Russia³ Lomonosov Moscow State University, Moscow, Russia

Infected SARS-CoV-2 virus occurs not only through contact with an infected person, but also through surfaces with which the illness has contacted. The problem of preserving an infectious virus over time capable of infecting remains actual. We evaluated the SARS-CoV-2 viability preservation on different model surfaces over time. Ceramic tiles, metal (aluminum foil), wood (chipboard), plastic and cloth (towel) were used as model materials. Assessment of the presence of SARS-CoV-2 RNA was carried out by quantitative RT-PCR. Viable virus was determined by tissue culture assay on 293T/ACE2 cells. It was found that the SARS-CoV-2 RNA was detected on all studied surfaces for 360 minutes, but a significant decrease RNA by 1 log₁₀ copies/ml was detected after contact of the virus with cloth (towel). While the viability of the virus was completely lost after 120 minutes. Type of experimental surface significantly affects viability preservation.

Keywords: coronavirus, SARS-CoV-2, viability, surface, PCR

Funding: this research was funded by the grant #056 - 00119 - 21-00 provided by the Ministry of Health of the Russian Federation, Russia.

Acknowledgments: the authors are grateful to Dr. I.V. Korobko for the general idea and discussion of the study design.

Author contribution: Nikiforova MA — experiment planning, working with the virus and determining SARS-CoV-2 viability, data analyzing, writing-original draft preparation; Siniavin AE — working with the virus and determining SARS-CoV-2 viability, data analysing, writing-original draft preparation; Shidlovskaya EV — PCR-analysis, data processing, writing-original draft preparation; Kuznetsova NA — PCR-analysis; Gushchin VA — experiment planning, writing-original draft preparation.

✉ **Correspondence should be addressed:** Maria A. Nikiforova
Gamaleya, 18, Moscow, 123098; marianikiforova@inbox.ru

Received: 25.06.2021 **Accepted:** 09.07.2021 **Published online:** 13.07.2021

DOI: 10.24075/brsmu.2021.033

ОЦЕНКА ЖИЗНЕСПОСОБНОСТИ SARS-COV-2 НА ЭКСПЕРИМЕНТАЛЬНЫХ ПОВЕРХНОСТЯХ ВО ВРЕМЕНИМ. А. Никифорова¹✉, А. Э. Синявин^{1,2}, Е. В. Шидловская¹, Н. А. Кузнецова¹, В. А. Гущин^{1,3}¹ Научный исследовательский центр эпидемиологии и микробиологии имени Н. Ф. Гамалеи, Москва, Россия² Институт биоорганической химии имени М. М. Шемякина и Ю. А. Овчинникова, Москва, Россия³ Московский государственный университет имени М. В. Ломоносова, Москва, Россия

Зарождение вирусом SARS-CoV-2 происходит не только при непосредственном контакте с инфицированным человеком, но и через поверхности, с которыми соприкасался больной. Вопрос сохранения инфекционного вируса, способного заразить спустя время, остается открытым. Целью исследования было изучить жизнеспособность SARS-CoV-2 на различных модельных поверхностях с течением времени. В качестве модельных материалов были использованы керамическая плитка, металл (алюминиевая фольга), дерево (ДСП), пластик и ткань (полотенце). В ходе исследования проводили оценку наличия РНК SARS-CoV-2 методом количественной RT-ПЦР. Жизнеспособность вируса определяли на клеточной линии 293T/ACE2. Показано, что РНК SARS-CoV-2 продолжала детектироваться спустя 360 мин, но значительное снижение РНК на 1 log₁₀ копий/мл обнаружено после контакта вируса с тканью (полотенцем). Жизнеспособный вирус практически полностью отсутствовал через 120 мин. На жизнеспособность вируса значительно влияет тип экспериментальной поверхности.

Ключевые слова: коронавирус, SARS-CoV-2, жизнеспособность, поверхность, ПЦР

Финансирование: данное исследование было финансировано Министерством здравоохранения РФ в рамках государственного задания #056-00119-21-00

Благодарности: авторы выражают благодарность И. В. Коробко за идею и обсуждение дизайна исследования.

Вклад авторов: М. А. Никифорова — планирование эксперимента, работа с вирусом и определение его жизнеспособности, анализ данных, написание текста; А. Э. Синявин — работа с вирусом и определение его жизнеспособности, анализ данных, написание текста; Е. В. Шидловская — ПЦР-анализ, обработка данных, написание текста; Н. А. Кузнецова — ПЦР-анализ; В. А. Гущин — планирование эксперимента, написание текста.

✉ **Для корреспонденции:** Мария Андреевна Никифорова
ул. Гамалея, д. 18, г. Москва, 123098; marianikiforova@inbox.ru

Статья получена: 25.06.2021 **Статья принята к печати:** 09.07.2021 **Опубликована онлайн:** 13.07.2021

DOI: 10.24075/vrgmu.2021.033

Environmental surfaces are suspected to be contaminated with the SARS-CoV-2 and are likely sources of COVID-19 transmission [1]. The World Health Organization (WHO) has found that there is still not enough scientific evidence of the viability of SARS-CoV-2 on inert surfaces. Scientific reports on the viability of SARS-CoV-2 report that the virus can persist differently according to the surface, from hours to days. For example, the SARS-CoV-2 is stable on glass, stainless steel, cardboard, and copper with durations detected up to 84, 72, 24, and 4 h, respectively [2].

However, the fact that the virus is present on the surface does not mean that the surface itself is dangerous and can

become a source of infection [3, 4]. At the same time, there is data showing that SARS-CoV-2 is transmitted between people by touching surfaces that have recently been in contact with COVID-19 patients (coughing or sneezing), and then directly touching the mouth, nose or eyes [5, 6].

Other studies show that after a 3-hour incubation the infectious virus is not detected on the paper for printer and napkins or on treated wood and cloth in one day. In contrast, SARS-CoV-2 was more stable on smooth surfaces. Thus 39 non-infectious samples were positive, which indicates that non-infectious viruses could still be detected [7].

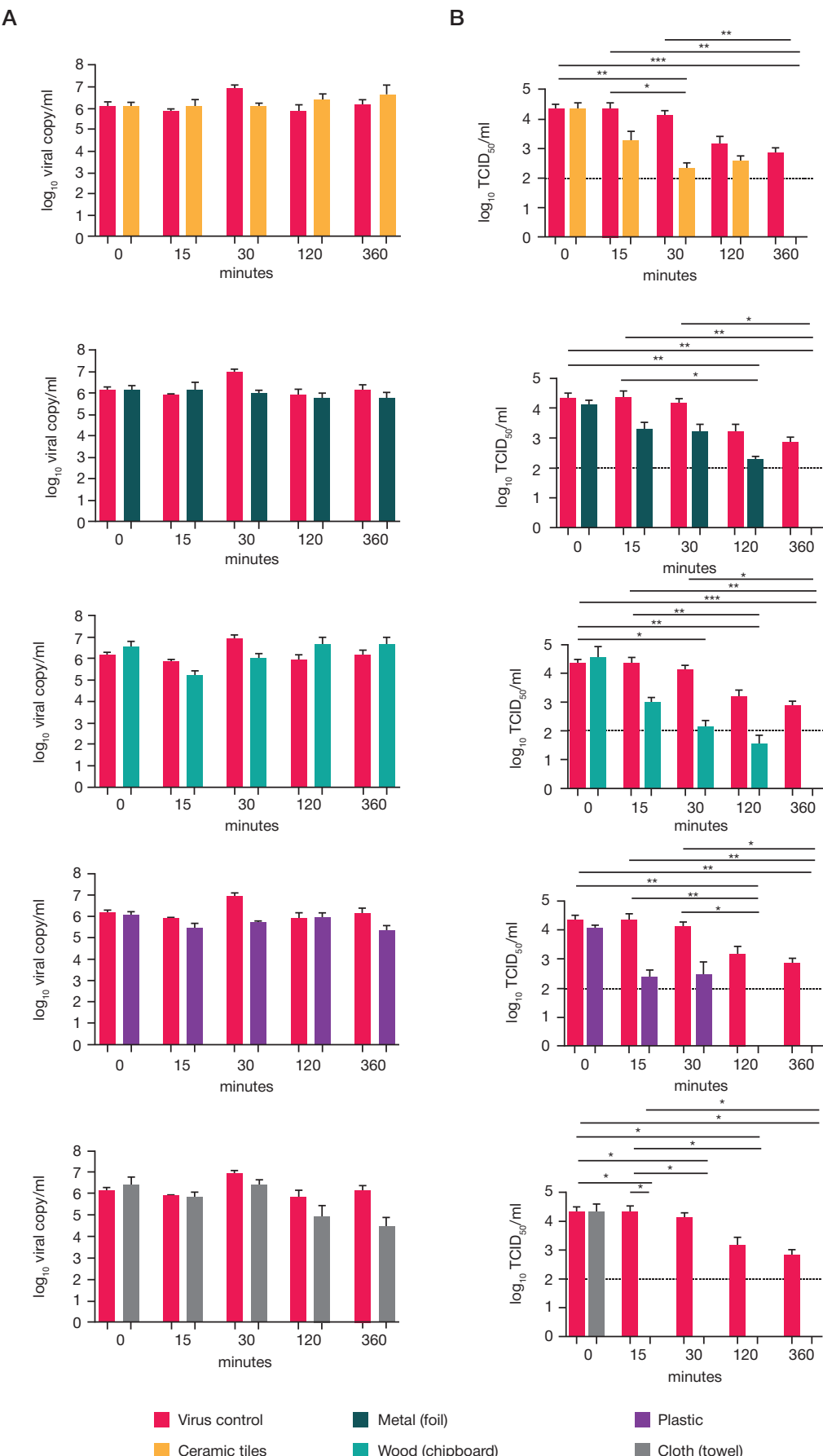


Fig. 1. Stability of SARS-CoV-2 on model surfaces under different conditions. Various experimental surfaces were inoculated with $0.4 \times 10^5 \text{ TCID}_{50}/\text{ml}$ SARS-CoV-2 and incubated at room temperature. At indicating time points the virus were eluted and residual virus was detected by (A) qRT-PCR or (B) viable virus titer was determined by tissue culture assay on 293T/ACE2 cells.

Therefore, our study is paid to the types of surfaces that are most common around us and can pose a risk in terms of transmission of the SARS-CoV-2. We also compare the viability of the virus on different surfaces over time using quantitative RT-PCR and cell culture.

METHODS

Modeling of the SARS-CoV-2 in time viability preservation upon contact with five model materials was carried out in laboratory controlled experimental conditions, steady relative humidity (55–60%) and temperature (22–24°C). The most common materials including ceramic tile, metal (aluminum foil), wood (chipboard), plastic, and cloth (towel) had been used. SARS-CoV-2 strain PMVL-3 (GISaid: EPI_ISL_470897) was isolated from naso/oropharyngeal swab and propagated on Vero E6 cells (ATCC CRL-1586). A 15 µl of viral culture the SARS-CoV-2 (containing 0.4×10^5 TCID₅₀/ml) was pipetted on a surface (~ 1.5–2 cm²) of each material in quintuplicate. Groups of sample material and virus control were incubated for 0 min, 15 min and 30 min (wet surface) or 120 min and 360 min (dried at room temperature). After virus exposure, the virus was eluted from the experimental surface with 200 µL of PBS.

Assessment of the presence of SARS-CoV-2 RNA was carried out by quantitative RT-PCR. Viable virus was determined by tissue culture assay on 293T/ACE2 cells and virus titer was calculated using the Reed and Muench method. The data was processed in the GraphPad Prism 7 software and analyzed using the ANOVA Kruskal-Wallis test. Differences were considered statistically significant at $p < 0.05$.

RESULTS

According to the results of the experiments, it was found that SARS-CoV-2 RNA is detected on all experimental surfaces. Significant reduction of $0.5 \log_{10}$ copies/ml SARS-CoV-2 RNA was observed upon contact of the virus with wood (chipboard) for 15 min, as well as on $1 \log_{10}$ copies/ml SARS-CoV-2 RNA on contact with metal and plastic, after 15 min and 30 min respectively. However, in all eluates from experimental materials at both 120- and 360-minutes exposure were detected a high level of SARS-CoV-2 RNA (Fig. 1A). A significant reduction by $1 \log_{10}$ copies/ml of SARS-CoV-2 was noted after exposure for 6 h on a cloth (towel) sample. But, in general, the amount of SARS-CoV-2 RNA was stably high in all kinds of surface and did not differ from virus control (sample not in contact with the material).

Determination of the infectivity of SARS-CoV-2 after contact with model materials on 293T/ACE2 cells showed a sharp decreased viability of SARS-CoV-2 after 120 min (Fig. 1B). The

virus titer gradually decreased depending on the material in the following order: ceramic tile → metal → wood (chipboard) → plastic → cloth (towel). After 120 min exposure of virus on materials such as plastic and a cloth (towel), the infectious virus was not detected while SARS-CoV-2 RNA was still there.

During the assessment of the infectivity of the virus upon contact with model materials it was shown that SARS-CoV-2 RNA is detected on all experimental surfaces, regardless of the conditions and time of exposure to the virus. Even after 360 min the amount of virus on the surface, measured by quantitative RT-PCR, varies insignificant (within the order). However, the detection of SARS-CoV-2 RNA is not indicating the presence of a viable virus. Most significantly reduce the infectivity of the virus when the virus contacts with cloth (towel) samples, as well as plastic. Longer persistence of the infectious virus has been observed on surfaces such as metal, wood (chipboard) and ceramic tile. The decrease in the infectivity of SARS-CoV-2 occurs 120 min after contact with model materials and is completely lost for 360 min of exposure, when drying is achieved. It can be assumed that the complete loss of viability and the infectivity of the virus occurs at an earlier point in time (between 120–360 minutes) for all investigated materials

DISCUSSION

Our research is not without its flaws. We used culture fluid to simulate contamination. Its composition will be significantly different from human excreta formed because of natural contact with surfaces. In addition, the method itself for viable virus isolating using a cell culture may differ significantly in susceptibility to infection [8, 9]. Individual strains circulating in people with different genetic backgrounds may also differ in their ability to persist on surfaces. Nevertheless, accepting these limitations, the results can be useful for planning further research and preparing practical recommendations.

CONCLUSIONS

The results obtained in the framework of this study show that positive RT-PCR data do not allow us to speak about the viability of the virus. For at least 360 minutes on the surface, the amount of RNA SARS-CoV-2 on the surface practically does not change, while the virus viability drops by many orders of magnitude in 120 minutes and after 360 minutes is not detected for any of the experimental surfaces. Thus, in the context of environmental safety assessment, the use of RT-PCR alone can lead to highly distorted judgments. At the very least, the interpretation of RT-PCR results in the context of potential surface contamination with SARS-CoV-2 should be done with great care.

References

1. Jayaweera M, Perera H, Gunawardana B, Manatunge J. Transmission of COVID-19 Virus by Droplets and Aerosols: A Critical Review on the Unresolved Dichotomy. Environ. Res. 2020; 188: 109819.
2. van Doremalen N, Bushmaker T, Morris DH, Holbrook MG, Gamble A, Williamson BN, et al. Aerosol and Surface Stability of SARS-CoV-2 as Compared with SARS-CoV-1. N Engl J Med. 2020; 382: 1564–7.
3. Fernández-Raga M, Díaz-Marugán L, García Escolano M, Bort C, Fanjul V. SARS-CoV-2 Viability under Different Meteorological Conditions, Surfaces, Fluids and Transmission between Animals. Environ Res. 2021; 192: 110293.
4. Xue X, Ball JK, Alexander C, Alexander MR. All Surfaces Are Not Equal in Contact Transmission of SARS-CoV-2. Matter. 2020; 3: 1433–41.
5. Cai J, Sun W, Huang J, Gamber M, Wu J, He G. Indirect Virus Transmission in Cluster of COVID-19 Cases, Wenzhou, China. 2020; Emerg Infect Dis. 2020; 26: 1343–5.
6. Xie C, Zhao H, Li K, Zhang Z, Lu X, Peng H, et al. The Evidence of Indirect Transmission of SARS-CoV-2 Reported in Guangzhou,

- China. BMC Public Health. 2020; 20: 1202.
7. Chin AWH, Chu JTS, Perera MRA, Hui KPY, Yen H-L, Chan MCW, et al. Stability of SARS-CoV-2 in Different Environmental Conditions. Lancet Microbe. 2020; 1: e10.
 8. Yao H, Lu X, Chen Q, Xu K, Chen Y, Cheng M, et al. Patient-Derived SARS-CoV-2 Mutations Impact Viral Replication Dynamics and Infectivity in Vitro and with Clinical Implications in Vivo. Cell Discov. 2020; 6: 76.
 9. Cevik M, Kuppalli K, Kindrachuk J, Peiris M. Virology, Transmission, and Pathogenesis of SARS-CoV-2. BMJ. 2020; 371: m3862.

Литература

1. Jayaweera M, Perera H, Gunawardana B, Manatunge J. Transmission of COVID-19 Virus by Droplets and Aerosols: A Critical Review on the Unresolved Dichotomy. Environ. Res. 2020; 188: 109819.
2. van Doremalen N, Bushmaker T, Morris DH, Holbrook MG, Gamble A, Williamson BN, et al. Aerosol and Surface Stability of SARS-CoV-2 as Compared with SARS-CoV-1. N Engl J Med. 2020; 382: 1564–7.
3. Fernández-Raga M, Díaz-Marugán L, García Ecolano M, Bort C, Fanjul V. SARS-CoV-2 Viability under Different Meteorological Conditions, Surfaces, Fluids and Transmission between Animals. Environ Res. 2021; 192: 110293.
4. Xue X, Ball JK, Alexander C, Alexander MR. All Surfaces Are Not Equal in Contact Transmission of SARS-CoV-2. Matter. 2020; 3: 1433–41.
5. Cai J, Sun W, Huang J, Gamber M, Wu J, He G. Indirect Virus Transmission in Cluster of COVID-19 Cases, Wenzhou, China. 2020; Emerg Infect Dis. 2020; 26: 1343–5.
6. Xie C, Zhao H, Li K, Zhang Z, Lu X, Peng H, et al. The Evidence of Indirect Transmission of SARS-CoV-2 Reported in Guangzhou, China. BMC Public Health. 2020; 20: 1202.
7. Chin AWH, Chu JTS, Perera MRA, Hui KPY, Yen H-L, Chan MCW, et al. Stability of SARS-CoV-2 in Different Environmental Conditions. Lancet Microbe. 2020; 1: e10.
8. Yao H, Lu X, Chen Q, Xu K, Chen Y, Cheng M, et al. Patient-Derived SARS-CoV-2 Mutations Impact Viral Replication Dynamics and Infectivity in Vitro and with Clinical Implications in Vivo. Cell Discov. 2020; 6: 76.
9. Cevik M, Kuppalli K, Kindrachuk J, Peiris M. Virology, Transmission, and Pathogenesis of SARS-CoV-2. BMJ. 2020; 371: m3862.

FEATURES OF THE PATHOGENETIC MECHANISMS OF TUBERCULOUS PERITONITIS IN AN EXPERIMENT

Plotkin DV^{1,2}✉, Vinogradova TI³, Reshetnikov MN¹, Ariel BM³, Zyuzya YuR¹, Zhuravlev VYu³, Sinitsyn MV¹, Bogorodskaya EM¹, Yablonsky PK³¹ Moscow Research and Clinical Center for TB Control, Moscow, Russia² Pirogov Russian National Research Medical University, Moscow, Russia³ Saint-Petersburg State Research Institute of Phthisiopulmonology, Saint Petersburg, Russia

The prevalence of tuberculous peritonitis that has been observed in the recent decades is the result of lymphohematogenous spread of *Mycobacterium tuberculosis* (MBT) from lungs and other extrapulmonary sources. It is still unclear why certain organs and anatomical regions get involved in the inflammatory process during generalization of the tuberculosis infection. Why do some cases develop into peritoneal tuberculosis and others into kidney tuberculosis? Thus, this study aimed to investigate the pathogenesis of tuberculous peritonitis in a reproducible biological model. Tuberculous peritonitis was modeled in 18 rabbits (10 in the test group, 8 in control) by intraperitoneal inoculation of the MBT suspension. In order to suppress peritoneal macrophages and major cytokines, test group rabbits were injected with the TNFα inhibitor and iron (III) hydroxide sucrose complex before being infected, while control group rabbits received no immunosuppressive drugs. Autopsy of the control group animals revealed changes characteristic of pulmonary tuberculosis in 37.5% of cases, with no damage to other organs and systems registered. Conversely, test group rabbits had the signs of tuberculous peritonitis in their abdominal cavities. The results of this study suggest that it is the local immunity of an anatomical area that largely determines whether a secondary focus of extrapulmonary tuberculosis infection will develop there or not. For the peritoneum, a smaller pool of peritoneal macrophages and weaker cytokine production is a necessary and sufficient condition to have tuberculous peritonitis developing therein.

Keywords: peritonitis, animal model, tuberculous peritonitis, abdominal tuberculosis, TNFα, tumor necrosis factor, rabbit

Conflict of interests: Plotkin DV, Vinogradova TI, Reshetnikov MN, Zyuzya YuR, Sinitsyn MV, Bogorodskaya EM, Yablonsky PK have filed a request to the Federal intellectual property service "Federal Institute for Industrial Property" to register the Russian Federation patent for the invented "Method for modeling tuberculous peritonitis" (registration #2021114954 of May 25, 2021). Ariel BM, Zhuravlev VYu claim to have no conflict of interest.

Author contributions: Plotkin DV, Vinogradova TI, Sinitsyn MV, Bogorodskaya EM — study concept and design development; Plotkin DV, Reshetnikov MN, Zhuravlev VYu, Zyuzya YuR — material collection; Reshetnikov MN, Zhuravlev VYu — statistical processing; Plotkin DV, Vinogradova TI, Ariel BM, Yablonsky PK — analysis of the data obtained; Plotkin DV, Ariel BM, Sinitsyn MV, Bogorodskaya EM — text preparation; Vinogradova TI, Zyuzya YuR, Yablonsky PK — editing.

Compliance with ethical standards: the study was approved by the Ethics Committee of the Saint Petersburg Research Institute of Phthisiopulmonology (protocol № 73 of December 23, 2020). All manipulations with animals conformed to the requirements of the European Convention for the Protection of Vertebral Animals Used for Experimental and Other Scientific Purposes (CETS # 170) and followed guidelines provided in GOST 33216-2014 Rules for Working with Laboratory Rodents and Rabbits.

✉ Correspondence should be addressed: Dmitry Vladimirovich Plotkin
Ostrovityanova, 1, Moscow, 117997; kn13@list.ru

Received: 30.06.2021 Accepted: 21.07.2021 Published online: 04.07.2021

DOI: 10.24075/rsmu.2021.036

ОСОБЕННОСТИ ПАТОГЕНЕТИЧЕСКИХ МЕХАНИЗМОВ ТУБЕРКУЛЕЗНОГО ПЕРИТОНИТА В ЭКСПЕРИМЕНТЕ

Д. В. Плоткин^{1,2}✉, Т. И. Виноградова³, М. Н. Решетников¹, Б. М. Ариэль³, Ю. Р. Зюзя¹, В. Ю. Журавлев³, М. В. Синицын¹, Е. М. Богородская¹, П. К. Яблонский³

¹ Московский городской научно-практический центр борьбы с туберкулезом, Москва, Россия

² Российский национальный исследовательский медицинский университет имени Н. И. Пирогова, Москва, Россия

³ Санкт-Петербургский научно-исследовательский институт фтизиопульмонологии, Санкт-Петербург, Россия

Наблюдаемый в последние десятилетия рост числа случаев туберкулезного перитонита обусловлен лимфогематогенным распространением микобактерий туберкулеза (МБТ) из легких и других экстрапулмональных источников. До сих пор остается неясным, почему при генерализации туберкулезной инфекции в воспалительный процесс вовлекаются те или иные органы и анатомические области. Почему в одних случаях развивается туберкулез брюшины, а в других туберкулез почек? Целью работы было изучить патогенез туберкулезного перитонита с помощью создания воспроизводимой биологической модели. Туберкулезный перитонит моделировали на 18 кроликах (10 особей — экспериментальная группа, 8 — контрольная) путем внутрибрюшинной инокуляции взвеси МБТ. Кроликам экспериментальной группы перед заражением вводили ингибитор TNF — и железа (III) гидроксид сахарозный комплекс с целью подавления активности перitoneальных макрофагов и основных цитокинов; в контрольной группе введение иммуносупрессивных препаратов не производили. При аутопсии животных контрольной группы в 37,5% случаев выявлены изменения, характерные для туберкулеза легких, поражения других органов и систем не отмечено. Напротив, у кроликов экспериментальной группы в брюшной полости выявлены признаки туберкулезного перитонита. По результатам проведенной работы, анатомическая область, где развивается вторичный очаг внелегочной туберкулезной инфекции, во многом зависит от местной иммунной защиты. Так, для брюшины таким необходимым и достаточным условием развития туберкулезного перитонита являются уменьшение пула перitoneальных макрофагов и снижение цитокиновой продукции.

Ключевые слова: перитонит, животная модель, туберкулезный перитонит, абдоминальный туберкулез, TNFα, фактор некроза опухолей, кролик

Конфликт интересов: Д. В. Плоткин, Т. И. Виноградова, М. Н. Решетников, Ю. Р. Зюзя, М. В. Синицын, Е. М. Богородская, П. К. Яблонский — подали заявку в Федеральную службу по интеллектуальной собственности «Федеральный институт промышленной собственности» на регистрацию заявления о выдаче патента Российской Федерации на изобретение «Способ моделирования туберкулезного перитонита» (регистрационный № 2021114954 от 25 мая 2021 г.). Б. М. Ариэль, В. Ю. Журавлев — заявляют об отсутствии у них конфликта интересов.

Вклад авторов: Д. В. Плоткин, Т. И. Виноградова, М. В. Синицын, Е. М. Богородская — разработка концепции и дизайна исследования; Д. В. Плоткин, М. Н. Решетников, В. Ю. Журавлев, Ю. Р. Зюзя — сбор материала; М. Н. Решетников, В. Ю. Журавлев — статистическая обработка; Д. В. Плоткин, Т. И. Виноградова, Б. М. Ариэль, П. К. Яблонский — анализ полученных данных; Д. В. Плоткин, Б. М. Ариэль, М. В. Синицын, Е. М. Богородская — подготовка текста; Т. И. Виноградова, Ю. Р. Зюзя, П. К. Яблонский — редактирование.

Соблюдение этических стандартов: исследование одобрено этическим комитетом Санкт-Петербургского научно-исследовательского института фтизиопульмонологии (протокол № 73 от 23 декабря 2020 г.). Все манипуляции с животными проводили в соответствии с требованиями European Convention for the Protection of Vertebral Animals Used for Experimental and Other Scientific Purposes (CETS No. 170), а также руководствуясь «Правилами работы с лабораторными грызунами и кроликами» (ГОСТ 33216-2014).

✉ Для корреспонденции: Дмитрий Владимирович Плоткин
ул. Островитянова, д. 1, г. Москва, 117997; kn13@list.ru

Статья получена: 30.06.2021 Статья принята к печати: 21.07.2021 Опубликована онлайн: 04.07.2021

DOI: 10.24075/vrgmu.2021.036

Currently, it is believed that a quarter of the world's population is infected with tuberculosis; more than 10 million new cases of the disease and 1.2 million deaths from tuberculosis are registered annually. According to the World Health Organization, 15–20% of tuberculosis cases are extrapulmonary, and tuberculous peritonitis (TP) is the sixth most common of them [1, 2].

The concepts of pathogenesis of extrapulmonary tuberculosis were formed in the 30s–60s of the last century on the basis of clinical observations, experimental work and results of autopsies. TP was considered as part of polyserositis that simultaneously involved peritoneum, pericardium, pleura and synovial membranes of large joints in a specific process [3, 4] that was a typical manifestation of progressive primary tuberculosis.

The TP observed in the recent decades in the vast majority of patients develops during late stages of tuberculosis infection. Its pathogenesis is studied insufficiently; probably, TP is the result of lymphohematogenous spread of *Mycobacterium tuberculosis* (MBT) from the lungs, intra-abdominal lymph nodes, intestines, fallopian tubes [5, 6]. It is still unclear why, in such cases, generalization of the infection induces inflammatory process in certain organs and what are the conditions that promote the development of pathological changes in the given anatomical region.

Until recently, it was believed that such conditions were mainly shaped by microcirculatory disorders, when the initial focal lesions appeared only against the background of certain functional restructuring of the microvasculature: its increase in volume, slowed blood flow, close contact with tissues (semi-closed microcirculation system, with pores and fenestra in the walls of capillaries) [7].

It is known that each form of extrapulmonary tuberculosis has its own locus minoris resistentiae, where the initial focal lesions develop in a strictly regular sequence. In the abdominal cavity, such locus is the ileocecal zone, where the blood flow can grow weaker because of the slowed intestinal passage (ileostasis) and presence of a relatively large mass of lymphoid tissue in mesenteric lymph nodes and Peyer's patches, which get "swamped" when the blood flow is slow [3, 8].

Microvasculature disorders cannot but play a significant role in the development of TP, although, of course, they are not the only reasons behind the disease's pathogenesis. Poorly understood immune defense mechanisms also play a certain part here, as they do in any other pathological process. With regard to TP, it is the protective part played by the peritoneum MBT interact with, as well as local immunity [9].

These insufficiently studied mechanisms can be investigated under experimental conditions on models that reproduce human TP with all its characteristic features. There is reason to believe that with this approach, it will be possible to understand how and to what extent damage to the peritoneum and protective reactions therein "work" and balance out on the level of the body as a whole.

We searched for publications covering TP modeling methods in the PubMed database and found nothing in the current literature. Deepening the search, we discovered works published in the 19th century and first half of the 20th century [10, 11] that contained a few descriptions of unsuccessful attempts at intraperitoneal infection of laboratory animals with MBT culture for the purpose of experimental reproduction of TP.

Thus study aimed to investigate the pathogenesis of tuberculous peritonitis in a reproducible biological model.

METHODS

The study involved 18 male Sovetskaya Chinchilla rabbits weighing 2.60–3.25 kg, obtained from the Rappolovo laboratory

animal nursery (Kurchatov Institute; Russia). The animals had no external manifestations of a disease; they were quarantined for two weeks in the certified vivarium of the St. Petersburg Scientific Research Institute of Phthisiopulmonology. The conditions were similar for all the animals, the food regimen standard, with access to water ad libitum.

The rabbits were divided into two groups, test and control. The division factored in age of the animals, i.e., all rabbits in a group were of the same age, obtained from the nursery at the same time.

We relied on the original technique we have developed to model TP: intraperitoneal inoculation of 6 ml of suspension of *M. tuberculosis* H₃₇Rv standardized virulent test strain (10⁶ mycobacterial cells in 6 ml). To infect control group and test group animals, we used saline or aluminum hydroxide gel MBT suspensions, respectively. *M. tuberculosis* H₃₇Rv test strain (TBC #1/47, Institute of Hygiene and Epidemiology; Prague, 1976), taken from the collection of the Scientific Centre for Expert Evaluation of Medicinal Products, was cultured on the Lowenstein–Jensen medium (Becton, Dickinson and Company; USA). The mycobacterial suspension of the three-week (second generation) *M. tuberculosis* H₃₇Rv test strain was prepared *ex tempore* on the day of infection.

The animals were infected intraperitoneally with immunodeficiency in the background. To induce immunodeficiency, we decreased the concentration of tumor necrosis factor TNF α (the main cytokine, regulator of the formation and resistance of granulomas) by intravenous administration of the TNF α inhibitor infliximab (chimeric mouse-human monoclonal antibody) (BIOCAD; Russia). We also suppressed the phagocytic activity of peritoneal agranulocytes (peritoneal macrophages) through intraperitoneal administration of iron (III) hydroxide sucrose complex (PHARMASINTEZ; Russia). This drug was chosen as a donor of ferric iron to create the effect of "iron overload" in immunocompetent cells that absorb excess non-transferrin bound iron [12, 13].

The test group consisted of 10 rabbits, who were injected infliximab (once, into the marginal ear vein, 16 mg/kg) [14] one day before intraperitoneal infection with MBT culture, and 5 ml of iron (III) hydroxide of the sucrose complex intraperitoneally 1 hour before infection.

Eight rabbits of the control group were infected in a similar way, but they did not receive the TNF α inhibitor and the iron sucrose complex.

After infection, we monitored body weight of the animals (weighed them once every 10 days), observed their behavior, applied intradermal recombinant tuberculosis antigen (Diaskintest \circledast) tests to confirm the development of tuberculosis infection. The animals were removed from the experiment on the 45th day from the moment of infection with the help of a general anesthetic overdose: sodium thiopental 250 mg and pipcuronium bromide 1 mg intravenously.

During autopsy, we looked for effusion in serous cavities and tubercles on the serous integuments of the liver, spleen, intestines and lungs, and assessed the shape and size of the intrathoracic and intra-abdominal lymph nodes, the size and structure of the kidneys. For microscopic examination, we sampled tissues of the parietal peritoneum, liver, kidneys, spleen, lungs, heart and lymph nodes. The samples were embedded in paraffin wax. Slices were stained with hematoxylin and eosin; we also applied the Van Gieson and Perls staining methods to identify collagen fibers and have a qualitative reaction to ferric iron, respectively. Besides, to detect MBT, we stained the samples following the Ziehl–Neelsen technique and then performed a bacterioscopic study. Also with the aim

of detecting MBT DNA, we subject peritoneal and omentum tissues to PCR test using the Amplitub-RV reagent kit (Syntol; Russia).

RESULTS

Dynamic post-infection observation of the animals did not reveal any weight loss. On the contrary, all rabbits gained an average of 132 ± 42.6 g over the entire period of the experiment. On the 20th — 22nd day after the infection, the recombinant tuberculosus allergen (Diaskintest®) test returned hyperergic in all 18 rabbits.

Autopsy and histological examination of the samples revealed significant differences between the rabbits of test and control groups.

On the 45th day from the moment of intraperitoneal infection, serous cover of the abdominal cavity of control group animals remained intact at both macro- and microscopic levels. There were no specific changes identified either in the parenchymal organs of the abdominal cavity or in the kidneys. PCR test did not detect MBT DNA in the animals' peritoneum and omentum.

At the same time, 3 animals (37.5%) had clear signs of tuberculous pneumonia. Lung tissue microscopy revealed BLURRY, fused macrophage granulomas with small areas of necrosis and mild leukocytic infiltration along the periphery, and occasional larger foci of caseous necrosis infiltrated by decaying leukocytes. Distelectasae dominated by atelectasae, focal exudative reaction, vasculitis products were found in the adjacent lung tissue (Fig. 1A, C). In such areas, the pleura was thickened due to edema and mononuclear infiltration. Van Gieson staining revealed no encapsulation of foci of caseous necrosis, nor signs of organization in the areas of tuberculous inflammation. Ziehl–Neelsen staining allowed detecting microcolonies of MBT in the necrosis foci (Fig. 1B).

It is worth noting mild character of reactive changes in individual lymph nodes of the abdominal cavity and mediastinum and lack of signs of specific tuberculous lymphadenitis. Microscopic examination revealed focal nonspecific infiltration of the peritoneum with MBT, where bacterioscopy failed to detect the bacteria. Their absence in such areas of the peritoneal cover was confirmed by the PCR test.

In the test group, in the first week after infection all animals were showing clinical symptoms of intoxication: physical inactivity, lack of appetite, loss of body weight by 75–110 g

(average — 84 g). In the next 35 days, the dynamics of their state was positive, with physical activity, appetite returning to norm and some body weight gained.

Forty-five days after infection, autopsy of all test group animals presented characteristic macroscopic signs of TP: yellowish serous effusions in the abdominal cavity (maximum volume — 5 ml), dense and loose adhesions of varying degrees of maturity between the small intestine loops, the greater omentum and the anterior abdominal wall, multiple small and large tubercles measuring 2–6 mm on the parietal and visceral peritoneum (Fig. 2). Histological examination of the adhesions and serous cover fragments revealed macrophage granulomas with single giant multinucleated Langhans cells, as well as extensive foci of caseous necrosis with perifocal accumulation of macrophage granulomas merging with each other (Fig. 3A, B). Similar changes were also present in the mesentery of the small intestine and the greater omentum.

Nine out of ten (90%) test group animals had active pulmonary tuberculosis in the form of foci of caseous necrosis with small accumulations of lymphocytes along the periphery and specific granulations. Van Gieson staining revealed no signs of organization in the tuberculous inflammation foci in the lungs. Ziehl–Neelsen staining allowed discovering MBT microcolonies in caseous masses.

Perls staining uncovered multiple accumulations of macrophages with a high content of iron in the cytoplasm. Such were found both in the tissues of the peritoneum and those of the lungs (Fig. 3C, D). One case (10%) was diagnosed as tuberculous splenitis, another (10%) as tuberculous hepatitis. In the lymph nodes of the small intestine mesentery both specific changes and nonspecific reactive hyperplasia of lymphocytes were revealed. At the same time, all rabbits had dystrophic changes in the kidney convoluted tubes epithelium, liver and myocardium, which were accompanied by pronounced plethora and edema of the organ stroma.

Changes in the serous membrane of the intestine were of two kinds: in some cases, productive tuberculous peritonitis was detected without signs of organization, and in others it was nonspecific reactive inflammation. No specific inflammatory changes were found in the serous membrane of the stomach. Tests for MBT DNA in the tissues of the greater omentum returned positive in all 10 cases.

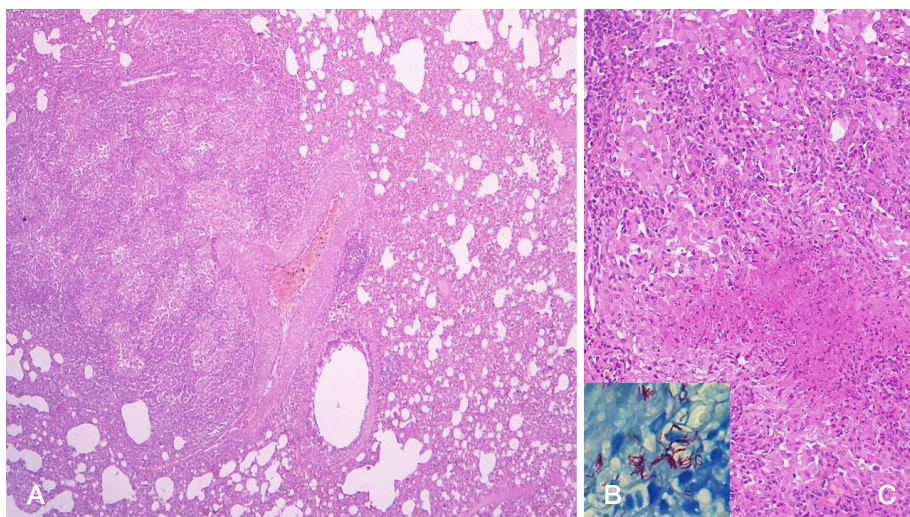


Fig. 1. Foci of tuberculous lesions in the lung of a rabbit. **A.** Lung area under tuberculous granulomatous inflammation with distelectasis (micropreparation, stained with hematoxylin and eosin; $\times 40$). **B.** Acid-resistant mycobacteria in the focus of tuberculous inflammation (micropreparation, staining according to Ziehl–Neelsen; $\times 1000$). **C.** Lung: a focus of caseous necrosis with leukocyte infiltration and perifocal macrophage-epithelioid granulomas (micropreparation, stained with hematoxylin and eosin; $\times 100$)

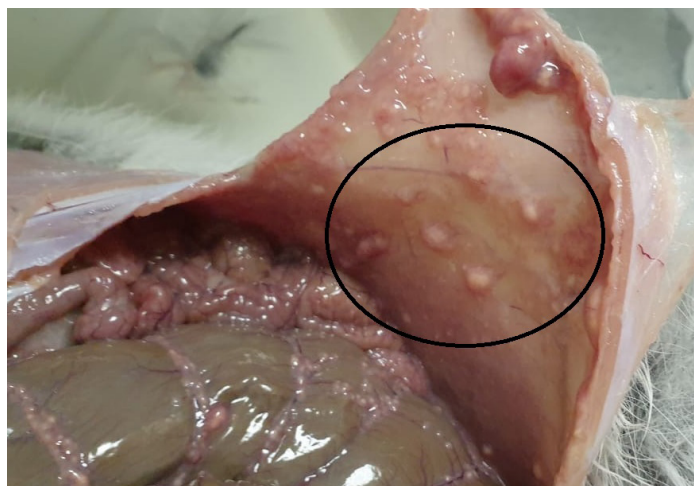


Fig. 2. There are multiple tuberculous tubercles on the parietal peritoneum of a rabbit-disseminates (circled in a round frame) (macro specimen)

DISCUSSION

The choice of rabbit (*Oryctolagus cuniculus domesticus*) as a laboratory animal in the development of the experimental TP model was a thought-out decision. According to Claude Bernard, a good choice of animal is often enough to solve the most difficult general questions.

Previous research has shown that rabbits, which are considered resistant to *M. tuberculosis*, under certain conditions can naturally develop specific chronically progressive granulomatous inflammation or latent tuberculosis infection, depending on the MBT virulence [15–17]. From the morphological point of view, the subject is the evolution of granulomas — their formation, maturation and decay. In rabbits, these processes run the same way as they do in human being. Rabbits are fairly large laboratory animals, so selecting them as experimental subjects researcher can reliably monitor pathophysiological changes from the very beginning of the infectious process until its completion, even without resorting to euthanasia [18].

According to our observations, in case of intraperitoneal infection with MBT rabbits with an intact immune status develop not TP but tuberculous inflammation of the lungs and mediastinum lymph nodes. Only half of the infected animals fall ill; the changes in their lungs and lymph nodes are transient and

disappear 1.5 months after infection. As inflammatory changes disappear from the organs, so do the MBT. The absence of inflammatory changes in the abdominal cavity is due to the serous membrane playing the part of a mechanical barrier in the pathological process, as does, for example, the greater omentum, which limits inflammatory foci in the abdominal cavity independently and as a *sui generis* organ of the humoral and cellular defense system.

It is now generally accepted that there are three cellular systems opposing the invasion of microorganisms in the abdominal cavity: lymphocytes, mesotheliocytes, and peritoneal macrophages. They are the first line of defense, which relies on phagocytic activity and production of inflammatory cytokines [19]. Secretory function of the mesothelium also contributes to the body's defensive capabilities, both under normal and pathological conditions [20]. It makes the MBT release into the free abdominal cavity, where they die in the exudate containing free antibodies, peritoneal macrophages and neutrophilic leukocytes, which, taken together, produce bacteriostatic and bactericidal effects. In other words, we consider the peritoneum not as a morphologically formed statically permanent formation but as an organ of humoral and cellular immunity [21].

Obviously, physiological activity of the peritoneal macrophages is important for the peritoneum's protective properties. Having suppressed it with infliximab (TNF α

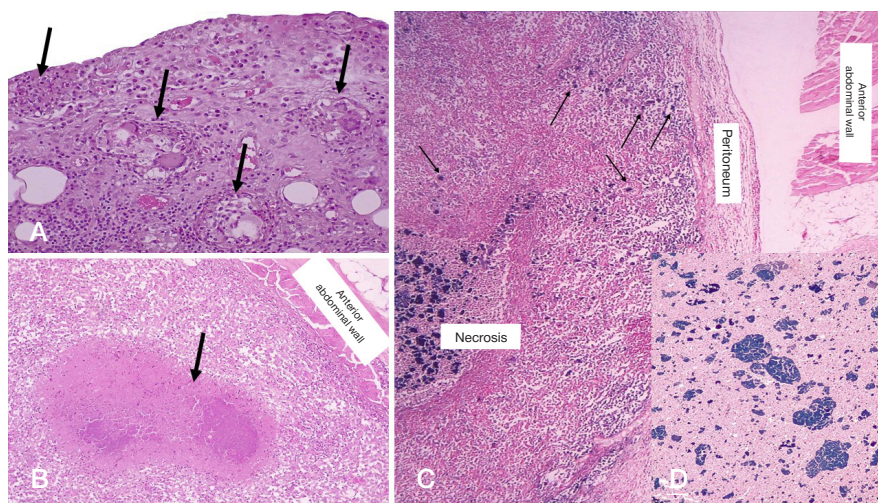


Fig. 3. Tuberculous peritonitis in rabbits. Micropreparation. **A.** Tuberculous granulomatous peritonitis (granulomas are shown by arrows) (staining with hematoxylin and eosin; $\times 200$). **B.** Caseous peritonitis (a focus of caseous necrosis is shown by the arrow) (stained with hematoxylin and eosin; $\times 100$). **C.** Accumulations of iron-containing pigment in necrotic masses and in adjacent macrophages (iron-containing pigment is blue-green, some of the macrophages with pigments are shown by arrows) (Perls reaction; $\times 100$). **D.** Fragment of Fig. C (Perls reaction; $\times 200$)

inhibitor) and overloaded with iron, we were able to reproduce chronically progressive TP with the formation of alternative and granulomatous changes against the background of MBT reproduction. Speaking about the importance of protective reactions in the pathogenesis of TP, we mean not only phagocytosis of pathogens by macrophages but also the further fate of both. MBT partially or completely die in the macrophages' cytoplasm, while the affected cells themselves are removed by the body naturally: secreted into the free abdominal cavity from the peritoneum and cleared and from the lungs.

Thus, in addition to presence of an etiological factor in the abdominal cavity TP development requires inactivation of peritoneal macrophages and regulatory cytokines, the main of which is TNF α . The latter plays an important part in tuberculosis protection in human beings, too. It performs many immunoregulatory functions, including early induction of chemokines that leads to the recruitment of leukocytes, and it also participates in the morphogenesis of granulomas, which always appear in people suffering from a mycobacterial disease [22, 23].

Genetic studies have shown that toll-like receptors, such as TLR-2, significantly affect the susceptibility (consequently, resistance) to tuberculosis. Variants of their polymorphism were examined mainly in pulmonary tuberculosis; however, a significant relationship was found between the TLR-2 Arg753Gln polymorphism and the incidence of TP. This suggests that individuals with a TLR2 gene Arg753Gln polymorphism run an increased risk of TP [24].

Our experimental TP modeling allowed discovering and number of important features of its pathogenesis.

1. With a TNF α inhibitor and an iron (III) hydroxide sucrose complex administered, all animals naturally develop a widespread, actively progressive tuberculous inflammation of the peritoneum dominated by granulomatous-necrotic changes that sometimes turn into caseosis. Its expansive character is proven by the fact that, in addition to the parietal peritoneum and the greater omentum, tuberculous inflammation spreads into the visceral peritoneum of the mesentery and intestinal loops.

2. With the described method for TP modeling there also develops a destructive pulmonary tuberculosis with lymphadenopathy of intrathoracic and intra-abdominal lymph nodes where specific granulomatous and nonspecific hyperplastic changes can be found.

3. As for the other organ lesions of hematogenous genesis (those of liver, spleen, kidneys), this method of modeling only allowed finding them in isolated cases as evidence of hematogenous generalization of the infection.

Our experimental TP model has reliably reproduced the clinical, morphological and pathogenetic features of tuberculous lesions of the peritoneum of human beings. They can be observed in case of hematogenous dissemination of pulmonary tuberculosis, which develops against a particular comorbid background that has the peritoneum's local immunity compromised and/or general immunosuppression developed.

As we learned from the literature and our own clinical observations, peritoneal tuberculosis develops during pregnancy, in patients with diabetes mellitus, liver cirrhosis, cardiovascular diseases comorbid with ascites, as well as peritoneal dialysis, congenital and acquired immunodeficiencies.

Immunosuppression is common in pregnancy. It is associated with a complex system of immunological interaction between the mother and the fetus. Progesterone and cortisol, the levels of which go up during pregnancy, suppress T- and

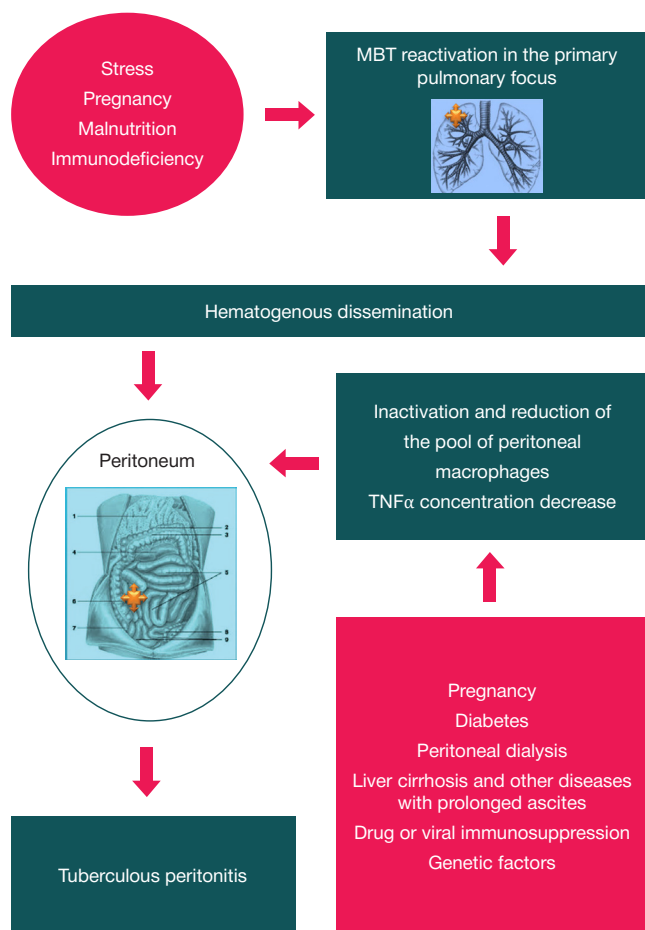


Fig. 4. Tuberculous peritonitis pathogenesis pattern

B-cell immunity, and after 2–3 months after childbirth, the pool of agranulocytes is depleted [25]. It affects the number and activity of peritoneal macrophages, as indicated by the incidence of TP in the first months after birth.

Both during the carbohydrate metabolism decompensation stage and when the compensation is achieved, diabetes mellitus patients have the induced production of IL1 and TNF α by peripheral blood mononuclear cells (compared with healthy individuals) going down and spontaneous — going up [26], which leads to disruption of the morphogenesis of granulomas and reduces their resistance. This explains the cases of detection of TP in such patients.

With the above pathology in the background, persisting ascites, as well as with carcinomatosis, lead to chronic aseptic inflammation of the peritoneum, the outcome of which significantly decreases the number of macrophages, including peritoneal ones. At the same time, the local concentration of TNF α decreases [27].

Chronic peritoneal dialysis is also directly associated with the development of peritoneal tuberculosis. Dialysis solutions contain an increased concentration of glucose and have a non-physiological pH value, which entails disturbance of the functional activity of phagocytes and lymphocytes in the peritoneum [28].

Immunodeficiency states, both congenital and acquired, including after the use of immunomodulatory drugs (TNF α inhibitors) and glucocorticosteroids, entail a decrease in the number of agranulocytes and TNF α synthesis. Low concentrations of TNF α and inactivation of macrophages in the peritoneum directly contribute to the development of TP. And, of course, HIV infection with its characteristic

immunosuppression can become a trigger in the pathogenesis of peritoneal tuberculosis [29, 30].

Analyzing the results of our experiment and taking into account clinical observations and literature data, we can propose the following pattern of TB pathogenesis in humans. Stressful influences, such as malnutrition, pregnancy, a sudden change in social status, immunosuppressive diseases etc., lead to the reactivation of the primary tuberculous focus and destruction of previously formed granulomas and lymphohematogenous by the spread of MBT [31]. Where, in which anatomical region the secondary focus of extrapulmonary tuberculosis infection will develop directly depends not only on the characteristics of microcirculation in this region but also on the local immune protection (local immunity according to A. M. Bezredka). For the peritoneum, a smaller pool of peritoneal macrophages and weaker cytokine production is a necessary and sufficient condition to have TP developing therein. Figure 4 shows the pattern of TP pathogenesis.

CONCLUSIONS

Clinical manifestations, methods of detection, diagnosis and treatment of respiratory tuberculosis are well studied and fully covered in the scientific and medical literature. Tuberculosis

mainly affects the pulmonary parenchyma, but under certain conditions associated with changes in local and humoral immunity, the process can localize in almost all organs and tissues of a human being. As a rule, actively progressive pulmonary tuberculosis receives the bulk of attention while much less effort goes into investigating extrapulmonary manifestations of the infection with severe destructive changes. Over the past decades, about 15% of the detected tuberculosis cases worldwide are extrapulmonary. Their clinical diagnosis is fraught with objective difficulties, since in extrapulmonary tuberculosis, the results of the gold diagnostics standard — testing sputum for MBT — often return negative. And, in the most paradoxical way, the presence of *M. tuberculosis* in extrapulmonary foci often causes a wide range of nonspecific symptoms, thereby creating additional diagnostic difficulties. TP is one of the extrapulmonary forms of tuberculosis that are difficult to diagnose and treat. In this work we have experimentally shown the role of peritoneal macrophages in the formation of local protective immunity and TNF α in the humoral aspects of the protective processes. The data obtained will make the features of the modern pathogenesis of tuberculous peritonitis more clear and enable development of the diagnostic criteria and therapeutic (including surgical) protocols for such patients.

References

- Behr MA, Edelstein PH, Ramakrishnan L. Is Mycobacterium tuberculosis infection life long? BMJ. 2019; 367: i5770. PubMed PMID: 31649096. DOI: 10.1136/bmj.i5770.
- WHO. Global Tuberculosis Report 2020. World Health Organization, Geneva, 2020. Available at: https://www.who.int/tb/publications/global_report/en.
- Mirzajan JeZ. Tuberkulez kishechnika i brjushiny. V knige: V. L. Jejnisi, redaktor. Mnogotomnoe rukovodstvo po tuberkulezu. T. 3. M.: Medgiz, 1960; s. 125–146. Russian.
- Onosovskij VV. O lechenii tuberkuleznogo peritonita u detej, po materialam Ol'ginskoj detskoy bol'nicy v Moskve za 36 let. Problemy tuberkuleza. 1923; 5–6 (1): 148–155. Russian.
- Savonenkova LN, Arjamikina OL. Patogenezi i morfogenез abdominal'nogo tuberkuleza s porazheniem gastrointestinal'nogo trakta. Nizhegorodskij medicinskij zhurnal. 2006; 2: 89–94. Russian.
- Dülgör AC, Karadaş S, Mete R, Türkdoğan MK, Demirkiran D, Gültepe B. Analysis of cases with tuberculous peritonitis: a single-center experience. Turk J Gastroenterol. 2014; 25 (1): 72–8. PubMed PMID: 24918135. DOI: 10.5152/tjg.2014.5145.
- Bellendir JeN. Patogenezi vnelegochnykh lokalizacij tuberkuleza. V knige: A. V. Vasil'ev, redaktor. Vnelegochnyj tuberkulez. SPb., 2000; s. 36–48. Russian.
- Singh MM, Bhargava AN, Jain KP. Tuberculous peritonitis. An evaluation of pathogenetic mechanisms, diagnostic procedures and therapeutic measures. N Engl J Med. 1969; 281 (20): 1091–4. PubMed PMID: 5824174. DOI: 10.1056/NEJM196911132812003.
- Bezredka AM. Ocherki po immunitetu. M-L., 1929; 267 c. Russian.
- Kishenskij DN. Vlijanie chrevosechenija na tuberkulez brjushiny. Jeksperimental'noe issledovanije [dissertacija]. M.: Tovarishhestvo tipografii A. I. Mamontova, 1894; 82 c. Russian.
- Lurie MB. The fate of tubercle bacilli in the organs of reinfected rabbits. J Exp Med. 1929; 50 (6): 747–765. PubMed PMID: 19869661. DOI: 10.1084/jem.50.6.747.
- Roach DR, Bean AG, Demangel C, France MP, Briscoe H, Britton WJ. TNF regulates chemokine induction essential for cell recruitment, granuloma formation, and clearance of mycobacterial infection. J Immunol. 2002; 168 (9): 4620–7. PubMed PMID: 11971010. DOI: 10.4049/jimmunol.168.9.4620.
- Brissot E, Bernard DG, Loréal O, Brissot P, Troadec MB. Too much iron: A masked foe for leukemias. Blood Rev. 2020; 39: 100617. PubMed PMID: 31753415. DOI: 10.1016/j.blre.2019.100617.
- Shekunova EV, Kovaleva MA, Makarova MN, Makarov VG. Vybor dozy preparata dlja doklinicheskogo issledovanija: mezhvidovoj perenos doz. Vedomosti Nauchnogo centra jekspertizy sredstv medicinskogo primeneniya. 2020; 10 (1): 19–28. DOI: 10.30895/1991-2919-2020-10-1-19-28. Russian.
- Zemskova ZS, Arijei BM, Babaeva IJu, Erohin VV, Zjuzja JuR., Lepeha LN. Tuberkulez (vklad otechestvennyh uchenyh HH stoletija v razvitiye ftiziatrii). M.: Izd-vo Sechenovskogo universiteta, 2020; 352 s. Russian.
- Shepelkova GS, Evstifeev VV, Apt AS. Issledovanie molekularnykh mehanizmov patogeneza tuberkuleza na jekspertimental'nyh modeljah. Tuberkulez i bolezni legkih. 2012; 89 (7): 3–11. Russian.
- Singhal A, Aliouat el M, Hervé M, Mathys V, Kiass M, Creusy C, et al. Experimental tuberculosis in the Wistar rat: a model for protective immunity and control of infection. PLoS One. 2011; 6 (4): e18632. PubMed PMID: 21533270. DOI: 10.1371/journal.pone.0018632.
- Graur D, Duret L, Gouy M. Phylogenetic position of the order Lagomorpha (rabbits, hares and allies). Nature. 1996; 379 (6563): 333–5. PubMed PMID: 8552186. DOI: 10.1038/379333a0.
- Bujanov VM, Rodoman GV, Belous GG. Jeksperimental'naja model' ostrogo gnojnogo peritonita. Hirurgija. Zhurnal im. N. I. Piropova. 1997; 1: 25–28. Russian.
- Knutsen KM, Skuterud B, Halvorsen S. Hemoperfusion ved forgiftninger [Hemoperfusion in poisoning]. Tidsskr Nor Laegeforen. 1979; 99 (3): 172–4. PubMed PMID: 419497.
- Dobbie JW. Serositis: comparative analysis of histological findings and pathogenetic mechanisms in nonbacterial serosal inflammation. Perit Dial Int. 1993; 13 (4): 256–69. PubMed PMID: 8241326.
- Mohan VP, Scanga CA, Yu K, Scott HM, Tanaka KE, Tsang E, et al. Effects of tumor necrosis factor alpha on host immune response in chronic persistent tuberculosis: possible role for limiting pathology. Infect Immun. 2001; 69 (3): 1847–55. PubMed PMID: 11179363. DOI: 10.1128/IAI.69.3.1847-1855.2001.
- Roach DR, Bean AG, Demangel C, France MP, Briscoe H, Britton WJ. TNF regulates chemokine induction essential for cell recruitment, granuloma formation, and clearance of mycobacterial

- infection. *J Immunol.* 2002; 168 (9): 4620–7. PubMed PMID: 11971010. DOI: 10.4049/jimmunol.168.9.4620.
24. Saleh MA, Ramadan MM, Arram EO. Toll-like receptor-2 Arg753Gln and Arg677Trp polymorphisms and susceptibility to pulmonary and peritoneal tuberculosis. *APMIS.* 2017; 125 (6): 558–64. PubMed PMID: 28332241. DOI: 10.1111/apm.12680.
 25. Aleshkin VA, Lozhkina AN, Zagorodnjaja JeD. *Immunologija reprodukcii.* Chita, 2004; 79 s. Russian.
 26. Krekova JuV. Izmenenie funkcion'nogo sostojaniya immunnoj sistemy u bol'nyh razlichnymi tipami saharnogo diabeta [dissertacija]. 2002; 122 s. Russian.
 27. Shatalin JuV, Naumov AA, Pocelueva MM. Izmenenie sostava kletochnyh populacij i urovnya aktivnyh form kisloroda v krovi i asciticheskoy zhidkosti opuholenositelja. *Citologija.* 2010; 52 (2): 131–35. Russian.
 28. Rohit A, Abraham G. Peritoneal dialysis related peritonitis due to *Mycobacterium* spp.: A case report and review of literature. *J Epidemiol Glob Health.* 2016; 6 (4): 243–8. PubMed PMID: 27443487. DOI: 10.1016/j.jegh.2016.06.005.
 29. Pornprasert S, Leechanachai P, Klinbuayaem V, Leenasirimakul P, Promping C, Inta P, et al. Unmasking tuberculosis-associated immune reconstitution inflammatory syndrome in HIV-1 infection after antiretroviral therapy. *Asian Pac J Allergy Immunol.* 2010; 28 (2–3): 206–9. PubMed PMID: 21038792.
 30. Roth S, Delmont E, Heudier P, Kaphan R, Cua E, Castela J, et al. Anticorps anti-TNF alpha (infliximab) et tuberculose: à propos de trois cas [Anti-TNF alpha monoclonal antibodies (infliximab) and tuberculosis: apropos of 3 cases]. *Rev Med Interne.* 2002; 23 (3): 312–6. PubMed PMID: 11928379. DOI: 10.1016/s0248-8663(01)00556-2.
 31. Moule MG, Cirillo JD. Mycobacterium tuberculosis Dissemination Plays a Critical Role in Pathogenesis. *Front Cell Infect Microbiol.* 2020; 10: 65. PubMed PMID: 32161724. DOI: 10.3389/fcimb.2020.00065.

Литература

1. Behr MA, Edelstein PH, Ramakrishnan L. Is *Mycobacterium tuberculosis* infection life long? *BMJ.* 2019; 367: l5770. PubMed PMID: 31649096. DOI: 10.1136/bmj.l5770.
2. WHO. Global Tuberculosis Report 2020. World Health Organization, Geneva, 2020. Available at: https://www.who.int/tb/publications/global_report/en.
3. Мирзоян Э. З. Туберкулез кишечника и брюшины. В книге: В. Л. Эйнис, редактор. Многотомное руководство по туберкулезу. Т. 3. М.: Медгиз, 1960; с. 125–146.
4. Оносовский В. В. О лечении туберкулезного перитонита у детей, по материалам Ольгинской детской больницы в Москве за 36 лет. Проблемы туберкулеза. 1923; 5–6 (1): 148–155.
5. Савоненкова Л. Н., Арямкина О. Л. Патогенез и морфогенез абдоминального туберкулеза с поражением гастроинтестинального тракта. *Нижегородский медицинский журнал.* 2006; 2: 89–94.
6. Dülger AC, Karadaş S, Mete R, Türkdoğan MK, Demirkiran D, Gültepe B. Analysis of cases with tuberculous peritonitis: a single-center experience. *Turk J Gastroenterol.* 2014; 25 (1): 72–8. PubMed PMID: 24918135. DOI: 10.5152/tjg.2014.5145.
7. Беллендир Э. Н. Патогенез внелегочных локализаций туберкулеза. В книге: А. В. Васильев, редактор. Внелегочный туберкулез. СПб., 2000; с. 36–48.
8. Singh MM, Bhargava AN, Jain KP. Tuberculous peritonitis. An evaluation of pathogenetic mechanisms, diagnostic procedures and therapeutic measures. *N Engl J Med.* 1969; 281 (20): 1091–4. PubMed PMID: 5824174. DOI: 10.1056/NEJM196911132812003.
9. Безредка А. М. Очерки по иммунитету. М–Л., 1929; 267 с.
10. Кишенский Д. Н. Влияние чревосечения на туберкулез брюшины. Экспериментальное исследование [диссертация]. М.: Товарищество типографии А. И. Мамонтова, 1894; 82 с.
11. Lurie MB. The fate of tubercle bacilli in the organs of reinfected rabbits. *J Exp Med.* 1929; 50 (6): 747–765. PubMed PMID: 19869661. DOI: 10.1084/jem.50.6.747.
12. Roach DR, Bean AG, Demangel C, France MP, Briscoe H, Britton WJ. TNF regulates chemokine induction essential for cell recruitment, granuloma formation, and clearance of mycobacterial infection. *J Immunol.* 2002; 168 (9): 4620–7. PubMed PMID: 11971010. DOI: 10.4049/jimmunol.168.9.4620.
13. Brissot E, Bernard DG, Loréal O, Brissot P, Troadec MB. Too much iron: A masked foe for leukemias. *Blood Rev.* 2020; 39: 100617. PubMed PMID: 31753415. DOI: 10.1016/j.bbrev.2019.100617.
14. Шекунова Е. В., Ковалева М. А., Макарова М. Н., Макаров В. Г. Выбор дозы препарата для доклинического исследования: межвидовой перенос доз. *Ведомости Научного центра экспертизы средств медицинского применения.* 2020; 10 (1): 19–28. DOI: 10.30895/1991-2919-2020-10-1-19-28.
15. Земскова З. С., Ариэль Б. М., Бабаева И. Ю., Ерохин В. В., Зюзя Ю. Р., Лепеха Л. Н. Туберкулез (вклад отечественных ученых XX столетия в развитие фтизиатрии). М.: Изд-во Сеченовского университета, 2020; 352 с.
16. Шепелькова Г. С., Евстифеев В. В., Айт А. С. Исследование молекулярных механизмов патогенеза туберкулеза на экспериментальных моделях. *Туберкулез и болезни легких.* 2012; 89 (7): 3–11.
17. Singhal A, Aliouat el M, Hervé M, Mathys V, Kiass M, Creusy C, et al. Experimental tuberculosis in the Wistar rat: a model for protective immunity and control of infection. *PLoS One.* 2011; 6 (4): e18632. PubMed PMID: 21533270. DOI: 10.1371/journal.pone.0018632.
18. Graur D, Duret L, Gouy M. Phylogenetic position of the order Lagomorpha (rabbits, hares and allies). *Nature.* 1996; 379 (6563): 333–5. PubMed PMID: 8552186. DOI: 10.1038/379333a0.
19. Буюнов В. М., Родоман Г. В., Белоус Г. Г. Экспериментальная модель острого гнойного перитонита. *Хирургия. Журнал им. Н. И. Пирогова.* 1997; 1: 25–28.
20. Knutsen KM, Skuterud B, Halvorsen S. Hemoperfusion ved forgiftninger [Hemoperfusion in poisoning]. *Tidsskr Nor Laegeforen.* 1979; 99 (3): 172–4. PubMed PMID: 419497.
21. Dobbie JW. Serositis: comparative analysis of histological findings and pathogenetic mechanisms in nonbacterial serosal inflammation. *Perit Dial Int.* 1993; 13 (4): 256–69. PubMed PMID: 8241326.
22. Mohan PV, Scanga CA, Yu K, Scott HM, Tanaka KE, Tsang E, et al. Effects of tumor necrosis factor alpha on host immune response in chronic persistent tuberculosis: possible role for limiting pathology. *Infect Immun.* 2001; 69 (3): 1847–55. PubMed PMID: 11179363. DOI: 10.1128/IAI.69.3.1847-1855.2001.
23. Roach DR, Bean AG, Demangel C, France MP, Briscoe H, Britton WJ. TNF regulates chemokine induction essential for cell recruitment, granuloma formation, and clearance of mycobacterial infection. *J Immunol.* 2002; 168 (9): 4620–7. PubMed PMID: 11971010. DOI: 10.4049/jimmunol.168.9.4620.
24. Saleh MA, Ramadan MM, Arram EO. Toll-like receptor-2 Arg753Gln and Arg677Trp polymorphisms and susceptibility to pulmonary and peritoneal tuberculosis. *APMIS.* 2017; 125 (6): 558–64. PubMed PMID: 28332241. DOI: 10.1111/apm.12680.
25. Алешкин В. А., Ложкина А. Н., Загородняя Э. Д. Иммунология репродукции. Чита, 2004; 79 с.
26. Крекова Ю. В. Изменение функционального состояния иммунной системы у больных различными типами сахарного диабета [диссертация]. 2002; 122 с.
27. Шаталин Ю. В., Наумов А. А., Поцелуева М. М. Изменение состава клеточных популяций и уровня активных форм кислорода в крови и асцитической жидкости опухоленосителя. *Цитология.* 2010; 52 (2): 131–35.
28. Rohit A, Abraham G. Peritoneal dialysis related peritonitis due to *Mycobacterium* spp.: A case report and review of literature. *J Epidemiol Glob Health.* 2016; 6 (4): 243–8. PubMed PMID: 27443487. DOI: 10.1016/j.jegh.2016.06.005.
29. Pornprasert S, Leechanachai P, Klinbuayaem V, Leenasirimakul

- P, Promping C, Inta P, et al. Unmasking tuberculosis-associated immune reconstitution inflammatory syndrome in HIV-1 infection after antiretroviral therapy. *Asian Pac J Allergy Immunol.* 2010; 28 (2–3): 206–9. PubMed PMID: 21038792.
30. Roth S, Delmont E, Heudier P, Kaphan R, Cua E, Castela J, et al. Anticorps anti-TNF alpha (infliximab) et tuberculose: à propos de trois cas [Anti-TNF alpha monoclonal antibodies (infliximab) and tuberculosis: apropos of 3 cases]. *Rev Med Interne.* 2002; 23 (3): 312–6. PubMed PMID: 11928379. DOI: 10.1016/s0248-8663(01)00556-2.
31. Moule MG, Cirillo JD. Mycobacterium tuberculosis Dissemination Plays a Critical Role in Pathogenesis. *Front Cell Infect Microbiol.* 2020; 10: 65. PubMed PMID: 32161724. DOI: 10.3389/fcimb.2020.00065.

LABELLING OF DATA ON FUNDUS COLOR PICTURES USED TO TRAIN A DEEP LEARNING MODEL ENHANCES ITS MACULAR PATHOLOGY RECOGNITION CAPABILITIES

Takhchidi HP¹, Gliznitsa PV²✉, Svetozarskiy SN³, Bursov AI⁴, Shusterzon KA⁵

¹ Pirogov Russian National Research Medical University, Moscow, Russia

² OOO Innovatsionniye Tekhnologii (Innovative Technologies, LLC), Nizhny Novgorod, Russia

³ Volga District Medical Center under the Federal Medical-Biological Agency, Nizhny Novgorod, Russia

⁴ Ivannikov Institute for System Programming of RAS, Moscow, Russia

⁵ L.A. Melentiev Energy Systems Institute, Irkutsk, Russia

Retinal diseases remain one of the leading causes of visual impairments in the world. The development of automated diagnostic methods can improve the efficiency and availability of the macular pathology mass screening programs. The objective of this work was to develop and validate deep learning algorithms detecting macular pathology (age-related macular degeneration, AMD) based on the analysis of color fundus photographs with and without data labeling. We used 1200 color fundus photographs from local databases, including 575 retinal images of AMD patients and 625 pictures of the retina of healthy people. The deep learning algorithm was deployed in the Faster RCNN neural network with ResNet50 for convolution. The process employed the transfer learning method. As a result, in the absence of labeling, the accuracy of the model was unsatisfactory (79%) because the neural network selected the areas of attention incorrectly. Data labeling improved the efficacy of the developed method: with the test dataset, the model determined the areas with informative features adequately, and the classification accuracy reached 96.6%. Thus, image data labeling significantly improves the accuracy of retinal color images recognition by a neural network and enables development and training of effective models with limited datasets.

Keywords: retinal diseases, fundus camera, machine learning, screening, biomedical visualization, data labeling

Funding: this work was financially supported by the Foundation for Assistance to Small Innovative Enterprises in Science and Technology (contract №150ГС1ЦТНТИС5/64226 dated December 22, 2020)

Author contribution: Takhchidi HP — manuscript editing; Gliznitsa PV — study concept and design, data collection and processing, results analysis, manuscript writing; Svetozarskiy SN — participation in data collection, literature and results analysis, manuscript writing; Bursov AI — literature analysis, algorithms development, manuscript editing; Shusterzon KA — algorithms development and validation, illustrations preparation, text writing.

✉ Correspondence should be addressed: Pavel V. Gliznitsa
Belinskogo, 58/60, et. 5, 603000, Nizhny Novgorod; gliznitsap@icloud.com

Received: 27.07.2021 **Accepted:** 15.08.2021 **Published online:** 28.08.2021

DOI: 10.24075/brsmu.2021.040

РАЗМЕТКА ЦВЕТНЫХ ФОТОГРАФИЙ ГЛАЗНОГО ДНА УЛУЧШАЕТ РАСПОЗНАВАНИЕ МАКУЛЯРНОЙ ПАТОЛОГИИ С ПОМОЩЬЮ ГЛУБОКОГО ОБУЧЕНИЯ

Х. П. Тахчиди¹, П. В. Глизница²✉, С. Н. Светозарский³, А. И. Бурсов⁴, К. А. Шустерзон⁵

¹ Российский национальный исследовательский медицинский университет имени Н. И. Пирогова, Москва, Россия

² ООО «Инновационные технологии», Нижний Новгород, Россия

³ Приволжский окружной медицинский центр Федерального медико-биологического агентства, Нижний Новгород, Россия

⁴ Институт системного программирования имени В. П. Иванникова РАН, Москва, Россия

⁵ Институт систем энергетики имени Л. А. Мелентьева, Иркутск, Россия

Заболевания сетчатки остаются одной из ведущих причин слабовидения в мире. Разработка методов автоматизированной диагностики может повысить эффективность и доступность программ массового скрининга патологии макулярной области. Целью работы было разработать и провалидировать алгоритмы машинного обучения для диагностики макулярной патологии на основе анализа цветных фотографий глазного дна с предварительной разметкой данных и без нее на примере возрастной макулярной дегенерации (ВМД). В исследовании использовали 1200 цветных фотографий глазного дна из локальных баз данных, включая 575 изображений сетчатки пациентов с ВМД и 625 ретинальных фотографий здоровых пациентов. Алгоритм глубокого обучения был реализован на основе нейронной сети Faster RCNN с ResNet50 в качестве сверточной основы с использованием трансферного обучения. В результате, при отсутствии разметки валидация показала неудовлетворительную точность модели (79%), что было связано с неправильным выбором нейросетью областей внимания. Выполнение разметки повысило эффективность разработанной методики, на тестовом наборе данных модель продемонстрировала адекватное определение информативных участков, точность классификации достигла 96.6%. Таким образом, применение разметки изображений значительно повышает точность распознавания цветных изображений сетчатки с помощью нейросетевых технологий и позволяет создавать эффективные модели при использовании ограниченных по объему наборов данных.

Ключевые слова: болезни сетчатки, фундус-камера, машинное обучение, скрининг, биомедицинская визуализация, разметка данных

Финансирование: работа выполнена при финансовой поддержке Фонда содействия инновациям (договор №150ГС1ЦТНТИС5/64226 от 22.12.2020).

Вклад авторов: Х. П. Тахчиди — редактирование рукописи. П. В. Глизница — концепция и дизайн исследования, сбор и обработка данных, анализ результатов, написание текста рукописи; С. Н. Светозарский — участие в сборе данных, анализ результатов, работа с литературой, написание текста рукописи; А. И. Бурсов — работа с литературой, разработка алгоритмов, редактирование рукописи; К. А. Шустерзон — разработка и валидация алгоритмов, подготовка иллюстраций, участие в написании текста.

✉ Для корреспонденции: Павел Викторович Глизница
ул. Белинского, д. 58/60, эт. 5, 603000, г. Нижний Новгород; gliznitsap@icloud.com

Статья получена: 27.07.2021 **Статья принята к печати:** 15.08.2021 **Опубликована онлайн:** 28.08.2021

DOI: 10.24075/vrgmu.2021.040

In the Russian Federation, retinal diseases rank second and cause 28.9% of the visual impairment cases [1]. An effective retinal pathology early detection system that would be part of the mass preventive examination campaigns is yet to be deployed. Such systems require special logistics and dedicated staff, which, in addition to the one-time deployment expenses, translates into the need for regular funding to support the system and pay the people powering it. Computers can analyze big data faster, and machine learning algorithms automate the time-consuming and labor-intensive screening of patients to nominate those who need extensive examination. Thus, artificial intelligence capable of screening for eye diseases can mitigate the primary health care personnel shortage and reduce the clinical examination costs while increasing the number of patients reasonably referred to an ophthalmologist because of the suspected ophthalmic pathology [2].

Age-related macular degeneration (AMD), a retinal disease common among people aged 50 and over, remains one of the main causes of poor eyesight. The disease manifests in soft drusen measuring 63 µm or above in the macular zone, hyperpigmentation and/or hypopigmentation of the pigment epithelium, detachment of pigment and neuroepithelium, pigment epithelium geographic atrophy, retinal hemorrhages and cicatricial changes in the retina [3].

AMD is of great clinical and social importance. The prevalence of AMD among people aged 50 to 85 years is 8.69%, with 8.01% being early AMD and 0.37% late stage AMD [4]. Mathematical model forecasts growth of the absolute number of AMD patients from 196 million in 2020 to 288 million in 2040. [4]. Late stage AMD translates into a pronounced degradation of central vision, which worsens quality of life, limits daily living activities and impairs working capacity. Timely detection of the disease and adequate monitoring of the patients are instrumental to successful treatment of neovascular AMD because the efficacy of antiangiogenic therapy directly depends on the time elapsed from the moment of manifestation to administration of the first dose of the drug [5]. Fundus photography is a widely adopted and highly sensitive method of macular pathology visualization; it has been used in a number of countries for mass screening and yielded a significant increase of the early stage AMD detection rates [6].

The objective of this work was to develop and validate machine learning algorithms diagnosing macular pathology (AMD) based on the analysis of color pictures of the fundus with data labeled and unlabeled, and to assess sensitivity and specificity of the developed method with the help of a test dataset.

METHODS

The sets of color images of the fundus used in this study were collected at the Tsentr Zreniya clinic (Chelyabinsk) and the ophthalmological department of the Volga District Medical Center under FMBA of Russia (Nizhny Novgorod). All the pictures were taken with Visucam 500 fundus camera (Carl Zeiss; USA). The inclusion criteria applied to the images were: diagnosed AMD in one eye, registered in the patient's digital

medical record; presence of specific signs of AMD on the image; absence of signs of other retinal diseases (diabetic retinopathy, etc). Image quality was assessed in points on a scale from 1 to 4, the assessment relied on the method by Klais C et al., with 1 point given to high quality pictures, 2 points to average quality images, 3 points to those of low quality and 4 points to indiscernible pictures [7]. The images that scored 3–4 points were rejected. We used the widely adopted clinical classification of AMD that distinguishes early, intermediate and late stages of the disease (Table 1) [8]. The initial set of images was anonymized and blind classified independently by two ophthalmologists with over 5 years of experience.

The resulting set included 1200 color fundus photographs, including 575 retinal images of AMD patients and 625 pictures of the retina of healthy people. Under the AMD classification, 127 images were classified into the early AMD group, 341 were marked as intermediate stage and 107 as late stage AMD pictures.

The data were distributed into training and test sets randomly, with 994 images used in the neural network training (475 eyes with AMD, 519 eyes of healthy people) and 206 photographs used for testing (100 from patients with AMD, 106 from healthy people).

To accomplish the task set, we practiced two approaches to training:

1) training a convolutional neural network (CNN) on a dataset consisting of binary classified images without specified regions of interest;

2) training a CNN on a dataset consisting of binary classified images with the regions of interest specified in bounding boxes;

We relied on the ResNet-50 deep learning architecture and transfer learning for both approaches [9]. Transfer learning involves use of CNNs that are pretrained on a large set of third-party data. Following pretraining, the network, which already has its weighing system set up, goes through training on a small set of data of immediate interest. The large set of third-party data used for pretraining in this work was the ImageNET dataset, which includes millions of images divided into 1000 different classes [10].

Fundus pictures from the local databases were preprocessed (converted to 512 × 512 pixel images) and then processed by a pretrained Faster RCNN neural network with ResNet50 enabling convolution. Each output window was linked with a category tag and a softmax score at [0, 1]. A score threshold of 0.7 was used to display these images. The execution time needed to obtain these results was 120 ms per image, all steps included. All in all, the image analysis sequence can be outlined as follows: preprocessing, processing by the CNN with a feature map as output, highlighting regional suggestions thereon, determining regions of interest and classifying the image as either an AMD picture or a normal eye photograph based on the features found within the regions of interest (Fig. 1).

All algorithms were developed in Python 3.7 using libraries PyTorch 1.5.0, TorchVision 0.6.0, Tensorflow 1.14.0, Keras 2.0.8, Pillow 7.2, OpenCV 4.5.2, Cuda 10.1, cudnn 7.6.5. The hardware configuration of the computer used to do the

Table 1. Clinical classification of AMD [8]

Stage	Symptoms
Normal age-related changes	Small druses up to 63 µm, no pigmentation defects
Early	Drusen with a diameter of 63–125 microns, no pigmentation defects
Intermediate	Drusen with a diameter over 125 microns, pigmentation defective
Late	Neovascular form or geographic atrophy

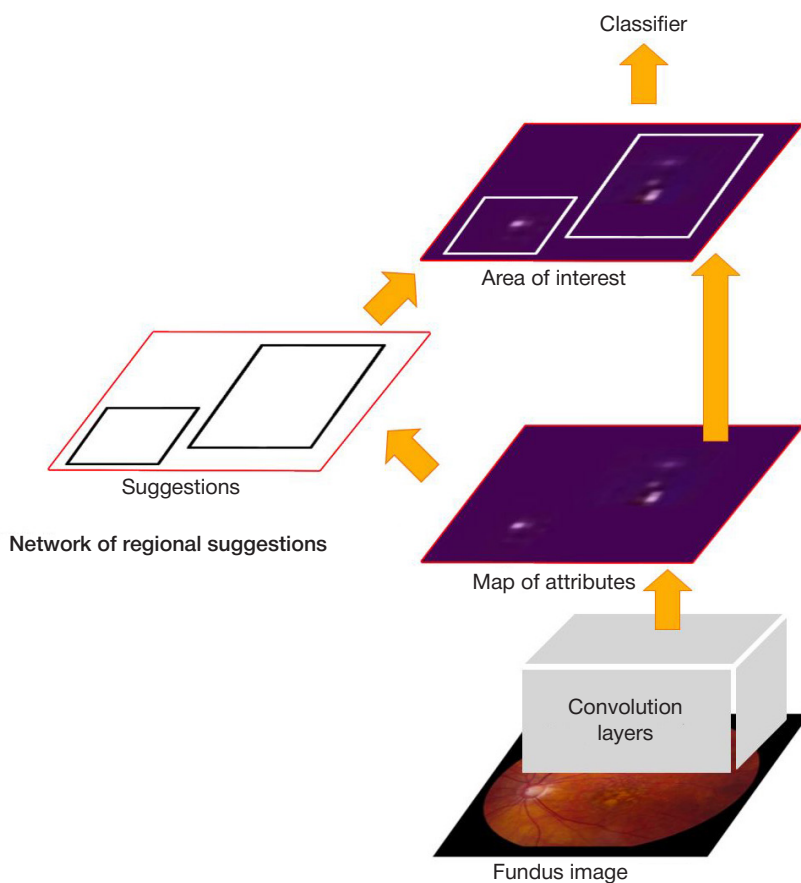


Fig. 1. Stages of image analysis by Faster RCNN

calculations was as follows: Intel Core i7 9750H (Intel; USA), RTX 2070 Max-Q 8GB GDDR6, 16 GB RAM 2666 MHz.

RESULTS

Image classification by a CNN without specified regions of interest

All color images of the fundus belonging to the training set were reduced to a resolution of 512×512 pixels and normalized to the average pixel. Then the dataset was submitted to the neural network for training. The training lasted 193 min and took 50 iterations. A batch (combined load) included 10 images. Nesterov accelerated gradient was used as an optimizer; the learning rate parameter was 0.0005, the moment was 0.9. Loss function — categorical cross-entropy, metric — accuracy.

Validation of the resulting model on the test dataset revealed that its specificity reached 77.4%, sensitivity — 80.9%, accuracy — 79% (Table 2). To learn what regions of the images the model used for classification we imported the class activation heatmaps (Fig. 2).

Table 2. Developed models' performance indicators reflecting the quality of detection of AMD in color fundus photographs

Indicator	Machine learning without labeling	Machine learning with pre-labeling
Sensitivity	80,9%	99,0%
Specificity	77,4%	94,3%
Accuracy	79%	96,6%
Positive result predictability	74%	94,3%
Negative result predictability	82%	99,0%

As a result, it was found that the network selected the areas of attention incorrectly: one of them was the area of the optic nerve head, which is not involved in AMD's pathological process, another — paramacular area. Thus, the neural network used incorrect features in training, which nevertheless correlate with the classification result.

Image classification by a CNN with regions of interest pre-specified

The training dataset was the same as for the first approach, but for this case, we marked the macular region as the region of interest with the help of bounding boxes. All the images were reduced to a resolution of 512×512 pixels and normalized to the average pixel. Faster RCNN + FPN network combination enabled object detection [11]. The training lasted 158 min and took 10 iterations. A batch included 10 images. Nesterov accelerated gradient was used as an optimizer; the learning rate parameter was 0.0001, the moment was 0.05, weight decay — 0.0005. Classification categorical cross-entropy was the loss function, mean average accuracy was the classification accuracy metric,

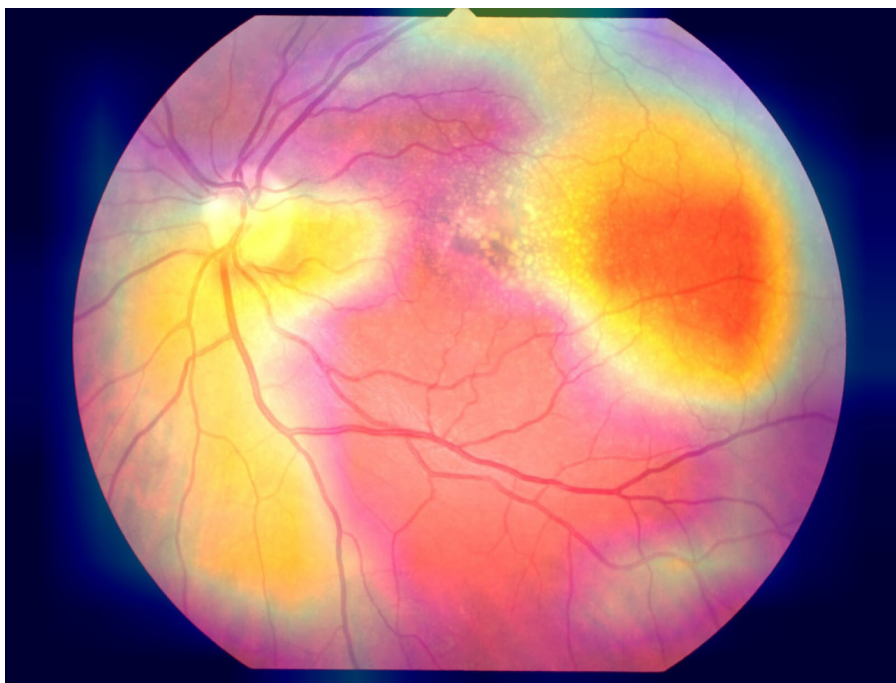


Fig. 2. Class activation heatmap visualization example, fundus photograph of an AMD patient

intersection over union — detection accuracy metric. The training was stopped after 10 iterations because of the emerging overtraining effect [12].

On the test dataset, the model demonstrated the classification accuracy of 96.6% at sensitivity of 99.0% and specificity of 94.3% (Table 2). Visualization of the areas of interest showed that the model identified informative areas of the images adequately (Fig. 3).

DISCUSSION

This study showed that Faster RCNN neural network with ResNet50 enabling convolution can effectively differentiate between AMD patient fundus pictures and those of healthy

retina. We have also established that even with a small sample (1200 images) the resulting classification accuracy can be high if the data are pre-labeled.

Researchers investigating application of neural networks to diagnose AMD through analysis of color pictures of the retina reported sensitivity of 84.5–89.0%, specificity of 83.1–89.0% and accuracy of 88.4–91.6% [13, 14]. One study aimed to detect AMD at the early stage using images of the fundus; its authors claimed to have achieved sensitivity and specificity of 96.7%, 96.4% [15]. The datasets used in these works were not pre-labeled, but each of them relied on the sample comprised of over 50000 images, which is an order of magnitude greater than the sample used for this study [13–15]. In this connection, it is interesting to note that, considering the

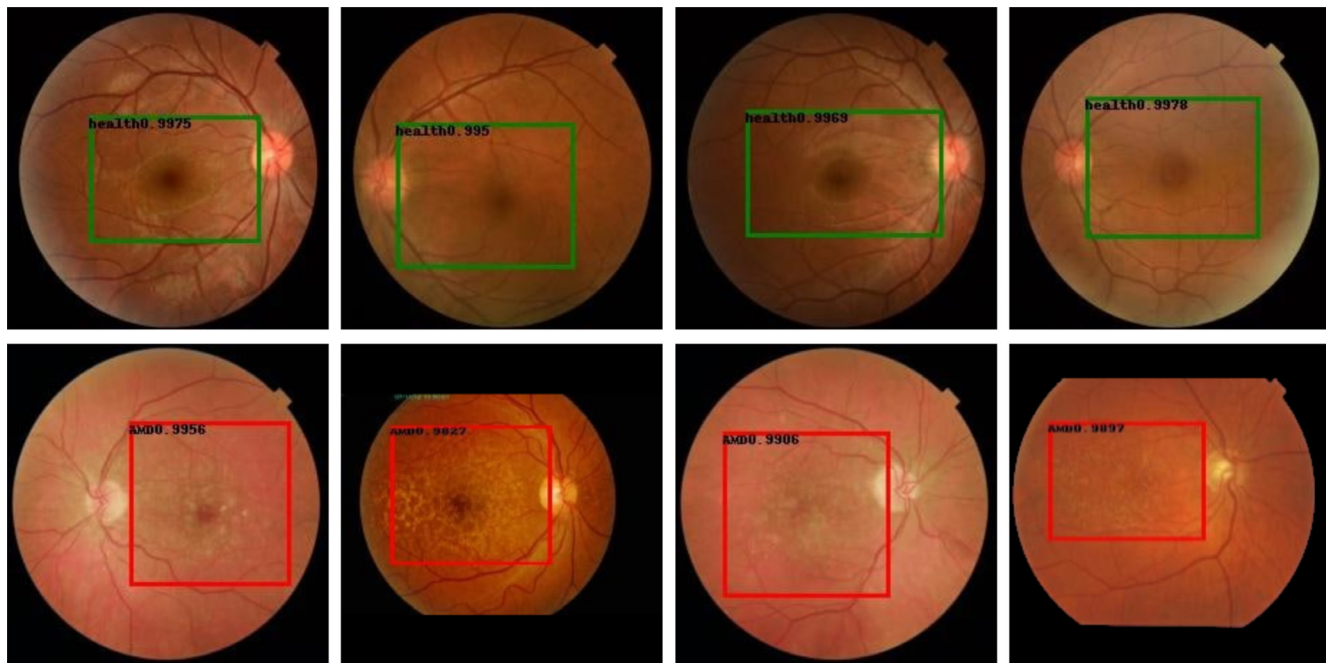


Fig. 3. Results of detection of regions of interest and classification of images from the test dataset by Faster RCNN with ResNet50 for convolution. Images correctly identified by the model as healthy retina photographs have green boxes, those with AMD detected have red boxes

relatively small dataset employed, by some parameters we received comparable results with the help of a simple and fast labeling procedure.

A meta-analysis of 13 studies averaged the neural networks' sensitivity and specificity in AMD detection at 0.92 and 0.89, respectively [16]. However, this analysis included studies that made use of fundus camera images exclusively and works that relied on the pictures obtained with optical coherence tomography. Another meta-analysis considered papers reporting on the automated AMD diagnosing models that processed only color photographs of the retina; this analysis averaged the models' sensitivity and specificity at 0.88 and 0.90, respectively [17]. Thus, the level of accuracy we have achieved is comparable to the results of studies based on much larger datasets.

It should be noted that instant AMD diagnostics using color images of the fundus traditionally underpins the relevant mass screening programs, but has limited application in specialized care. What shows promise in this field is the determination of AMD stages from the available dataset [18–20] and the identification of individual pathological elements in the images [21], which can serve the purposes of monitoring in the context of clinical observation and during clinical trials.

On the one hand, small size of the training dataset and the decision to not differentiate between stages of AMD (we used one class for all of them) can be considered a limitation of this work. On the other hand, with these prerequisites, we managed

to answer the questions posed. The small dataset confirmed that, with a limited sample available at a local database, it is possible to successfully develop models capable of automated retinal disease diagnosing provided the training dataset is pre-labeled. The clinical heterogeneity of pathological changes allows simulation of a real life screening situation, where it is necessary to detect various pathologies with high sensitivity in order to refer the patients for further examination.

CONCLUSIONS

Automated diagnostics of retinal diseases, which are among the top causes of blindness and poor eyesight, opens new opportunities for mass screening for AMD. The fast and easy-to-use method of image markup with bounding boxes significantly increases accuracy of the developed methods of recognition of medical images relying on neural networks. As a result, it is possible to achieve high classification accuracy even when there are only small local databases available. At the same time, it underscores the importance of the role played by medical specialists in the development of new diagnostic methods based on machine learning, which requires consolidation of efforts of ophthalmologists and IT engineers in order to create large annotated databases of retinal images collected with various models of fundus cameras, which, when labeling the data thereon, would ensure high accuracy and reproducibility of the results in real clinical practice.

References

- Nazarjan MG, Vertash OYu. Analiz pokazatelej pervichnoj i povtornoj invalidnosti vsledstvie boleznej glaza u lic pensionnogo vozrasta v Rossijskoj Federacii i Moskve. Uspehi gerontologii. 2019; 32 (1–2): 215–17. Russian.
- Armstrong GW, Lorch AC. A(eye): A Review of Current Applications of Artificial Intelligence and Machine Learning in Ophthalmology. *Int Ophthalmol Clin.* 2020; 60 (1): 57–71. DOI: 10.1097/IIO.0000000000000298. PMID: 31855896.
- Bird AC, Bressler NM, Bressler SB, Chisholm IH, Coscas G, Davis MD, et al. An international classification and grading system for age-related maculopathy and age-related macular degeneration. The International ARM Epidemiological Study Group. *Surv Ophthalmol.* 1995; 39 (5): 367–74.
- Wong WL, Su X, Li X, et al. Global prevalence of age-related macular degeneration and disease burden projection for 2020 and 2040: a systematic review and meta-analysis. *Lancet Glob Health.* 2014; 2 (2): e106–e116. DOI: 10.1016/S2214-109X(13)70145-1.
- Schwartz R, Warwick A, Olvera-Barrios A, Pikoula M, Lee AY, Denaxas S, et al. Evolving treatment patterns and outcomes of neovascular age-related macular degeneration over a decade. *Ophthalmol Retina.* 2021; 5 (8): e11–e22. DOI: 10.1016/j.oret.2021.04.001. Epub ahead of print. PMID: 33866023.
- Danis RP, Domalpally A, Chew EY, et al. Methods and reproducibility of grading optimized digital color fundus photographs in the Age-Related Eye Disease Study 2 (AREDS2 Report Number 2). *Invest Ophthalmol Vis Sci.* 2013; 54 (7): 4548–54.
- Klais C, et al. Photoscreening for diabetic retinopathy: a comparison of image quality between film photography and digital imaging. *Clin Experiment Ophthalmol.* 2004; 32: 393–6.
- Ferris 3rd FL, Wilkinson CP, Bird A, et al. Clinical classification of age-related macular degeneration. *Ophthalmology.* 2013; 120 (4): 844–51.
- He K, Zhang X, Ren S, Sun J. Deep Residual Learning for Image Recognition. 2016 IEEE Conference on Computer Vision and Pattern Recognition (CVPR). 2016, pp. 770–778. DOI: 10.1109/CVPR.2016.90.
- Deng J, Dong W, Socher R, Li L, Li K, Fei-Fei L. ImageNet: A large-scale hierarchical image database. 2009 IEEE Conference on Computer Vision and Pattern Recognition. 2009; pp. 248–255. DOI: 10.1109/CVPR.2009.5206848.
- Ren S, He K, Girshick R, Sun J. Faster R-CNN: Towards Real-Time Object Detection with Region Proposal Networks. *IEEE Transactions on Pattern Analysis and Machine Intelligence.* 2017; 39 (6): 1137–49. DOI: 10.1109/TPAMI.2016.2577031.
- Lee CS, Baughman DM, Lee AY. Deep learning is effective for the classification of OCT images of normal versus Age-related Macular Degeneration. *Ophthalmol Retina.* 2017; 1 (4): 322–7. DOI: 10.1016/j.oret.2016.12.009.
- Burlina P, Joshi N, Pacheco KD, Freund DE, Kong J, Bressler NM. Utility of Deep Learning Methods for Referability Classification of Age-Related Macular Degeneration. *JAMA Ophthalmol.* 2018; 136 (11): 1305–7. DOI: 10.1001/jamaophthalmol.2018.3799.
- Burlina PM, Joshi N, Pekala M, Pacheco KD, Freund DE, Bressler NM. Automated Grading of Age-Related Macular Degeneration From Color Fundus Images Using Deep Convolutional Neural Networks. *JAMA Ophthalmol.* 2017 Nov 1; 135 (11): 1170–6. DOI: 10.1001/jamaophthalmol.2017.3782. PMID: 28973096; PMCID: PMC5710387.
- Keel S, Li Z, Scheetz J, Robman L, Phung J, Makeyeva G, et al. Development and validation of a deep-learning algorithm for the detection of neovascular age-related macular degeneration from colour fundus photographs. *Clin Exp Ophthalmol.* 2019 Nov; 47 (8): 1009–18. DOI: 10.1111/ceo.13575. Epub 2019 Jul 25. PMID: 31215760.
- Cheung R, Chun J, Sheidow T, Motolko M, Malvankar-Mehta MS. Diagnostic accuracy of current machine learning classifiers for age-related macular degeneration: a systematic review and meta-analysis. *Eye (Lond).* 2021 May 6. DOI: 10.1038/s41433-021-01540-y. Epub ahead of print. PMID: 33958739.
- Dong L, Yang Q, Zhang RH, Wei WB. Artificial intelligence for the detection of age-related macular degeneration in color fundus photographs: A systematic review and meta-analysis.

- E Clinical Medicine. 2021 May 8; 35: 100875. DOI: 10.1016/j.eclinm.2021.100875. PMID: 34027334; PMCID: PMC8129891.
18. Grassmann F, Mengelkamp J, Brandl C, Harsch S, Zimmermann ME, Linkohr B, et al. A Deep Learning Algorithm for Prediction of Age-Related Eye Disease Study Severity Scale for Age-Related Macular Degeneration from Color Fundus Photography. *Ophthalmology*. 2018 Sep; 125 (9): 1410–20. DOI: 10.1016/j.ophtha.2018.02.037. Epub 2018 Apr 10. PMID: 29653860.
 19. Peng Y, Dharssi S, Chen Q, Keenan TD, Agrón E, Wong WT, et al. DeepSeeNet: A Deep Learning Model for Automated Classification of Patient-based Age-related Macular Degeneration Severity from Color Fundus Photographs. *Ophthalmology*. 2019 Apr; 126 (4): 565–75. DOI: 10.1016/j.ophtha.2018.11.015. Epub 2018 Nov 22. PMID: 30471319; PMCID: PMC6435402.
 20. Keenan TD, Dharssi S, Peng Y, Chen Q, Agrón E, Wong WT, et al. A Deep Learning Approach for Automated Detection of Geographic Atrophy from Color Fundus Photographs. *Ophthalmology*. 2019 Nov; 126 (11): 1533–40. DOI: 10.1016/j.ophtha.2019.06.005. Epub 2019 Jun 11. PMID: 31358385; PMCID: PMC6810830.
 21. Keenan TDL, Chen Q, Peng Y, Domalpally A, Agrón E, Hwang CK, et al. Deep Learning Automated Detection of Reticular Pseudodrusen from Fundus Autofluorescence Images or Color Fundus Photographs in AREDS2. *Ophthalmology*. 2020 Dec; 127 (12): 1674–87. DOI: 10.1016/j.ophtha.2020.05.036. Epub 2020 May 21. PMID: 32447042.

Литература

1. Назарян М. Г., Верташ О. Ю. Анализ показателей первичной и повторной инвалидности вследствие болезней глаза у лиц пенсионного возраста в Российской Федерации и Москве. Успехи геронтологии. 2019; 32 (1–2): 215–17.
2. Armstrong GW, Lorch AC. A(eye): A Review of Current Applications of Artificial Intelligence and Machine Learning in Ophthalmology. *Int Ophthalmol Clin*. 2020; 60 (1): 57–71. DOI: 10.1097/IIO.0000000000000298. PMID: 31855896.
3. Bird AC, Bressler NM, Bressler SB, Chisholm IH, Coscas G, Davis MD, et al. An international classification and grading system for age-related maculopathy and age-related macular degeneration. The International ARM Epidemiological Study Group. *Surv Ophthalmol*. 1995; 39 (5): 367–74.
4. Wong WL, Su X, Li X, et al. Global prevalence of age-related macular degeneration and disease burden projection for 2020 and 2040: a systematic review and meta-analysis. *Lancet Glob Health*. 2014; 2 (2): e106–e116. DOI: 10.1016/S2214-109X(13)70145-1.
5. Schwartz R, Warwick A, Olvera-Barrios A, Pikoula M, Lee AY, Denaxas S, et al. Evolving treatment patterns and outcomes of neovascular age-related macular degeneration over a decade. *Ophthalmol Retina*. 2021; 5 (8): e11–e22. DOI: 10.1016/j.oret.2021.04.001. Epub ahead of print. PMID: 33866023.
6. Danis RP, Domalpally A, Chew EY, et al. Methods and reproducibility of grading optimized digital color fundus photographs in the Age-Related Eye Disease Study 2 (AREDS2 Report Number 2). *Invest Ophthalmol Vis Sci*. 2013; 54 (7): 4548–54.
7. Klaas C, et al. Photoscreening for diabetic retinopathy: a comparison of image quality between film photography and digital imaging. *Clin Experiment Ophthalmol*. 2004; 32: 393–6.
8. Ferris 3rd FL, Wilkinson CP, Bird A, et al. Clinical classification of age-related macular degeneration. *Ophthalmology*. 2013; 120 (4): 844–51.
9. He K, Zhang X, Ren S, Sun J. Deep Residual Learning for Image Recognition. 2016 IEEE Conference on Computer Vision and Pattern Recognition (CVPR). 2016, pp. 770–778. DOI: 10.1109/CVPR.2016.90.
10. Deng J, Dong W, Socher R, Li L, Li K, Fei-Fei L. ImageNet: A large-scale hierarchical image database. 2009 IEEE Conference on Computer Vision and Pattern Recognition. 2009; pp. 248–255. DOI: 10.1109/CVPR.2009.5206848.
11. Ren S, He K, Girshick R, Sun J. Faster R-CNN: Towards Real-Time Object Detection with Region Proposal Networks. *IEEE Transactions on Pattern Analysis and Machine Intelligence*. 2017; 39 (6): 1137–49. DOI: 10.1109/TPAMI.2016.2577031.
12. Lee CS, Baughman DM, Lee AY. Deep learning is effective for the classification of OCT images of normal versus Age-related Macular Degeneration. *Ophthalmol Retina*. 2017; 1 (4): 322–7. DOI: 10.1016/j.oret.2016.12.009.
13. Burlina P, Joshi N, Pacheco KD, Freund DE, Kong J, Bressler NM. Utility of Deep Learning Methods for Referability Classification of Age-Related Macular Degeneration. *JAMA Ophthalmol*. 2018; 136 (11): 1305–7. DOI: 10.1001/jamaophthalmol.2018.3799.
14. Burlina PM, Joshi N, Pekala M, Pacheco KD, Freund DE, Bressler NM. Automated Grading of Age-Related Macular Degeneration From Color Fundus Images Using Deep Convolutional Neural Networks. *JAMA Ophthalmol*. 2017 Nov 1; 135 (11): 1170–6. DOI: 10.1001/jamaophthalmol.2017.3782. PMID: 28973096; PMCID: PMC5710387.
15. Keel S, Li Z, Scheetz J, Robman L, Phung J, Makeyeva G, et al. Development and validation of a deep-learning algorithm for the detection of neovascular age-related macular degeneration from colour fundus photographs. *Clin Exp Ophthalmol*. 2019 Nov; 47 (8): 1009–18. DOI: 10.1111/ceo.13575. Epub 2019 Jul 25. PMID: 31215760.
16. Cheung R, Chun J, Sheidow T, Motolko M, Malvankar-Mehta MS. Diagnostic accuracy of current machine learning classifiers for age-related macular degeneration: a systematic review and meta-analysis. *Eye (Lond)*. 2021 May 6. DOI: 10.1038/s41433-021-01540-y. Epub ahead of print. PMID: 33958739.
17. Dong L, Yang Q, Zhang RH, Wei WB. Artificial intelligence for the detection of age-related macular degeneration in color fundus photographs: A systematic review and meta-analysis. *E Clinical Medicine*. 2021 May 8; 35: 100875. DOI: 10.1016/j.eclinm.2021.100875. PMID: 34027334; PMCID: PMC8129891.
18. Grassmann F, Mengelkamp J, Brandl C, Harsch S, Zimmermann ME, Linkohr B, et al. A Deep Learning Algorithm for Prediction of Age-Related Eye Disease Study Severity Scale for Age-Related Macular Degeneration from Color Fundus Photography. *Ophthalmology*. 2018 Sep; 125 (9): 1410–20. DOI: 10.1016/j.ophtha.2018.02.037. Epub 2018 Apr 10. PMID: 29653860.
19. Peng Y, Dharssi S, Chen Q, Keenan TD, Agrón E, Wong WT, et al. DeepSeeNet: A Deep Learning Model for Automated Classification of Patient-based Age-related Macular Degeneration Severity from Color Fundus Photographs. *Ophthalmology*. 2019 Apr; 126 (4): 565–75. DOI: 10.1016/j.ophtha.2018.11.015. Epub 2018 Nov 22. PMID: 30471319; PMCID: PMC6435402.
20. Keenan TD, Dharssi S, Peng Y, Chen Q, Agrón E, Wong WT, et al. A Deep Learning Approach for Automated Detection of Geographic Atrophy from Color Fundus Photographs. *Ophthalmology*. 2019 Nov; 126 (11): 1533–40. DOI: 10.1016/j.ophtha.2019.06.005. Epub 2019 Jun 11. PMID: 31358385; PMCID: PMC6810830.
21. Keenan TDL, Chen Q, Peng Y, Domalpally A, Agrón E, Hwang CK, et al. Deep Learning Automated Detection of Reticular Pseudodrusen from Fundus Autofluorescence Images or Color Fundus Photographs in AREDS2. *Ophthalmology*. 2020 Dec; 127 (12): 1674–87. DOI: 10.1016/j.ophtha.2020.05.036. Epub 2020 May 21. PMID: 32447042.

ROLE OF MAST CELLS IN SKIN REGENERATION AFTER THERMAL BURN TREATED WITH MELATONIN-ENRICHED DERMAL FILM

Osikov MV^{1,2}, Ageeva AA^{1✉}, Fedosov AA³, Ushakova VA¹

¹ South-Ural State Medical University, Chelyabinsk, Russia

² Chelyabinsk Regional Clinical Hospital, Chelyabinsk, Russia

³ Pirogov Russian National Research Medical University, Moscow, Russia

The development of novel local therapies for thermal burns (TB) and their pathogenetic rationale are a pressing challenge. Melatonin (MT) is an endogenous factor of hemostasis regulation with pleiotropic potential. The aim of this study was to assess some parameters of tissue regeneration, the functional state of mast cells and the levels of matrix metalloproteinase-9 (MMP-9) and vascular endothelial growth factor (VEGF) in the experimentally induced TB treated with the original MT-enriched dermal film (DF). A second-degree burn (3.5% of the total body surface area) was modelled by exposing a patch of skin to hot water. Applications of 12 cm² DF enriched with 5 mg/g MT were performed every day for 5 days. The following parameters were calculated: the wound area, the rate of wound epithelization, the number of MC in the wound, the intensity of degranulation, and the levels of MMP-9 and VEGF expression. Over the course of treatment, the absolute wound area shrank by 35%, its epithelization rate increased, the number of MC rose, their functional state changed, and the expression of MMP-9 and VEGF increased. A negative correlation was established between the wound area and the expression of MMP-9 and VEGF, as well as between the wound area and the degranulation coefficient. Applications of MT-enriched DF resulted in the reduction of the wound area, higher epithelization rate, an increase in the total MC count and degranulation intensity on days 5 and 10; it also led to a reduction in the total MC count and a loss in degranulation intensity on day 20 (166.87 (154.95; 178.78) un/mm² vs. 464.84 (452.92; 476.76) un/mm²) in the group of intact animals), an increase in MMP-9 expression on day 5 (14.20 (11.30; 18.10) vs. 3.30 (2.20; 4.40) in the intact group), an increase in VEGF expression on days 5 and 10 (33.00 (30.20; 34.90) vs 25.40 (22.20; 29.30) in the intact group), and a reduction in MMP-9 expression on days 10 and 20 after thermal injury.

Keywords: thermal burn, melatonin, dermal film, regeneration, VEGF, MMP-9

Funding: the study was supported by the Russian Foundation for Basic Research and the government of Chelyabinsk region (Project ID 20-415-740016).

Author contribution: Osikov MV — study concept and design; integral analysis of the obtained data; manuscript preparation and editing; Ageeva AA — data acquisition; statistical analysis; analysis of study results; manuscript preparation; Fedosov AA — analysis of study results; manuscript editing; Ushakova VA — synthesis of the dermal film; analysis of study results.

Compliance with ethical standards: the study was approved by the Ethics Committee of South-Ural State Medical University (Protocol № 10 dated November 15, 2019). The study was conducted at a standard vivarium in strict compliance with guidelines on the care and euthanasia of laboratory animals outlined in the European Convention for the Protection of Vertebrate Animals used for Experimental and other Scientific Purposes (ETS № 123 , March 18, 1986, Strasburg), the EU Commission Recommendation 2007/526/EC on Guidelines for the Accommodation and Care of Animals used for Experimental and other Scientific Purposes (June 18, 2007), and the Directive 2010/63/EU of the European Parliament and of the Council on the Protection of Animals used for Scientific Purposes (September 22, 2010).

✉ Correspondence should be addressed: Anna A. Ageeva
Vorovskogo, 64, Chelyabinsk, 454092; anne.ageeva.r@yandex.ru

Received: 28.06.2021 **Accepted:** 12.07.2021 **Published online:** 07.08.2021

DOI: 10.24075/brsmu.2021.035

РОЛЬ ТУЧНЫХ КЛЕТОК В РЕПАРАЦИИ КОЖИ ПОСЛЕ ТЕРМИЧЕСКОЙ ТРАВМЫ ПРИ ПРИМЕНЕНИИ ДЕРМАЛЬНОЙ ПЛЕНКИ С МЕЛАТОНИНОМ

М. В. Осиков^{1,2}, А. А. Агеева^{1✉}, А. А. Федосов³, В. А. Ушакова¹

¹ Южно-Уральский государственный медицинский университет, Челябинск, Россия

² Челябинская областная клиническая больница, Челябинск, Россия

³ Российский национальный исследовательский медицинский университет имени Н. И. Пирогова, Москва, Россия

Разработка и патогенетическое обоснование применения новых средств для локальной терапии термической травмы (ТТ) — одна из актуальных проблем медицины. Мелатонин (МТ) — эндогенный фактор регуляции гомеостаза с плейотропным потенциалом. Целью работы было оценить показатели репарации, функциональное состояние тучных клеток (ТК), содержание матриксной металлопротеиназы-9 (ММР-9) и фактора роста сосудистого эндотелия (VEGF) в очаге повреждения кожи в динамике экспериментальной ТТ в условиях применения оригинальной дермальной пленки (ДП) с МТ. ТТ степени IIIA площадью 3,5% моделировали погружением участка кожи в кипящую воду. ДП площадью 12 см² с МТ в концентрации 5 мг/г наносили ежедневно в течение пяти суток. Вычисляли площадь раны и скорость ее эпителизации, в ожоговой ране определяли число ТК и интенсивность дегрануляции, экспрессию ММР-9 и VEGF. В динамике ТТ абсолютная площадь ожоговой раны уменьшается на 35%, увеличивается скорость ее эпителизации, в очаге ТТ увеличивается число ТК, изменяется их функциональная характеристика; увеличивается экспрессия ММР-9 и VEGF. Выявлена обратная связь площади ожоговой раны с экспрессией ММР-9 и VEGF, коэффициентом дегрануляции ТК. Применение МТ при ТТ ведет к уменьшению площади ожоговой раны, увеличению скорости ее эпителизации, увеличению в ожоговой ране общего числа ТК и дегрануляции на 5-е и 10-е сутки, снижению общего числа и дегрануляции ТК на 20-е сутки ТТ (166,87 (154,95; 178,78) ед./мм²; в контроле — 464,84 (452,92; 476,76) ед./мм²), увеличению экспрессии ММР-9 на 5-е сутки (14,20 (11,30; 18,10); в контроле — 3,30 (2,20; 4,40)), экспрессии VEGF на 5-е и 10-е сутки (33,00 (30,20; 34,90); в контроле — 25,40 (22,20; 29,30)), снижению экспрессии ММР-9 на 10-е и 20-е сутки ТТ.

Ключевые слова: термическая травма, мелатонин, дермальная пленка, тучные клетки, репарация, VEGF, MMP-9

Финансирование: исследование выполнено при финансовой поддержке РФФИ и Челябинской области в рамках научного проекта № 20-415-740016

Вклад авторов: М. В. Осиков — концепция и дизайн исследования, интегральный анализ полученных данных, написание текста, редактирование рукописи; А. А. Агеева — набор экспериментального материала, статистическая обработка и анализ полученных данных, написание текста; А. А. Федосов — анализ результатов, редактирование рукописи; В. А. Ушакова — создание дермальной пленки, анализ полученных данных.

Соблюдение этических стандартов: исследование одобрено этическим комитетом Южно-Уральского государственного медицинского университета г. Челябинск (протокол № 10 от 15 ноября 2019 г.), выполнено в стандартных условиях вивария при строгом соблюдении требований по уходу и содержанию животных, а также выводу их из эксперимента с последующей утилизацией в соответствии с Европейской конвенцией о защите позвоночных животных, используемых для экспериментов или в иных научных целях (ETS № 123 от 18 марта 1986 г., Страсбург), Рекомендациями Европейской комиссии 2007/526/ EC от 18 июня 2007 г. по содержанию и уходу за животными, используемыми в экспериментальных и других научных целях, а также Директивой 2010/63/ EU Европейского парламента и совета Европейского союза от 22 сентября 2010 г. по охране животных, используемых в научных целях в соответствии с правилами гуманного отношения к животным, методическими рекомендациями по их выведению из опыта и эвтаназии.

✉ Для корреспонденции: Анна Алексеевна Агеева
ул. Воровского, д. 64, г. Челябинск, 454092; anne.ageeva.r@yandex.ru

Статья получена: 28.06.2021 **Статья принята к печати:** 12.07.2021 **Опубликована онлайн:** 07.08.2021

DOI: 10.24075/vrgmu.2021.035

Thermal burns are often associated with high mortality and temporary disability. According to WHO, about 11 million people seek medical care for burns every year; many of them sustain a temporary disability. It is estimated that 200,000 people die from burns annually [1]. Despite significant advances in the therapy of burns (skin grafting, stem cell therapy, etc.), slow wound healing, infection and scarring still pose a serious therapeutic challenge as they result in prolonged hospital stay, disfigurement, reduced quality of life, and emotional distress [2]. This can be largely explained by the complexity and diversity of pathogenetic mechanisms underlying the response to heat exposure and the progression and outcomes of thermal burns (TB). Burn researchers hold the opinion that knowledge of TB pathophysiology is essential for finding ways to effectively stop burn wound progression and develop pathogenetically informed methods for burn healing [3]. Neutrophils, macrophages, various subpopulations of lymphocytes, changes in the cytokine profile, oxidative stress, and events of the acute phase response play the key role in the pathogenesis of TB and determine the intensity and success of wound healing [4]. Mast cells (MC), which are abundant in the skin, are among the first responders to TB. They are resident inflammatory cells containing secretory granules filled with preformed and de novo mediators that participate in vascular and exudative responses, pain signaling, fibroblast proliferation, collagen synthesis, and scar remodeling. Regulation of MC function in TB holds promise for novel therapeutic approaches [5].

Apart from protecting the wound from infection and trauma, modern wound dressings promote healing and keep the wound adequately moist. They are fabricated as hydrogels, textile-based gel dressings, hydrocolloids, polyurethane foam, calcium alginate fibers, etc. [6]. Most dressing materials are produced by non-Russian companies, so the development of an original dermal film (DF) for burn care may be high on the Russian research agenda. Dressings for TB contain antiseptics, hemostatic agents, antioxidants, healing-promoting agents, stimulators of tissue regeneration, etc. The Russian State Registry of Medicinal Products has a few entries on medicated films: nitroglycerin films for buccal administration, sildenafil orodispersible films and ocular inserts with taurine. The search for novel therapeutic approaches to TB treatment has a special focus on endogenous regulators of homeostasis [7, 8]. There is theoretical evidence that melatonin (MT) may have a therapeutic potential for TB. MT is mostly known for regulating the sleep-wake cycle and neuronal excitation, as well as synchronizing circadian rhythms and physiological functions [9]. In contemporary science, MT is considered an endogenous factor with multifaceted effects, including antioxidant, pro/anti-inflammatory, immunomodulatory, and antiapoptotic effects, and a regulator of cell proliferation and differentiation, which makes MT an attractive candidate therapeutic agent [10]. The literature on novel MT-enriched wound dressings is scarce; the mechanism of local MT effects on TB has not been studied yet, and there are no topical MT-enriched formulations for the therapy of burns on the Russian pharmaceutical market [11, 12]. Mammalian skin has its own melatonergic system [13]. MT receptors have been detected not only in keratinocytes and fibroblasts, hair follicles and melanocytes but also in MC, suggesting MT involvement in the regulation of the functional activity of MC, especially in mitigating vascular and exudative responses and stimulating tissue regeneration after TB [14]. Besides, skin cells, including MC, are capable of producing and secreting MT. However, the mechanism of possible MT effects on MC involvement in skin regeneration after TB is not fully clear and cannot be associated with the secretion of matrix

metalloproteinase-9 (MMP-9) and vascular endothelial growth factor (VEGF) by mast cells. The aim of this study was to assess some parameters of tissue regeneration, the functional state of mast cells and the levels of MMP-9 and VEGF in the experimentally induced thermal burn treated with an original MT-enriched dermal film.

METHODS

The experiment was conducted in 70 male Wistar rats weighing 200–240 g. The animals were randomized in 4 groups: group 1 ($n = 7$) — intact animals; group 2 ($n = 21$) — animals with TB treated with aseptic dressings (TI + AD); group 3 ($n = 21$) — animals with TB treated with DF and aseptic dressings (TB + DF); group 4 ($n = 21$) — animals with TB treated with MT-enriched DF and aseptic dressings (TB + MT DF). Aseptic dressings and DF were changed every day for 20 days after TB.

Thermal burns are most commonly caused by hot liquids and flames; in two thirds of the patients, less than 10% of the total body surface area is involved [15]. So, to model a second-degree burn (ICD-10 codification, corresponds to a IIIA degree burn according to the classification proposed at the 27th All-Soviet Congress of Surgeons held in 1960) involving 3.5% of the total animal body surface, the area of skin between the shoulder blades was exposed to distilled water at 98–99 °C for 12 s. Burn depth was verified morphologically. The animals were anesthetized with 20 mg/kg tiletamine-zolazepam. The DF matrix and the MT-enriched DF (12 cm²) were applied immediately after inducing TB (groups 3 and 4, respectively). The matrix was fixed with an aseptic dressing. The dressing was changed every day for 5 days. In our preliminary experiment, we designed a sodium carboxymethylcellulose film (sodium poly-1,4-β-O-carboxymethyl-D-pyranosyl-D-glycopyranose) enriched with 5 mg/g MT. The matrix was evaluated for its pharmacological and fabrication characteristics: organoleptic properties (appearance, color, transparency, elasticity, presence of impurities, microcracks), adhesiveness, tensile strength, and thickness [16]. In group 3, we used an MT-free DF matrix similar in size and properties to the MT-enriched DF.

The wound area was measured by digital planimetry on days 5, 10 and 20 after TB using a Nikon Coolpix S2800 camera (Nikon; China) and Microsoft Office Visio software (Microsoft; USA). The rate of wound epithelialization (VS) was calculated by the formula: $VS = S - Sn / t$, where S is the wound area before treatment (the area at previous measurement); Sn is the area at subsequent measurement; t is days between measurements. The wound area at subsequent measurements was calculated as % of the initial wound area and expressed as % / day.

On days 5, 10 and 20 after TB, the burned skin and a small amount of healthy skin at the wound margin were excised for pathomorphological and immunohistochemical examinations. Microscopy was performed using a DMRXA microscope (Leika; Germany) and ImageScope M software (Germany) at $\times 100$ and $\times 400$ magnifications.

After staining the tissue sections with toluidine blue (pH = 2,0) (Biovitrum; Russia), a total mast cell count was performed. Mast cells were typed by the degree of degranulation: 1st degree (1–2 granules visualized outside the cell), 2nd degree (3–10 granules outside the cell), 3rd degree (over 10 granules outside the cell); mast cells of each degranulation type were counted. Additionally, the average MC brightness was assessed. The degranulation coefficient was calculated as the ratio of degranulated MC to the total number of mast cells in 10 random fields of view.

The abundance of MMP-9 and VEGF in the wound was determined immunohistochemically using MMP-9 rabbit anti-rat polyclonal antibodies (catalog item PAA553Ra01, Cloud-Clone Corp.; China), VEGF rabbit anti-rat polyclonal antibodies (catalog item PAA143Ra01, Cloud-Clone Corp., China) and a Rabbit Specific HRP/DAB Detection IHC Kit (Abcam; Latvia). Diaminobenzidine was used as a chromogenic substrate to visualize the polymer complex. We calculated the relative surface area of MMP-9-positive and VEGF-positive structures; the integral indicator of MMP-9 and VEGF content was calculated as the product of the relative surface area of the positively stained structures and the intensity of staining. The result was presented in arbitrary units ($\mu\text{m}/\text{mm}^2$).

The obtained data were processed in IBM SPSS Statistics 19 (SPSS: An IBM Company; USA). The results were presented as a median (Me) and quartiles (Q_1 ; Q_3). The significance of differences was assessed using the Kruskal-Wallis, Mann-Whitney U and Wald-Wolfowitz runs tests. Correlations between the studied parameters were tested using the Spearman's correlation coefficient (R). The Bonferroni-adjusted significance threshold was $p < 0.01$.

RESULTS

In group 2, there was a reduction in the absolute wound area on day 10, compared to day 5 of the experiment; the rate of epithelialization had increased by day 10, and the relative wound area had decreased (Table 1). On day 20, there was a reduction in the absolute wound area, compared to days 5 and 10; the relative wound area on day 20 was also smaller than on day 5. Thus, by day 20 the rate of epithelialization had increased in comparison with day 5, and the wound reduction area had grown in comparison with days 5 and 10. The median wound area measured on day 20 was 35% smaller than on day 5.

To investigate the role of MC in the pathophysiology of wound healing, we measured their abundance and activity from the intensity of degranulation in the burn (Table 2). On day 5 the median total MC count in the wound in group 2 was 43% higher than in the group of intact animals; this may be explained by active basophile migration from the bloodstream to the wound site. The number of degranulated MC was more than 3 times higher in group 2 than in the group of intact animals;

of them the number of MC in the 1st degree of degranulation was 3 times higher, the number of MC in the 2nd degree of degranulation was 4 times higher, and the number of MC in the 3rd degree of degranulation was 10 times higher. The median value of the degranulation coefficient was 3.5 times higher than in the group of intact animals. Notably, many MC (mostly those in the 3rd degree of degranulation) had a "ghostly" appearance due to the loss or release of their granules. This was reflected in the significant loss of average MC brightness on day 5 of the experiment. On day 10, the rise in the total MC count was even more pronounced than on day 5: the median total number of MC cells in the wound in group 2 was 72% higher than in the group of intact animals. On day 10, the number of MC in the 1st and 2nd degrees of degranulation was 3 times higher than in the intact group; the number of MC in the 3rd degree of degranulation had risen tenfold in comparison with the intact group. The median value of the degranulation coefficient now was 2.5 times higher than in the group of intact animals. The average MC brightness measured on day 10 was 2 times lower than in the intact group. By day 20, the total MC count in group 2 had reached its peak and was 1.7 times higher than in the intact group; the number of degranulated MC, MC in the 1st and 3rd degrees of degranulation and the degranulation coefficient were significantly higher than in the group of intact animals, and the average MC brightness was lower. The highest total MC count, the highest number of degranulated MC and the highest number of MC in the 1st degree of degranulation were observed on day 20; the number of MC in the 2nd degree of degranulation peaked on day 5, and the number of MC in the 3rd degree of degranulation reached its maximum on days 5 and 10. The highest value of the degranulation coefficient was observed on day 5; the lowest MC brightness was observed on days 5 and 10. Summing up, the MC count peaked on day 20 after inducing the burn, and degranulation was the most pronounced on days 5 and 10 of the experiment.

Figure shows the dynamics of MMP-9 and VEGF expression in the wound throughout the experiment. On days 5, 10 and 20 after TB, VEGF expression was significantly elevated in comparison with the intact group. MMP-9 expression was significantly elevated on days 10 and 20. On day 10, VEGF expression in the wound was higher than on day 5; on day 20 it was lower than on day 10. MMP-9 expression on days 10 and

Table 1. Parameters of tissue regeneration after experimentally induced thermal burn treated with MT-enriched DF (Me (Q_{25} ; Q_{75}))

Parameter	Group 2 (TB + AD)			Group 3 (TB + DF)			Group 4 (TB + MT DF)		
	Day 5 (n = 7)	Day 10 (n = 7)	Day 20 (n = 7)	Day 5 (n = 7)	Day 10 (n = 7)	Day 20 (n = 7)	Day 5 (n = 7)	Day 10 (n = 7)	Day 20 (n = 7)
Absolute wound area, cm^2	11,66	9,48	7,59	11,59	9,4	7,29	10,33	8,34	5,54
	(11,50; 11,94)	(9,28; 9,93)	(7,23; 7,84)	(11,00; 11,99)	(9,22; 9,81)	(7,01; 7,52)	(10,17; 10,56)	(8,19; 8,51)	(5,24; 5,88)
	*	***					#	#	#
Relative wound area, %	3,34	3,17	2,99	3,31	3,16	2,81	3,36	3,02	1,98
	(3,25; 3,39)	(3,10; 3,29)	(2,94-3,12)	(3,22; 3,42)	(3,10; 3,28)	(2,74-3,09)	(3,23; 3,42)	(2,91; 3,13)	(1,87; 2,23)
			*					#	#
Epithelialization rate, % /day	0,89	1,9	2,26	0,91	2,01	3,06	1,33	6,57	14,3
	(0,86; 0,89)	(1,88; 1,95)	(2,14; 2,55)	(0,85; 0,92)	(1,93; 2,05)	(2,73; 3,15)	(1,29; 1,35)	(5,92; 6,93)	(13,38; 15,17)
		*	***				#	#	#
Reduction in wound area, %	2,61	3,68	11,49	2,6	3,71	13,58	9,8	16,1	19,98
	(2,59; 2,64)	(3,53; 4,23)	(11,43; 11,64)	(2,58; 2,64)	(3,63; 4,31)	(12,93; 14,01)	(9,64; 10,08)	(14,62; 17,73)	(19,30; 20,38)
		*	***				#	#	#

Note: * — differences are significant ($p < 0.01$) for comparisons with group 2 on day 5; ** — with group 2 on day 10; # — with group 3 on the specified day.

Table 2. Functional characteristics of mast cells in the burn wound treated with MT-enriched DF (Me (Q₂₅; Q₇₅))

Parameter	Group 1 Intact animals (n = 7)	Group 2 (TB + AD)			Group 3 (TB + DF)			Group 4 (TB + MT DF)		
		Day 5 (n = 7)	Day 10 (n = 7)	Day 20 (n = 7)	Day 5 (n = 7)	Day 10 (n = 7)	Day 20 (n = 7)	Day 5 (n = 7)	Day 10 (n = 7)	Day 20 (n = 7)
Total mast cell count, un/mm ²	166,87	238,38	286,05	441	226,46	286,06	464,84	250,3	369,49	166,87
	(160,91; 172,82)	(226,46; 238,38) *	(274,14; 286,05) *	(441,00; 452,92) * # ##	(202,62; 262,22)	(274,14; 297,97)	(452,92; 476,76)	(250,30; 250,30)	(357,57; 381,41)	(154,95; 178,78)
				*	*	*	*	* &	* &	&
Number of degranulated mast cells, un/mm ²	35,76	178,78	166,87	214,54	178,78	166,87	226,46	202,62	190,7	83,43
	(35,76; 41,72)	(166,87; 178,78) *	(154,95; 178,78) *	(202,62; 214,54) * # ##	(154,95; 190,70)	(166,87; 178,78)	(226,46; 250,30)	(190,70; 214,54)	(178,78; 202,62)	(83,43; 83,43)
				*	*	*	*	* &	* &	* &
Number of mast cells in the 1st degree of degranulation, un/mm ²	23,84	83,43	59,59	178,78	83,43	59,6	178,78	143,03	154,95	59,6
	(11,92; 29,79)	(71,51; 83,43)	(47,68; 71,51)	(178,78; 178,78) * # ##	(71,51; 95,35)	(59,60; 71,51)	(178,78; 202,62)	(143,03; 154,95)	(131,11; 154,95)	(59,60; 59,60)
		*	* #		*	*	*	* &	* &	* &
Number of mast cells in the 2nd degree of degranulation, un/mm ²	11,92	47,68	35,76	11,92	47,68	47,68	13,84	35,76	23,84	13,84
	(0; 17,88)	(35,76; 47,68)	(35,76; 47,68)	(11,92; 11,92)	(35,76; 47,68)	(23,84; 59,60)	(13,84; 13,84)	(35,76; 59,60)	(23,84; 39,20)	(11,92; 15,76)
		*	* #	# ##	*	*		*	* &	
Number of mast cells in the 3rd degree of degranulation, un/mm ²	5,96	59,59	59,59	11,92	59,6	59,6	23,84	11,92	11,92	11,92
	(0; 11,92)	(47,68; 59,59)	(59,59; 83,43)	(11,92; 11,92)	(35,76; 59,60)	(47,68; 71,51)	(11,92; 23,84)	(11,92; 23,84)	(0,00; 11,92)	(0,00; 11,92)
		*	*	# ##	*	*	*	* &	* &	* &
Degranulation coefficient, au	0,22	0,75	0,59	0,49	0,76	0,6	0,5	0,81	0,5	0,5
	(0,21; 0,26)	(0,73; 0,76)	(0,56; 0,63)	(0,49; 0,49)	(0,71; 0,77)	(0,56; 0,61)	(0,48; 0,53)	(0,81; 0,86)	(0,48; 0,53)	(0,47; 0,54)
		*	* #	* # ##	*	*	*	* &	* &	*
Average mast cell brightness, au	79,51	57,14	33,83	37,69	57,38	38	36,38	51,36	38,13	37,87
	(73,14; 83,76)	(51,36; 64,76)	(33,67; 39,22)	(37,69; 39,33)	(50,0; 58,42)	(33,26; 39,57)	(34,36; 37,9599)	(48,50; 59; 32)	(33,83; 40,78)	(32,50; 39,33)
		*	* #	* #	*	*	*	*	*	*

Note: * — differences are significant ($p < 0,01$) for comparisons with group 1, # — with group 2 on day 5, ## — with group 2 on day 10, & — with group 3 on the specified day.

20 was higher than on day 5. Thus, VEGF expression reached its peak on day 10, whereas MMP-9 expression, on days 10 and 20. MC can be a source of MMP-9 and VEGF, factors that promote effective tissue regeneration in the wound. In this study, we established a correlation between the degranulation coefficient of MC and the expression of MMP-9 and VEGF in the burn wound (Table. 3). On day 10, MMP-9 expression in the wound was directly moderately correlated with the value of the degranulation coefficient. On day 20, we detected a direct weak correlation between VEGF expression in the wound and the degranulation coefficient. We think that MC activity and the expression of MMP-9 and VEGF in the wound play a role in wound healing and systemic response to TB. While analyzing possible correlations between the absolute wound area and the degranulation coefficient, we established a weak negative correlation on day 5 and a moderate negative correlation on days 10 and 20 between these 2 variables. The absolute wound area was negatively correlated with MMP-9 expression on day 10 (the correlation was weak) and also negatively correlated with MMP-9 expression on day 20 (the correlation was moderate; Table 4). On day 10, a weak negative correlation was observed between the absolute wound area and VEGF expression. No significant correlations were established between the absolute wound area and VEGF expression on days 5 and 20 and between the absolute wound area and MMP-9 expression on day 5.

The effect of local application of MT-enriched DF (group 4) was assessed and compared with the effect of MT-free DF in

group 3 over the course of 5 days. MT causes a significant reduction in the absolute wound area on days 5, 10 and 20 and in the relative wound area on days 10 and 20 of the experiment (Table 1). On days 5, 10 and 20, the rate of epithelization and the reduction in the wound size in group 4 were increased in comparison with group 3. On day 5, the median value of the absolute wound area in group 4 was 12.2% smaller than in group 3; peak values of the absolute wound area were observed on day 20 when it was 31.6% smaller than in group 4 and the median rate of epithelization was 4.7-fold lower than in the DF group. On days 10 and 20 in comparison with day 5 and on day 20 in comparison with day 10, the absolute wound area was significantly reduced; the rate of epithelization and the rate of wound size reduction were significantly increased ($p < 0,01$). Notably, from day 5 to day 20 the absolute wound area decreased by 46% vs 37% in the group treated with MT-free DF.

MT incorporated in DF changes the abundance and functional activity of MC in the experimentally induced burn wound (Table 2). On day 5, the total count of MC in the wound was significantly higher in group 4 than in group 3 (no MT). Besides, on day 5 the total number of degranulated MC and the number of MC in the 1st degree of degranulation was increased in comparison with group 3; the degranulation coefficient in group 4 was also higher on day 5, and the number of MC in the 2nd and 3rd degrees of degranulation was lower; the average MC brightness did not differ between the two groups on day 5. On day 10, there was a significant increase in the total MC count in the wound and a rise in the

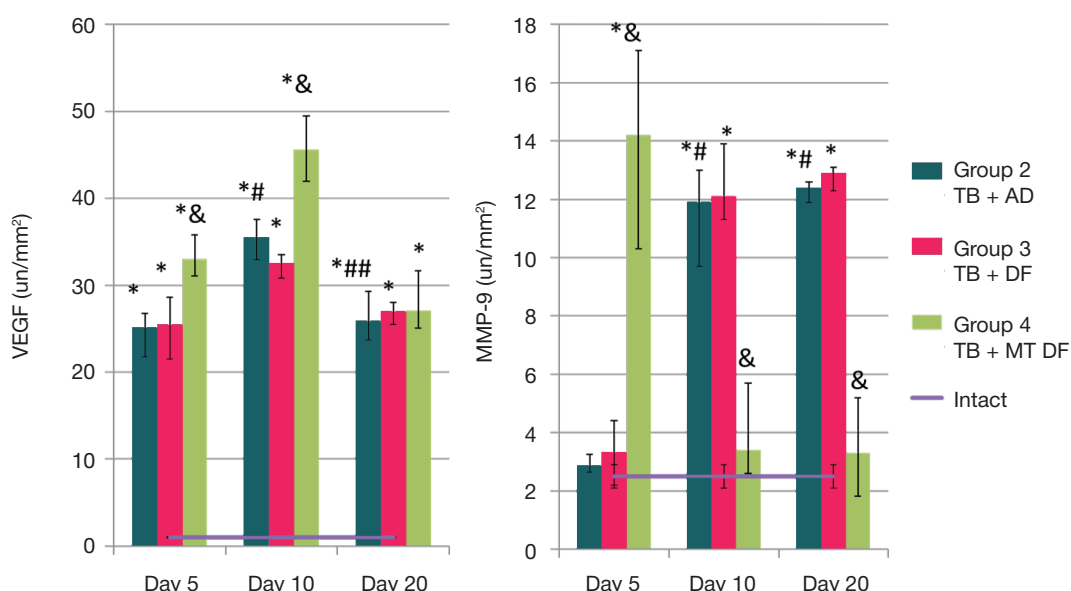


Figure. Effects of melatonin-enriched dermal film on the immunohistochemical parameters of burn wound tissue (Me ($Q_{25}; Q_{75}$)). * — differences are significant ($p < 0.01$) for comparisons with group 1; # — with group 2 on day 5; ## — with group 2 on day 10; & — with group 3 on the specified day

number of degranulated MC and the number of MC in the 1st degree of degranulation in group 4, but the number of MC in the 2nd and 3rd degrees of degranulation was lower, and the degranulation coefficient had fallen, in comparison with group 3. Finally, on day 20 the total MC count and the number of MC in the 1st and 3rd degrees of degranulation were significantly decreased. So, local applications of MT-enriched DF result in the increased number and degranulation of MC on days 5 and 10 after thermal injury; by day 20, the abundance and activity of MC shifts towards reduction. The degranulation coefficient and average MC brightness, which are the integral indicators of MC activity, were significantly higher and lower, respectively, than in the group of intact animals at all time points of the experiment.

In group 4 (treated with MT-enriched DF), MMP-9 and VEGF expression was significantly elevated on day 5; by day 10, MMP-9 expression had fallen significantly, whereas VEGF expression continued to increase. On day 20, MMP-9 expression was decreasing, while VEGF expression showed no significant changes. VEGF expression was significantly higher ($p < 0.01$) on day 10 than on day 5; on day 20, it was lower than on days 5 and 10. MMP-9 expression was lower ($p < 0.01$) on days 10 and 20 than on day 5. Notably, VEGF expression on days 5, 10 and 20 and MMP-9 expression on day 5 were significantly higher in group 4 than in the group of intact animals. MMP-9 expression on days 10 and 20 did not differ significantly from that in the group of intact animals.

DISCUSSION

We think that the detected dynamics of tissue regeneration parameters in the burn wound are associated with the participation of MC in the key events of wound healing. In the first 5 days after thermal injury the process is dominated by secondary alteration vascular, exudative and leukocyte responses, MC degranulation and release of preformed

mediators, like histamine, TNF α , IL1 β , IL6, etc., leading to arterial and venous hyperemia, exudation and phagocyte activation. Protease-4 released by MC acts as a chemoattractant for leukocytes in the inflammation phase. Later, on days 10–15, mast cells start to secrete the keratinocyte growth factor and VEGF, activating fibroblasts and collagen synthesis, which is often excessive and leads to hypertrophic scarring. Increased collagen synthesis is associated, among other things, with the activation of the TGF β 1/Smads signaling pathway by chymase secreted by MC and fibroblast proliferation [17]. Serotonin secreted into the wound primarily by MC inhibits apoptosis and improves survival of fibroblasts and keratinocytes, thereby participating in the regulation of wound healing; inhibitors of endogenous serotonin release reduce the rate of epithelialization [18].

The intensity of MMP-9 expression in the burn wound and serum levels of MMP-9 are risk markers for a systemic inflammatory response syndrome (SIRS) and predictors of poor outcomes in patients with burns [19]. Neutrophils activated by GM-CSF, IL8, TNF α and other cytokines, as well as some other cells, including MC, are the major source of MMP-9 at the early stages after thermal injury. MMP-9 expression reflects the abundance and activity of neutrophils and macrophages in the wound. MMP-9 is involved in the degradation of the extracellular matrix (especially collagen types IV and V), increases vascular permeability in the wound, participates in neutrophil chemotaxis, activation and deactivation of autacoids, and thus creates the right conditions for tissue regeneration and successful epithelialization. MMP-9 can be inhibited by alpha1-antichymotrypsin, a proteinase-1 inhibitor [20]. MMP-9 plays a special role in the dynamics of chronic wounds: overexpression of MMP-9 results in the degradation of the extracellular matrix, inhibition of growth factors and tissue regeneration. According to some reports, the knockout of the MMP-9-encoding gene or MMP-9 inhibition accelerates wound healing [21]. As a rule,

Table 3. Correlations between the degranulation coefficient of mast cells and immunohistochemical parameters of the experimentally induced thermal wound

Parameter	Day 5 ($n = 7$)	Day 10 ($n = 7$)	Day 20 ($n = 7$)
VEGF, un/mm ²	0,26	0,37	0,31
MMP-9, un/mm ²	0,23	0,64	0,37

Note: The table features Spearman's correlation coefficient. Significant correlations ($p < 0.05$) are shown in semibold.

Table 4. Correlations between the absolute burn wound area and VEGF/MMP-9 expression and between the absolute burn wound area and the degranulation coefficient

Parameter	Day 5 (<i>n</i> = 7)	Day 10 (<i>n</i> = 7)	Day 20 (<i>n</i> = 7)
VEGF, un/mm ²	- 0,13	- 0,37	0,17
MMP-9, un/mm ²	- 0,31	- 0,47	- 0,54
Degranulation coefficient, au	- 0,37	- 0,51	- 0,64

Note: The table features Spearman's correlation coefficient. Significant correlations (*p* < 0.05) are shown in semibold.

low MMP-9 activity in the acute wound is associated with its inhibition by alpha1-antichymotrypsin.

Members of the VEGF family (VEGF-A, VEGF-B, VEGF-C, VEGF-D) in general and VEGF-A in particular are produced in the wound by keratinocytes, mast cells, macrophages, monocytes, and activated fibroblasts. VEGF-A receptors have been detected on endothelial cells, fibroblasts and other cells [22]. GM-CSF stimulates VEGF production in the wound and directly increases keratinocyte and fibroblast activity [23]. VEGF participates in the regulation of angiogenesis, collagen synthesis and production of other connective tissue components; it is also involved in scar formation. Inhibition of VEGF prevents excessive scarring and formation of hypertrophic and keloid scars after TB, thus holding promise for the therapy of burns. However, the mechanism underlying these VEGF effects is not fully clear and may be associated with direct activation of fibroblast migration, fibroblast proliferation and collagen synthesis and/or indirect activation of endothelial cells, neutrophils, macrophages, and mast cells accompanied by the production of profibrogenic mediators (cytokines, growth factors) [24]. Specifically, the therapeutic effect of interferon alpha2b in patients with hypertrophic and keloid scars is associated with mitigation of VEGF effects and angiogenesis. It is reported that bevacizumab, a humanized anti-VEGF antibody, exerts a positive effect against hypertrophic scarring [25]. In this regard, the correlations established in our study are very illustrative, including the negative correlation between the wound area and the abundance of MMP-9 and VEGF in the wound, the direct correlation between the wound area and the degranulation coefficient, and the direct correlation between the degranulation coefficient and the levels of MMP-9 and VEGF in the wound. Therefore, it can be hypothesized that the wound area after thermal injury shrinks as MMP-9 and VEGF levels grow; in turn, MMP-9 and VEGF levels in the wound increase as MC undergo degranulation.

We believe that the therapeutic effects of MT-enriched DF can be explained by the pleiotropic properties of MT. The antioxidant effect of MT can curb the progression of secondary injury expansion after TB, which occurs due to the activation and recruitment of neutrophils, monocytes and lymphocytes to the affected site. Previously, we demonstrated that MT-enriched DF limits the growing levels of lipid peroxidation products and proteins in the burn wound and thus accelerates healing [26]. Modulation of the inflammatory response by MT may be associated with a reduction in secondary alteration, mitigation of vascular-exudative responses, suppression of cytokine and autacoid production, thus leading to changes in the wound and the acute phase response. MT-enriched DF limits the death of leukocytes in an experimentally induced TB [27]. MT may exert direct effects on the synthesis and activity of factors involved in tissue regeneration. In the experiment *in vitro* conducted on the endothelial cells of cerebral vessels, MT has been shown to reduce the permeability IL1 β -activated cells by inhibiting MMP-9 [28]. MT has the ability to directly bind MMP-9. Specifically, MT binds excessive MMP-9 in COVID-19-mediated immune response and squamous-cell carcinoma of the oral cavity [29]. MT downregulates overexpression and reduces excessive

activity of MMP-9 by regulating the NOTCH3/NF- κ B and TLR4/NF- κ B signaling pathways [30]. In the experiments *in vitro* involving the serum of rats with experimentally induced thermal burns, MT has been shown to reduce the permeability of endothelial cells due to MMP-9 inhibition and the antioxidant activity [31]. MT is protective against MC damage by chemical agents and may affect the secretory activity of MC [32]. Besides, MT effects on MC may vary depending on the type of receptor MT interacts with (M1 or M2). Thus, a complex effect of locally applied MT on the expression of MMP-9 in the burn wound may be associated with protection of MC against injurious factors in the wound on day 5; in turn, the increased secretion of MMP-9 by MC may ensure more effective and rapid removal of cell detritus from the wound, preparing tissue for regeneration. On days 10 and 20, the decline in MMP-9 expression in the wound may be associated with direct or indirect inhibition and reduced synthesis of this proteinase following exposure to MT; this halts tissue destruction in the wound, activates cell proliferation and differentiation driven by growth factors and results in rapid tissue regeneration. Therefore, stimulation of VEGF expression in the wound on days 5 and 10 by the local application of MT has a rationale.

The reports on MT effects on VEGF synthesis and expression are controversial. On the one hand, MT inhibits VEGF synthesis by SH-SY5Y human neuroblastoma cells, prostate cancer cells and other malignancies, exerting an antiangiogenic effect and inhibiting tumor growth [33]. This phenomenon is associated with the inhibition of STAT3 and HIF-1 α stabilization and the genes they control, including VEGF and the VEGFR2 receptor [34]. According to other studies, MT does not change VEGF expression in ischemic lesions [35]. However, recent data suggest that multifunctional regulatory MT effects on angiogenesis are dose-dependent and determined by the initial tissue condition. MT directly or indirectly enhances angiogenesis during fractured bone healing, skin healing after mechanical or chemical damage, in experimentally induced gastric ulcers and myocardial or cerebral ischemia [33]. MT boosts the angiogenic potential of mesenchymal stem cells in the wound due to Erk1/2-mediated VEGF synthesis [36]. Besides, MT can stimulate production of platelet-derived growth factor, which is a known angiogenesis stimulator, and confers resistance to ischemic stress.

CONCLUSIONS

In our study, the absolute area of the experimentally induced burn shrank by 35% from day 5 to day 20, the wound epithelialization rate and the total MC count in the wound increased, and the functional activity of MC changed: the cells lost their granularity and underwent significant degranulation. MMP-9 and VEGF expression in the wound was elevated. A negative correlation was established between the wound area and the expression of MMP-9 and VEGF; the wound area and the degranulation coefficient were also negatively correlated. MMP-9 and VEGF expression in the wound increased as the degranulation of mast cells intensified. MT-enriched DF caused a reduction in the wound area observed on days 5, 10 and

20 after thermal injury and increased the wound epithelization rate. The medicated film increased the total MC count in the wound and stimulated MC degranulation on days 5 and 10. On day 20, there was a reduction in the total MC count in the wound and a decline in degranulation. The application of MT-enriched DF resulted in elevated MMP-9 expression on day 5 and elevated VEGF expression on days 5 and 10; MMP-9 expression on days 10 and 20 was reduced. The obtained results expand our knowledge of the contribution of changes in MC activity and the dynamics of MMP-9 and VEGF expression to the pathogenesis of TB. They create a basis for further clinical studies into the role of MC in skin burns and help to identify diagnostic markers, predictors of

complications and markers of treatment efficacy among their secretory products. Established at the preclinical stage, the stimulatory effect of MT-enriched DF on tissue regeneration is associated with changes in the abundance and activity of mast cells and MMP-9 and VEGF expression in the wound. It paves the way for the study of mechanisms underlying the effects and efficacy of MT in the clinical setting in patients with TB. Considering that wound healing mechanisms, regardless of their nature, act in alliance, we believe that our findings suggesting a stimulatory effect of MT-enriched DF on tissue regeneration due to changes in mast cells activity and in the abundance of MMP-9 and VEGF in the wound can be extrapolated to wounds of other etiologies.

References

- WHO Fact Sheet: Burns. [(accessed on 6 March 2018)]; Available online: <https://www.who.int/news-room/fact-sheets/detail/burns>.
- Wang Y, Beekman J, Hew J, Jackson S, Issler-Fisher AC, Parungao R, et al. Burn injury: Challenges and advances in burn wound healing, infection, pain and scarring. *Adv Drug Deliv Rev.* 2018; 123: 3–17. DOI: 10.1016/j.addr.2017.09.018.
- Saavedra PA, deBrito ES, Areda CA, Escalda PM, Galato D. Burns in the Brazilian Unified Health System: a review of hospitalization from 2008 to 2017. *Int J Burns Trauma.* 2019 Oct 15; 9 (5): 88–98.
- Yang P, Li Y, Xie Y, Liu Y. Different faces for different places: heterogeneity of neutrophil phenotype and function. *J Immunol Res.* 2019 Feb 28; 2019: 8016254. DOI: 10.1155/2019/8016254.
- Nguyen AV, Soulka AM. The Dynamics of the Skin's Immune System. *Int J Mol Sci.* 2019 Apr 12; 20 (8). pii: E1811. DOI: 10.3390/ijms20081811.
- Murray RZ, West ZE, Cowin AJ, Farrugia BL. Development and use of biomaterials as wound healing therapies. *Burns Trauma.* 2019 Jan 25; 7: 2. DOI: 10.1186/s41038-018-0139-7-6
- Osikov MV, Teleshova LF, Ageev YI. Antioxidant effect of erythropoietin during experimental chronic renal failure. *Bulletin of Experimental Biology and Medicine.* 2015; 160 (2): 202–4.7
- Osikov MV, Teleshova LF, Ageev Yul. Vlijanie jeritropojetina na apotoz limfocitov pri jeksperimental'noj hronicheskoy pochechnoj nedostatochnosti. *Bjulleten' jeksperimental'noj biologii i mediciny.* 2015; 3: 326–9. Russian.
- Tordjman S, Chokron S2, Delorme R, et al. Melatonin: pharmacology, functions and therapeutic benefits. *Curr Neuropharmacol.* 2017 Apr; 15 (3): 434–43.
- Varoni EM, Soru C, Pluchino R, et al. The impact of melatonin in research. *Molecules.* 2016 Feb 20; 21 (2): 240. DOI: 10.3390/molecules21020240.
- Lopes RCV, Assis Martins J, Ribeiro de Souza T, de Castro Nunes Rincon G, Pacheco Miguel M, Borges de Menezes L, Correa Amaral A. Melatonin loaded lecithin-chitosan nanoparticles improved the wound healing in diabetic rats. *Int J Biol Macromol.* 2020 Nov 1; 162: 1465–75. DOI: 10.1016/j.ijbiomac.2020.08.027.
- Kaczmarek-Szczepańska B, Ostrowska J, Kozłowska J, Szota Z, Brożyna AA, Dreier R, et al. Evaluation of polymeric matrix loaded with melatonin for wound dressing. *Int J Mol Sci.* 2021 May 26; 22 (11): 5658. DOI: 10.3390/ijms22115658.
- Rusanova I, Martínez-Ruiz L, Florido J, Rodríguez-Santana C, Guerra-Libero A, Acuña-Castroviejo D, et al. Protective effects of melatonin on the skin: future perspectives. *Int J Mol Sci.* 2019 Oct 8; 20 (19): 4948. DOI: 10.3390/ijms20194948.
- Theoharides TC. Neuroendocrinology of mast cells: Challenges and controversies. *Exp Dermatol.* 2017 Sep; 26 (9): 751–9.
- Li H, Yao Z, Tan J, et al. Epidemiology and outcome analysis of 6325 burn patients: a five-year retrospective study in a major burn center in Southwest China. *Sci Rep.* 2017 Apr 6; 7: 46066. DOI: 10.1038/srep46066.
- Ageeva AA, Osikov MV, Simonjan EV, Toporec TA, Potekhina EA, avtory. Federal'noe gosudarstvennoe bjudzhetnoe obrazovatel'noe uchrezhdenie vysshego obrazovanija «Juzhno-Ural'skij gosudarstvennyj medicinskij universitet» Ministerstva zdravoochronenija Rossijskoj Federacii, patentobladatel'. Sredstvo v vide plenki lekarstvennoj, soderzhashhej melatonin, dlja lechenija termicheskoy travmy patent # 2 751 048 07.07.2021. Russian.
- Chen H, Xu Y, Yang G, Zhang Q, Huang X, Yu L, et al. X. Mast cell chymase promotes hypertrophic scar fibroblast proliferation and collagen synthesis by activating TGF- β 1/Smads signaling pathway. *Exp Ther Med.* 2017 Nov; 14 (5): 4438–42.
- Sadiq A, Shah A, Jeschke MG, et al. The Role of Serotonin during Skin Healing in Post-Thermal Injury. *Int J Mol Sci.* 2018 Mar 29; 19(4). pii: E1034. DOI: 10.3390/ijms19041034. 12.
- Nagy B, Szélíg L, Rendeki S, et al. Dynamic changes of matrix metalloproteinase 9 and tissue inhibitor of metalloproteinase 1 after burn injury. *J Crit Care.* 2015; 30 (1): 162–6. DOI: 10.1016/j.jcrc.2014.07.008.
- Lang TC, Zhao R, Kim A, et al. A Critical Update of the Assessment and Acute Management of Patients with Severe Burns. *Adv Wound Care (New Rochelle).* 2019; 8 (12): 607–33. DOI: 10.1089/wound.2019.0963.
- Wilgus TA, Roy S, McDaniel JC. Neutrophils and wound repair: positive actions and negative reactions. *Adv Wound Care (New Rochelle).* 2013; 2 (7): 379–88. DOI: 10.1089/wound.2012.0383
- Johnson KE, Wilgus TA. Vascular endothelial growth factor and angiogenesis in the regulation of cutaneous wound repair. *Adv Wound Care (New Rochelle)* 2014; 3: 647–61.
- Yamakawa S, Hayashida K. Advances in surgical applications of growth factors for wound healing. *Burns Trauma.* 2019 Apr 5; 7: 10. DOI: 10.1186/s41038-019-0148-1.
- Wilgus TA. Vascular endothelial growth factor and cutaneous scarring. *Adv Wound Care (New Rochelle).* 2019 Dec 1; 8 (12): 671–8.
- Kwak DH, Bae TH, Kim WS, Kim HK. Anti-vascular endothelial growth factor (Bevacizumab) therapy reduces hypertrophic scar formation in a rabbit ear wounding model. *Arch Plast Surg.* 2016; 43: 491–7.
- Osikov MV, Simonyan EV, Ageeva AA, Ageev YI, Sinitsky AI, Fedosov AA. Local antioxidant effect of original dermal film with melatonin in thermal injury. *Bulletin of Russian State Medical University.* 2020; 6: 104–12.
- Osikov MV, Simonjan EV, Ageeva AA, Ageev Yul. Melatonin v sostave dermal'noj plenki ogranichivaet gibel' limfocitov v krovi pri jeksperimental'noj termicheskoy travme. *Medicinskaja immunologija.* 2021; 23 (2): 389–94. Russian.
- Alluri H, Wilson RL, Anasooya Shaji C, et al. Melatonin Preserves Blood-Brain Barrier Integrity and Permeability via Matrix Metalloproteinase-9 Inhibition. *PLoS One.* 2016; 11 (5): e0154427. DOI: 10.1371/journal.pone.0154427.
- Hazra S, Chaudhuri AG, Tiwary BK, Chakrabarti N. Matrix metallopeptidase 9 as a host protein target of chloroquine and melatonin for immunoregulation in COVID-19: A network-based meta-analysis. *Life Sci.* 2020; 257: 118096. DOI: 10.1016/j.

- Ifs.2020.118096.
30. Qin W, Li J, Zhu R, et al. Melatonin protects blood-brain barrier integrity and permeability by inhibiting matrix metalloproteinase-9 via the NOTCH3/NF-κB pathway. *Aging (Albany NY)*. 2019; 11 (23): 11391–415. DOI: 10.18632/aging.102537.
 31. Wiggins-Dohlvik K, Han MS, Stagg HW, Alluri H, Shaji CA, Oakley RP, et al. Melatonin inhibits thermal injury-induced hyperpermeability in microvascular endothelial cells. *J Trauma Acute Care Surg.* 2014; 77: 899–905.
 32. Maldonado MD, Garcia-Moreno H, Calvo JR. Melatonin protects mast cells against cytotoxicity mediated by chemical stimuli PMACl: possible clinical use. *J Neuroimmunol.* 2013 Sep 15; 262 (1–2): 62–5.
 33. Rahbarghazi A, Siahkouhian M, Rahbarghazi R, et al. Role of melatonin in the angiogenesis potential; highlights on the cardiovascular disease. *J Inflamm (Lond)*. 2021; 18 (1): 4. DOI: 10.1186/s12950-021-00269-5.
 34. Bhattacharya S, Patel KK, Dehari D, Agrawal AK, Singh S. Melatonin and its ubiquitous anticancer effects. *Mol Cell Biochem.* 2019 Dec; 462 (1–2): 133–55.
 35. Zhu P, Liu J, Shi J, Zhou Q, Liu J, Zhang X, et al. Melatonin protects ADSCs from ROS and enhances their therapeutic potency in a rat model of myocardial infarction. *J Cell Mol Med.* 2015; 19 (9): 2232–43.
 36. Lee JH, Han YS, Lee SH. Melatonin-Induced PGC-1α Improves Angiogenic Potential of Mesenchymal Stem Cells in Hindlimb Ischemia. *Biomol Ther (Seoul)*. 2020; 28 (3): 240–9. DOI: 10.4062/biomolther.2019.131.

Литература

1. WHO Fact Sheet: Burns. [(accessed on 6 March 2018)]; Available online: <https://www.who.int/news-room/fact-sheets/detail/burns>
2. Wang Y, Beekman J, Hew J, Jackson S, Issler-Fisher AC, Parungao R, et al. Burn injury: Challenges and advances in burn wound healing, infection, pain and scarring. *Adv Drug Deliv Rev.* 2018; 123: 3–17. DOI: 10.1016/j.addr.2017.09.018.
3. Saavedra PA, de Brito ES, Areca CA, Escalda PM, Galato D. Burns in the Brazilian Unified Health System: a review of hospitalization from 2008 to 2017. *Int J Burns Trauma.* 2019 Oct 15; 9 (5): 88–98.
4. Yang P, Li Y, Xie Y, Liu Y. Different faces for different places: heterogeneity of neutrophil phenotype and function. *J Immunol Res.* 2019 Feb 28; 2019: 8016254. DOI: 10.1155/2019/8016254.
5. Nguyen AV, Soulka AM. The Dynamics of the Skin's Immune System. *Int J Mol Sci.* 2019 Apr 12; 20 (8). pii: E1811. DOI: 10.3390/ijms20081811.
6. Murray RZ, West ZE, Cowin AJ, Farrugia BL. Development and use of biomaterials as wound healing therapies. *Burns Trauma.* 2019 Jan 25; 7: 2. DOI: 10.1186/s41038-018-0139-7.
7. Osikov MV, Teleshova LF, Ageev YI. Antioxidant effect of erythropoietin during experimental chronic renal failure. *Bulletin of Experimental Biology and Medicine.* 2015; 160 (2): 202–4.
8. Осиков М. В., Телешева Л. Ф., Агеев Ю. И. Влияние эритропоэтина на апоптоз лимфоцитов при экспериментальной хронической почечной недостаточности. *Бюллетень экспериментальной биологии и медицины.* 2015; 3: 326–9.
9. Tordjman S, Chokron S2, Delorme R, et al. Melatonin: pharmacology, functions and therapeutic benefits. *Curr Neuropharmacol.* 2017 Apr; 15 (3): 434–43.
10. Varoni EM, Soru C, Pluchino R, et al. The impact of melatonin in research. *Molecules.* 2016 Feb 20; 21 (2): 240. DOI: 10.3390/molecules21020240.
11. Lopes RCV, Assis Martins J, Ribeiro de Souza T, de Castro Nunes Rincon G, Pacheco Miguel M, Borges de Menezes L, Correa Amaral A. Melatonin loaded lecithin-chitosan nanoparticles improved the wound healing in diabetic rats. *Int J Biol Macromol.* 2020 Nov 1; 162: 1465–75. DOI: 10.1016/j.ijbiomac.2020.08.027.
12. Kaczmarek-Szczepańska B, Ostrowska J, Kozłowska J, Szota Z, Brożyna AA, Dreier R, et al. Evaluation of polymeric matrix loaded with melatonin for wound dressing. *Int J Mol Sci.* 2021 May 26; 22 (11): 5658. DOI: 10.3390/ijms22115658.
13. Rusanova I, Martínez-Ruiz L, Florido J, Rodríguez-Santana C, Guerra-Librero A, Acuña-Castroviejo D, et al. Protective effects of melatonin on the skin: future perspectives. *Int J Mol Sci.* 2019 Oct 8; 20 (19): 4948. DOI: 10.3390/ijms20194948.
14. Theoharides TC. Neuroendocrinology of mast cells: Challenges and controversies. *Exp Dermatol.* 2017 Sep; 26 (9): 751–9.
15. Li H, Yao Z, Tan J, et al. Epidemiology and outcome analysis of 6325 burn patients: a five-year retrospective study in a major burn center in Southwest China. *Sci Rep.* 2017 Apr 6; 7: 46066. DOI: 10.1038/srep46066.
16. Агеева А. А., Осиков М. В., Симонян Е. В., Топорец Т. А., Потехина Е. А., авторы. Федеральное государственное бюджетное образовательное учреждение высшего образования «Омский государственный медицинский университет» Министерства здравоохранения Российской Федерации, патентообладатель. Средство в виде пленки лекарственной, содержащей мелатонин, для лечения термической травмы патент № 2 751 048 07.07.2021.
17. Chen H, Xu Y, Yang G, Zhang Q, Huang X, Yu L, et al. X. Mast cell chymase promotes hypertrophic scar fibroblast proliferation and collagen synthesis by activating TGF-β1/Smads signaling pathway. *Exp Ther Med.* 2017 Nov; 14 (5): 4438–42.
18. Sadiq A, Shah A, Jeschke MG, et al. The Role of Serotonin during Skin Healing in Post-Thermal Injury. *Int J Mol Sci.* 2018 Mar 29; 19(4). pii: E1034. DOI: 10.3390/ijms19041034.
19. Nagy B, Szélig L, Rendeki S, et al. Dynamic changes of matrix metalloproteinase 9 and tissue inhibitor of metalloproteinase 1 after burn injury. *J Crit Care.* 2015; 30 (1): 162–6. DOI: 10.1016/j.jcrc.2014.07.008.
20. Lang TC, Zhao R, Kim A, et al. A Critical Update of the Assessment and Acute Management of Patients with Severe Burns. *Adv Wound Care (New Rochelle).* 2019; 8 (12): 607–33. DOI: 10.1089/wound.2019.0963.
21. Wilgus TA, Roy S, McDaniel JC. Neutrophils and wound repair: positive actions and negative reactions. *Adv Wound Care (New Rochelle).* 2013; 2 (7): 379–88. DOI: 10.1089/wound.2012.0383.
22. Johnson KE, Wilgus TA. Vascular endothelial growth factor and angiogenesis in the regulation of cutaneous wound repair. *Adv Wound Care (New Rochelle)* 2014; 3: 647–61.
23. Yamakawa S, Hayashida K. Advances in surgical applications of growth factors for wound healing. *Burns Trauma.* 2019 Apr 5; 7: 10. DOI: 10.1186/s41038-019-0148-1.
24. Wilgus TA. Vascular endothelial growth factor and cutaneous scarring. *Adv Wound Care (New Rochelle).* 2019 Dec 1; 8 (12): 671–8.
25. Kwak DH, Bae TH, Kim WS, Kim HK. Anti-vascular endothelial growth factor (Bevacizumab) therapy reduces hypertrophic scar formation in a rabbit ear wounding model. *Arch Plast Surg.* 2016; 43: 491–7.
26. Osikov MV, Simonyan EV, Ageeva AA, Ageev YI, Sinitsky AI, Fedosov AA. Local antioxidant effect of original dermal film with melatonin in thermal injury. *Bulletin of Russian State Medical University.* 2020; 6: 104–12.
27. Осиков М. В., Симонян Е. В., Агеева А. А., Агеев Ю. И. Мелатонин в составе дермальной пленки ограничивает гибель лимфоцитов в крови при экспериментальной термической травме. *Медицинская иммунология.* 2021; 23 (2): 389–94.
28. Alluri H, Wilson RL, Anasooya Shaji C, et al. Melatonin Preserves Blood-Brain Barrier Integrity and Permeability via Matrix Metalloproteinase-9 Inhibition. *PLoS One.* 2016; 11 (5): e0154427. DOI: 10.1371/journal.pone.0154427.
29. Hazra S, Chaudhuri AG, Tiwary BK, Chakrabarti N. Matrix metallopeptidase 9 as a host protein target of chloroquine and melatonin for immunoregulation in COVID-19: A network-based meta-analysis. *Life Sci.* 2020; 257: 118096. DOI: 10.1016/j.lfs.2020.118096.
30. Qin W, Li J, Zhu R, et al. Melatonin protects blood-brain barrier

- integrity and permeability by inhibiting matrix metalloproteinase-9 via the NOTCH3/NF- κ B pathway. *Aging (Albany NY)*. 2019; 11 (23): 11391–415. DOI: 10.18632/aging.102537.
31. Wiggins-Dohlvik K, Han MS, Stagg HW, Alluri H, Shaji CA, Oakley RP, et al. Melatonin inhibits thermal injury-induced hyperpermeability in microvascular endothelial cells. *J Trauma Acute Care Surg*. 2014; 77: 899–905.
 32. Maldonado MD, Garcia-Moreno H, Calvo JR. Melatonin protects mast cells against cytotoxicity mediated by chemical stimuli PMACl: possible clinical use. *J Neuroimmunol*. 2013 Sep 15; 262 (1–2): 62–5.
 33. Rahbarghazi A, Siahkouhian M, Rahbarghazi R, et al. Role of melatonin in the angiogenesis potential; highlights on the cardiovascular disease. *J Inflamm (Lond)*. 2021; 18 (1): 4. DOI: 10.1186/s12950-021-00269-5.
 34. Bhattacharya S, Patel KK, Dehari D, Agrawal AK, Singh S. Melatonin and its ubiquitous anticancer effects. *Mol Cell Biochem*. 2019 Dec; 462 (1–2): 133–55.
 35. Zhu P, Liu J, Shi J, Zhou Q, Liu J, Zhang X, et al. Melatonin protects ADSCs from ROS and enhances their therapeutic potency in a rat model of myocardial infarction. *J Cell Mol Med*. 2015; 19 (9): 2232–43.
 36. Lee JH, Han YS, Lee SH. Melatonin-Induced PGC-1 α Improves Angiogenic Potential of Mesenchymal Stem Cells in Hindlimb Ischemia. *Biomol Ther (Seoul)*. 2020; 28 (3): 240–9. DOI: 10.4062/biomolther.2019.131.

EFFECTIVENESS OF HYBRID INTRAPERITONEAL MESH REPAIR FOR PARACOLOSTOMY HERNIA

Malgina NV^{1,2}, Dolgina TYu^{1,2}✉, Epifanova AD³, Rodoman GV^{1,2}

¹ City Clinical Hospital № 24, Moscow, Russia

² Pirogov Russian National Research Medical University, Moscow, Russia

³ Sechenov First Moscow State Medical University, Moscow, Russia

Due to advances in medical science, the frequency of surgical interventions that once ended in end-stoma formation has decreased significantly. An ostomy is a life-saving surgery performed when there are no other options. Unfortunately, the number of patients with life-threatening conditions requiring colostomy or ileostomy is growing. A stoma in itself is a cause of social alienation; stoma-associated complications reduce the quality of life and debilitate the patient. The aim of this study was to assess the effectiveness of hybrid intraperitoneal mesh repair of paracolostomy hernia using a modified EUROQOL 5D-5L questionnaire. Sixty patients with paracolostomy hernias included in the study were divided in 2 groups (30 persons per group). The experimental group (10 (33%) men and 20 (67%) women) and the control group (11 (37%) men and 19 (63%) women) were comparable in terms of sex ($p = 0.787$) and age (66.5 (62.2; 72.0) years vs. 65.0 (61.25; 71.75) years, respectively; $p = 0.246$). Patients included in the control group underwent a classic Sugarbaker procedure; the experimental group underwent hybrid intraperitoneal mesh repair. The quality of life of the patients was evaluated before surgery and then 1 and 2 years after surgery using a modified EUROQOL 5D-5L questionnaire. Hybrid intraperitoneal mesh repair proved to be effective in the early and late postoperative periods. Based on the significant improvement of the patients' quality of life after hybrid intraperitoneal mesh repair, we conclude that this technique is an effective surgical treatment for paracolostomy hernias.

Keywords: paracolostomy hernia, quality of life, questionnaire, surgery

Author contribution: Rodoman GV — the final version of the manuscript; Malgina NV — study concept and design; Dolgina TYu — data acquisition, manuscript draft; Epifanova AD — statistical analysis.

Compliance with ethical standards: the study was approved by the Ethics Committee of Pirogov Russian National Research Medical University (Protocol № 160 dated December 19, 2016)

✉ **Correspondence should be addressed:** Tamara Yu. Dolgina
Pistsovaya, 10, 127015, Moscow; dolgina-tamara@yandex.ru

Received: 10.07.2021 **Accepted:** 25.07.2021 **Published online:** 17.08.2021

DOI: 10.24075/rsmu.2021.037

ОЦЕНКА ЭФФЕКТИВНОСТИ ПРИМЕНЕНИЯ ГИБРИДНОЙ ИНТРАПЕРИТОНЕАЛЬНОЙ АЛЛОПЛАСТИКИ ПРИ ПАРАКОЛОСТОМИЧЕСКИХ ГРЫЖАХ

Н. В. Мальгина^{1,2}, Т. Ю. Долгина^{1,2}✉, А. Д. Епифанова³, Г. В. Родоман^{1,2}

¹ Городская клиническая больница № 24, Москва, Россия

² Российский национальный исследовательский медицинский университет имени Н. И. Пирогова, Москва, Россия

³ Первый Московский государственный медицинский университет имени И. М. Сеченова, Москва, Россия

Современный уровень развития медицины позволил значительно сократить частоту операций, сопровождающихся формированием концевых кишечных стом. Такие операции предпринимают для спасения жизни, когда невозможно поступить другим образом. К сожалению, из-за роста числа такого рода заболеваний число стомированных пациентов во всем мире увеличивается. Наличие стомы само по себе приводит человека к социальной дезадаптации, а осложненная стома стойко снижает качество жизни и трудоспособность. Целью исследования было оценить эффективность применения операции гибридной интраперitoneальной аллопластики параколостомических грыж при помощи оценки качества жизни пациентов на основании опросника EUROQOL 5D-5L. Включенные в исследование 60 пациентов с параколостомическими грыжами были разделены на две группы по 30 человек в каждой. Группа исследования (мужчины 10 (33%), женщины 20 (67%)) и группа сравнения (мужчины 11 (37%), женщины 19 (63%)) были сопоставимы по полу ($p = 0,787$) и возрасту (66,5 (62,2; 72,0) лет и 65,0 (61,25; 71,75), соответственно; $p = 0,246$). Пациентам первой группы была выполнена операция Sugarbaker, второй — гибридная интраперitoneальная аллопластика. Оценку качества жизни пациентов до операции, через год и через два года после нее осуществляли при помощи опросника EUROQOL 5D-5L. Показана эффективность гибридной интраперitoneальной аллопластики до операции и в раннем и позднем послеоперационных периодах. На основании значительного улучшения качества жизни пациентов после гибридной интраперitoneальной аллопластики можно сделать вывод о том, что эта операция является эффективным методом хирургического лечения пациентов с параколостомическими грыжами.

Ключевые слова: параколостомическая грыжа, качество жизни, опросник, хирургическое лечение

Вклад авторов: Г. В. Родоман — утверждение окончательного варианта статьи для публикации; Н. В. Мальгина — концепция и дизайн работы; Т. Ю. Долгина — сбор данных, написание текста статьи; А. Д. Епифанова — статистический анализ.

Соблюдение этических стандартов: исследование одобрено этическим комитетом РНИМУ им. Н. И. Пирогова (протокол заседания № 160 от 19 декабря 2016 г.)

✉ **Для корреспонденций:** Тамара Юрьевна Долгина
ул. Писцовая, д. 10, г. Москва, 127015; dolgina-tamara@yandex.ru

Статья получена: 10.07.2021 **Статья принята к печати:** 25.07.2021 **Опубликована онлайн:** 17.08.2021

DOI: 10.24075/vrgmu.2021.037

Paracolostomy hernia is one of the late colostomy complications. According to different estimates, the rate of herniation after colostomy or ileostomy varies from 28 to 100% [1–6]. While a stoma in itself is a source of emotional distress for the patient, a parastomal hernia significantly reduces the patient's quality

of life. Parastomal hernias can become painful, incarcerated or strangulated, lead to chronic evacuation difficulties, cause aesthetic discomfort and make it difficult to attach a colostomy bag [6–9].

To this day, paracolostomy hernias remain a surgical challenge [10]. Despite the diversity of surgical options for

their repair, parastomal hernias recur in 14–50% of patients; reoperations increase the rate of recurrence up to 20–64% [11–13]. Local tissue repair is characterized by a very high rate of parastomal hernia recurrence (46–100%) [14]. Repair with synthetic mesh placed in a potentially contaminated wound (near the stoma site) is associated with a high risk of infection (27.6%); therefore, a need may arise to remove hernia mesh in the early postoperative period, which may lead to hernia recurrence. Stoma relocation through open extraperitoneal ostomy is also associated with high hernia recurrence (75–100%). Today, these methods have only historical value [10]. By contrast, the Sugarbaker technique and its modifications ensure the lowest rate of parastomal hernia recurrence (15% on average) [15; 16]. The high recurrence rate drives the search for new surgical techniques for parastomal hernia repair. One of such techniques, hybrid intraperitoneal mesh alloplasty, was proposed in our previous publication [17].

The aim of this study was to evaluate the effectiveness of hybrid intraperitoneal mesh alloplasty of paracolostomy hernia using a modified quality-of-life EUROQOL 5D-5L questionnaire.

METHODS

The study was conducted on 60 patients with paracolostomy hernias undergoing hernia repair between 2013 and 2019 at the City Clinical Hospital № 4, Moscow. Our study was a prospective single-center controlled continuous pilot trial of hybrid intraperitoneal mesh alloplasty effectiveness in patients with parastomal hernias. Sample size calculations were not performed. The study included patients with permanent stomas. The extent of surgical intervention which involved stoma formation was determined by the type of rectal disease: total abdominoperineal resection of the rectum for anal canal cancer; partial abdominoperineal resection for cancer of the rectal ampulla; colostomy for severe trauma of the anal sphincter [9].

The following inclusion criteria were applied: parastomal hernia confirmed by imaging tests which significantly compromised the patient's quality of life; clinical symptoms indicative of episodes of incarceration, documented bowel obstruction; informed consent to be treated, participate in the study and be followed-up for 2 years after surgery; willingness to follow medical advice. Exclusion criteria: allergies to iodine-containing drugs; class IV–V of cardiac complications risk on the MNOAR (Moscow Scientific Society for Anesthesiology and Critical Care Resuscitation) scale [18]; Lee's class IV of cardiac complications risk (revised cardiac risk index) [19]; severe chronic obstructive pulmonary disease with FVC reduced to 70%; mental disorders; impaired cognitive function; progressing or metastatic cancer; the possibility of stoma reversal surgery.

Patients included in the study were randomized into 2 groups. The control group comprised patients with paracolostomy hernia who were operated on using a classic Sugarbaker technique, i.e. tension-free intraperitoneal prosthetic mesh repair without defect closure [20]. The experimental group consisted of 30 patients who underwent hybrid intraperitoneal hernioplasty with composite mesh. This surgical intervention is a modification of the Sugarbaker technique. Briefly, the defect in the abdominal wall is closed with individual interrupted sutures so that it would match the diameter of the colon. Then the suture line and the anterior abdominal wall are reinforced with a composite mesh placed around the stoma to form an envelope for the colon. The mesh is secured with tacks to the parietal peritoneum and sutured to the serosa of the colon (Fig. 1–3). If properly performed, this technique prevents hernia recurrence during

mesh integration with the native tissue. To sum up, the groups differed in terms of the applied surgical technique; the patients were randomly assigned to either group.

The groups were comparable in terms of parastomal hernia size: there were 20 (67%) patients with type III hernia and 10 (33%) patients with type IV hernia in the experimental group vs. 15 (50%) and 15 (50%) patients with type III and type IV hernia, respectively, in the control group ($p = 0.191$).

The overwhelming majority of our patients had a permanent stoma for anal canal cancer; of them 22 (73%) were in the experimental group and 20 (67%) were in the control group. The groups were comparable in terms of the underlying condition that necessitated a permanent colostomy ($p = 0.763$). The groups were also comparable in terms of initial surgical intervention ($p = 0.394$): 22 (73%) patients in the experimental group and 17 (57%) patients in the control group had total abdominoperineal resection of the rectum. Table shows the distribution of patients in the groups by their initial characteristics.

Early postoperative complications were evaluated using the Clavien–Dindo classification [21]. No deaths were registered in any of the groups. Most complications (surgical wound complications like seromas, postoperative hematomas, gastrointestinal paresis) were classified as grade I complications. Surgical site seromas were detected in 7% (2–21%) of patients from the experimental group and in 10% (4–25%) of patients from the control group (the difference was insignificant; $p > 0.05$, Fisher's exact test). Surgical site hematomas were detected in 3% (1–17%) of control group patients vs. no hematomas in the experimental group. The proportion of patients with early postoperative gastrointestinal paresis was equal in both groups: 7% (2–21%). Thus, the frequency of early postoperative complications did not differ significantly between the groups [17].

Late postoperative complications (parastomal hernia recurrence) were evaluated using follow-up contrast-enhanced CT scans of the abdomen performed 1 and 2 years after parastomal hernia repair. Two years after surgery, there were 3 parastomal hernia recurrences in the experimental group (10% (3–26%)) vs. 13 recurrences in the control group (43% (27–61%)); the difference was statistically significant ($p = 0.01$; Yates-corrected χ^2). The most common late postoperative complications, besides parastomal hernia recurrence, are colostomy stricture and prolapse. In our study, there were no postoperative colostomy strictures in any of the groups. This may be explained by the use of composite mesh that does not erode into the bowel wall, cause deformation or stenosis of the



Fig. 1. An intraoperative image of the parastomal fascial defect

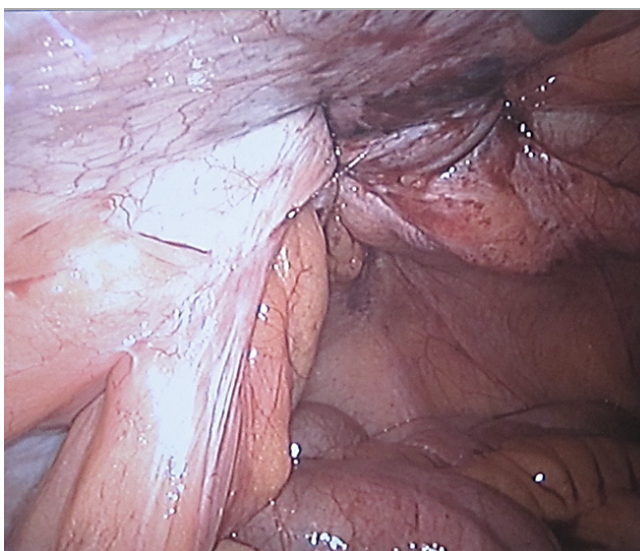


Fig. 2. An intraoperative image showing defect closure with sutures

bowel [22]. No cases of colostomy prolapse were observed in the experimental group. There were 3 cases of colostomy prolapse (10%) in the control group. This complication was most likely due to the absence of fixation of the colon to the anterior abdominal wall at the ostomy site and higher colonic mobility. During hybrid intraperitoneal hernia mesh alloplasty, the colon is secured in place by adjusting the size of the defect to the colonic diameter so as not to leave any free space in this zone.

The quality of life of our patients was assessed using a European EQOL 5D-5L questionnaire. Our patients were mostly elderly people with chronic neurological comorbidities (cerebrovascular disease, chronic brain ischemia). It may be difficult for such patients to complete extensive questionnaires, and thus the results may be invalid and unreliable [9]. In our study, the quality of life was measured using a EQOL 5D-5L questionnaire before hernia repair and 1 and 2 years after hernia repair. These time points were chosen based on the international literature reports of paracolostomy hernia recurrences and our own data. Usually, paracolostomy hernias recur within one year after surgical repair [15; 21].

The EQOL 5D-5L questionnaire consists of 2 sections. The first section focuses on 5 dimensions: mobility, self-care, usual activities, pain and discomfort, anxiety and depression. There are 5 levels of severity for each dimension: no problems, slight problems, moderate problems, severe problems, and extreme problems. In total, the questionnaire generates 3,125 different health states [23; 24].

We modified the questionnaire so that our respondents understood that they were evaluating the impact of paracolostomy hernia (but not other conditions) on their everyday activities and emotional state.

Below, we provide a modified version of the EQOL 5D-5L questionnaire [9].

1. Mobility:

- a) My parastomal hernia does not cause any problems walking — 1 point;
- b) I have slight problems walking because of parastomal hernia — 2 points;
- c) I have moderate problems walking because of parastomal hernia — 3 points;
- d) I have severe problems walking because of parastomal hernia — 4 points;
- e) I am unable to walk because of parastomal hernia — 5 points.



Fig. 3. An intraoperative image of the “envelope” for the colon

2. Self-care:

- a) I have no problems dressing or washing myself — 1 point;
- b) I have slight problems dressing or washing myself — 2 points;
- c) I have moderate problems dressing or washing myself — 3 points;
- d) I have severe problems dressing or washing myself — 4 points;
- e) I am unable to dress or wash myself because of parastomal hernia — 5 points.

3. Usual activities (work, housework, family activities, leisure):

- a) I have no problems doing my usual activities — 1 point;
- b) I have slight problems doing my usual activities because of parastomal hernia — 2 points;
- c) I have moderate problems doing my usual activities because of parastomal hernia — 3 points;
- d) I have severe problems doing my usual activities because of parastomal hernia — 4 points;
- e) I am unable to do my usual activities because of parastomal hernia — 5 points.

4. Pain and discomfort:

- a) I have no pain or discomfort — 1 point;
- b) I sometimes have slight pain or discomfort that I link to parastomal hernia — 2 points;
- c) I sometimes have moderate pain or discomfort that I link to parastomal hernia — 3 points;
- d) I often have severe pain or discomfort that I link to parastomal hernia — 4 points;
- e) I almost always have extreme pain or discomfort that I link to parastomal hernia — 5 points.

5. Anxiety and depression:

- a) I am not anxious or depressed — 1 point;
- b) I am slightly anxious or depressed — 2 points;
- c) I am moderately anxious or depressed — 3 points;
- d) I am severely anxious or depressed — 4 points;
- e) I am extremely anxious or depressed — 5 points.

The second section of the questionnaire is a visual analogue scale (VAS) that allows the patient to self-rate their general health from 0 to 100 (Fig. 4).

The respondent completes the questionnaire independently; it normally takes 2–3 min and does not pose any difficulty even for elderly patients with memory problems or cognitive impairment. The quality of life was evaluated by calculating a

Table. Initial characteristics of patients included in the study

Characteristic	Total number of patients (n = 60)	Experimental group (hybrid intraperitoneal mesh alloplasty) (n = 30)	Control group (classic Sugerbaker technique) (n = 30)	p	Statistical test
Sex Male Female	21 (35%) 39 (65%)	10 (33%) 20 (67%)	11 (37%) 19 (63%)	0,787	χ^2
Median age, years	65,5 (61,75; 72,0)	66,5 (62,25; 72,0)	65,0 (61,25; 71,75)	0,246	Манна–Уитни
CParastomal hernia type III IV	35 (58%) 25 (42%)	20 (67%) 10 (33%)	15 (50%) 15 (50%)	0,191	χ^2
Underlying condition					
Cancer of rectal ampulla Anal canal cancer Diverticular disease complications Rectal sphincter trauma	15 (25%) 42 (70%) 1 (2%) 2 (3%)	7 (23%) 22 (73%) 0 (0%) 1 (3%)	8 (27%) 20 (67%) 1 (3%) 1 (3%)	0,763	χ^2
Initial surgery					
Subtotal abdominoperineal resection of rectum Colostomy Total abdominoperineal resection of rectum	18 (30%) 3 (5%) 39 (65%)	7 (23%) 1 (3%) 22 (73%)	11 (37%) 2 (7%) 17 (57%)	0,394	χ^2

crosswalk index (weighted coefficient) using a EUROQOL 5D-5L Crosswalk Index Value Calculator for Windows [24]. The difference between the crosswalk indices before and after treatment indicates the effectiveness of treatment. The following grading scale for treatment effectiveness was applied:

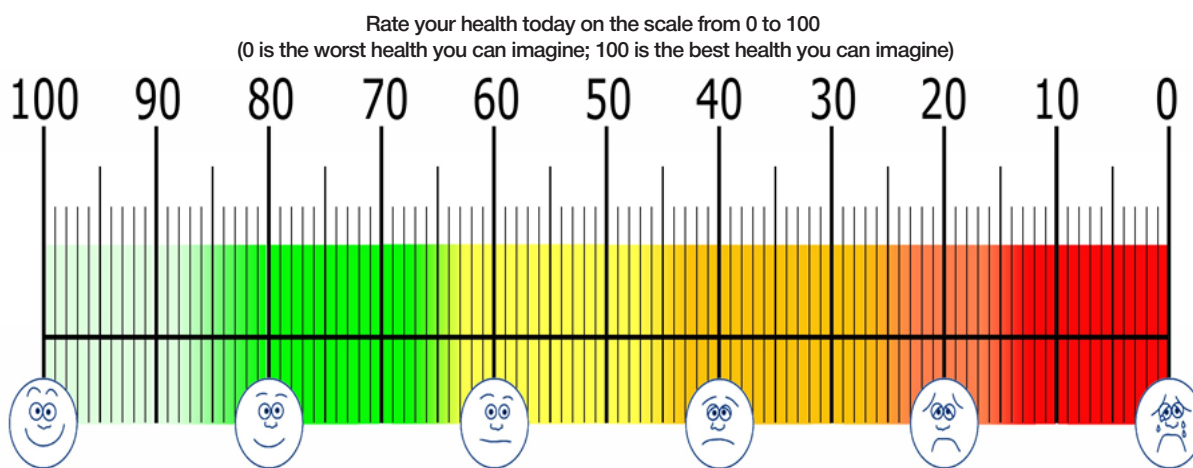
- Δ EQ-5D-5L < 0.10 points — no effect
- 0.10 ≤ Δ EQ-5D-5L ≤ 0.24 — minimal effect
- 0.24 ≤ Δ EQ-5D-5L < 0.31 — satisfactory effect
- Δ EQ-5D-5L ≥ 0.31 points — pronounced effect

The obtained data were processed in Python 3.8. (Guido van Rossum; Netherlands). Calculations were done using algorithms from the SciPy library. The Shapiro-Wilk test was applied to test the normality of distribution of quantitative variables. The test showed that the variables had non-normal distribution. Therefore, further analysis was performed using nonparametric statistics. Variables that had non-normal distribution are presented below as median values (Me), upper and lower quartiles (Q_1 ; Q_3). Independent samples were compared using the Mann-Whitney U test; dependent samples were compared using the Wilcoxon test.

Possible correlations between quantitative variables were investigated using nonparametric statistics (Spearman's rank correlation coefficient, rs). Qualitative variables are presented below as absolute values, proportions (%) and 95%-CI calculated by the Wilson method. Categorical variables were compared using Pearson's χ^2 . If the expected count in at least 1 cell was < 10, Yates' correction for continuity was applied. If the expected count per cell was < 5, Fisher's exact test was applied to measure the level of statistical significance. The significance threshold was set at $p \leq 0.05$.

RESULTS

Preoperative median values of the crosswalk index were comparable between the groups: 0.56 (0.42; 0.69) in the experimental group and 0.46 (0.29; 0.68) in the control group ($p = 0.113$). Median VAS scores calculated before surgery were also comparable: 52.5 (41.25; 67.5) in the experimental group and 47.5 (40.0; 60.0) in the control group ($p = 0.156$).

**Fig. 4.** The EUROQOL 5D-5L visual analogue scale

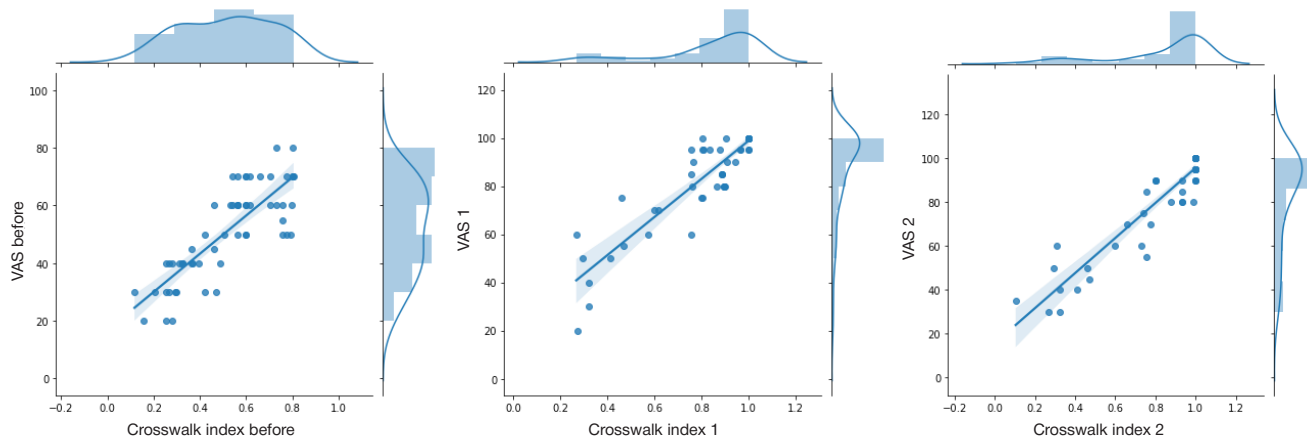


Fig. 5. Correlations between the crosswalk index and the VAS score

A year after surgery, the median crosswalk index and the median VAS score differed significantly between the groups ($p < 0.001^*$ and $p < 0.001^*$, respectively; * designates statistically significant differences, i.e. $p < 0.05$). The median crosswalk index and the median VAS score were significantly higher in the experimental group than in the control group (crosswalk index: 0.92 (0.81; 1.0) in the experimental group vs. 0.89 (0.5; 1.0) in the control group, $p = 0.046^*$; VAS score: 95.0 (86.25; 100.0) in the experimental group vs. 85.0 (62.5; 100.0) in the control group, $p = 0.021^*$).

Two years after surgery, the median crosswalk index was still significantly higher in the experimental group (1.0 (0.93; 1.0) than in the control group (0.8 (0.46; 1.0); $p = 0.048^*$). Notably, the crosswalk index increased significantly in the experimental group in the second year after surgery from 0.92 (0.81; 1.0) to 1.0 (0.93; 1.0) ($p = 0.033^*$), whereas in the control group it fell from 0.89 (0.5; 1.0) to 0.8 (0.46; 1.0) ($p = 0.028^*$).

During the second year after surgery, the values of the crosswalk index in the experimental group were tight around 1 ((0.93, 1.0)), whereas in the control group they ranged from 0.46 to 1.0, suggesting an unstable effect of surgery (measured by the crosswalk index) after 2 years. VAS scores were also higher in the experimental group than in the control group two years after surgery but the differences

were insignificant: 95.0 (85.0; 100.0) in the experimental group and 85.0 (50.0; 95.0) in the control group ($p = 0.054$). By year 2, the median VAS score in the experimental group stabilized at 95, without any significant dynamics. In the control group, the median VAS score remained at the same level (85) but the interquartile range expanded and shifted towards lower values, which was reflected in the statistically significant difference in VAS scores between years 1 and 2 after surgery: 85.0 (62.5; 100.0) in year 1 vs. 85.0 (50.0; 95.0) in year 2 ($p = 0.004^*$).

Importantly, the crosswalk index and the VAS score were well-correlated at all time points of measurement: before surgery ($rs = 0.8246$; $p < 0.001^*$), 1 year after surgery ($rs = 0.8909$; $p < 0.001^*$) and 2 years after surgery ($rs = 0.9161$; $p < 0.001^*$). In other words, the results generated by these two scales were in good agreement with each other (Fig. 5).

DISCUSSION

After hernia repair, median values of quality-of-life indicators improved significantly in both groups. However, the effectiveness of paracolostomy hernia repair is determined not only by an improvement in the quality of life but also by the proportion of patients without recurrent herniation [25].

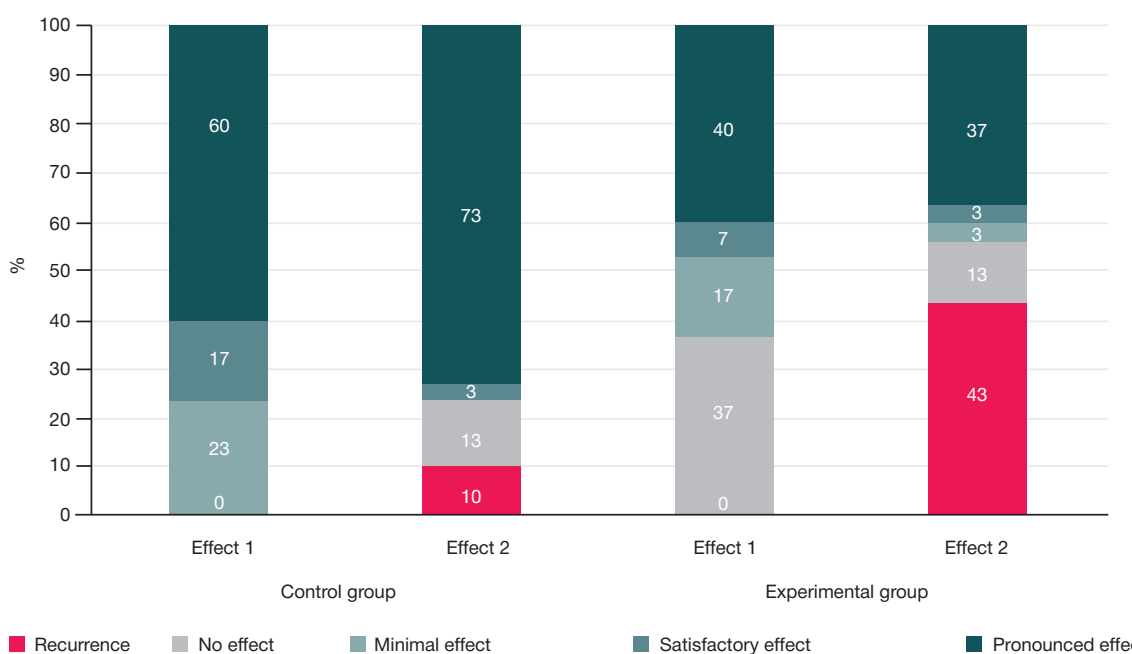


Fig. 6. Effectiveness of paracolostomy hernia repair

The analysis of differences in the crosswalk index measured before surgery and 1 year after it (effect 1) and differences in this parameter measured 1 and 2 years after surgery (effect 2) showed that the effect of the delivered treatment was statistically significant (Fig. 6) in both groups 1 year after (effect 1; $p = 0.004^*$) and 2 years after surgery (effect 1; $p = 0.028^*$).

In terms of prevention of hernia recurrence, hybrid intraperitoneal hernia mesh repair in the experimental group had a significantly stronger effect (90% (74; 97%) than the classic Sugarbaker technique in the control group (57% (39; 73%); ($p = 0.009^*$; Yates-corrected χ^2). The difference between the crosswalk indices before and after treatment allows assessing the effectiveness of the proposed surgical treatment based on the grading scale for effectiveness. Our findings may be useful for the planning of further studies and development of practical recommendations.

Our findings suggest that a follow-up abdominal CT scan might not be necessary in the late postoperative period after colostomy hernia repair. In a clinical setting, using the modified EUROQOL 5D-5L questionnaire may help to avoid a costly CT procedure. If the questionnaire shows that the patient's quality of life has not improved significantly after surgery and hernia

recurrence is suspected, then a follow-up CT scan should be ordered.

In the late postoperative period, recurrent herniation was observed in 3 patients in the experimental group (10%; 95%CI: 3–26%) and 13 patients in the control group (43%; 95%CI: 27–61%; $p = 0.01$; Yates-corrected χ^2). The rate of recurrence in the experimental group was quite high. This raises the need for further refinement of the surgical technique and for new effective methods of parastomal hernia prevention [26–28].

The limitation of our study was a small sample size due to stringent inclusion criteria.

CONCLUSIONS

Parastomal hernia repair is a challenging surgical procedure without a clear standard of optimal surgical approach. Data collected by means of the modified EUROQOL 5D-5L questionnaire suggest that hybrid intraperitoneal hernia mesh alloplasty is an effective surgical treatment for patients with paracolostomy hernias that significantly improves the patient's quality of life. This technique can be recommended as a surgical treatment option for parastomal hernia.

References

- Allen-Mersh TG, Thomson JP. Surgical treatment of colostomy complications. *Br J Surg.* 1988 May; 416–8.
- Israelson LA. Preventing and treating Parastomal hernia. *World Journal of Surgery.* 2005; 1086–9.
- Israelson LA. Parastomal hernias. *Surgical Clinics of North America.* 2008; 113–25.
- Hiranyakas A, Ho YH. Laparoscopic parastomal hernia repair. *Diseases of the Colon & Rectum.* 2010; 53 (9): 1334–6.
- Śmietański M, Bury K, Matyja A, et al. Polish guidelines for treatment of patients with parastomal hernia. *Pol Przegl Chir.* 2013; 85: 152–80.
- De Robles MS, Young CJ. BMC. Parastomal hernia repair with onlay mesh remains a safe and effective approach. 2020; 24; 20 (1): 296. DOI: 10.1186/s12893-020-00964-9.
- Tivenius M, Näsvall P, Sandblom G. Int J. Parastomal hernias causing symptoms or requiring surgical repair after colorectal cancer surgery-a national population-based cohort study. *Colorectal Dis.* 2019; 34 (7): 1267–72. DOI: 10.1007/s00384-019-03292-4.
- Van Dijk SS, Timmermans L, Deerenberg EB, et al. Parastomal Hernia: Impact on Quality of Life? *World J Surg.* 2015; 39: 2596–601.
- Rodoman GV, Malgina NV, Razbirin VN, Dolgina TYu. Ocena individual'nogo kachestva zhizni pacienta s parakolostomicheskoy gryzhej. *Hirurg.* 2019; 3–4: 14–23. Russian.
- Rodoman GV, Malgina NV, Razbirin VN, Dolgina TYu. Sostojanie problemy operativnogo lechenija parakolostomicheskikh gryzh. *Hirurg.* 2016; 10 (144): 24–30. Russian.
- Hansson BM, Slater NJ, Schouten van der Velden AP, et al. Surgical techniques for parastomal hernia repair: a systematic review of the literature. *Ann Surg.* 2012; 255: 685–95.
- Tadeo-Ruiz G, Picazo-Yeste JS, Moreno-Sanz C, Herrero-Bogajo ML. Parastomal hernias: background, current status and future prospects. *Cirugía Española (English Edition).* 2010; 87 (6): 339–49.
- Antoniou SA, Agresta F, Garcia Alamino JM, et al. European Hernia Society guidelines on prevention and treatment of parastomal hernias. *Hernia.* 2018; 22: 183–98.
- Gregg ZA, Dao HE, Schechter S, Shah N. Paracolostomal Hernia Repair: who and when? *Journal of the American College of Surgeons.* 2014; 1105–12.
- Szczepkowski M, Gil G, Kobus A. Parastomal hernia repair: Bielański hospital experience. *Acta chirurgica jugoslavica.* 2006; 53 (2): 99–102.
- Okorji LM, Kasten KR. Diagnosis and Management of Parastomal Hernias. *Dis Colon Rectum.* 2019 Feb; 62 (2): 158–62. DOI: 10.1097/DCR.0000000000001293.
- Rodoman GV, Malgina NV, Razbirin VN, Epifanova SV, Dolgina TYu, Kuznecov AI. Primenenie mul'tispiral'noj komp'juternoj tomografii dlja ocenki effektivnosti hirurgicheskogo lechenija pacientov s parakolostomicheskoy gryzhej. *Hirurgija. Zhurnal im. N. I. Pirogova.* 2021; (3): 36–41. Russian.
- Burov NE. Kratkij obzor istorii MNOAR. K 50-letiju MNOAR. *Anesteziologija i reanimatologija.* 2013; (4): 77–82. Russian.
- Lee TH, Marcantonio ER, Mangione CM, et al. Derivation and prospective validation of a simple index for prediction of cardiac risk of major noncardiac surgery. *Circulation.* 1999; 100 (10): 1043–9.
- Sugarbaker PH. Peritoneal approach to prosthetic mesh repair of parastomy hernias. *Ann Surg.* 1985; 201: 344–6.
- Dindo D, Demartines N, Clavien P. Classification of surgical complications: a new proposal with evaluation in a cohort of 6336 patients and results of a survey. *Ann Surg.* 2004; 240: 205–13.
- Rodoman GV, Malgina NV, Razbirin VN, Dolgina TYu. Vybor sinteticheskogo allotransplantata dlja operacij po povodu parakolostomicheskikh gryzh. *Hirurg.* 2018; 9–10: 3–12. Russian.
- The EuroQol group. EuroQol — a new facility for the measurement of health related quality of life. *Health Policy.* December 1990; 16: 199–208. Available from: [https://doi.org/10.1016/0168-8510\(90\)90421-9](https://doi.org/10.1016/0168-8510(90)90421-9).
- Notes on the use of EQ-5D developed by the EuroQol Group, 2003, EuroQol Business Management, PO Box 4445 3006 AK Rotterdam, the Netherlands, Available from: www.euroqol.org.
- Blackwell S, Pinkney T. Quality of life and parastomal hernia repair: the PROPHER study. *Hernia.* 2020; 24: 429–30.
- Gachabayov M, Orujova L, Latifi LA, Latifi R. Use of Biologic Mesh for the Treatment and Prevention of Parastomal Hernias. *Surg Technol Int.* 2020 Nov; 28; 37: 115–9.
- Cross AJ, Buchwald PL, Frizelle FA, Eglinton TW. Meta-analysis of prophylactic mesh to prevent parastomal hernia. *Br J Surg.* 2017 Feb; 104 (3): 179–186. DOI: 10.1002/bjs.10402. Epub 2016 Dec 22.
- Pich J. Prosthetic mesh for the prevention of parastomal hernias. *Am J Nurs.* 2019 Apr; 119 (4): 49. DOI: 10.1097/01.NAJ.0000554548.93403.64.

Литература

1. Allen-Mersh TG, Thomson JP. Surgical treatment of colostomy complications. *Br J Surg.* 1988 May; 416–8.
2. Israelson LA. Preventing and treating Parastomal hernia. *World Journal of Surgery.* 2005; 1086–9.
3. Israelson LA. Parastomal hernias. *Surgical Clinics of North America.* 2008; 113–25.
4. Hiranyakas A, Ho YH. Laparoscopic parastomal hernia repair. *Diseases of the Colon & Rectum.* 2010; 53 (9): 1334–6.
5. Śmietański M, Bury K, Matyja A, et al. Polish guidelines for treatment of patients with parastomal hernia. *Pol Przegl Chir.* 2013; 85: 152–80.
6. De Robles MS, Young CJ. BMC. Parastomal hernia repair with onlay mesh remains a safe and effective approach. 2020; 24; 20 (1): 296. DOI: 10.1186/s12893-020-00964-9.
7. Tivenius M, Näsvall P, Sandblom G. Int J. Parastomal hernias causing symptoms or requiring surgical repair after colorectal cancer surgery-a national population-based cohort study. *Colorectal Dis.* 2019; 34 (7): 1267–72. DOI: 10.1007/s00384-019-03292-4.
8. Van Dijk SS, Timmermans L, Deerenberg EB, et al. Parastomal Hernia: Impact on Quality of Life? *World J Surg.* 2015; 39: 2596–601.
9. Родоман Г. В., Мальгина Н. В., Разбираин В. Н., Долгина Т. Ю. Оценка индивидуального качества жизни пациента с параколостомической грыжей. *Хирург.* 2019; 3–4: 14–23.
10. Родоман Г. В., Мальгина Н. В., Разбираин В. Н., Долгина Т. Ю. Состояние проблемы оперативного лечения параколостомических грыж. *Хирург.* 2016; 10 (144): 24–30.
11. Hansson BM, Slater NJ, Schouten van der Velden AP, et al. Surgical techniques for parastomal hernia repair: a systematic review of the literature. *Ann Surg.* 2012; 255: 685–95.
12. Tadeo-Ruiz G, Picazo-Yeste JS, Moreno-Sanz C, Herrero-Bogajo ML. Parastomal hernias: background, current status and future prospects. *Cirugía Española (English Edition).* 2010; 87 (6): 339–49.
13. Antoniou SA, Agresta F, Garcia Alamino JM, et al. European Hernia Society guidelines on prevention and treatment of parastomal hernias. *Hernia.* 2018; 22: 183–98.
14. Gregg ZA, Dao HE, Schechter S, Shah N. Paracolostomal Hernia Repair: who and when? *Journal of the American College of Surgeons.* 2014; 1105–12.
15. Szczepkowski M, Gil G, Kobus A. Parastomal hernia repair: Bielański hospital experience. *Acta chirurgica jugoslavica.* 2006; 53 (2): 99–102.
16. Okorji LM, Kasten KR. Diagnosis and Management of Parastomal Hernias. *Dis Colon Rectum.* 2019 Feb; 62 (2): 158–62. DOI: 10.1097/DCR.0000000000001293.
17. Родоман Г. В., Мальгина Н. В., Разбираин В. Н., Епифанова С. В., Долгина Т. Ю., Кузнецов А. И. Применение мультиспиральной компьютерной томографии для оценки эффективности хирургического лечения пациентов с параколостомической грыжей. *Хирургия. Журнал им. Н. И. Пирогова.* 2021; (3): 36–41.
18. Буров Н. Е. Краткий обзор истории МНОАР. К 50-летию МНОАР. Анетезиология и реаниматология. 2013; (4): 77–82.
19. Lee TH, Marcantonio ER, Mangione CM, et al. Derivation and prospective validation of a simple index for prediction of cardiac risk of major noncardiac surgery. *Circulation.* 1999; 100 (10): 1043–9.
20. Sugarbaker PH. Peritoneal approach to prosthetic mesh repair of parastomy hernias. *Ann Surg.* 1985; 201: 344–6.
21. Dindo D, Demartines N, Clavien P. Classification of surgical complications: a new proposal with evaluation in a cohort of 6336 patients and results of a survey. *Ann Surg.* 2004; 240: 205–13.
22. Родоман Г. В., Мальгина Н. В., Разбираин В. Н., Долгина Т. Ю. Выбор синтетического аллотрансплантата для операций по поводу параколостомических грыж. *Хирург.* 2018; 9–10: 3–12.
23. The EuroQol group. EuroQol — a new facility for the measurement of health related quality of life. *Health Policy.* December 1990; 16: 199–208. Available from: [https://doi.org/10.1016/0168-8510\(90\)90421-9](https://doi.org/10.1016/0168-8510(90)90421-9).
24. Notes on the use of EQ-5D developed by the EuroQol Group, 2003, EuroQol Business Management, PO Box 4445 3006 AK Rotterdam, the Netherlands, Available from: www.euroqol.org.
25. Blackwell S, Pinkney T. Quality of life and parastomal hernia repair: the PROPHER study. *Hernia.* 2020; 24: 429–30.
26. Gachabayov M, Orujova L, Latifi LA, Latifi R. Use of Biologic Mesh for the Treatment and Prevention of Parastomal Hernias. *Surg Technol Int.* 2020 Nov; 28; 37: 115–9.
27. Cross AJ, Buchwald PL, Frizelle FA, Eglinton TW. Meta-analysis of prophylactic mesh to prevent parastomal hernia. *Br J Surg.* 2017 Feb; 104 (3): 179–186. DOI: 10.1002/bjs.10402. Epub 2016 Dec 22.
28. Pich J. Prosthetic mesh for the prevention of parastomal hernias. *Am J Nurs.* 2019 Apr; 119 (4): 49. DOI: 10.1097/01.NAJ.0000554548.93403.64.

EXPERIMENTAL ASSESSMENT OF BIOLOGICAL POTENTIAL OF COLLAGEN MEMBRANES IN RECONSTRUCTION OF FULL-THICKNESS HYALINE CARTILAGE DEFECTS

Lazishvili GD¹✉, Egiazaryan KA¹, Nikishin DV², Voroncov AA³, Klinov DV⁴

¹ Pirogov Russian National Research Medical University, Moscow, Russia

² OOO Aptos Group, Moscow, Russia

³ Doctor Vorontsov's Veterinary Center for Surgery and Oncology, Moscow, Russia

⁴ Federal Research and Clinical Center of Physical-Chemical Medicine under the Federal Medical Biological Agency, Moscow, Russia

Investigation of the efficacy of collagen membranes used in the full-thickness hyaline cartilage defect surgery is extremely urgent from the point of view of everyday healthcare. However, there is no information about the collagen membrane transformation timeframe, patterns and type of tissue the membrane transforms into, nor on the quality of the newly formed cartilage, which hinders the use of collagen membranes in clinical practice. This study aimed to investigate the biological potential of collagen membranes and their capacity to transform into cartilage tissue. The study involved four pigs as subjects. We induced a full-thickness cartilage defect on their right hind limb joint and implanted an Ortokeep collagen membrane to remedy it. Two full-thickness cartilage defects were induced on the left hind limb joints of the animals, one was treated with an implanted Chondro-Gide collagen membrane, the other remained without a membrane. The animals were withdrawn from the experiment at 2, 3, 4, 6 months after the operation. This report contains results of the macroscopic and microscopic analyses revealing the character of cartilage tissue regeneration at various timepoints post-surgery. The collagen membranes proved to have a high biological potential and a capacity to transform into cartilage tissue. The cartilages were identifiable from the 3rd month of the study. Their thickness was growing significantly ($p < 0.05$) up to the 4th month post-surgery, gaining 18.7% in group 1 and 12.8% in group 2; afterwards, the formed tissue "matured". We have shown that the AMIC technique allows significant ($p < 0.05$) reduction of the bone tissue destruction area.

Keywords: cartilage, local defect, knee joint, AMIC technology, osteochondral defect, collagen membrane, mosaicplasty

Author contribution: Lazishvili GD — design of the experiment, participation in the experimental surgery, analysis of literature and experimental materials, article authoring; Egiazaryan KA — analysis of literature, experimental results; Nikishin DV — processing and analysis of the experimental data, article authoring; Vorontsov AA — execution of the experimental surgery; Klinov DV — Ortokeep collagen membrane design and development.

Compliance with ethical standards: the study was approved by the Ethics Committee of the Center for Preclinical Research of Penza (Minutes № 1–19 of March 11, 2019). The animals were kept and used in compliance with the ethical standards and International requirements for humane treatment of laboratory (experimental) animals, as well as GOST R ISO 10993-1-2009 Medical Devices.

✉ Correspondence should be addressed: Guram D. Lazishvili
Ostrovyanova, 1, 117997, Moscow; guramlaz@gmail.com

Received: 19.07.2021 Accepted: 05.08.2021 Published online: 20.08.2021

DOI: 10.24075/rbsmu.2021.038

ЭКСПЕРИМЕНТАЛЬНАЯ ОЦЕНКА БИОЛОГИЧЕСКОГО ПОТЕНЦИАЛА КОЛЛАГЕНОВЫХ МЕМБРАН ПРИ РЕКОНСТРУКЦИИ ПОЛНОСЛОЙНЫХ ДЕФЕКТОВ ГИАЛИНОВОГО ХРЯЩА

Г. Д. Лазишвили¹✉, К. А. Егиазарян¹, Д. В. Никишин², А. А. Воронцов³, Д. В. Клинов⁴

¹ Российский национальный исследовательский медицинский университет имени Н. И. Пирогова, Москва, Россия

² ООО «Аптос групп», Москва, Россия

³ Клиника «Ветеринарный центр хирургии и онкологии доктора Воронцова», Москва, Россия

⁴ Федеральный научно-клинический центр физико-химической медицины Федерального медико-биологического агентства, Москва, Россия

Изучение эффективности применения коллагеновых мембран при хирургическом лечении полнослойных дефектов гиалинового хряща крайне актуально для практического здравоохранения. Отсутствие сведений о том, в какие сроки, как и в какую хрящевую ткань трансформируются коллагеновые мембранны, каково качество вновь образованного хряща, сдерживает их применение в клинической практике. Целью исследования было изучить биологический потенциал коллагеновых мембран и их способность к трансформации в хрящевую ткань. Исследование проводили на четырех свиньях. На суставах правых задних конечностей формировали полнослойный дефект хряща и имплантировали коллагеновую мембрану Ortokeep. На суставах левых задних конечностей формировали по два полнослойных дефекта хряща. На один дефект имплантировали коллагеновую мембрану Chondro-Gide, на второй дефект мембрану не имплантировали. Животных выводили из эксперимента в сроки 2, 3, 4, 6 месяцев после операции. Представлены макроскопический и микроскопический анализ характера регенерации хрящевой ткани в различные сроки после операции. Результаты показали высокий биологический потенциал коллагеновых мембран и их возможность трансформироваться в хрящевую ткань. Хрящ выявлялся с 3-го месяца исследования. Отмечена тенденция к статистически достоверному ($p < 0,05$) увеличению его толщины вплоть до 4-го месяца (в группе 1 — на 18,7%, во группе 2 — на 12,8%) с последующим его «созреванием». Показано, что при использовании технологии AMIC статистически достоверно ($p < 0,05$) уменьшается область деструкции костной ткани.

Ключевые слова: хрящ, локальный дефект, коленный сустав, технология AMIC, костно-хрящевой дефект, коллагеновая мембрана, мозаичная пластика

Вклад авторов: Г. Д. Лазишвили — дизайн эксперимента, участие в выполнении экспериментальных операций, анализ данных литературы и материалов эксперимента, написание статьи; К. А. Егиазарян — анализ данных литературы, результатов эксперимента; Д. В. Никишин — обработка и анализ данных эксперимента, участие в написании статьи; А. А. Воронцов — выполнение экспериментальных операций; Д. В. Клинов — автор и разработчик коллагеновой мембраны Ortokeep.

Соблюдение этических стандартов: исследование одобрено этическим комитетом Центра доклинических исследований г. Пенза (протокол № 1–19 от 11 марта 2019 г.). Содержание животных и манипуляции с ними соответствуют этическим нормам и Международным требованиям по гуманному отношению к лабораторным (экспериментальным) животным, а также ГОСТ Р ИСО 10993-1-2009 «Изделия медицинские».

✉ Для корреспонденции: Гурам Давидович Лазишвили
ул. Островитянова, д. 1, 117997, г. Москва; guramlaz@gmail.com

Статья получена: 19.07.2021 Статья принята к печати: 05.08.2021 Опубликована онлайн: 20.08.2021

DOI: 10.24075/vrgmu.2021.038

In the recent years, AMIC (autologous matrix induced chondrogenesis) has grown widely popular as a full-thickness hyaline cartilage defect restoration technique [1–4]. The method relies on holes made in the subchondral bone and allowing passage of bone marrow to the defect's surface, which delivers bone marrow stromal cells inducing regeneration. The resulting red bone marrow "superclot" is stabilized by a collagen membrane implanted in the cartilage defect area. The natural cell scaffolding protects and binds progenitor cells inside the "biological chamber", stimulating their differentiation and subsequent cartilage repair [3, 5].

The benefits of AMIC are clear. It is a minimally invasive single step procedure that does not require chondrocyte culturing; it enables restoration of large cartilage defects ($\geq 6\text{--}8 \text{ cm}^2$); it is a simple surgical technique; its efficacy in relieving pain, restoring joint function and ensuring patient satisfaction with treatment outcomes has been proven.

Despite the wide popularity of AMIC, many controversial and unresolved issues remain. In particular, little is known about the time it takes the membrane to degrade, the nature of its transformation into cartilage tissue and the quality of cartilage tissue formed at the membrane implantation site [6, 7].

Currently, collagen membrane is the most demanded biological material used in cartilage tissue restorations. Unfortunately, the high cost of imported membranes disallows widespread introduction of AMIC into everyday clinical practice at domestic medical institutions. At the same time, cartilage restoration is one of the highly demanded operations. This fact determined the need to develop a domestic analogue that meets all the current requirements practitioners have for collagen membranes.

This study aimed to experimentally investigate the biological potential of collagen membranes and their capacity to transform into cartilage tissue.

METHODS

We used two types of collagen membranes, different in composition, structure and nature of production.

The main (tested) membrane was the Ortokeep membrane developed by Russian scientists (Ortosoft; Russia). It is formed by electrospinning from nanofibers (300–500 nm in diameter), which are a mixture of bovine type I collagen and polylactide. Both sides of the membrane have similar microrelief and wettability. By the formation method and structure of the nanofibers, Ortokeep is radically different from the foreign analogues, which allows an objective comparative analysis of their biological potential.

We selected a Chondro-Gide collagen membrane (Geistlich Pharma; Switzerland) as a control membrane for our experiments. Chondro-Gide is synthesized from pork collagen types I and III through natural resorption. This membrane is the most popular bioproduct, it is widely used to repair full-thickness cartilage defects, which is why we took it as a control membrane.

Experiment model

The experimental animals were four White Russian breed pigs, 6 months old, weighing 68/67.4/79/73 kg. They were kept in the subsidiary farm of the Center for Preclinical Research (Penza), isolated from the general livestock. At the beginning of the experiment, the animals were in a satisfactory condition, had a light color, independently took food and water, showed no external manifestations of a disease. Their records contained no entries describing diseases. All animals spent 3 weeks before the experiment in isolation, with their feeding dosed. The animals received individually calculated doses of systemic analgesics (xylazine, etc.) used in veterinary and clinical medicine. The depth of anesthesia was controlled by systemic reactions: spontaneous breathing, heart rate, blood pressure, state of the pupil, pulse oximetry. For respiratory support, we employed an anesthesia and respiratory device that delivered oxygen-air (anesthetic gas) mixture of oxygen (75–85%), air and 1.0–3.0 vol.% of Isoflurane (aerran) in a semi-closed circuit.

On the right hind limb joints of each animal, using a round bur, we made one full-thickness cartilage defect (defect № 1) of rectangular shape, measuring $1 \times 0.5 \text{ cm}$, reaching the subchondral bone (Fig. 1A). With a thin drill (diameter of 1.5 mm),

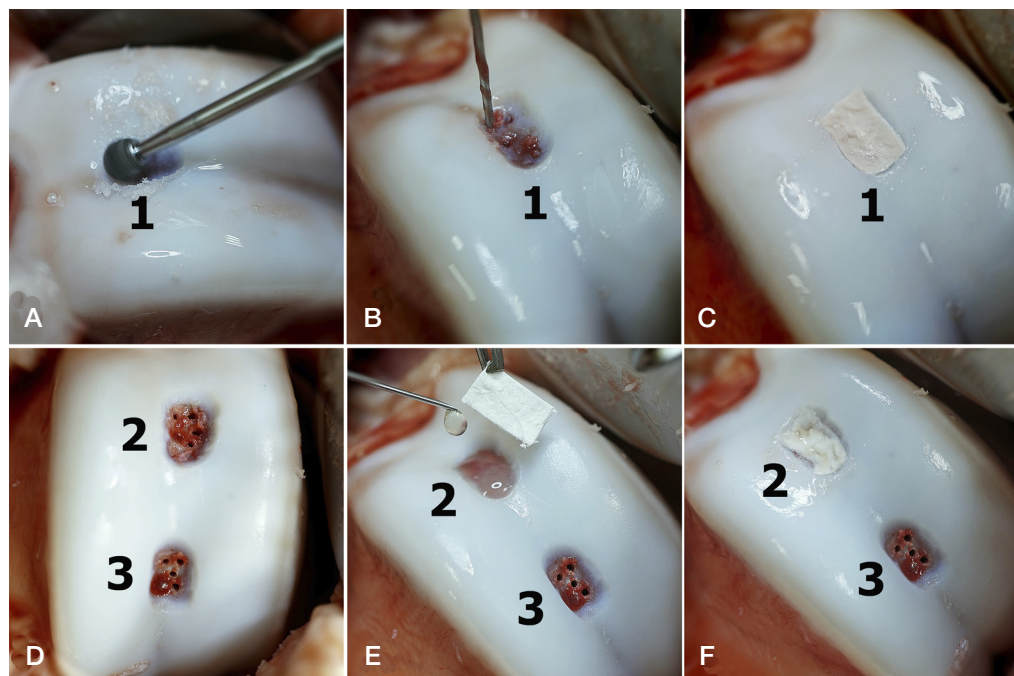


Fig. 1. Stages of formation of full-thickness defects and implantation of collagen membranes. 1 — defect № 1 (implantation of the Ortokeep membrane); 2 — defect № 2 (implantation of the Chondro-Gide membrane); 3 — defect № 3 (no membrane implantation)

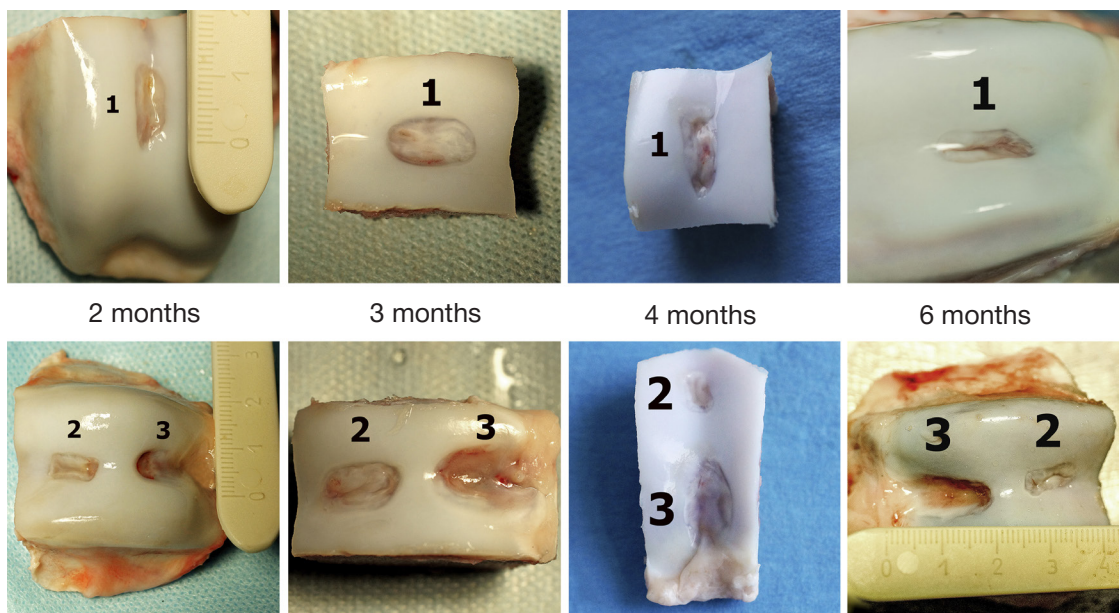


Fig. 2. Macro specimen at various timepoints post surgery. 1 — defect № 1 after implantation of the Ortokeep membrane; 2 — defect № 2 after implantation of the Chondro-Gide membrane; 3 — defect № 3, no membrane implantation

we reamed the subchondral bone to a depth of 1 cm, thus letting bone marrow onto the surface of the defect (Fig. 1B). The Ortokeep collagen membrane was shaped appropriately for the defect and attached to the subchondral bone with fibrin glue (Fig. 1C).

On the left hind limb joints we made two defects, defect No. 2 to be covered with the Chondro Gide membrane and defect № 3 to remain as is for control purposes (Fig. 1D). The collagen membrane was modeled according to the shape and size of the defect. After reaming the subchondral bone, we applied fibrin glue to defect № 2 and implanted the Chondro-Gide collagen membrane (Fig. 1E). No membrane was implanted onto the control defect № 3 (Fig. 1F).

The animals were removed from the experiment 2, 3, 4, 6 months post-surgery by anesthesia (xylazine 15 ml, zoletil 1.5 ml I.M.) followed by bloodletting (transection of the carotid arteries). For subsequent histological examination, we collected large bone-cartilage fragments containing the studied defects. For the purpose of microscopic examination, one biopsy fragment was taken from the central part of each defect.

The bone-cartilage underwent gentle acid decalcification followed by the standard histological preparation. Histological sections 7–8 μm thick were stained with hematoxylin and eosin (Van Gieson's stain). Using a microscope with a digital 12-megapixel camera attachment (Sony; Japan) we took micrographs of at least 5 views of each histological section, studied the inflammatory response, structure of the tissues, their percentage ratio in the defect area, state of the microvasculature.

The obtained data were processed with the help of Statistica v.10 software packages (StatSoft; USA). The assessment of normality of distribution relied on the Shapiro-Wilk test. All the parameters described in this work had a distribution close to normal. For each parameter, we calculated the arithmetic mean (M) and the arithmetic mean error (m).

The significance of differences between groups was determined with the help of Fisher's exact test and nonparametric Kolmogorov-Smirnov test. The differences were considered significant at 95% probability threshold ($p < 0.05$).

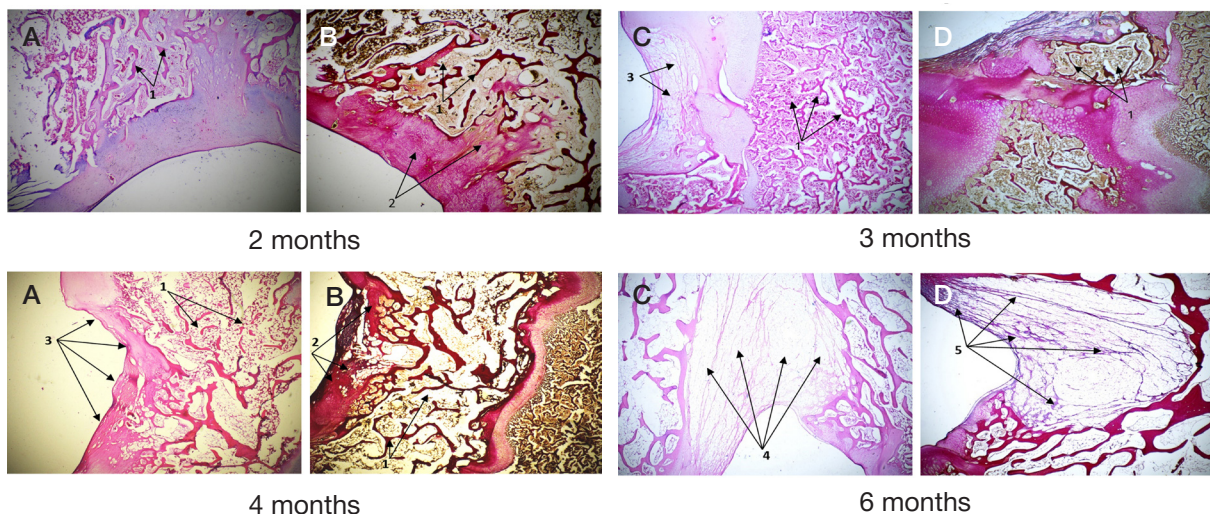


Fig. 3. Microscopic examination of defect № 3, control group; staining with hematoxylin and eosin, $\times 40$ (A); Van Gieson's stain, $\times 40$ (B). 1 — osteodystrophy; 2 — coarse fibrous connective tissue; 3 — developing "crater" defect in cartilage and bone tissues; 4 — groups of adipocytes filling the "crater" defect; 5 — bundles of collagen fibers between islets of adipocytes

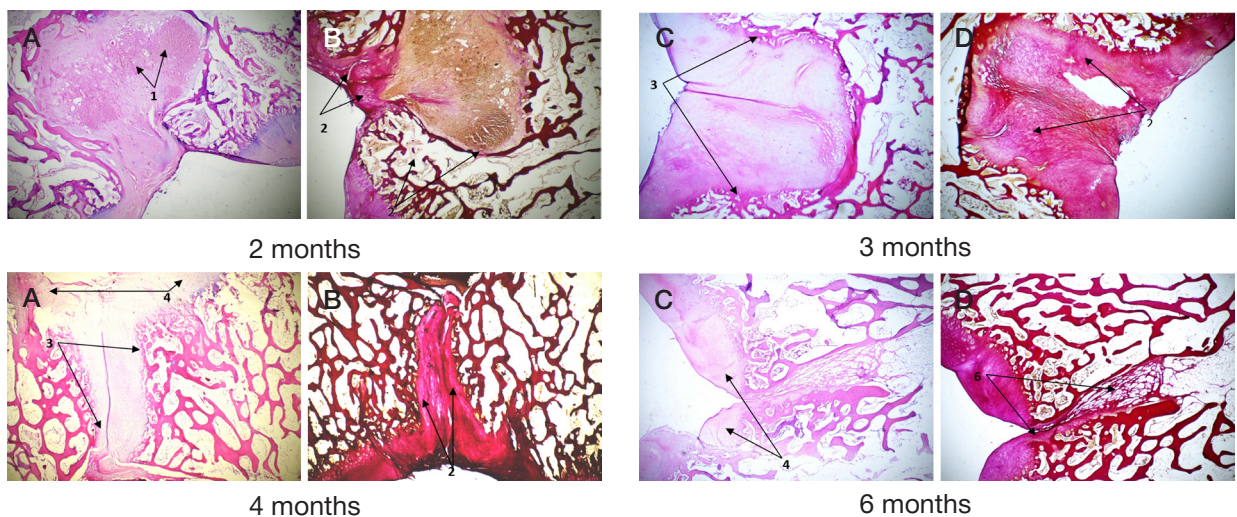


Fig. 4. Microscopic examination of defect № 1 after implantation of the Ortokeep membrane; staining with hematoxylin and eosin, $\times 40$ (A); Van Gieson's stain, $\times 40$ (B). 1 — fibrin; 2 — coarse fibrous connective tissue; 3 — developing cylindrical defect, active neoosteogenesis evident at the edges; 4 — neochondrogenesis; 5 — the defect shrunk sharply with formation of a slit cavity in the center

RESULTS

Macroscopic examination

Macroscopic examination of the control group samples (defect № 3, no membrane) revealed defect expansion without signs of cartilage tissue regeneration on its surface. The situation progressed into the 6th month post-surgery (Fig. 2).

At the same time, there was no pronounced expansion of the defects detected in the experimental groups (defects № 1 and № 2). The bed of the defects was even, but not uniform. Palpation revealed the bed to be elastic. Both defects were covered with a viable stable cartilage tissue (see Fig. 2).

Microscopic examination

Microscopic examination of the control group defect (defect № 3) revealed progression of the bone tissue destruction process and very weak signs of chondrogenesis, seen only in the immediate vicinity of the intact cartilage (Fig. 3).

Examination of the histological slides of samples with the Ortokeep membrane revealed no inflammatory process and

leukocyte infiltration at all animal withdrawal timepoints. Up to the 4th month, the border of the intact cartilage is clearly visible, but by the 6th month it becomes indistinguishable. The underlying bone tissue underwent significant resorption in the immediate vicinity of the defect. However, there were no signs of osteodystrophy in the surrounding spongy substance (Fig. 4).

Coarse fibrous connective tissue appeared at the site of the removed cartilage and resorbed bone tissue. The formation and maturation of the connective tissue was first noted at the first animal withdrawal timepoint, and by the 6th month its volume decreased (see Table). In parallel, active reparative processes of bone tissue — neoosteogenesis — were evident along the edges of the bone defect. Initially, the defect had a bulbous shape, but later it turned cylindrical and by the 6th month became wedge-shaped. From the 2nd to the 4th months, the defect was mainly filled with coarse fibrous tissue, and by the 6th month it was almost completely covered with bone tissue. Chondrocytes formed actively (neochronogenesis) not only at the edge of the intact cartilage but also in the center of the defect (see Fig. 4). In the center of the defect there was a deep slit cavity extending relatively deep into the spongy substance.

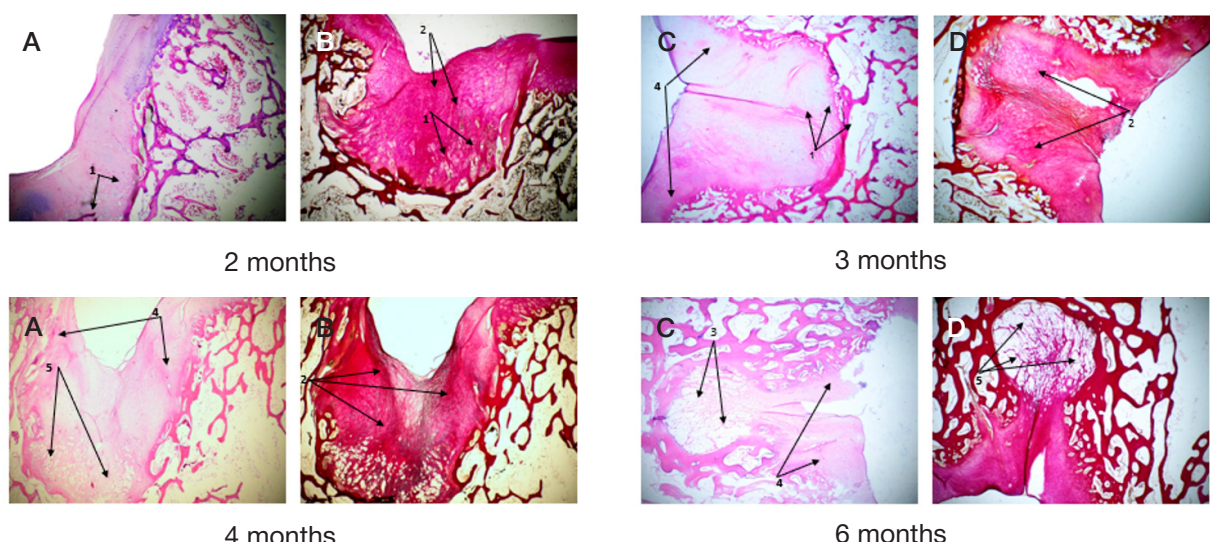


Fig. 5. Microscopic examination of defect № 2 after implantation of the Chondro-Gide membrane, stained with hematoxylin and eosin, $\times 40$ (A); Van Gieson's stain, $\times 40$ (B). 1 — fibrin; 2 — coarse fibrous connective tissue; 3 — emerging bulbous defect, active neoosteogenesis evident along the edges; 4 — neochondrogenesis; 5 — the bed of the bone defect filled with adipocytes

Table. Dimensional characteristics of the histological structure of the defect's center, various types of treatment

	Group	2 months (M ± m)	3 months (M ± m)	4 months (M ± m)	6 months (M ± m)
Intact cartilage thickness, µm	Control	734,0 ± 16,12	2247,5 ± 36,94	2359,8 ± 38,79	842,10 ± 21,23
	Chondro-Gide	1118,5 ± 21,81	1230,4 ± 23,99	1291,9 ± 25,19	838,67 ± 19,12
	Ortokeep	1519,0 ± 38,42	1670,5 ± 42,26	1341,3 ± 25,08	886,35 ± 10,44
Cartilage thickness at the treatment site's center, µm	Control	0	0	0	0
	Chondro-Gide	0	503,9 ± 22,74	571,4 ± 29,96	252,68 ± 12,19
	Ortokeep	0	534,0 ± 36,42	657,1 ± 34,46	335,94 ± 13,47
Connective tissue thickness at the site of implantation, µm	Control	1635,2 ± 187,33	1152,2 ± 124,80	1094,6 ± 118,56	2406,98 ± 178,05
	Chondro-Gide	1648,2 ± 137,34	1615,2 ± 134,60	1534,5 ± 127,87	900,58 ± 72,43
	Ortokeep	2072,0 ± 339,89	1968,6 ± 322,90	2905,7 ± 204,92	1688,66 ± 71,60
Cortical plate thickness in the intact area, µm	Control	162,9 ± 6,33	121,9 ± 7,27	134,0 ± 8,00	53,22 ± 4,08
	Chondro-Gide	162,2 ± 8,37	181,6 ± 9,38	199,8 ± 10,32	102,18 ± 6,60
	Ortokeep	181,0 ± 9,92	198,6 ± 10,91	226,0 ± 12,03	84,53 ± 5,15
Cortical plate thickness at the treatment site, µm	Control	121,6 ± 7,73	96,8 ± 5,53	106,5 ± 6,08	147,54 ± 18,67
	Chondro-Gide	140,4 ± 13,67	157,3 ± 15,31	173,0 ± 16,84	184,76 ± 5,48
	Ortokeep	149,0 ± 11,01	164,4 ± 12,11	163,9 ± 14,81	142,66 ± 19,93
Bone tissue volume, %	Control	18,9 ± 0,63	18,5 ± 0,62	20,4 ± 0,68	10,42 ± 0,67
	Chondro-Gide	16,3 ± 0,28	19,2 ± 0,33	21,1 ± 0,36	17,41 ± 0,36
	Ortokeep	27,0 ± 0,67	29,8 ± 0,73	27,1 ± 0,57	30,23 ± 0,34
Cartilage tissue volume, %	Control	15,4 ± 0,51	22,4 ± 0,74	24,6 ± 0,82	10,64 ± 0,38
	Chondro-Gide	23,1 ± 0,29	25,8 ± 0,33	28,4 ± 0,36	15,04 ± 0,72
	Ortokeep	27,0 ± 0,57	29,4 ± 0,63	32,1 ± 1,88	19,99 ± 0,43
Connective tissue volume, %	Control	53,3 ± 0,70	52,3 ± 0,69	44,4 ± 0,58	13,31 ± 1,04
	Chondro-Gide	53,2 ± 0,50	40,4 ± 0,48	34,4 ± 0,41	17,03 ± 0,56
	Ortokeep	43,0 ± 0,47	33,7 ± 0,47	31,2 ± 0,46	18,19 ± 0,53
Volume of blood vessels, %	Control	5,8 ± 0,16	7,1 ± 0,20	6,8 ± 0,19	8,39 ± 0,42
	Chondro-Gide	7,5 ± 0,45	8,9 ± 0,53	8,4 ± 0,50	11,91 ± 0,42
	Ortokeep	9,0 ± 0,36	9,5 ± 0,40	10,7 ± 0,83	12,79 ± 0,65

Examination of the histological slides of samples with the Chondro-Gide membrane revealed no inflammatory process and leukocyte infiltration at all animal withdrawal timepoints. The border of the destroyed cartilage was indistinct. In the center of the defect area there appeared a slit cavity, and the underlying bone tissue underwent resorption (the depth of resorption was less than registered in the control group). Coarse fibrous connective tissue appeared where the resorbed bone tissue was, with bone tissue tending to form along the edge of the defect, same as the multiple islets of chondrocytes in the thickness of the defect. The defect had a bulbous shape; neochondrocytes formed more actively in the direction from the periphery to the center. There were separate slit cavities in the thickness of the coarse fibrous connective tissue. A rather pronounced layer of fat cells has formed between connective tissue and bone tissue at the bed of the defect. The neoangiogenesis processes were intense. Islets of chondrocytes also formed in the thickness of the connective tissue, but, in contrast to defect № 1, they were found closer to the developing callus (Fig. 5).

Analyzing results of the measurements, we noted that in the control group a new cartilage has never fully formed in the center of the operation area (Table). The same is true for groups 1 and 2 at the 2nd month of the study, but starting from the 3rd month, the cartilage became detectable and its thickness was increasing significantly ($p < 0.05$) up to the

4th month, with the gain being 18.7% (657.1 ± 34.46 µm) in the 1st group and 12.8% (571.4 ± 29.96 µm) in the second group. However, by the 6th month the thickness decreased significantly ($p < 0.05$), by 51.1% in the 1st group and by 44.2% in the 2nd group (335.94 ± 13.47 µm and 252.68 ± 12.19 µm, respectively), which is most likely associated with the process of "organization" of the cartilaginous tissue. This fact underscores the efficacy of membranes.

The thickness of the connective tissue in the control group increased by 32.1% ($p < 0.05$) by the 6th month, while in groups 1 and 2 it decreased ($p < 0.05$) by 18.5% (1688.66 ± 71.60 µm) and 46.4% (900.58 ± 72.43 µm), respectively. Shrinking connective tissue indicates reparative processes in the area of operation. In group 2, the thickness of the connective tissue was decreasing rapidly because it was replaced with adipose tissue, which somewhat worsens the ultimate repair with bone tissue.

By the 6th month, the thickness of the cortical plate at the surgery site increased by ($p < 0.05$) by 17.6 and 24.0% in the control and 2nd groups, respectively, while in the 1st group it was decreasing from month 2 to month 6 ($p > 0.05$) by 4.3%. For the most part, the cortical plate gained in thickness due to the formation of the new tissue (osteoid). Subsequently, that tissue matured, with maturation starting earlier in group 1, which suggests the surgery site in that group offered more favorable conditions therefor.

The above changes at the surgery sites zones are confirmed by the component percentage ratio data shown in the Table.

It is also worth noting the processes of neoangiogenesis. The area of blood vessels increased significantly ($p < 0.05$) in all groups, But the fastest growth thereof was registered in the 1st group (up to $12.79 \pm 0.65\%$), which indicates the trophism of the surgery site tissues was best there. In group 2, the area of connective tissue increased to $11.91 \pm 0.42\%$.

DISCUSSION

The demonstrated poor efficacy of bone tunneling applied without additions to the treatment casts doubt on the feasibility of performing such operations in clinical practice, which is confirmed in studies by other authors [1]. The high efficacy of collagen membranes in regeneration of cartilage tissue that we have witnessed in this study accords with the results reported by other researchers [1–4]. Unfortunately, it is not possible to correctly compare the digital values, since the works cited employed different biomodels. It also seems important to study the data describing more long-term results and set up a study to investigate the efficacy of membranes of different compositions.

CONCLUSIONS

Both of the tested materials (Ortokeep and Chondro-Gide collagen membranes) showed excellent results in regeneration of a full-thickness cartilage defect. Almost identical macroscopic and microscopic results were registered in both experimental groups. However, a more detailed analysis of the histological examination data revealed the following features: 1) in both groups, the area of collagen membrane implantation was a patch of fibrous connective tissue with inclusions of chondrocytes; 2) at the defect sites, collagen membranes created better conditions for reparative processes, which is confirmed by the shortest terms of closure of the defect with the body's connective tissue; 3) maturation of the connective tissue took less time; 4) in the zone of membrane implantation, chondrogenesis was "scattered", with islets of hyaline cartilage appearing in the formed coarse fibrous connective tissue, such islets detectable by the 3rd month of the experiment and initially distant from each other but tending to merge at later withdrawal timepoints; neochondrogenesis was evident not only at the healthy tissue border but also in the thickness of the connective tissue callus; 5) the figures reflecting bone and cartilage tissue volumes prove the efficacy of collagen membranes.

References

- Garkavi AV, Blokov MYu. Artroskopicheskaja hondroplastika lokal'nyh hrjashhevih defektov kolennogo sustava s ispol'zovaniem kollagenovoj membrany Chondro-Gide. Kafedra travmatologii i ortopedii. 2015; 15 (3): 4–7. Russian.
- Gao L, Orth P, Cucchiari M, Madry H. Autologous Matrix-Induced Chondrogenesis: A Systematic Review of the Clinical Evidence. Am J Sports Med. 2019; 47 (1): 222–31.
- Bentien JP, Behrens P. Autologous Matrix-Induced Chondrogenesis (AMIC) combining Microfracturing and a Collagen I/III Matrix for Articular Cartilage Resurfacing. Cartilage. 2010; 1 (1): 65–8.
- Girolamo L, Schönhuber HI, Vigano M, et al. Autologous Matrix-Induced Chondrogenesis (AMIC) and AMIC Enhanced by Autologous Concentrated Bone Marrow Aspirate (BMAC) Allow for Stable Clinical and Functional Improvements at up to 9 Years Follow-Up: Results from a Randomized Controlled Study. Journal of Clinical Medicine. 2019; 8 (3): 392–405.
- Kon E, Filardo G, Brittberg M, Busacca M, et al. Multilayer biomaterial for osteochondral regeneration shows superiority vs microfractures for the treatment of osteochondral lesions in a multicentre randomized trial at 2 years. Knee Surgery Sports Traumatology Arthroscopy. 2018; 26 (2): 2704–15.
- Egiazaryan KA, Lazishvili GD, Hramenkova IV, Shpak MA, Badriev DA. Knee osteochondritis desiccans: surgery algorithm. Bulletin of RSMU. 2018; 2: 73–80. Russian.
- Lazishvili GD, Egiazaryan KA, Ratev AP, Gordienko DI, But-Gusaim AB, Chulovskaja IG, i dr. Gibridnaja kostno-hrjashhevaja transplantacija — innovacionnaja tehnologija dlja hirurgicheskogo lechenija obshirnyh kostno-hrjashhevih defektov kolennogo sustava. Hirurgicheskaja praktika. 2019; 40 (4): 10–18. Russian.

Литература

- Гаркави А. В., Блоков М. Ю. Артроскопическая хондропластика локальных хрящевых дефектов коленного сустава с использованием коллагеновой мембраны Chondro-Gide. Кафедра травматологии и ортопедии. 2015; 15 (3): 4–7.
- Gao L, Orth P, Cucchiari M, Madry H. Autologous Matrix-Induced Chondrogenesis: A Systematic Review of the Clinical Evidence. Am J Sports Med. 2019; 47 (1): 222–31.
- Bentien JP, Behrens P. Autologous Matrix-Induced Chondrogenesis (AMIC) combining Microfracturing and a Collagen I/III Matrix for Articular Cartilage Resurfacing. Cartilage. 2010; 1 (1): 65–8.
- Girolamo L, Schönhuber HI, Vigano M, et al. Autologous Matrix-Induced Chondrogenesis (AMIC) and AMIC Enhanced by Autologous Concentrated Bone Marrow Aspirate (BMAC) Allow for Stable Clinical and Functional Improvements at up to 9 Years Follow-Up: Results from a Randomized Controlled Study. Journal

- of Clinical Medicine. 2019; 8 (3): 392–405.
- Kon E, Filardo G, Brittberg M, Busacca M, et al. Multilayer biomaterial for osteochondral regeneration shows superiority vs microfractures for the treatment of osteochondral lesions in a multicentre randomized trial at 2 years. Knee Surgery Sports Traumatology Arthroscopy. 2018; 26 (2): 2704–15.
- Егиязарян К. А., Лазишвили Г. Д., Храменкова И. В., Шпак М. А., Бадриев Д. А. Алгоритм хирургического лечения больных с рассекающим остеохондритом коленного сустава. Вестник РГМУ. 2018; 2: 77–83.
- Лазишвили Г. Д., Егиязарян К. А., Ратьев А. П., Гордиенко Д. И., Бут-Гусаим А. Б., Чуловская И. Г., и др. Гибридная костно-хрящевая трансплантация — инновационная технология для хирургического лечения обширных костно-хрящевых дефектов коленного сустава. Хирургическая практика. 2019; 40 (4): 10–18.

FLUORESCENCE DETECTION OF AMYLOID DEPOSITS IN HUMAN TISSUES USING HISTOCHEMICAL DYES

Guselnikova VV^{1,2}✉, Sufieva DA¹, Tsyba DL¹, Korzhevskii DE¹

¹ Institute of Experimental Medicine, Saint Petersburg, Russia

² Saint Petersburg State University, Saint Petersburg, Russia

Recently, fluorescence microscopy becomes more available, presenting new opportunities to face several challenges of experimental biology and medicine. The study was aimed to assess the effectiveness of fluorescence microscopy for the identification of amyloid deposits in human tissues. Post-mortem samples of the myocardium ($n = 12$) and cerebral cortex ($n = 8$) obtained from subjects of both sexes aged 60–98 with verified amyloidosis were used as a material for the study. The specimens were stained using 11 different histochemical dyes and subsequently analyzed by light and fluorescence microscopy. Qualitative and quantitative analysis has shown that Thioflavin T is the most effective stain for fluorescence detection of β - and transthyretin amyloid in human tissues. Congo red staining is highly effective for the detection of transthyretin amyloidosis, however, it is ill-suited for the identification of β -amyloid plaques. It has been found that the ability of Congo red to exhibit fluorescence when binding to amyloid fibrils can be used for verification of amyloid deposits instead of the traditional polarized light microscopy. As has been first noted, methyl violet can selectively bind to β -amyloid with fluorescent complex formation. In addition, methyl violet treatment effectively reduces the autofluorescent background in the nervous tissue. This makes methyl violet staining a promising diagnostic tool for Alzheimer's-type pathology.

Keywords: fluorescence microscopy, amyloid, amyloid plaques, histochemistry, congo red, thioflavin, methyl violet

Author contribution: Guselnikova VV — literature analysis, study planning, staining specimens, analysis and interpretation of the results, manuscript draft writing; Sufieva DA — quantitative data analysis; Tsyba DL — quantitative data analysis; Korzhevskii DE — conceptual development, study planning, manuscript editing.

Compliance with ethical standards: the study was conducted in accordance with the requirements of the World Medical Association Declaration of Helsinki (2013) and approved by the Ethics Committee of the Institute of Experimental Medicine (protocol № 3/18 dated November 22, 2018).

✉ Correspondence should be addressed: Valeria V. Guselnikova
Acad. Pavlov, 12, Saint Petersburg, 197376; Guselnicova.Valeria@yandex.ru

Received: 12.07.2021 Accepted: 25.07.2021 Published online: 31.07.2021

DOI: 10.24075/brsmu.2021.034

ПРИМЕНЕНИЕ ГИСТОХИМИЧЕСКИХ КРАСИТЕЛЕЙ ДЛЯ ФЛУОРЕСЦЕНТНОГО ВЫЯВЛЕНИЯ АМИЛОИДНЫХ СКОПЛЕНИЙ В ТКАНЯХ ЧЕЛОВЕКА

В. В. Гусельникова^{1,2}✉, Д. А. Суфиева¹, Д. Л. Цыба¹, Д. Э. Коржевский¹

¹ Институт экспериментальной медицины, Санкт-Петербург, Россия

² Санкт-Петербургский государственный университет, Санкт-Петербург, Россия

В последнее время метод флуоресцентной микроскопии приобретает все большее распространение, открывая новые возможности для решения целого ряда задач экспериментальной биологии и медицины. Целью настоящей работы было оценить эффективность применения метода флуоресцентной микроскопии для идентификации амилоидных скоплений в тканях человека. В качестве материала для исследования были использованы фрагменты миокарда ($n = 12$) и коры головного мозга ($n = 8$) людей обоих полов в возрасте от 60 до 98 лет с верифицированным амилоидозом. Препараты окрашивали с применением 11 разных гистохимических красителей с последующим анализом методами световой и флуоресцентной микроскопии. Проведенные качественный и количественный анализ показали, что тиофлавин Т является наиболее эффективным красителем для флуоресцентного выявления β - и транстиреинового амилоида в тканях человека. Методика окраски конго красным обладает высокой эффективностью в отношении транстиреинового амилоидоза, но плохо подходит для идентификации β -амилоидных бляшек. Установлено, что способность конго красного флуоресцировать при связывании с амилоидными фибрillами может быть использована для верификации амилоидных скоплений вместо традиционной поляризационной микроскопии. Впервые отмечено, что краситель метиловый фиолетовый обладает способностью специфично связываться с β -амилоидными скоплениями с формированием флуоресцирующего комплекса, одновременно подавляя автофлуоресценцию нервной ткани. Это делает методику окраски метиловым фиолетовым перспективной для диагностики патологии альцгеймеровского типа.

Ключевые слова: флуоресцентная микроскопия, амилоид, амилоидные бляшки, гистохимия, конго красный, тиофлавин, метиловый фиолетовый

Вклад авторов: В. В. Гусельникова — анализ литературы, планирование исследования, окраска препаратов, анализ и интерпретация результатов, подготовка черновика рукописи; Д. А. Суфиева — количественный анализ данных; Д. Л. Цыба — количественный анализ данных; Д. Э. Коржевский — разработка концепции, планирование исследования, редактирование рукописи.

Соблюдение этических стандартов: исследование проведено в соответствии с требованиями Хельсинской декларации Всемирной медицинской ассоциации (2013) и одобрено этическим комитетом ФГБНУ «ИЭМ» (протокол № 3/18 от 22 ноября 2018 г.).

✉ Для корреспонденции: Валерия Владимировна Гусельникова
ул. Акад. Павлова, д. 12, г. Санкт-Петербург, 197376; Guselnicova.Valeria@yandex.ru

Статья получена: 12.07.2021 Статья принята к печати: 25.07.2021 Опубликована онлайн: 31.07.2021

DOI: 10.24075/vrgmu.2021.034

In recent years, fluorescence microscopy is being increasingly used for morphological studies. This method becoming a research tool available together with rapid introduction of the method into clinical diagnostic practice provide new opportunities to face a number of challenges of experimental biology and medicine. Improving methods for morphological diagnosis of amyloidosis is one of those challenges.

Amyloidosis is a group of protein-conformational diseases characterized by extracellular deposition of pathological

insoluble fibrillar proteins, amyloids, in organs and tissues [1]. Amyloidosis is a severe condition having high mortality rate. The most malignant forms of amyloidosis occur in individuals of working age. Accumulation of amyloid in various organs (heart, kidney, liver, lungs, gastrointestinal tract, etc.) results in impaired organ function and can cause cardiomyopathy, heart and kidney failure, hepatic vein thrombosis, etc. Accumulation of amyloid in brain is a histopathological sign of such neurodegenerative diseases, as Alzheimer's disease and Parkinson's disease [2–4].

Differential diagnosis of amyloidosis is difficult due to great diversity of clinical manifestations and lack of pathognomonic symptoms. To date, histological examination of tissue specimens with the use of Congo red stain, and subsequent investigation of specimens using light and polarized light microscopy remains the most reliable diagnosis method [5]. However, application of such an approach often results in false positive and/or false negative findings [6], which indicates imperfect nature of the existing methods. This explains the urgency of the problem of searching for new approaches to improving the quality of amyloidosis morphological diagnosis. The use of fluorescence microscopy can make a definite contribution to that objective. Currently, many clinical and diagnostic centers are equipped with fluorescence microscopes, allowing them to use fluorescent properties of some dyes for diagnosis, including for diagnosis of amyloidosis.

The study was aimed to assess the effectiveness of fluorescence microscopy for identification of amyloid deposits in human tissues.

METHODS

Samples of myocardium ($n = 12$) and cerebral cortex ($n = 8$), obtained from patients of both sexes (4 men and 8 women, 3 men and 5 women respectively) aged 60–98 with amyloidosis detected by immunohistochemistry, were used as a material for the study. Inclusion criteria: immunopositive β -amyloid plaques in cerebral cortex and accumulation of aggregated transthyretin in myocardium. Exclusion criteria: marked postmortem autolytic changes in brain tissue or myocardium.

Rabbit OC polyclonal antibody (Anti-Amyloid Fibrils OC Antibody) against the conformational epitopes of amyloid fibrils (1:1000 dilution, catalogue number AB2286, Sigma-Aldrich; USA) and mouse monoclonal (clone TA5F4) antibody targeting aggregated transthyretin (1:600 dilution, catalogue number 848102, BioLegend; USA) were used to verify the presence of amyloid deposits.

Biomaterial was received from the archive of the Department of General and Special Morphology, Institute of Experimental Medicine. Samples were fixed in 10% formalin and embedded in paraffin. Paraffin blocks were sectioned in order to obtain the slices 5, 7 and 14 μm thick. Human cerebral cortex and myocardium specimens were stained using a number of histochemical stains in order to assess the potential of using histochemical dyes for fluorescence detection of amyloid (Table 1).

Specimen analysis and imaging were performed using Leica DM750 light microscope (Leica Microsystems; Germany) and Leica DM2500 fluorescence microscope (Leica Microsystems;

Table 1. List of dyes used

Dye	Manufacturer and producer country	Staining dye solution
Congo red	Sigma, USA	0.1% aqueous solution
Thioflavin T	Fluka, USA	1% aqueous solution
Alcian blue	BioVitrum, Russia	Commercially available solution
Toluidine blue	Acros Organics, USA	1% alcohol solution
Methyl violet	Pr. G. Grubler, Germany	0.1% aqueous solution
Methylene green	Ferak Berlin, Germany	0.1% aqueous solution
Eosin Y solution, alcoholic	BioVitrum, Russia	Commercially available solution
Janus green	Merck, Germany	0.1% aqueous solution
Pyronin G	British Drug Houses, UK	0.1% aqueous solution
Basic fuchsin	Serva, Germany	0.1% aqueous solution
Neutral red	National Aniline Division, USA	0.1% aqueous solution

Germany), equipped with a set of fluorescence filters 340–560 nm. The filter set included the following excitation filters: BP=340–380 nm (the first — "A"), BP=450–490 nm (the second — "I3") and BP=515–560 nm (the third — "N2.1").

Amyloid plaques detected by various techniques were counted in serial sections of cerebral cortex of the same case. The plaques were counted by three different researchers under identical conditions using the objective lens with a magnification of $\times 40$. Since the distribution of amyloid plaques in the nervous tissue was very uneven, the plaques were counted across the entire area of the slice (0.67 cm^2), and after that the number of plaques per cm^2 was calculated. The number of amyloid plaques detected by immunofluorescence assay was used as a reference value. Mouse monoclonal (clone DE2B4) antibody against β -amyloid (1:200 dilution, catalogue number ab11132, Abcam; UK) was used for that purpose; biotin-conjugated Fab fragment from a donkey anti-mouse immunoglobulin (Jackson ImmunoResearch; USA) and Cy2-conjugated streptavidin (Jackson ImmunoResearch; USA) were used as secondary reagents.

Statistical analysis of the data obtained was performed using the GraphPad Prism 9 software (GraphPad Software Inc.; USA). The indicators were compared using the analysis of variance (ANOVA) with subsequent pairwise comparison of groups (Thioflavin T, Congo red, methyl violet) with the control (immunohistochemistry) using the Dunnett's post-hoc test. The differences were considered significant when $p < 0.05$. The data were presented in the following format: mean \pm standard error of the mean.

RESULTS

Analysis of histochemical dye effectiveness for fluorescence detection of amyloid deposits

The results of using various histochemical dyes for identification of β -amyloid and transthyretin amyloid by light and fluorescence microscopy are presented in Tables 2 and 3 respectively.

Three dyes are capable of binding to amyloid fibrils to form fluorescent complexes: Thioflavin T (ThT), Congo red and methyl violet.

When stained with ThT, amyloid plaques in cerebral cortex are clearly visible even at low magnification ($\times 10$) of a microscope. The deposits detected look like compact focal lesions fluorescent in the blue range (Fig. 1A). Amyloid plaques are characterized by morphological heterogeneity: some plaques have a roundish intensely fluorescent dense central core surrounded by a fibrillar peripheral halo (Fig. 1A; arrow 1), while

Table 2. Results of β -amyloid staining in human cerebral cortex

Dye	Color of amyloid deposits when viewed in transmitted light	Fluorescence of amyloid deposits
Congo red	Salmon pink	+
Thioflavin T	-	+
Alcian blue	Blue	-
Toluidine blue	-	-
Methyl violet	-	+
Methylene green	-	-
Eosin Y	Light pink	-
Janus green	-	-
Pyronin G	-	-
Basic fuchsin	-	-
Neutral red	-	-

other plaques look like deposits formed of nothing but fibrillar structures (Fig. 1A; arrow 2). Fluorescence is characteristic of amyloid plaques of both types. When stained with ThT, these are visualized with uniform effectiveness (Fig. 1A). Analysis of specimens revealed low background fluorescence of cell nuclei and autofluorescent lipofuscin (pigment accumulated in neurons during aging).

When stained with ThT, transthyretin amyloid in human myocardium is also characterized by intense fluorescence in the blue range (Fig. 1B). Similarly to the cerebral cortex specimens assessment, background fluorescence of cell nuclei (Fig. 1B; arrow head, turquoise) was observed in myocardium together with autofluorescence of lipofuscin granules (Fig. 1B, short arrow, orange), the accumulation of which is characteristic both of neurons and cardiomyocytes. It is important to highlight the following: despite the fact that the color of fluorescence in non-amyloid tissue component differs from the color of fluorescence in amyloid fibrils bound to ThT, the presence of additional fluorescent elements complicates identification and quantification of amyloid deposits.

Analysis of specimens stained with Congo red using fluorescence microscope showed that congophilic amyloid deposits in human tissues were fluorescent in the red range (Fig. 1C; 1D). When examining cerebral cortex specimens, it was noted that after staining with Congo red amyloid plaques were detected not in every studied specimen. Few congophilic deposits in brain tissue were identified only in three cases out of eight cases under investigation. When stained with Congo red, maximum fluorescence intensity was observed in the dense central core of amyloid plaque. Fibrillar peripheral halo was

poorly visualized. Plaques with no compact core were poorly distinguishable compared to plaques with intensely fluorescent central area. Significant background fluorescence (in the red range) was also noted in the cell nuclei of cerebral cortex cells, red blood cells and lipofuscin (Fig. 1C).

When examining myocardium specimens stained with Congo red, amyloid deposits looked like fibrillar aggregates of varying size, located in the myocardial interstitial space, and intensely fluorescent in the red range (Fig. 1D). Lipofuscin autofluorescence was observed, which made it difficult to identify amyloid deposits, especially in case of accumulation of a large amount of this pigment by cardiomyocytes.

Analysis of specimens stained with methyl violet using fluorescence microscope showed that in that case amyloid plaques were intensely fluorescent in the blue range (Fig. 1E). Moreover, tissue background fluorescence was totally absent. Only weak dark crimson staining of nervous tissue was observed, which enhanced the contrast of the detected amyloid plaques (Fig. 1E). Total lack of background fluorescence significantly simplified identification of amyloid plaques. The plaques with or without the dense central core were visualized with equal effectiveness. It should be noted that transthyretin amyloid in human myocardium was not fluorescent when stained with methyl violet (in contrast to amyloid plaques in cerebral cortex), although when the stained specimens were viewed in transmitted light, amyloid deposits in myocardium were clearly visible due to metachromatic (deep purple) staining (Fig. 2A).

Staining of transthyretin amyloid with basic fuchsin was an interesting object found during the study. After application of this dye amyloid deposits become deep red when viewed in

Table 3. Results of transthyretin amyloid staining in human myocardium

Dye	Color of amyloid deposits when viewed in transmitted light	Fluorescence of amyloid deposits
Congo red	Salmon pink	+
Thioflavin T	-	+
Alcian blue	Blue	-
Toluidine blue	Light purple	-
Methyl violet	Deep purple	-
Methylene green	-	-
Eosin Y	Light pink	-
Janus green	Grayish purple	-
Pyronin G	Light pink	-
Basic fuchsin	Red	-
Neutral red	Dark red	-

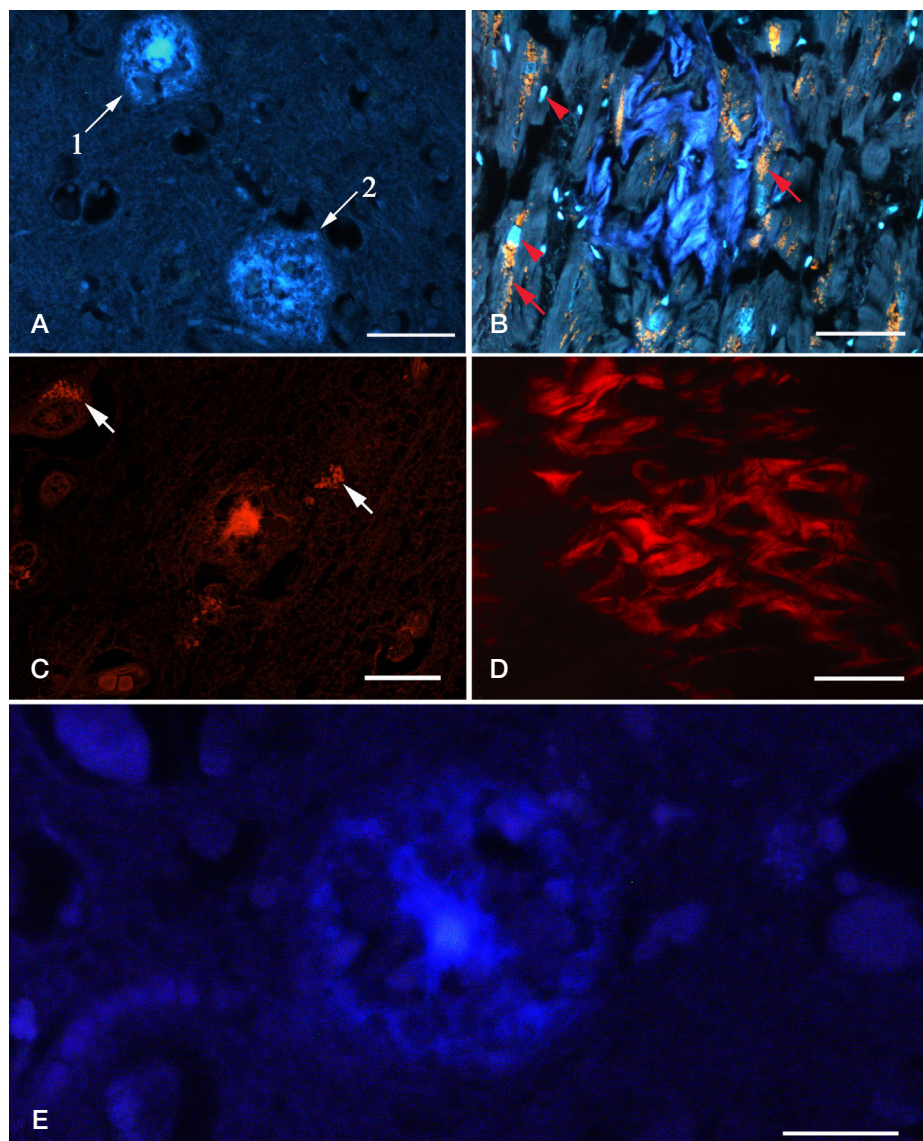


Fig. 1. Fluorescence detection of amyloid deposits in human cerebral cortex (A, C, E) and myocardium (B, D). Thioflavin T (A, B), Congo red (C, D) and methyl violet (E) staining. Arrow 1 points at amyloid plaque with dense central core, arrow 2 points at fibrillar amyloid plaque (no dense core), short arrow points at lipofuscin deposits, and the arrow head points at cell nucleus. The scale bar shows 50 μm (A, B, D) and 20 μm (C, E)

transmitted light (Fig. 2B). According to our data, metachromatic properties of basic fuchsin when staining amyloid have not been described earlier.

Quantitative analysis of amyloid plaques detected using various dyes

During analysis of human cerebral cortex specimens, it was noted that the visually detected number of amyloid plaques varied greatly depending on staining method. Therefore, the quantitative study was performed, which included counting of amyloid plaques in the specimens of the same case stained with different dyes by three different researchers. The quantitative analysis results are presented in Fig. 3. The results obtained were compared with the results of immunohistochemical assay for detecting β -amyloid fibrils, being the most sensitive method for amyloid plaque identification.

As shown in the histogram, the number of amyloid plaques detected using any histochemical dye is significantly lower than the number of immunopositive plaques. The average number of amyloid plaques detected by immunofluorescence staining in the sample, collected for quantitative analysis, was

1106 ± 76.72 per cm^2 of brain tissue. The minimum quantitative differences with the control group were observed when the slices were stained with ThT. After application of this stain the average number of amyloid plaques was 810.9 ± 44.49 per cm^2 . Maximum differences with the control group were observed when the slices were stained with Congo red: the number of visualized plaques was 268.1 ± 15.34 per cm^2 . The average number of amyloid plaques when stained with methyl violet was 399.0 ± 60.03 per cm^2 , which was the intermediate value between the results obtained for ThT and Congo red staining.

DISCUSSION

The ability to form fluorescent complexes when binding to cellular and tissue structures has been previously reported for a wide range of histochemical dyes. Thus, fluorescent properties of eosin are used for visualization of elastic fibers [7], liver injury assessment [8], spleen morphology evaluation [9], as well as for assessment of periodontal structure and function [10]. Basic fuchsin also demonstrates fluorescent properties when binding to elastic fibers [11]. Therefore, the search for new

amyloid fibril-specific fluorescent probes among the known histochemical dyes may contribute to development of new approaches to the diagnosis of amyloidosis.

Staining of slices with ThT is the most well-known technique of amyloid fluorescence detection. It has been shown that molecules of this dye are able to specifically integrate into the β -sheet structure of amyloid fibrils. According to researchers, such integration blocks the rotation of the dimethylaminobenzene ring relative to the benzothiazole ring in the dye molecule, which leads to a significant (by thousand times) increase in fluorescence quantum yield [12].

According to literature, upon binding to amyloid fibrils, ThT demonstrates a dramatic shift of the excitation maximum from 385 nm to 450 nm and the emission maximum from 445 nm to 482 nm [13]. Therefore, it is common practice to assess fluorescence of ThT-stained amyloid deposits in the green range (with the use of excitation filter "I3" BP=450–490 nm). Our studies indicate that staining with ThT is an effective method of β - and transthyretin amyloidosis visualization in human tissues. It is interesting that after ThT staining of human cerebral cortex and myocardium slices the intense amyloid fluorescence was observed not only in green, but also in blue range (with the use of excitation filter BP=340–380 nm). Moreover, in this case the color of nervous and muscle tissue autofluorescent elements (lipofuscin, accumulating in neurons and cardiomyocytes during aging, NADPH, contained in mitochondria, etc.) was different from the color of ThT-stained amyloid fluorescence. This significantly enhances the contrast when detecting amyloid.

Despite the fact that ThT can selectively interact with proteins in the state of amyloid fibrils to form the intensely fluorescent complex, it is much less frequently used for clinical diagnosis than the other dye with similar mechanism of action, Congo red. Currently, Congo red stain is the gold standard for detection of amyloid. It is widely used in scientific research and clinical diagnostic practice [14, 5]. Like ThT, Congo red integrates into β -sheet structure of amyloid fibrils acquiring the ability to rotate the plane of light polarization. Therefore, polarized light microscopy is a traditional method used to verify the type of congophilic deposits detected [14]. However, the color of fluorescence in congophilic deposits viewed under polarized light may vary greatly, which makes interpretation of the results obtained increasingly complicated [15].

We have shown that it can be recommended to use fluorescence microscopy instead of polarized light microscopy for verification of amyloid deposits after staining with Congo red. The ability of Congo red to exhibit fluorescence when binding to amyloid fibrils was reported back in 1959 [16]. However, the use of Congo red fluorescent properties was not widely implemented at the time. It was probably due to the fact that fluorescence microscopes were available only to a few diagnostic laboratories upon the time of the abovementioned article release. The use of Congo red ability to exhibit fluorescence when binding to amyloid may help to reduce the number of false positive and false negative findings, resulting from erroneous interpretation of the results due to variability of green hue of congophilic deposits fluorescence in polarized light. It is important to emphasize however that, according to our studies, staining with Congo red is ineffective for detection of β -amyloid plaques. This is evidenced by the fact that, when using Congo red, amyloid can be identified not in every specimen of cerebral cortex, containing β -amyloid plaques (based on immunohistochemical assay data). Moreover, the number of congophilic plaques in the specimen, selected for quantitative analysis, is four times lower than the value obtained after immunohistochemical staining.

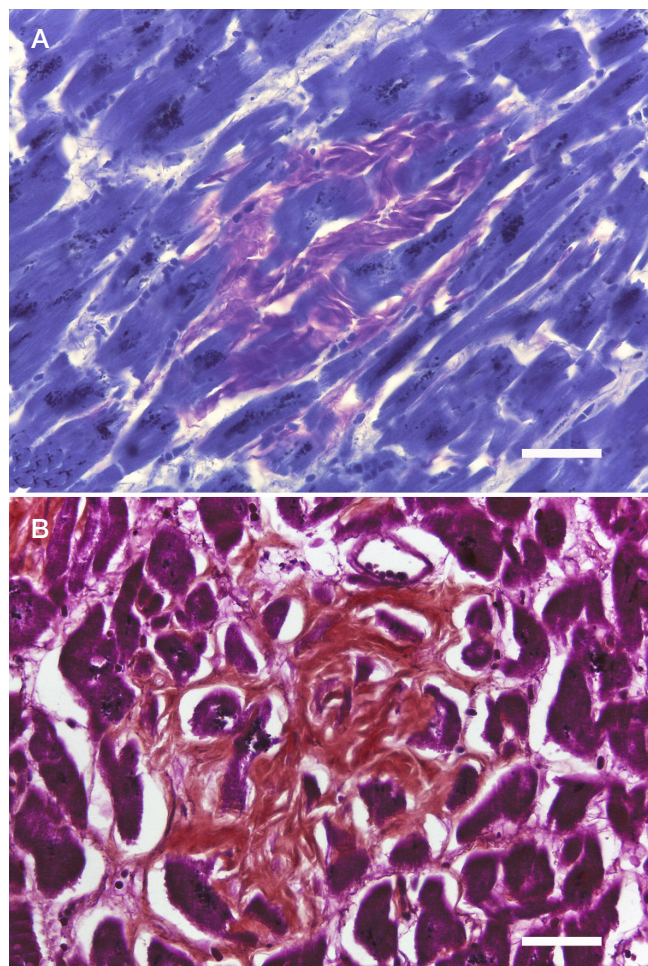


Fig. 2. Metachromatic staining of transthyretin amyloid in human myocardium. **A.** Methyl violet stain. **B.** Basic fuchsin stain. The scale bar shows 50 μ m

The first attempts to detect amyloid using metachromatic dyes, such as toluidine blue, crystal violet, and methyl violet, began at the end of the last century. According to the studies of those years, these methods were significantly less effective in amyloid detection compared to staining with Congo red and ThT [17]. It should be noted that the assessment of specimens stained with metachromatic dyes has been earlier performed only by transmitted light microscopy. We have found that staining with methyl violet with subsequent verification of amyloid by fluorescence microscopy is an effective method for detection of β -amyloid plaques. In this case, it is much easier to identify amyloid plaques within the slice due to totally absent background fluorescence of non-amyloid tissue components. It has been previously shown that applying crystal violet, having the chemical structure similar to methyl violet, to paraffin tissue sections results in significantly reduced autofluorescence [18]. Methyl violet probably possesses similar properties. It is interesting that this staining method is ineffective for transthyretin myocardial amyloidosis. In this case amyloid demonstrates metachromasia when viewed in transmitted light. However, it is characterized by total absence of fluorescence. This may indicate specific nature of methyl violet molecule binding to amyloid fibrils of certain type.

Identification of amyloid plaques in human cerebral cortex is an urgent challenge, since the presence of amyloid plaques is considered one of the main histological signs of Alzheimer's disease. During our studies, we have found that histochemical dyes analyzed interact with amyloid plaques to form fluorescent complexes with varying degrees of effectiveness. The observed

differences in the number of amyloid plaques detected using different methods may be due to varying specificity of binding to β -amyloid fibrils shown by the dyes. Significant differences from immunofluorescence assays suggest that the histochemical dyes used don't bind to all amyloid plaques in the tissue, but only to some of them. This may be due to structural differences between different types of amyloid plaques. Thus, it has been found that diffuse (immature) amyloid plaques do not have fibrillar structure. Such plaques are the compact deposits of β -amyloid peptide [19]. Due to lack of amyloid fibrils, these plaques are unable to interact with such dyes, as Congo red and ThT, the molecules of which are incorporated into structures with certain conformation. From this perspective, histochemical methods of amyloid detection are not entirely analogous to immunohistochemical methods, since the use of antibodies makes it possible to define where certain protein (β -amyloid, transthyretin, etc.) is located. In this case histochemical methods are a more effective way of detecting conformational pathology.

In spite of the fact that quantitative data indicate lower effectiveness of using any histochemical stain for detection of amyloid plaques compared to immunofluorescence method, the results obtained could be of interest for future research. Immunofluorescence method is complicated and expensive due to high cost of reagents and disposables required. As a result, it can be used as a routine method in a minority of scientific, clinical diagnostics and pathomorphological laboratories. In contrast, histochemical methods are simple and cost-effective, being more widely available. The problem of these methods' lower effectiveness for amyloid detection can be partly solved by modifying the existing histochemical dyes and developing the analogues of those [12, 20].

CONCLUSIONS

The use of fluorescence microscopy gives rise to new approaches to visualization of amyloid in human tissues,

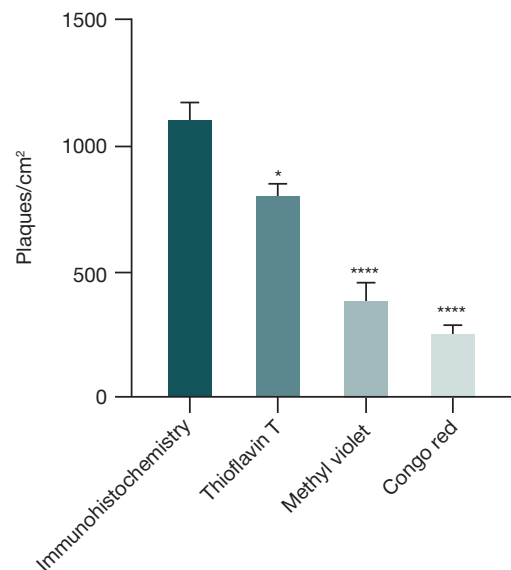


Fig. 3. Quantitative assessment of amyloid plaques stained using various methods. The differences with the control group (immunohistochemistry) are considered significant when $p = 0.01$ (*) and $p < 0.0001$ (****)

which can be successfully used to improve the effectiveness of amyloidosis morphological diagnosis. Thioflavin T is the most effective histochemical dye for fluorescence detection of β - and transthyretin amyloidosis in human tissues. Congo red staining method is highly effective for detection of transthyretin amyloidosis. However, it is ill-suited for identification of β -amyloid plaques. The ability of Congo red to exhibit fluorescence when binding to amyloid fibrils may be used for verification of amyloid deposits instead of polarized light microscopy. Methyl violet is able to specifically bind to β -amyloid deposits with fluorescent complex formation, simultaneously suppressing autofluorescence in nervous tissue. This makes methyl violet staining a promising method for the Alzheimer's-type pathology diagnosis.

References

- Picken MM. The pathology of amyloidosis in classification: A review. *Acta Haematol.* 2020; 143 (4): 322–34. DOI: 10.1159/000506696.
- Cuddy SAM, Falk RH. Amyloidosis as a systemic disease in context. *Can J Cardiol.* 2020; 36 (3): 396–407. DOI: 10.1016/j.cjca.2019.12.033.
- DeTure MA, Dickson DW. The neuropathological diagnosis of Alzheimer's disease. *Mol Neurodegener.* 2019; 14 (1): 32. DOI: 10.1186/s13024-019-0333-5.
- Dickson DW. Neuropathology of Parkinson disease. *Parkinsonism Relat Disord.* 2017; 46 (Suppl 1): S30–S33. DOI: 10.1016/j.parkreldis.2017.07.033.
- Dapsone RW. Amyloid from a histochemical perspective. A review of the structure, properties and types of amyloid, and a proposed staining mechanism for Congo red staining. *Biotech Histochem.* 2018; 93 (8): 543–56. DOI: 10.1080/10520295.2018.1528385.
- Yakupova EI, Bobyleva LG, Vikhlyantsev IM, Bobylev AG. Congo Red and amyloids: history and relationship. *Bioscience Reports.* 2019; 39 (1): BSR20181415. DOI: 10.1042/BSR20181415.
- De Carvalho HF, Taboga SR. The applicability of hematoxylin-eosin staining plus fluorescence or confocal laser scanning microscopy to the study of collagen fibers in cartilages. *Coll R Acad Sci III.* 1996; 319: 991–6. PMID: 9064122.
- Hamid A, Safdar A, Maryam M, Amjad A, Azra J, Abid A. Eosin fluorescence: A diagnostic tool for quantification of liver injury. *Photodiagnosis Photodyn Ther.* 2017; 19: 37–44. DOI: 10.1016/j.pdpdt.2017.03.016.
- Jakubovsky J, Guller L, Cerna M et al. Fluorescence of hematoxylin and eosin-stained histological sections of the human spleen. *Acta Histochem.* 2002; 104 (4): 353–6. DOI: 10.1078/0065-1281-00684.
- De Rossi A, Rocha LB., Rossi MA. Application of fluorescence microscopy on hematoxylin and eosin-stained sections of healthy and diseased teeth and supporting structures. *J Oral Pathol Med.* 2007; 36 (6): 377–81. DOI: 10.1111/j.1600-0714.2007.00542.x.
- Pihlman K, Linder E. Fluorescence microscopical visualization of elastic fibres using basic fuchsin. *Histochemistry.* 1983; 79 (2):157–65. DOI: 10.1007/BF00489778.
- Sapozhnikov SP, Karyshev PB, Sheptukhina AI, Nikolayeva OV, Avruyskaya AA, Mitrasov YN, Kozlov VA. Novel fluorescent probes for amyloid detection. *CTM.* 2017; 9 (2): 91–8. DOI: 10.17691/stm2017.9.2.11.
- Biancalana M, Koide S. Molecular mechanism of Thioflavin-T binding to amyloid fibrils. *Biochim Biophys Acta.* 2010; 1804 (7): 1405–12. DOI: 10.1016/j.bbapap.2010.04.001.
- Sipe JD, Benson MD, Buxbaum JN., Ikeda S-I, Merlini G, Saravia MJM, Westerman P. Amyloid fibril proteins and amyloidosis: chemical identification and clinical classification International Society of Amyloidosis 2016 Nomenclature Guidelines. *Amyloid.* 2016; 23 (4): 209–13. DOI: 10.1080/13506129.2016.1257986.
- Howie AJ, Mared P O-C. 'Apple-green birefringence' of amyloid stained by Congo red. *Kidney Int.* 2012; 82 (1): 114. DOI: 10.1038/ki.2012.89.
- Cohen AS, Calkins E, Levene CI. Studies on experimental amyloidosis. Analysis of histology and staining reactions of

- casein-induced amyloidosis in the rabbit. *Am J Pathol.* 1959; 35: 971–89. PMID: 13810917.
17. Elghetany MT, Saleem A. Methods for staining amyloid in tissues: a review. *Stain Technol.* 1988; 63 (4): 201–12. DOI: 10.3109/10520298809107185.
 18. Buchynska L, Kashuba E, Szekely L. Immunofluorescence staining of paraffin sections: creating DAB staining like virtual digital images using CMYK color conversion. *Exp Oncol.* 2008; 30 (4): 327–9. PMID: 19112433.
 19. Mott RT, Hulette CM. Neuropathology of Alzheimer's disease. *Neuroimaging Clin N Am.* 2005; 15: 755–65. DOI: 10.1016/j.nic.2005.09.003.
 20. Styren SD, Hamilton RL, Styren GC, Klunk WE. X-34, a fluorescent derivative of Congo red: a novel histochemical stain for Alzheimer's disease pathology. *J Histochem Cytochem.* 2000; 48 (9): 1223–32. DOI: 10.1177/002215540004800906.

Литература

1. Picken MM. The pathology of amyloidosis in classification: A review. *Acta Haematol.* 2020; 143 (4): 322–34. DOI: 10.1159/000506696.
2. Cuddy SAM, Falk RH. Amyloidosis as a systemic disease in context. *Can J Cardiol.* 2020; 36 (3): 396–407. DOI: 10.1016/j.cjca.2019.12.033.
3. DeTure MA, Dickson DW. The neuropathological diagnosis of Alzheimer's disease. *Mol Neurodegener.* 2019; 14 (1): 32. DOI: 10.1186/s13024-019-0333-5.
4. Dickson DW. Neuropathology of Parkinson disease. *Parkinsonism Relat Disord.* 2017; 46 (Suppl 1): S30–S33. DOI: 10.1016/j.parkreldis.2017.07.033.
5. Dapson RW. Amyloid from a histochemical perspective. A review of the structure, properties and types of amyloid, and a proposed staining mechanism for Congo red staining. *Biotech Histochem.* 2018; 93 (8): 543–56. DOI: 10.1080/10520295.2018.1528385.
6. Yakupova El, Bobyleva LG, Vikhlyantsev IM, Bobylev AG. Congo Red and amyloids: history and relationship. *Bioscience Reports.* 2019; 39 (1): BSR20181415. DOI: 10.1042/BSR20181415.
7. De Carvalho HF, Taboga SR. The applicability of hematoxylin-eosin staining plus fluorescence or confocal laser scanning microscopy to the study of collagen fibers in cartilages. *Coll R Acad Sci Ill.* 1996; 319: 991–6. PMID: 9064122.
8. Hamid A, Safdar A, Maryam M, Amjad A, Azra J, Abid A. Eosin fluorescence: A diagnostic tool for quantification of liver injury. *Photodiagnosis Photodyn Ther.* 2017; 19: 37–44. DOI: 10.1016/j.pdpdt.2017.03.016.
9. Jakubovsky J, Guller L, Cerna M et al. Fluorescence of hematoxylin and eosin-stained histological sections of the human spleen. *Acta Histochem.* 2002; 104 (4): 353–6. DOI: 10.1078/0065-1281-00684.
10. De Rossi A, Rocha LB., Rossi MA. Application of fluorescence microscopy on hematoxylin and eosin-stained sections of healthy and diseased teeth and supporting structures. *J Oral Pathol Med.* 2007; 36 (6): 377–81. DOI: 10.1111/j.1600-0714.2007.00542.x.
11. Pihlman K, Linder E. Fluorescence microscopical visualization of elastic fibres using basic fuchsin. *Histochemistry.* 1983; 79 (2): 157–65. DOI: 10.1007/BF00489778.
12. Sapozhnikov SP, Karyshev PB, Sheptukhina AI, Nikolayeva OV, Avruyskaya AA, Mitrasov YN, Kozlov VA. Novel fluorescent probes for amyloid detection. *CTM.* 2017; 9 (2): 91–8. DOI: 10.17691/stm2017.9.2.11.
13. Biancalana M, Koide S. Molecular mechanism of Thioflavin-T binding to amyloid fibrils. *Biochim Biophys Acta.* 2010; 1804 (7): 1405–12. DOI: 10.1016/j.bbapap.2010.04.001.
14. Sipe JD, Benson MD, Buxbaum JN., Ikeda S-I, Merlini G, Saraiva MJM, Westerman P. Amyloid fibril proteins and amyloidosis: chemical identification and clinical classification International Society of Amyloidosis 2016 Nomenclature Guidelines. *Amyloid.* 2016; 23 (4): 209–13. DOI: 10.1080/13506129.2016.1257986.
15. Howie AJ, Mared P O-C. 'Apple-green birefringence' of amyloid stained by Congo red. *Kidney Int.* 2012; 82 (1): 114. DOI: 10.1038/ki.2012.89.
16. Cohen AS, Calkins E, Levene CI. Studies on experimental amyloidosis. Analysis of histology and staining reactions of casein-induced amyloidosis in the rabbit. *Am J Pathol.* 1959; 35: 971–89. PMID: 13810917.
17. Elghetany MT, Saleem A. Methods for staining amyloid in tissues: a review. *Stain Technol.* 1988; 63 (4): 201–12. DOI: 10.3109/10520298809107185.
18. Buchynska L, Kashuba E, Szekely L. Immunofluorescence staining of paraffin sections: creating DAB staining like virtual digital images using CMYK color conversion. *Exp Oncol.* 2008; 30 (4): 327–9. PMID: 19112433.
19. Mott RT, Hulette CM. Neuropathology of Alzheimer's disease. *Neuroimaging Clin N Am.* 2005; 15: 755–65. DOI: 10.1016/j.nic.2005.09.003.
20. Styren SD, Hamilton RL, Styren GC, Klunk WE. X-34, a fluorescent derivative of Congo red: a novel histochemical stain for Alzheimer's disease pathology. *J Histochem Cytochem.* 2000; 48 (9): 1223–32. DOI: 10.1177/002215540004800906.

HARDINESS AND PERSONAL RESOURCES OF RED ZONE STAFF: PSYCHOLOGICAL ANALYSIS

Yasko BA^{1,2}✉, Kazarin BV¹, Gorodin VN¹, Chugunova NA³, Pokul LV^{3,4}, Skripnichenko LS², Skorobogatov VV²

¹ Kuban State Medical University, Krasnodar, Russia

² Kuban State University, Krasnodar, Russia

³ Novorossiysk Clinical Center of FMBA, Novorossiysk, Russia

⁴ Peoples' Friendship University of Russia, Moscow, Russia

In light of the ongoing COVID-19 pandemic, it is becoming increasingly important to address the problem of resourcefulness in the healthcare personnel of COVID-19 red zones. The aim of this study was to assess hardiness and the state of vital resources in physicians continuously working in red zones and to test a hypothesis that long-term work in a COVID-19 red zone adversely affects the resourcefulness, reducing resistance to stress. Group 1 ($n = 94$) consisted of physicians with a history of employment in a COVID-19 red zone between May 2020 and June 2021; group 2 ($n = 77$) comprised physicians who were not involved in managing COVID-19 patients. The tests showed that hardiness and its components (commitment, control and challenge) were at high levels in group 2 (59.7%; 67.5%; 61.0%; 20.9%, respectively). The index of resourcefulness (RI; 1.24) reflected the prevalence of personal gains over losses in group 1 over the past year. In this group, there were no sex differences in the results. By contrast, hardiness was significantly reduced in 31.9% of the respondents in group 1 (red zone). Working in the red zone had a devastating effect on all hardiness components: the ratio of the percentages of high to low values was 8.5/27.7 for commitment, 9/6/34.0 for control and 10.6/35.1 for challenge. RI was reduced (0.77). The most pronounced loss of resources was observed in female physicians. The study found a significant mutual impact between challenge and the state of personality resources in red zone staff, which may indicate activation of proactive coping strategies and the acceptance of new professional experience.

Keywords: COVID-19, pandemic, pandemic consciousness, mental health, hardiness, personal resources

Acknowledgement: the authors thank Zotov SV, the Chief Medical Officer of the Specialized Clinical Hospital for Infectious Diseases for his assistance in organizing the study and Ostroshko MG, the Head of the HR Department of the Regional Clinical Hospital № 2, for her assistance in organizing psychological assessment.

Author contribution: Yasko BA proposed the idea and concept of the, systematized empirical data, discussed the results, and wrote the manuscript; Kazarin BV proposed the concept of the empirical study, provided tools to accumulate survey data; Gorodin VN recruited study participants, organized psychological assessment, proposed the theoretical and methodological basis of the study; Chugunova NA carried out data acquisition and analyzed the obtained data; Pokul LV participated in the discussion of the study design and wrote the draft version of the manuscript; Skripnichenko LS provided rationale for the study and participated in the discussion about delivering psychological counselling to red zone staff; Skorobogatov VV conducted statistical analysis.

Compliance with ethical standards: the study was approved by the Ethics Committee of Kuban State Medical University (Protocol № 12 dated June 29, 2021 and Protocol № 14 dated June 25, 2021); informed consent was obtained from all study participants.

✉ **Correspondence should be addressed:** Bella A. Yasko
Stavropolskaya, 149, 350040, Krasnodar; shabela@yandex.ru

Received: 12.08.2021 **Accepted:** 26.08.2021 **Published online:** 30.08.2021

DOI: 10.24075/brsmu.2021.042

ЖИЗНЕСТОЙКОСТЬ И ПЕРСОНАЛЬНЫЕ РЕСУРСЫ ВРАЧЕЙ «КРАСНЫХ ЗОН» КОВИД-ГОСПИТАЛЕЙ: ПСИХОЛОГИЧЕСКИЙ АНАЛИЗ

Б. А. Ясько^{1,2}✉, Б. В. Казарин¹, В. Н. Городин¹, Н. А. Чугунова³, Л. В. Покуль^{3,4}, Л. С. Скрипнichenko², В. В. Скоробогатов²

¹ Кубанский государственный медицинский университет, Краснодар, Россия

² Кубанский государственный университет, Краснодар, Россия

³ Новороссийский клинический центр Федерального медико-биологического агентства, Новороссийск, Россия

⁴ Российский университет дружбы народов, Москва, Россия

В связи с продолжающейся пандемией COVID-19 особенно актуален вопрос о состоянии психологических ресурсов у врачей, продолжительно работающих в условиях «красных зон». Целью работы было проанализировать специфику состояния жизнестойкости и персональных (вitalных) ресурсов врачей, продолжительно работающих в «красной зоне», и проверить гипотезу о том, что продолжительная профессиональная деятельность врачей в «красной зоне» оказывает негативное влияние на систему экзистенциальных и витальных ресурсов, сокращая потенциал стрессоустойчивости личности. Группу 1 ($n = 94$) составили врачи, вовлеченные с мая 2020 г. по июнь 2021 г. в «красную зону» ковид-госпиталей; группу 2 ($n = 77$) — врачи, не участвовавшие в клиническом процессе с ковидными пациентами. По результатам диагностики, врачи группы 2 характеризуются высоким уровнем жизнестойкости и ее компонентов «Вовлеченность», «Контроль», «Принятие риска» (59,7%; 67,5%; 61,0%; 20,9% соответственно). В индексе ресурсности (ИР) (1,24) отражено преобладание персональных приобретений над потерями за прошедший год. Отсутствуют различия по полу. У 31,9% врачей «красных зон» (группа 1) значительно сократился потенциал жизнестойкости. Разрушительному воздействию подверглись все компоненты жизнестойкости: соотношение %-долей высоких/низких значений следующее: «Вовлеченность» — 8,5/27,7; «Контроль» — 9,6/34,0; «Принятие риска» — 10,6/35,1. ИР снижен (0,77). Наиболее выражено сокращение ресурсов у врачей женского пола. Установлено значимое взаимовлияние принятия риска и динамики персональных ресурсов у врачей «красной зоны», что может указывать на активизацию проактивного совладания с опорой на принятие нового профессионального опыта.

Ключевые слова: пандемия, COVID-19, пандемическое сознание, психологическое здоровье, жизнестойкость, персональные ресурсы

Благодарности: главному врачу Специализированной клинической инфекционной больницы МЗ Краснодарского края С. В. Зотову — за организационную поддержку процесса исследования начальнику отдела кадров Краевой клинической больницы № 2 МЗ Краснодарского края М. Г. Остроушко — за организацию процедур психодиагностики групп врачей.

Вклад авторов: Б. А. Ясько — идея и концепция публикации, систематизация эмпирических данных, обсуждение результатов; подготовка статьи; Б. В. Казарин — концепция эмпирического исследования, предоставление базы кафедры для аккумуляции массива данных психодиагностики; В. Н. Городин — подбор испытуемых, организация психодиагностических обследований, обсуждение теоретико-методологических основ исследования; Н. А. Чугунова — предоставление эмпирической базы, сбор материала, анализ данных; Л. В. Покуль — обсуждение дизайна исследования, подготовка черновика статьи; Л. С. Скрипнichenko — обоснование актуальности исследования; обсуждение маршрутов психологической поддержки врачей «красных зон»; В. В. Скоробогатов — статистическая обработка данных.

Соблюдение этических стандартов: исследование одобрено этическим комитетом КубГМУ (протокол № 12 от 29 июня 2021 г. и протокол № 14 от 25 июня 2021 г.); все респонденты подписали добровольное информированное согласие на участие в исследовании.

✉ **Для корреспонденции:** Бэла Аслановна Ясько
ул. Ставропольская, д. 149, 350040, г. Краснодар; shabela@yandex.ru

Статья получена: 12.08.2021 **Статья принята к печати:** 26.08.2021 **Опубликована онлайн:** 30.08.2021

DOI: 10.24075/vrgmu.2021.042

The coronavirus has been rampant for over a year now. In all corners of the world, healthcare workers have been on the frontline of the battle against COVID-19. The losses suffered in the strenuous battle for patients' lives and the gains from this experience require detailed analysis.

The first steps in studying the impact of the COVID-19 pandemic on different demographic groups have been already made. The emotional response to the COVID threat in the early months of the pandemic was recognized by psychiatrists and psychologists as a mental health crisis. Prompt measures were expected of public health agencies to deliver psychological support to those in need [1, 2]. Today, questionnaire survey data collected during the first phase of the pandemic are being actively studied by psychology researchers. Their main focus is on coping strategies, risk factors of posttraumatic stress, and changes in the individual and collective consciousness provoked by the ongoing pandemic. An online survey conducted after the 2020 spring to summer lockdown revealed how proactive coping was implemented in different age groups [3]. Drawing on the concept of proactive coping [4], a group of researchers established that the most resourceful coping strategy for young people in the pandemic circumstances, given the low level of stress, was a search for information. At older age, proactive strategies were more diverse, regardless of the amount of stress, suggesting that older adults had a more stable coping system. Another research team analyzed psychological factors contributing to COVID-19-associated posttraumatic stress among Chinese students living in China and abroad. The analysis revealed that students who preferred proactive coping strategies had less pronounced symptoms of COVID-19-related posttraumatic stress disorder than those who resorted to passive coping [5].

The sociopsychological context of the pandemic was analyzed in a series of surveys conducted by the leading Russian psychologists [6]. A divide in society and in the expert community was exposed: there were confronting groups of COVID dissidents and COVID rigorists, which indeed disrupted the positive effect of containment measures. These findings are consistent with the conclusion about the lack of commitment to vaccination among different population groups. This creates barriers to effective communication between the doctor and the patient [7].

A review of the literature on the psychological impact of the pandemic reveals a paucity of data on the resourcefulness of healthcare personnel working in COVID hospitals. Here, the methodology of the resource-based approach that relies on the tenets of existential psychology and psychotherapy elaborated by Frankl, Maddi and Hobfoll [8–15] can serve as a theoretical and methodological basis for empirical research. Hardiness is the most important concept in the context of resourcefulness; it is defined as an attitude that helps a person to stay engaged and avoid the devastating effects of stress [9, 16]. According to Maddi, hardiness provides the courage to not deny stress and to turn stress into an opportunity [16]. A few recent studies demonstrated that high hardiness was a resource for patients with cardiovascular disorders [17], insomnia [18] and depression [19]. Within the scope of our interest are publications that unlock the potential of hardiness in resisting occupational stress in a clinical setting. For example, a study reports a negative correlation between low hardiness and high burnout levels in healthcare workers [20]. Another study demonstrates a link between hardiness and the attitude to work among healthcare professionals [21]. As an integral personality trait, hardiness is determined by professional engagement, satisfaction from work and is not significantly associated with age [22].

Foreign publications also discuss hardiness in the context of resistance to occupational stress. For example, hardiness is a mediator between perceived stress and happiness in nurses [23]. Resilience and well-being of hospice staff, their view of themselves as socially engaged and mentally healthy individuals are significantly correlated with high levels of hardiness [24]. A study conducted on a large sample size in China reports a strong positive correlation between hardiness and physical and mental health in hospital nurses [25].

Apart from the concept of hardiness as an existential resource that confers resistance to stressors, the concept of adaptive resources is also shared by many researchers [26–28]. According to Hobfoll, humans can draw from a variety of means to endure stress [26]. These resources can be broken down in 3 categories, one of them being significance for survival. Vital resources can be grouped into fundamental (essential for survival), secondary, which bolster fundamental resources (e.g., social support) and tertiary (social status, etc.). This approach was used to build a theoretical base for the psychological counseling of individuals facing a critical loss of resources or obstacles for their adequate repletion [28].

Based on the heuristic concepts of hardiness and adaptive resources and the concept of mental health formulated by WHO [29], we defined the aim of this study: to assess hardiness and the state of vital resources in red zone staff and to test the hypothesis that long-term (one year long) work in a COVID red zone adversely affects the resourcefulness of an individual, reducing their resistance to stress.

METHODS

The study was conducted on a sample of physicians from different healthcare institutions of Krasnodar and Krasnodar region during the COVID-19 pandemic (May 2020 – June 2021).

Two groups were formed. The main group (group 1) consisted of physicians who had been working in COVID-19 red zones during the specified period ($n = 94$); the control group (group 2) comprised physicians who had not been involved in managing COVID-19 patients ($n = 77$). In group 1, 60.0% ($n = 62$) of the participants were women and 34.0% ($n = 32$) were men; in group 2, women made up 66.2% ($n = 51$), whereas men, 33.8% ($n = 26$).

The following inclusion criteria were applied: physicians with a specialty in general medicine; age under 55 years; no life crisis accompanied by emotional distress during the specified period; a history of working in a COVID-19 red zone for group 1 and no such history for group 2.

Exclusion criteria: age above 55 years; a serious life crisis between May 2020 and June 2021.

The methodological principles of subjective activity and resourcefulness concepts [9, 10, 26, 27, 30] were used as a theoretical and methodological basis of our empirical research. Psychological assessment was conducted using surveys based on the theoretical constructs of hardiness [9, 10] and human resource psychology [26–28], including the Hardiness test [31] and the Loss and Gain of Resources test [32].

The Hardiness test is a tool for assessing 3 components that, according to the existential concept, make up hardiness: commitment, control and challenge. Commitment is defined as a conviction that involvement in life results in the highest chance to find something worthy and meaningful [31]. The lack of such conviction breeds a feeling of rejection, a sense of being an outcast in life. The control component shows how confident a person is in his/her ability to change the course of events. A low control score indicates helplessness in a given circumstance.

Table 1. Descriptive statistics for hardiness in the studies groups of red zone physicians

Groups	M ± SD, % relative to max	Level (abs./%)		
		high	medium	low
Hardiness				
Group 1 (<i>n</i> = 94)	57.0 ± 15.9* 42.2%	9/9.6% ^v	55/58.5% ^{vv}	30/31.9% ^{vvv}
Group 2 (<i>n</i> = 77)	81.6 ± 16.07* 60.5	46/59.7% ^v	27/35.1% ^{vv}	4/5.2% ^{vvv}
Commitment				
Group 1 (<i>n</i> = 94)	21.1 ± 6.84** 39.1%	8/8.5% ^u	60/63.8% ^{uu}	26/27.7% ^{uuu}
Group 2 (<i>n</i> = 77)	34.2 ± 7.39** 63.3%	52/67.5% ^u	19/24.7% ^{uu}	6/7.8% ^{uuu}
Control				
Group 1 (<i>n</i> = 94)	22.0 ± 5.58*** 43.1%	9/9.6% ^z	53/56.4% ^{zz}	32/34.0 ^{zzz}
Group 2 (<i>n</i> = 77)	31.5 ± 7.61*** 61.9%	47/61.0% ^z	23/29.9% ^{zz}	7/9.1 ^{zzz}
Challenge				
Group 1 (<i>n</i> = 94)	13.9 ± 4.65**** 46.4%	10/10.6% ^Δ	51/54.3%	33/35.1%
Group 2 (<i>n</i> = 77)	15.9 ± 5.25**** 52.9%	16/20.85% ^Δ	42/54.5%	19/24.7%

Note: Student's *t* test: * — *t* = 9.99; *p* < 0.001; ** — *t* = 11.9; *p* < 0.001; *** — *t* = 9.13; *p* < 0.001; **** — *t* = 2.57; *p* < 0.05. Fisher's criterion: ^v — φ^* = 7.39; *p* ≤ 0.001; ^{vv} — φ^* = 3.09; *p* ≤ 0.001; ^{vvv} — φ^* = 4.81; *p* ≤ 0.001; ^u — φ^* = 15.9; *p* ≤ 0.001; ^{uu} — φ^* = 9.65; *p* ≤ 0.001; ^{uuu} — φ^* = 6.47; *p* ≤ 0.001; ^z — φ^* = 7.56; *p* ≤ 0.001; ^{zz} — φ^* = 3.53; *p* ≤ 0.001; ^{zzz} — φ^* = 4.14; *p* ≤ 0.001; ^Δ — φ^* = 1.84; *p* ≤ 0.033.

Challenge exposes a conviction that whatever happens to a person, it promotes personal growth through knowledge gained from experience and the practical application of this knowledge [31]. The Hardiness test allows assessing the ability and willingness to be active and flexible in a difficult life situation and vulnerability to stress.

The respondents were offered to fill out a questionnaire that contained 45 statements describing different aspects of hardiness. The respondents reported their attitude to each statement by choosing one of four available options (no, more likely no than yes, more likely yes than no, yes). Each answer was rated on the scale from 0 to 3. Since the number of statements describing each hardiness component was different (18 statements for commitment, 17 statements for control and 10 statements for challenge), we compared the total score to the maximum possible total score and expressed the obtained value in %.

The "Loss and Gain of Resources" test [32] was used to analyze the interplay between vital resources during a certain time period (which in our case was from May 2020 to June 2021). The tests consisted of 2 identical lists of 30 resources (intrapersonal, social, material). The respondents rated their emotional response to the gain or loss of a resource on the list on a 5-point scale. The index of resourcefulness (RI) was calculated for each participant as a ratio of the total gain score to the total loss score. The authors of the test propose 3 levels of resourcefulness: low (RI < 0.8), medium (RI from 0.8 to 1.2) and high (RI > 1.2) [32].

Statistical analysis was carried out in SPSS 26.0 (An IBM Company; USA). Both parametric and nonparametric statistical methods were applied (means, standard deviations, Student's *t* test, Pearson's correlation coefficient *r*, and Fisher's φ^*). The decision to use parametric statistics was based on the results of Levene's F test for the homogeneity of variance. The

results of the F test for the entire sample and its subsamples corresponded to the significance level < 95.0% (*p* > 0.05), confirming the homogeneity of variance and justifying the use of parametric statistics.

RESULTS

Hardiness in Covid red zone staff (Group 1)

Of 94 respondents, high hardiness was observed in only 9 persons (9.6%). More than half of the respondents working in the red zone showed a medium level of hardiness (58.5%; *n* = 55); one-third of the red zone physicians (31.9%; *n* = 30) had low ability to tolerate stress and maintain inner balance (Table 1).

The average hardiness score in group 1 was 57 points (*SD* = 15.9), i.e. at the borderline between medium and low values (42.2%). The commitment score was the lowest (39.1% relative to the maximum on this scale). Only 8.5% of the respondents (*n* = 8) showed high levels of commitment. Eighty-six respondents had low (27.7%; *n* = 26) or medium (67.8%; *n* = 60) levels of commitment. Control and challenge scores in this group were in the lower part of the medium values spectrum: 43.1% and 46.4%, respectively, relative to the maximum possible scores on these scales. Eighty-five respondents from group 1 scored low (34.0%; *n* = 32) or medium (56.4%; *n* = 53) on the control scale. Only 9.6% of the physicians (*n* = 9) demonstrated high levels of subjective control over the course of events in the presence of occupational stress. High challenge scores were observed in 10 respondents (10.6%). Other 84 doctors in this group had low (35.1%; *n* = 33) or medium (54.3%; *n* = 51) challenge scores reflecting their level of willingness to grow from experience by taking risks.

There is a sex difference in hardiness among red zone physicians (Table 2).

Table 2. Descriptive statistics for hardness among male and female participants in group 1

Hardiness						
M ± SD	Men: 71.8 ± 12.10*			Women: 54.4 ± 15.5*		
Levels						
	high (total; %)		medium (total; %)		low (total; %)	
Men	4	6.5	35	56.5	23	37.1 ^v
Women	5	15.6	20	62.5	7	21.9 ^v
Commitment						
M ± SD	Men: 23.8 ± 5.78**			Women: 19.7 ± 6.90**		
	high (total; %)		medium (total; %)		low (total; %)	
Men	5	15.6	22	68.8	5	15.6 ^{vv}
Women	3	4.8	38	61.3	21	33.9 ^{vv}
Control						
M ± SD	Men: 23.5 ± 5.8			Women: 21.2 ± 5.3		
	high (total; %)		medium (total; %)		low (total; %)	
Men	4	12.5	21	65.6	7	21.9 ^{vv}
Women	5	8.1	32	51.6	25	40.3 ^{vv}
Challenge						
M ± SD	Men: 14.7 ± 5.20			Women: 13.5 ± 4.33		
	high (total; %)		medium (total; %)		low (total; %)	
Men	5	15.6	16	50	11	34.4
Women	5	8.1	35	56.4	22	35.5

Note: Student's *t* test: * — $t = 5.99$; $p < 0.001$; ** — $t = 3.1$; $p < 0.01$. Fisher's criterion: ^v — $\varphi^* = 1.54$; $p \leq 0.06$; ^{vv} — $\varphi^* = 2.0$; $p \leq 0.02$; ^{vv} — $\varphi^* = 1.85$; $p \leq 0.03$.

Medium hardness scores ($M \pm SD$) were prevalent in the male subsample ($t = 5.99$; $p < 0.001$), whereas the female subsample was dominated by low hardness scores ($\varphi^* = 1.54$; $p \leq 0.06$). The level of commitment also differed between the sexes ($t = 3.1$; $p < 0.01$). The female subsample was dominated by low commitment ($\varphi^* = 2.0$; $p \leq 0.03$) and low control ($\varphi^* = 1.85$; $p \leq 0.02$) scores.

Hardiness in physicians not involved in management of COVID-19 patients (group 2)

In group 2, the average hardness score was 81.6 points ($SD = 16.07$), i.e. high (60.5% relative to the maximum hardness score; see Table 1).

On the whole, these findings were consistent with the results of another study conducted in physicians [33]. In that study, physicians with over 5 years of professional experience scored an average of 70.4 points on hardness, and their commitment, control and challenge scores were 33.2, 24.1 and 13.08, respectively.

In our study, there was a significant difference in the level of hardness between the groups ($t = 9.99$; $p < 0.001$). Of 77 respondents in group 2, 59.7% ($n = 46$) demonstrated a higher level of hardness than those in group 1 ($\varphi^* = 7.39$; $p \leq 0.001$). Reduced tolerance to stress, compromising inner balance and preventing the person from succeeding in their activities, was observed in only 5.2% of the respondents in group 2 ($n = 4$); the difference in this parameter was significant between the groups ($\varphi^* = 4.81$; $p \leq 0.001$). Medium hardness was observed in 35.1% of the respondents ($n = 27$) in group 2, which was much lower than in group 1 ($\varphi^* = 3.09$; $p \leq 0.001$). In group 2, high

tolerance to stress was detected in 59.7% of the respondents ($n = 46$), which was a significantly higher value than in group 1 ($\varphi^* = 7.39$; $p \leq 0.001$).

Unlike red zone doctors, doctors from group 2 demonstrated significantly higher levels of commitment and control (see Table 1). More than half of the respondents in group 2 (67.5%; $n = 52$) reported being actively involved in their daily activities. Low commitment was detected in only 7.8% ($n = 6$) of the respondents in group 2. In comparison with group 1, individuals with high commitment prevailed in group 2; group 1 was dominated by individuals with low commitment ($\varphi^* = 15.9$ and $\varphi^* = 6.47$, respectively; $p \leq 0.001$).

The average control score (the ability to change the course of events) in group 2 was quite high ($M = 31.5 \pm 7.61$; 61.9% from the maximum on this subscale) and significantly higher than in group 1 ($t = 9.13$; $p < 0.001$). Only 7 respondents in group 2 (9.1%) scored low on the control scale, and 61.0% ($n = 47$) thought they were able to control events in their life and make a difference. High control scores were prevalent in group 2 ($\varphi^* = 7.56$; $p \leq 0.001$), as compared to group 1, dominated by low and medium control scores ($\varphi^* = 3.53$ and $\varphi^* = 4.14$, respectively; $p \leq 0.001$).

The average challenge score, i.e. a conviction that every event in life can promote personal growth, was 15.9 points in group 2 ($SD = 5.25$), which was significantly higher than in group 1 ($t = 2.57$; $p < 0.05$), although both parameters fell within the range of medium values. High willingness to take risks was observed in 20.8% of the participants in group 2 ($n = 16$), which again was significantly higher than in group 1 ($\varphi^* = 1.84$; $p \leq 0.033$). However, there were no significant differences in medium and low challenge scores between the groups.

Table 3. Descriptive statistics for hardness among male and female participants in group 2

Hardiness						
M ± SD	Men: 81.4 ± 17.10			Women: 81.7 ± 15.70		
levels						
	high (total; %)		medium (total; %)		low (total; %)	
Men	14	53.8	10	38.5	2	7.7
Women	32	62.7	17	33.4	2	3.9
Commitment						
M ± SD	Men: 33.1 ± 8.29			Women: 34.7 ± 7.49		
Levels						
	high (total; %)		medium (total; %)		low (total; %)	
Men	16	61.5	7	26.9	3	11.6
Women	36	70.6	12	23.5	3	5.9
Control						
M ± SD	Men: 31.0 ± 7.55			Women: 31.8 ± 7.70		
Levels						
	high (total; %)		medium (total; %)		low (total; %)	
Men	13	50	10	38.5	3	11.5
Women	34	66.7	13	25.5	4	7.8
Challenge						
M ± SD	Men: 17.3 ± 5.42			Women: 15.2 ± 5.07		
Levels						
	high (total; %)		medium (total; %)		low (total; %)	
Men	7	26.9	13	50	6	23.1
Women	9	17.6	29	56.9	13	25.5

Interestingly, there were no sex difference in the analyzed parameters among the male and female respondents in group 2 (Table 3).

Gain and loss of resources in red zone staff (group 1)

The average RI in group 1 was low (0.77), indicating the prevalence of personal losses over gains in the past year (Table 4). The RI was low for 53 respondents (56.4%) and medium in 32 (34.0%) respondents. Only 9 doctors (9.6%) scored slightly higher on total gains than on total losses; this was largely due to the maximum possible rates (4; 5) given to the following statements: I feel needed; My achievements are recognized by close others; I get support from colleagues.

Low RI was prevalent in the female subgroup vs. the male subgroup (61.3% and 37.5%, respectively; $\varphi^* = 2.21$; $p \leq 0.013$).

Table 4. Descriptive statistics for resource gains and losses in the compared groups

	M ± SD			RI (abs./%)		
	Losses	Gains	RI	low	medium	high
Group 1	107.1 ± 15.5 ^{*1}	79.9 ± 23.1 ^{*2}	0.77	53/56.4 ^{*1}	32/34.0 ^{*2}	9/9.6 ^{*3}
Men	107.3 ± 16.2 ^{*3^A}	87.8 ± 22.53	0.82	15/46.91°	13/40.6 ^{*1}	4/12.5 ^{Y1}
Women	107.0 ± 15.3 ^{*4^A}	75.9 ± 22.51 ^{*5}	0.71	38/61.31 ^{oV1}	19/30.6 ^{*2}	5/8.1 ^{Y2}
Group 2	88.4 ± 18.60 ^{*1}	102.05 ± 23.04 ^{*2}	1.24	20/26.0 ^{*1}	13/16.9 ^{*2}	44/57.1 ^{*3}
Men	90.8 ± 18.7 ^{*3}	98.9 ± 22.7	1.17	8/30.8	4/15.4 ^{*1}	14/53.8 ^{Y1}
Women	87.2 ± 18.0 ^{*4}	103.7 ± 23.3 ^{*5}	1.2	12/23.5 ^{V1}	9/17.6 ^{*2}	30/58.8 ^{Y2}

Note: Student's t test. Losses: ^{*1} — $t = 7.03$; $p < 0.001$; ^{*3} — $t = 3.56$; $p < 0.01$; ^{*4} — $t = 6.22$; $p < 0.001$; gains: ^{*2} — $t = 6.24$; $p < 0.001$; ^{*5} — $t = 6.41$; $p < 0.001$. Fisher's criterion. RI levels, low: ^o — $\varphi^* = 2.21$, $p \leq 0.013$; ^{*1} — $\varphi^* = 2.41$, $p \leq 0.007$; ^{V1} — $\varphi^* = 4.16$, $p \leq 0.001$; medium: ^{*2} — $\varphi^* = 2.59$, $p \leq 0.004$; ^{*1} — $\varphi^* = 2.17$, $p \leq 0.015$; ^{*2} — $\varphi^* = 1.61$, $p \leq 0.05$; high: ^{*3} — $\varphi^* = 7.04$, $p \leq 0.001$; ^{Y1} — $\varphi^* = 3.50$, $p \leq 0.001$; ^{V2} — $\varphi^* = 6.19$, $p \leq 0.001$.

Table 5. The correlation matrix (r) for hardness, its components and gain and loss scores on the self-assessment scale

Group 1			Group 2		
Total ($n = 94$)			Total ($n = 77$)		
	losses	gains		losses	gains
Commitment	-0.491	0.677	Commitment	-0.661	0.74
Control	-0.508	0.597	Control	-0.624	0.701
Challenge	-0.556	0.561	Challenge	-0.128*	0.238*
Hardiness	-0.551	0.663	Hardiness	-0.641	0.75
Women ($n = 62$)			Women ($n = 51$)		
Commitment	-0.501	0.623	Commitment	-0.608	0.72
Control	-0.484	0.54	Control	-0.577	0.717
Challenge	-0.453	0.498	Challenge	-0.069*	0.258*
Hardiness	-0.516	0.602	Hardiness	-0.573	0.752
Men ($n = 32$)			Men ($n = 26$)		
Commitment	-0.561	0.646	Commitment	-0.74	0.777
Control	-0.583	0.646	Control	-0.711	0.666
Challenge	-0.733	0.65	Challenge	-0.295*	0.273*
Hardiness	-0.665	0.723	Hardiness	-0.766	0.757

Note: * — r is below the significance threshold ($p > 0.05$).

r-coefficient in both samples. The established correlations were not sex-specific. Nevertheless, in group 2 the challenge score and the loss and gain score were mutually influential. Unlike group 1, in group 2 gains and losses were not associated significantly with experience acquired over the past year and the practical application of this experience. In general, in group 2 and male and female subgroups, the correlation coefficient was below the critical threshold for the corresponding sample size ($p > 0.05$).

DISCUSSION

Our findings indicate a negative psychological effect of long-term work in a COVID-19 red zone. All studied parameters were significantly lower in red zone staff than in healthcare workers not involved in the management of COVID-19 patients. Work overload and daily emotional distress undermine the ability to endure occupational stress and maintain inner balance (hardiness). This is most clearly manifested in reduced commitment, the feeling of being rejected or being an outsider to life, development of a non-constructive pandemic consciousness, i.e. a growing conviction that it is impossible to have control over one's own life or influence the course of events, and helplessness in difficult life situations and in the presence of occupational stress.

Direct consequences of low hardiness include low RI, the lack of personal resources, the prevalence of losses over gains, and a pessimistic assessment of personal gains.

The analysis of data generated by group 1 shows that men are slightly more successful in preserving their commitment than women. This is also reflected in higher RI among males, which falls within a domain of medium values (0.82 vs. 0.71 in women).

Group 2 was characterized by better hardiness potential and stronger vital resources. Drawing on the literature data [33], we conclude that the discovered characteristics of group 2 could be viewed as an element in the psychological profile of Russian physicians that enriches the psychological model of a medical doctor's personality [34].

The established correlations suggest a systemic link between existential and vital resources of a medical doctor. The

role of challenge in the perception of resource gains and losses by red zone staff, contrary to physicians not involved in the management of COVID-19 patients, may indicate the ongoing pursuit of meaning in the professional activity. The search for meaning may reflect the activation of proactive coping strategies (transformational coping, according to Maddi) in an effort to maintain resistance to stress. These findings are consistent with the literature [35].

High levels of resource losses reported by red zone physicians may be attributed to the weakness of their existential resources, whereas high levels of hardiness and its components among other physicians are directly associated with their optimistic assessment of resource dynamics, with gains prevailing over losses.

CONCLUSIONS

Modern psychology, including occupational medical psychology, is confronted with the psychosocial consequences of the COVID-19 pandemic that require thorough and prompt analysis. Our study has confirmed the hypothesized negative impact of long-term (one year long) work in a COVID-19 red zone on the system of existential and vital resources, compromising resistance to stress. The most pronounced manifestation of this process is significant depletion of personality resources, reduced hardiness (ability to endure stress), reduced adaptive potential of being involved in and having control over one's own life. As these tendencies progress, they may result in the existential vacuum, a personality crisis characterized by the lack of meaning of one's existence. This may breed noogenic neurosis, i.e. disruption of psychological well-being, which is the critical component of human health. Our findings may be used to create a roadmap for psychological counselling of healthcare workers during the ongoing pandemic. Such counseling should focus on the activation of commitment as a component of hardiness, finding the meaning in professional activities, acknowledging the significance of professional experience, repletion of vital resource, including rest, acquiring basic knowledge of psychophysiological self-regulation and stress reduction, and formation of proactive coping strategies.

References

1. Tverdohlebova TI, Kovaliov EV, Karpushhenko GV, Kulak MA, Dumbadze OS, Litovko AR i dr. Social'no-ekonomicheskie aspekty COVID-19 na primere Rostovskoj oblasti. Infekcionnye bolezni. 2020; 18 (4): 27–32. DOI: 10.20953/1729-9225-2020-4-27-32. Russian.
2. Sorokin MYu, Kasyanov ED, Rukavishnikov GV, Makarevich OV, Neznanov NG, Lutova NB, et al. Structure of anxiety associated with COVID-19 pandemic: the online survey results. Bulletin of RSMU. 2020; 3: 70–76.
3. Kuftjak EV, Behter AA. Stress i proaktivnoe sovladajushhee povedenie v period pandemii Covid-19: dannye onlajn-oprosa. Medicinskaia psihologija v Rossii. 2020; 12; 6 (65) [cited 2021 July 13]. Dostupno po ssylke: http://mpoj.ru/archiv_global/2020_6_65/nomer05.php. Russian.
4. Aspinwall LG, Taylor SE. Modeling cognitive adaptation: A longitudinal investigation of the impact of individual differences and coping on college adjustment and performance. Journal of Personality and Social Psychology. 1992; 63; 6: 989–1003. DOI: 10.1037/0022-3514.63.6.989.
5. Czyhan L, Sjao Gan V. Psihologicheskie faktory posttraumaticeskogo stressa, vyzvannogo pandemiej COVID-19. Psihologicheskiy zhurnal. 2021; 42; 1: 102–10. Russian.
6. Jurevich AV, Ushakov DV, Jurevich MA. COVID-19: rezul'taty tret'ego jekspertnogo oprosa. Psihologicheskiy zhurnal. 2021; 42; 3: 28–136. Russian.
7. Platonova TA, Golubkova AA, Smirnova SS, D'yachenko EV. Aktual'nye voprosy organizacii immunoprofilaktiki naselenija. Kommunikativnye riski — nereshennye problemy i novye vozmozhnosti. Infekcionnye bolezni. 2020; 18 (3): 112–8. DOI: 10.20953/1729-9225-2020-3-112-118. Russian.
8. Frankl V. Chelovek v poiskah smysla. M.: Progress, 1990; 368 s. Russian.
9. Maddi S. Hardiness: an Operationalization of Existential Courage. Journal of Humanistic Psychology. 2007; 44; 3: 279–98.
10. Maddi S. Hardiness: The courage to grow from stresses. The Journal of Positive Psychology. 2006; 1 (3): 160–8.
11. Odincova MA. Psihologija zhiznestoikosti. M.: FLINTA, 2015; 296 s. Russian.
12. Jaroshhuk IV. Psihologija zhiznestoikosti: obzor teoretycheskih koncepcij, jempiricheskikh issledovanij i metodik diagnostiki. Uchenye zapiski SPbGIPSR. 2020; 1; 33: 50–60. Russian.
13. Hobfoll SE. Stress, culture, and community. N.Y.: London, 1998; 296 p.
14. Vodopjanova N. E. Protivodejstvie sindromu vygoranija v kontekste resursnoj koncepcii cheloveka. Vestnik Sankt-Peterburgskogo universiteta. Serija: Psihologija. 2011; 3: 38–50. Russian.
15. Kobasa SC. Stressful life events, personality, and health — inquiry into hardiness. Journal of Personality and Social Psychology. 2011; 37 (1): 1–11.
16. Maddi S. The Courage and Strategies of Hardiness as Helpful in Crowing Despite Major, Destructive Stresses. American Psychologist. 2008; 63; 6: 563–4.
17. Bartone PT, Valdes JJ, Sandvik A. Psychological Hardiness Predicts Cardiovascular Health. Psychology, Health and Medicine. 2016; 21 (6): 743–9.
18. Nordmo M, Hystad SW, Sanden S, Johnsen BH. The effect of hardiness on symptoms of insomnia during a naval mission. International Maritime Health. 2017; 68 (3): 147–52.
19. Maddi SR. The Role of Hardiness and Religiosity in Depress and Anger. International Journal of Existential Psychology & Psychotherapy. 2004; 1; 1: 38–49.
20. Stecishin RI. Zhiznestoikost' kak akmeologicheskij resurs lichnosti vracha. Psihologicheskie problemy smysla zhizni i akme. V sbornike: Materialy XIII simpoziuma; 19 aprelya 2008 g.; M.: PI RAO, 2008; 63–65. Russian.
21. Soboleva AE. Vzaimosvjaz' zhiznestoikosti i otnoshenija k rabote u medicinskikh rabotnikov. Ustoichivoe razvitiye nauki i obrazovaniya. 2018; 8: 46–50. Russian.
22. Fomina NF, Fedoseeva TE. Issledovanie pokazatelej zhiznestoikosti v aspekte lichnosti professionala. Sovremennye problemy nauki i obrazovaniya [internet]. 2016; 6; [cited 2021 August 19]. Dostupno po ssylke: <https://science-education.ru/ru/article/view?id=25947>. Russian.
23. Abdollahi A, Abu Talib M, Yaacob SN, Ismail Z. Hardiness as a mediator between perceived stress and happiness in nurses. Journal of Psychiatry and Mental Health Nursing. 2014; 21; 9: 789–96.
24. Ablett J. Resilience and well-being in palliative care staff: a qualitative study of hospice nurses experience of work. Psycho-Oncology. 2007; 16; 8: 733–740.
25. Lambert V, Lambert C, Petrini M, Xiao M, Zhang Y. Workplace and social factors associated with physical and mental health in hospital nurses in China. Nursing and Health Sciences. 2007; 9: 120–6.
26. Hobfoll SE. Stress, culture, and community. N.Y.: London, 1998; 296 p.
27. Hobfoll SE, Lilly RS. Resource conservation as a strategy for community psychology. Journal of Community Psychology. 1993; 21: 128–48.
28. Vodopjanova NE. Protivodejstvie sindromu vygoranija v kontekste resursnoj koncepcii cheloveka. Vestnik Sankt-Peterburgskogo universiteta. Serija: Psihologija. 2011; 3: 38–50. Russian.
29. Ustav (Konstitucija) Vsemirnoj Organizacii. 2020; [cited 2021 July 13]. Dostupno po ssylke: <https://docs.cntd.ru/document/901977493>.
30. Noskova OG. Problemy psihologii dejatel'nosti i ee sub"ekta v tvorchestve E. A. Klimova (k 90-letiju so dnya rozhdenija). Psihologicheskiy zhurnal. 2021; 2; 42: 106–14. Russian.
31. Leontev D. A., Rasskazova E. I. Test zhiznestoikosti. M.: Smysl, 2006; 63 s. Russian.
32. Vodopjanova N. E. Stress-menedzhment. M.: Jurajt, 2018; 283 s. Russian.
33. Kostjuchenko EV, Romanchuk LN. Sviaz' zhiznestoikosti i optimizma medicinskikh rabotnikov. Aktual'nye problemy psihologii razvitiya lichnosti. Sbornik nauchnyh statej. Grodno: GrGU im. Janki Kupaly [internet]. 2017; 205–16 [cited 2021 August 19]. Dostupno po ssylke: <https://elib.grsu.by/doc/23846>. Russian.
34. Jasko BA, Kazarin BV. Model' lichnosti specialistika: metodologicheskoe obosnovanie i prakticheskaja vostrebovannost'. Organizacionnaja psihologija. 2020; 10; 4: 109–37. [cited 2021 August 19]. Dostupno po ssylke: [https://orgpsyjournal.hse.ru/data/2021/01/03/1344689973/OrgPsy_2020_4_\(6\)_Yasko-Kazarin_\(109-137\).pdf](https://orgpsyjournal.hse.ru/data/2021/01/03/1344689973/OrgPsy_2020_4_(6)_Yasko-Kazarin_(109-137).pdf). Russian.
35. Rasskazova EI, Gordeeva TO. Koping-strategii v strukture lichnostnogo potenciala. Lichnostnyj potencial: struktura i diagnostika. M.: Smysl, 2011; 267–99. Russian.

Литература

1. Твердохлебова Т. И., Ковалёв Е. В., Карпушченко Г. В., Кулак М. А., Думбадзе О. С., Литовко А. Р. и др. Социально-экономические аспекты COVID-19 на примере Ростовской области. Инфекционные болезни. 2020; 18 (4): 27–32. DOI: 10.20953/1729-9225-2020-4-27-32.
2. Сорокин М. Ю., Касьянов Е. Д., Рукавишников Г. В., Макаревич О. В., Незнанов Н. Г., Лутова Н. Б., и др. Структура тревожных переживаний, ассоциированных с распространением COVID-19: данные онлайн-опроса. Вестник

Российского Государственного Медицинского Университета [интернет]. 2020; 3: 77–84.

3. Куфтяк Е. В., Бехтер А. А. Стресс и проактивное совладающее поведение в период пандемии COVID-19: данные онлайн-опроса. Медицинская психология в России. 2020; 12; 6 (65) [cited 2021 July 13]. Доступно по ссылке: http://mpoj.ru/archiv_global/2020_6_65/nomer05.php.
4. Aspinwall LG, Taylor SE. Modeling cognitive adaptation: A longitudinal investigation of the impact of individual differences

- and coping on college adjustment and performance. *Journal of Personality and Social Psychology*. 1992; 63; 6: 989–1003. DOI: 10.1037/0022-3514.63.6.989.
5. Цыхань Л., Сяо Ган В. Психологические факторы посттравматического стресса, вызванного пандемией COVID-19. *Психологический журнал*. 2021; 42; 1: 102–10.
 6. Юревич А. В., Ушаков Д. В., Юревич М. А. COVID-19: результаты третьего экспериментального опроса. *Психологический журнал*. 2021; 42; 3: 28–136.
 7. Платонова Т. А., Голубкова А. А., Смирнова С. С., Дьяченко Е. В. Актуальные вопросы организации иммунопрофилактики населения. Коммуникативные риски — нерешенные проблемы и новые возможности. *Инфекционные болезни*. 2020; 18 (3): 112–8. DOI: 10.20953/1729-9225-2020-3-112-118.
 8. Франкл В. Человек в поисках смысла. М.: Прогресс, 1990; 368 с.
 9. Maddi S. Hardiness: an Operationalization of Existential Courage. *Journal of Humanistic Psychology*. 2007; 44; 3: 279–98.
 10. Maddi S. Hardiness: The courage to grow from stresses. *The Journal of Positive Psychology*. 2006; 1 (3): 160–8.
 11. Одинцова М. А. Психология жизнестойкости. М.: ФЛИНТА, 2015; 296 с.
 12. Ярошук И. В. Психология жизнестойкости: обзор теоретических концепций, эмпирических исследований и методик диагностики. Ученые записки СПбГИПСР. 2020; 1; 33: 50–60.
 13. Hobfoll SE. Stress, culture, and community. N.Y.: London, 1998; 296 р.
 14. Водопьянова Н. Е. Противодействие синдрому выгорания в контексте ресурсной концепции человека. Вестник Санкт-Петербургского университета. Серия: Психология. 2011; 3: 38–50.
 15. Kobasa SC. Stressful life events, personality, and health — inquiry into hardiness. *Journal of Personality and Social Psychology*. 2011; 37 (1): 1–11.
 16. Maddi S. The Courage and Strategies of Hardiness as Helpful in Crowing Despite Major, Destructive Stresses. *American Psychologist*. 2008; 63; 6: 563–4.
 17. Bartone PT, Valdes JJ, Sandvik A. Psychological Hardiness Predicts Cardiovascular Health. *Psychology, Health and Medicine*. 2016; 21 (6): 743–9.
 18. Nordmo M, Hystad SW, Sanden S, Johnsen BH. The effect of hardiness on symptoms of insomnia during a naval mission. *International Maritime Health*. 2017; 68 (3): 147–52.
 19. Maddi SR. The Role of Hardiness and Religiosity in Depress and Anger. *International Journal of Existential Psychology & Psychotherapy*. 2004; 1; 1: 38–49.
 20. Стецишин Р. И. Жизнестойкость как акмеологический ресурс личности врача. Психологические проблемы смысла жизни и акме. В сборнике: Материалы XIII симпозиума; 19 апреля 2008 г.; М.: ПИ РАО, 2008; 63–65.
 21. Соболева А. Е. Взаимосвязь жизнестойкости и отношения к работе у медицинских работников. Устойчивое развитие науки и образования. 2018; 8: 46–50.
 22. Фомина Н. Ф., Федосеева Т. Е. Исследование показателей жизнестойкости в аспекте личности профессионала. Современные проблемы науки и образования [интернет]. 2016; 6; [cited 2021 August 19]. Доступно по ссылке: <https://science-education.ru/ru/article/view?id=25947>.
 23. Abdollahi A, Abu Talib M, Yaacob SN, Ismail Z. Hardiness as a mediator between perceived stress and happiness in nurses. *Journal of Psychiatry and Mental Health Nursing*. 2014; 21; 9: 789–96.
 24. Ablett J. Resilience and well-being in palliative care staff: a qualitative study of hospice nurses experience of work. *Psycho-Oncology*. 2007; 16; 8: 733–740.
 25. Lambert V, Lambert C, Petrini M, Xiao M, Zhang Y. Workplace and social factors associated with physical and mental health in hospital nurses in China. *Nursing and Health Sciences*. 2007; 9: 120–6.
 26. Hobfoll SE. Stress, culture, and community. N.Y.: London, 1998; 296 р.
 27. Hobfoll SE, Lilly RS. Resource conservation as a strategy for community psychology. *Journal of Community Psychology*. 1993; 21: 128–48.
 28. Водопьянова Н. Е. Противодействие синдрому выгорания в контексте ресурсной концепции человека. Вестник Санкт-Петербургского университета. Серия: Психология. 2011; 3: 38–50.
 29. Устав (Конституция) Всемирной Организации. 2020; [cited 2021 July 13]. Доступно по ссылке: <https://docs.ctnd.ru/document/901977493>.
 30. Носкова О. Г. Проблемы психологии деятельности и ее субъекта в творчестве Е. А. Климова (к 90-летию со дня рождения). *Психологический журнал*. 2021; 2; 42: 106–14.
 31. Леонтьев Д. А., Рассказова Е. И. Тест жизнестойкости. М.: Смысл, 2006; 63 с.
 32. Водопьянова Н. Е. Стресс-менеджмент. М.: Юрайт, 2018; 283 с.
 33. Костюченко Е. В., Романчук Л. Н. Связь жизнестойкости и оптимизма медицинских работников. Актуальные проблемы психологии развития личности. Сборник научных статей. Гродно: ГрГУ им. Янки Купалы [интернет]. 2017; 205–16 [cited 2021 August 19]. Доступно по ссылке: <https://elib.grsu.by/doc/23846>.
 34. Ясько Б. А., Казарин Б. В. Модель личности специалиста: методологическое обоснование и практическая востребованность. *Организационная психология*. 2020; 10; 4: 109–37. [cited 2021 August 19]. Доступно по ссылке: [https://orgpsyjournal.hse.ru/data/2021/01/03/1344689973/OrgPsy_2020_4 \(6\)_Yasko-Kazarin \(109-137\).pdf](https://orgpsyjournal.hse.ru/data/2021/01/03/1344689973/OrgPsy_2020_4 (6)_Yasko-Kazarin (109-137).pdf).
 35. Рассказова Е. И., Гордеева Т. О. Копинг-стратегии в структуре личностного потенциала. *Личностный потенциал: структура и диагностика*. М.: Смысл, 2011; 267–99.